Lipid Bodies in Mycobacteria

Anna Louise Sherratt

Thesis submitted to the University of Leicester for the degree of Doctor of Philosopy

July 2008

Department of Infection, Immunity and Inflammation, Faculty of Medicine and Biological Sciences, University of Leicester, University Road, Leicester, LE1 7RH

ProQuest LLC
789 East Eisenhower Parkway
P.O. Box 1346
Ann Arbor, MI 48106-1346

Abstract

Lipid Bodies in Mycobacteria
Anna Sherratt (2008)

Lipid Bodies (LBs) are intracellular structures in mycobacteria that have been shown to consist of triacylglycerol (TAG) in *Mycobacterium smegmatis*. LB formation is environmentally regulated in *M. smegmatis in vitro* and LBs are thought to be linked with enhanced survival on exposure to antibiotics. LBs have not been demonstrated in *Mycobacterium tuberculosis* grown *in vitro*; however, LBs have been demonstrated in tubercle bacilli present in clinical sputum samples.

A survey of clinical samples revealed that LBs are a universal feature of tubercle bacilli in sputum. A number of conditions including hypoxia, Nitric Oxide ($NO^{\cdot}$) exposure, pH, heat and cold shock were shown to promote LB formation in *M. tuberculosis in vitro*. The formation of LBs in $NO^{\cdot}$ exposed *M. tuberc*ulosis was shown to correlate with the level of antibiotic tolerance displayed by the population. Antibiotic tolerance was thought to be a result of transitory growth arrest; however attempts to assess the growth status of LB positive *M. tuberculosis* cells were unsuccessful. The morphology of LBs in mycobacteria varied according to the growth condition of the cell and may be due to a change in lipid composition. The mechanism by which LBs are formed in mycobacteria remains unknown; however, there was some evidence to suggest that it follows a scheme similar to that which has been previously demonstrated in *Rhodococcus opacus*.

It was concluded that LB formation in mycobacteria may depend on a number of environmental factors, including conditions that promote growth arrest. The formation of LBs in *M. tuberculosis* may anticipate antibiotic tolerance. The presence of LBs in sputum tubercle bacilli may be used to assess treatment response in patients with tuberculosis; however, it remains to be shown that LB positive *M. tuberculosis* cells *in vitro* represent the physiological LB positive sputum bacilli.

Acknowledgements

I am extremely grateful for all the help and support I have received from my colleagues, family and friends throughout my studies and during writing up. I would particularly like to thank my supervisor Prof. Mike Barer for his support, advice, encouragement and giving me the opportunity to undertake this PhD study. Thanks also go to my co-supervisor, Prof. Colin Ockleford, for his support, guidance and helpful discussions, particularly in respect to the TEM work. I am especially grateful to Dr Natalie Garton, my third "unofficial supervisor". I would not have been able to carryout my laboratory work without her help and guidance. I would also like to thank Dr Primrose Freestone and Dr Caroline Beardsmore for their encouragement and advice.

My friends and colleagues in lab 136, both past and present, have not only been unfailingly supportive but also great fun to work with. Among them are Sarah, Hong-Yu, Ali, Eddy, Jo, Koirobi, Galina, Kumar and Gosia. Extra special thanks go to Su-Min Lee and Helen Smith for their help in the lab but particularly for their friendship and support. I am especially grateful to Helen for helping me set up and carry out all those NO experiments and teaching me to use Excel properly! Su-Min's help in using Endnote, proof reading and preparing the thesis document was invaluable and very much appreciated. I would also like to thank Dr Rebecca Smith for all her helpful advice on genetic manipulation, introducing me to primer design and answering all my endless questions with good humour! Thanks also go to Dr Bernard Burke for his collaboration in the macrophage experiments and letting me use his hypoxic incubator. I would also like to thank Sheila, Pam and Elizabeth, without whom the department of "3Is" would be unable to function!

I'd like to say a special thank-you to Stefan Hyman and Natalie Alcock of Leicester University EM unit, who kindly gave up their time to teach me how to process my samples for EM and use all the equipment. The TEM studies would have been impossible without their patience and advice. Thanks also go to Claire Senner of St George's

University for her collaboration in the NRP experiments. I would also like to thank Joanna Bacon who kindly donated the biomass from her chemostat cultures. Roger Meadows at the University of Manchester EM unit was kind enough to allow me to use of the Freeze Fracture equipment and give up his time to demonstrate the techniques involved and examine the specimens in the microscope.

My friends in the department have been wonderfully supportive and encouraging and I would like to say a big thank you to Kim Smith, Kim Earland, Jen, Adam, James, Abbey and Melissa. I'd also like to thank Nicola, Sophie, Nick, Steg, Tom and Sarah for their friendship and encouragement. Thanks go to Auntie Rita and Uncle Allen and Auntie Joan who have also been particularly supportive and encouraging. Finally I would like to express my appreciation for all the love and support my Mum, Dad and Holly have always given me. And last but certainly not least Bilbo Baggins the cat for keeping me company during writing up!

List of Common Abbreviations

ADC	Albumin Dextrose Catalase
AIDS	Acquired Immunodeficiency Disease
AFB	Acid-Fast Bacilli
APS	3'Aminopropyltriethoxysilane
ART	Antiretroviral therapy
ATP	Adenosine Triphosphate
BCG	Bacille Calmette-Guérin
BSA	Bovine Serum Albumin Fraction V
cDNA	Complementary DNA
CFDA/SE	Carboxyfluorescein diacetate, Succinimidyl ester
CFU	Colony Forming Unit
CoA	Co-enzyme A
COSHH	Control of substances hazardous to health
cm	Centimetre
DAG	Diacylglycerol
DGAT	Diacylglycerol acyl transferase
DMSO	Dimethyl sulfoxide
DNA	Deoxyribonucleic acid
DosR	Dormancy survival regulator
DOT	Dissolved oxygen tension
DOTs	Directly observed therapy
EEA	Early endosomal antigen
ER	Endoplasmic reticulum
FAD	Flavin adenine dinucleotide
FAME	Fatty Acid Methyl Esters
FAS	Fatty Acid Synthetase
GC-MS	Gas Chromotography Mass Spectrometry
GDP	Genome-directed primer
GFP	Green fluorescence protein
GSNO	S-nitrosglutathione
GTC	Guanidine thiocyanate
GTP	Guanosine Triphosphate
HIV	Human Immunodeficiency Virus
HLA	Human Leukocyte Antigen
ICL	Isocitrate lyase
IMP	Inter-membrane protein
IL	Inter Leukin
kDA	KiloDalton
L	Litre
LAM	Lipoarabinomannan
LB	Lipid Body
LCFA	Long Chain Fatty Acid

LCYB	Low carbon Youmans broth
LNYB	Low nitrogen Youmans broth
LM	Lipomannan
LSP	Large sequence polymorphism
M	Molar
mAGP	Mycolyl Arabinogalactan-Peptidoglycan
MDR-TB	Multi-drug resistant tuberculosis
MHC	Major Histocompatibility Complex
µg	Microgram
µm	Micrometre
mg	Milligram
ml	Millilitre
µl	Microlitre
MOI	Multiplicity of infection
MPN	Most probably number
mRNA	Messenger ribonucleic acid
MSM	Mineral salts medium
NAD	Nicotinamide-adenine dinucleotide
NALC	N-acetyl-L-cysteine
ng	Nanogram
nm	Nanometre
NO	Nitric oxide
NOS	Nitric oxide synthase
NRP	Non-replicating persistence
OA	Oleic Acid
OADC	Oleic Acid Albumin Dextrose Catalase
OD	Optical Density
PA	Phosphatidic acid
PBMC	Primary blood monocytes
PBS	Phosphate-buffered saline
PCR	Polymerase Chain Reaction
PDIM	Phthiocerol dimycocerosates
PHA	Polyhydroxyalkanotes
PHB	Poly-β-hydroxybutyrate
PIMS	Phosphatidylinositol mannosides
PO	Propylene oxide
RD	Regions of difference
RNA	Ribonucleic acid
RNI	Reactive nitrogen intermediates
ROI	Reactive oxygen intermediates
Rpf	Resuscitation promoting factor
rRNA	Ribosomal ribonucleic acid
RT-PCR	Reverse transcription Polymerase Chain Reaction
SCID	Severe combined immune deficiency
SD	Standard deviation
SNARE	Soluble NSF attachment receptor

TACO	Tryptophan aspartate rich coat protein
TA	Toxin-antitoxin
TAG	Triacylglycerol
TEM	Transmission Electron Microscopy
TGS	Triacylgylcerol Synthase
TLC	Thin Layer Chromatography
TLR	Toll-like receptor
TNF	Tumour Necrosis Factor
UV	Ultraviolet
WE	Wax Ester
WHO	World Health Organisation
WS	Wax synthase
XDR-TB	Extensively drug-resistant tuberculosis
YB	Youmans broth

List of Figures

List of Tables

Table of Contents

Chapter 1

Introduction

1.1 General Introduction

Tuberculosis is a global health problem and is caused by the pathogen *Mycobacterium tuberculosis* which belongs to the genus *Mycobacterium* (Dye, 2006). This group of bacteria are characterised by their high lipid content, which is largely attributable to their cell envelopes (Schweizer and Hofmann, 2004). This cell envelope is composed of unusual lipids derived from long chain fatty acids (LCFA) and this high requirement for LCFA of these organisms is reflected by their ability to synthesise medium and long chain fatty acids via the enzyme systems Fatty Acid Sythetase I and II, respectively (Takayama et al., 2005). In addition to *de novo* synthesis of fatty acids, LCFAs are also taken up by the cell and may be utilised with or without modification of the chain length in the biosynthesis of cell membrane phospholipids or cell envelope lipids (Takayama et al., 2005). It was believed that the entire cellular lipid content that was synthesised or taken up by the cell was located in the cell envelope (Garton et al., 2002). However, recent work has revealed that lipid in the form of triacylglycerol (TAG) is also present as intracellular droplets within the mycobacterial cell cytoplasm (Garton et al., 2002). The formation and occurrence of these droplets or Lipid Bodies (LBs), as they are now termed, is the focus of this thesis.

Significantly, LBs have been demonstrated in tubercle bacilli in sputum obtained from a patient with tuberculosis but LBs have not been observed in *M. tuberculosis* grown in the laboratory (Garton et al., 2002). This difference is indicative of *M. tuberculosis* adopting an altered physiology within the host (Garton et al., 2002). Indeed, there is a growing body of evidence to suggest that *M. tuberculosis* catabolism switches from carbohydrate to fatty acid utilisation and that the metabolic pathway involved in fatty acid metabolism is essential for survival in the host (Munoz-Elias and McKinney, 2005). The fatty acids that supply these metabolic pathways may be stored in LBs, however, the abundance of exogenous fatty acids in the host environment (Munoz-Elias and McKinney, 2005) suggest that the role of the mycobacterial LB is more dynamic than that of a simple storage structure.

Very little is known about the metabolism and physiology of *M. tuberculosis* during human infection. However, this is of particular interest because the two most distinguishing characteristics of human tuberculosis are thought to be due to marked changes in bacterial physiology that have not yet been elucidated. The first is the extended period of chemotherapy that is required to treat tuberculosis which takes 6 months. While, frontline drugs used to treat tuberculosis act rapidly on cultures of *M. tuberculosis in vitro*. The additional time required to eliminate *M. tuberculosis in vivo* is thought to be due to the existence of a group of physiologically distinct bacteria that are able to withstand the effects of these drugs (McKinney et al., 2000).

The second feature of tuberculosis is the long incubation period of the pathogen that characterises the latent, asymptomatic stage of disease. During this period, *M. tuberculosis* is thought to reside in the host tissue in a dormant-like state, although the location and state of the bacteria responsible for latent infection have yet to be defined (Parrish et al., 1998). The majority of research in this area has focussed on noculate latency in animal models and examining the response of *M. tuberculosis* to the assumed host environmental conditions (Wayne and Sohaskey, 2001). It is unknown whether the physiological states of the groups of bacteria underpinning these two disease phenomenon are equivalent or entirely discrete. Populations of sputum tubercle bacilli with LBs may be representative of one or both of these groups of bacteria. Therefore, the association of LBs in *M. tuberculosis* with antibiotic exposure and conditions that are thought to be involved in dormancy have been examined.

As the issues discussed are particularly relevant to studies related to LBs in mycobacteria, they will be considered in more detail in the following sections.

1.2 Mycobacteria and their lipids

1.2.1 Mycobacteria

The mycobacteria comprise the genus *Mycobacterium*, which are close relatives of *Corynebacterium* and *Norcardia* and common to these relatives, mycobacterial DNA has a high content of guanine and cytosine (G+C) (Wayne and Kubica, 1986). Mycobacteria are considered to be Gram-positive bacteria, despite the fact that cells are not readily stained by the Gram method. Members of the genus are aerobic, non-motile, slow-growing rod shaped bacteria that are characteristically acid-fast. Acid-fastness refers to the ability of mycobacteria stained with a cationic dye to resist decolourisation by acidified alcohol (Wayne and Kubica, 1986); it is a property that is associated with the high lipid content of the cell wall, of which waxes and mycolic acids are major constituents (see below for further discussion) (Goodfellow and Minnikin, 1980). Acid-fast staining techniques are routinely used to identify mycobacteria in clinical specimens (Mitchison, 2004).

The mycobacteria are usually divided into two groups based on the species generation time. The "slow growers" are the species of mycobacteria that require over 7 days of incubation at optimal temperatures to produce colonies from highly diluted inocula, while the "fast growers" are those that form colonies in less than 7 days in comparable conditions (Wayne and Kubica, 1986). The slow growing group of mycobacteria include some of the oldest pathogens known to man: *Mycobacterium tuberculosis* and *Mycobacterium leprae*, the causative agents of tuberculosis and leprosy, respectively. The fast growing mycobacteria are generally regarded as non-pathogenic; however, a number of species are able to establish infection of immunocompromised hosts (Howard and Byrd, 2000). These include *Mycobacterium smegmatis*, commonly used as a model organism for studying the biology and physiology of the mycobacteria because of its fast generation time and relative safety of use; *M. smegmatis* is only an occasional opportunistic pathogen, causing soft tissue infection (Howard and Byrd, 2000).

1.2.2 The *Mycobacterium tuberculosis* complex

The *M. tuberculosis* complex consists of closely related organisms of the genus *Mycobacterium* and that share 99% identity at the nucleotide level for some loci (Sreevatsan et al., 1997, Cole et al., 1998, Cosma et al., 2003). The *M. tuberculosis* complex was thought to comprise six members but recent taxonomic studies have identified a further two members (Aranaz et al., 2003, Cousins et al., 2003). Aside from *M. tuberculosis,* which causes the majority of human tuberculosis cases, the complex includes *Mycobacterium africanum*, a major cause of tuberculosis in sub-Saharan Africa. *Mycobacterium canetti*, is also capable of establishing human disease but is rarely encountered. While, *Mycobacterium bovis* is a pathogen of a number of mammalian species, including humans and cattle. The attenuated variant of *M. bovis*, known as nocula Calmette-Guérin (BCG), was isolated from 230 serial passages of *M. bovis* (Cole, 2002). It has since been extensively used as a live vaccine against tuberculosis and three billion doses have now been administered (Cole, 2002). The complex also includes three members which primarily infect non-human hosts. *Mycobacterium microti* is a vole pathogen and is avirulent in humans (Cole, 2002, Cosma et al., 2003). The two most recent additions to the complex are *Mycobacterium caprae* (Aranaz et al., 2003) and *Mycobacterium pinnipedii* (Cousins et al., 2003), the causative agents of tuberculosis in goats and seals, respectively.

1.2.3 The Mycobacterial Cell Wall

The mycobacteria have an extraordinary requirement for lipid, due to the high lipid content of the cell wall. The unique cell wall structure of the mycobacteria is arguably their most defining characteristic. The mycolic acids, high molecular weight α-alkyl,β-hydroxy branched fatty acids 60-90 carbons in length, are the key lipid components of the mycobacterial cell wall and a distinguishing feature of the mycobacteria (Brennan and Nikaido, 1995, Minnikin et al., 2002). Although mycolic acids are found in

Corynebacteria and *Nocardia*, the mycobacterial mycolic acids are much longer. The mycobacterial cell envelope comprises a cell membrane, and the outer and inner sections of the cell wall (Brennan, 2003). The inner section consists of a layer of peptidoglycan covalently attached to the polysaccharide, arabinogalactan, which in turn is attached to the mycolic acids. This is known as the mycolyl arabinogalactan-peptidoglycan complex (mAGP) and forms the core of the cell wall. The outer section consists of the free fatty acids and lipoarabinomannan (LAM) (Brennan, 2003, Brennan and Nikaido, 1995) (Figure 2). The components and structure of the cell envelope are discussed in more detail below.

The mycobacterial plasma membrane and peptidoglycan layer is thought to be similar to those of other bacteria (Minnikin et al., 2002). However, the appearance of the mycobacterial cell membrane is asymmetrical in that the outer, electron dense layer is thicker than the inner thin layer, as observed by electron microscopy (Paul and Beveridge, 1992). This electron transparent layer is thought to be where the phosphatidylinositol mannosides (PIMs) are located. PIMs are mannoside derivatives of phosphatidic acid and are major plasma membrane components. PIMs form the lipid base of lipomannan (LM) and lipoarabinomannan (LAM) (Brennan and Nikaido, 1995).

Mycobacterial peptidoglycan is similar to that which is most commonly found in bacteria. However, the muramic acid residue is N-glycolylated to glycolic acid in mycobacterial peptidoglycan, while this residue is N-acetylated in other bacteria (Brennan and Nikaido, 1995). The peptidoglycan is linked to arabinogalactan, a polysaccharide consisting of arabinose and galactan, through a phosphodiester link. In turn, the arabinogalactan is esterified through the terminal arabinose residues to the mycolic acids to form the cell wall core (Brennan and Nikaido, 1995).

The mycolic acids are made up of two structural groups: the meromycolate moiety (the main chain) and the α-branch. Except for length, the α-branch is invariant in mycolic acid, while functional changes are always found in the main chain. These are used to distinguish between the different mycolic acids (for the structure of the mycolic acids, see

Figure 1). Structural modifications usually consist of one or two functional groups, including double bonds, keto, methoxyl and alkenic groups and cyclopropane rings that are capable of introducing kinks in the molecule. The chain may also have oxygen functions further to the β-hydroxy group, in addition to methyl branches in the main carbon backbone (Brennan, 1988, Brennan and Nikaido, 1995).

In terms of the structure and arrangement of the cell wall, Minnikin (1982) proposed that the mycolic acid chains are packed side by side in a direction perpendicular to the plane of the cell surface. This is covered by an outer leaflet composed of extractable lipid to form a "pseudo" lipid bilayer structure (Chatterjee, 1997). The extractable lipids will be discussed separately below. The functional groups of the mycolic acids, discussed above, modulate the packing of the mycolic acids in this bilayer structure. The shorter α-branch chains are always saturated and without cyclopropane ring structures and the functional groups of the main chain are located at the distal end of the group, away from the carboxyl end of the molecule. This introduces a gradient of fluidity into the mycobacterial cell wall in which the external regions are more fluid, due to a disruption of the packing of mycolic acids, and the internal section is less fluid owing to the tight packing of the mycolic acid chains (Brennan and Nikaido, 1995).

Figure 1: The chemical structure of the mycolic acids of *M. tuberculosis*

Mycolic acids are composed of a long meromycolate chain and a saturated α-chain and can be distinguished by the chemical modifications of the former. The α-mycolic acids do not contain an oxygen function other than the β-hydroxyl group but possess two cyclopropane rings. This is the most abundant mycolic acid. The oxygenated keto- and methoxy-mycolic acids possess polar modifications containing oxygen functions in the distal part of the main chain. Non-polar modifications, such as cyclopropane rings are located in the distal and proximal ends of the chain (Bhatt et al., 2007, Takayama et al., 2005). Image taken from Takayama et al. (2005).

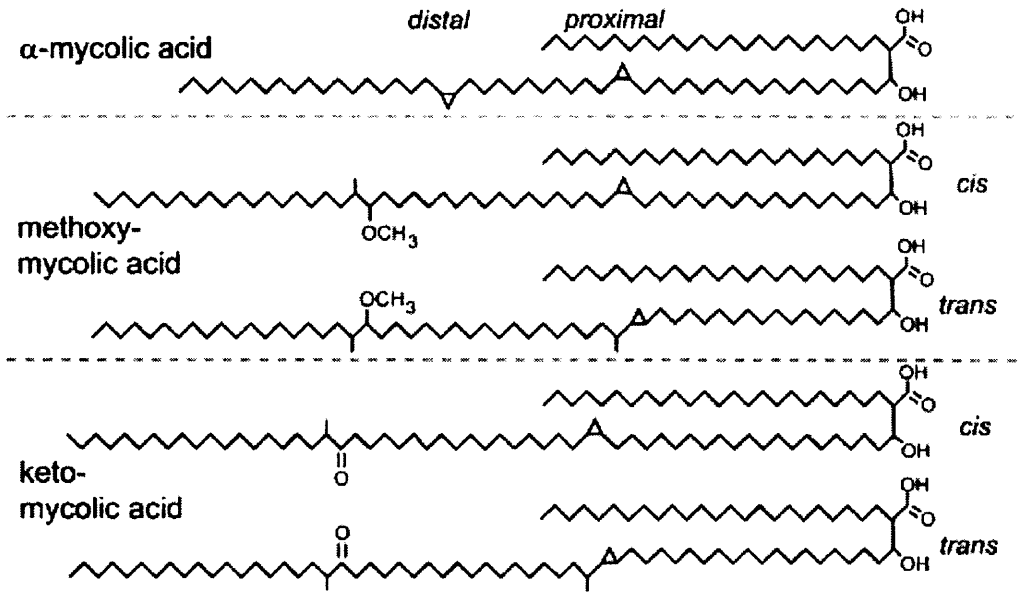

The waxy nature of the mycobacterial cell envelope can be attributed to the dimycocerosates of the phthiocerol family, the PDIMs. Waxes can be defined as esters of long chain alcohols and fatty acids, with the waxes of mycobacteria consisting of diesters of the phthiocerols. Phthiocerols are long chain methoxyglycols, with mycocerosic acids (mutimethyl branched fatty acids). PDIMS form part of the outer bilayer of the cell envelope structure and interact with the covalently bound mycolic acids (Minnikin et al., 2002, Brennan, 1988). PDIM is thought to have a role in regulating the immune response within infected tissue (Russell, 2007).

Interspersed between the mycolic acids are the lipopolysaccarides, LM and LAM, which span the whole cell wall. These are considered to form part of the free lipids of the envelope because they are extractable by various solvents. However, they are extensions of PIMs, which are anchored in the plasma membrane. LAM is also an immunologically active compound and is capable of inducing numerous signalling events that are important in the host response to *M. tuberculosis* (Brennan and Nikaido, 1995, Brennan, 2003).

The outer section of the envelope is characterised by a whole host of extractable glycolipids, of which trehalose is the basic component. Trehalose is a non-reducing disaccharide in which the two glucose units are linked in an α,α,-1,1-glycosidic linkage (Elbein et al., 2003). Members of the *M. tuberculosis* complex, such as *M. africanum* and *M. bovis*, form characteristic phenolic glycolipid antigens (Minnikin et al., 2002). In addition, the virulent W-Beijing *M. tuberculosis* family possess a unique phenolic glycolipid and loss of this lipid resulted in a marked reduction in their hypervirulence phenotype (Russell, 2007). Cord factor is perhaps the most widely studied trehalose based lipid of the mycobacteria. Cord factors are dimycolates of trehalose that cause the cells to aggregate in a cord like fashion during growth *in vitro* and in sputum they occur on the surface of the cell and provide a thick layer that protects the bacterium from chemicals and the host immune system (Takayama et al., 2005). In addition to this protective role, cord factor is extremely toxic to mice due to its ability to stimulate host NADase activity and thereby reduce the activities of NAD-dependent microsomal

enzymes (Brennan, 2003) and is also believed to act as a mycolic acid donor to cell wall arabinogalactan (Chatterjee, 1997).

The structure of the mycobacterial cell wall is the key to a number of characteristics of the mycobacteria. As discussed, a number of cell wall components are important in the host immunological response. In addition, the low permeability of the cell wall is thought to contribute to the resistance of mycobacteria to antibiotics and chemotherapeutic agents (Jarlier and Nikaido, 1994).

Figure 2: Schematic representation of the structure of the mycobacterial cell wall

The mycobacterial cell wall is composed of the plasma membrane and the outer and inner sections of the cell wall. The core element of the wall (inner section) consists of the mycolyl arabinogalactan-peptidoglycan complex (mAGP), which is linked to the plasma membrane. Lipoarabinomannan (LAM) is anchored in the plasma membrane by its base phosphatidylinositol mannosides (PIMS), which are indicated by the yellow boxes. Interspersed between the mycolic acid chains are the complex free lipids and waxes (PDIM) that comprise the upper section of the wall (Brennan, 2003). Diagram adapted from (Brennan, 1988, Christensen et al., 1999, Somoskovi et al., 2001).

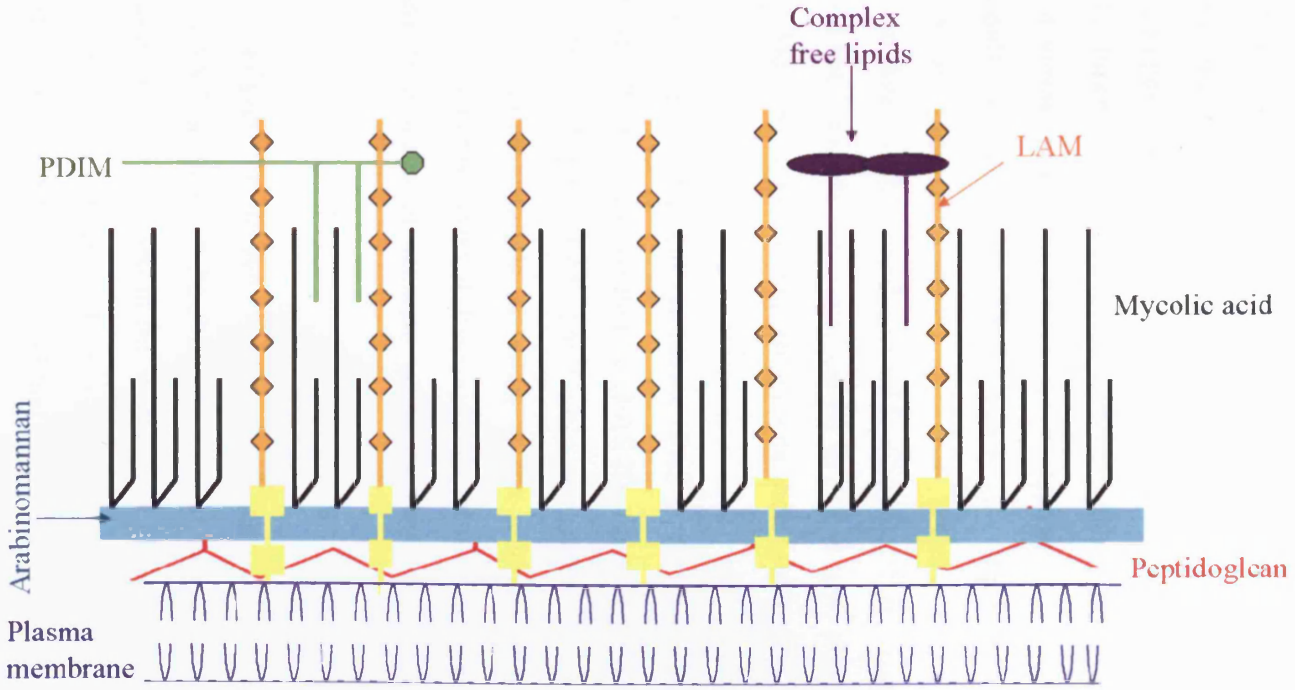

1.2.4 Lipid Metabolism

1.2.4.1 Fatty Acid Synthesis

Given the high requirement of the mycobacteria for lipids, up to 60% of the dry mass of the mycobacterial cell is composed of lipids (Schweizer and Hofmann, 2004), their synthesis is a crucial cellular function in cell envelope turnover. As we have seen, long chain fatty acids (LCFA) of various structures are the key components of a number of mycobacterial cell wall lipids, in addition to phospholipids and acylglycerols. The mycobacterial acylglycerols, as major constituents of Lipid Bodies, are discussed separately in this chapter, and their synthesis is described in Chapter 3. An overview of the cellular flux of environmental and *de novo* synthesised LCFA is also presented in Chapter 3. Therefore, this introduction is concerned simply with their synthetic pathways.

The mycobacteria possess both type I fatty acid synthetase (FAS-I), found in eukaryotes and some prokaryotes and type II fatty acid synthetase (FAS-II), found in bacteria and plants (Takayama et al., 2005). Type I FAS are highly integrated multi-enzyme complexes which contain the various catalytic activities of the reaction sequence as discrete functional domains. In contrast, type II FAS systems consist of independent proteins which are encoded by a series of separate genes (Schweizer and Hofmann, 2004).

The mycobacterial FAS I catalyses the *de novo* synthesis of short chain fatty acyl primers. The mycobacterial FAS I is unique in its ability to produce two classes of fatty acids: those with chain lengths of 16 to 18, used in the synthesis of phospholipids, and a second group with chain lengths of 24 to 26 carbon atoms, used in the synthesis of mycolic acids and multimethyl branched fatty acids (Bhatt et al., 2007, Schweizer and Hofmann, 2004, Takayama et al., 2005). This second function perhaps also serves to elongate conventional fatty acids obtained from the host environment to be used in mycolic acid synthesis. In contrast to the type II synthases of other bacteria, the mycobacterial type II is not capable of *de novo* fatty acid synthesis but instead the four

enzymes of FAS II elongate the medium chain length fatty acids generated by FAS I (Bhatt et al., 2007, Schweizer and Hofmann, 2004, Takayama et al., 2005).

In *M. tuberculosis*, the *fas* gene encodes the FAS-I polypeptide that contains all the domains required for the *de novo* synthesis of fatty acid (Smith et al., 2003). The mycobacterial FAS I consists of the following domains: acyltransferase, enoyl reductase, dehydratase, malony/palmitoyl transferase, acyl carrier protein, β-ketoacyl reductase and β-ketoacyl synthase (Takayama et al., 2005). The two carbon fragment, acetate, substrate for fatty acid synthesis is activated by the FAS I Coenzyme A (CoA), via a high energy thioester linkage between the carboxyl function of the fatty acid and the –SH group of the enzyme (Gurr and James, 1975). The first step in fatty acid synthesis is the carboxylation of acetyl-CoA to malonate (Gurr and James, 1975). Carboxylation is catalysed by a biotin dependent carboxylase, of which there may be three complete systems in *M. tuberculosis* (Cole et al., 1998). FAS-I then elongates acyl groups by two carbon units using acetyl-CoA and malonyl-CoA as substrates (Takayama et al., 2005). The substrates are transferred to the FAS I acyl carrier protein, where condensation reactions between the substrates take place to yield butyryl-ACP. Further elongation leads to the formation of 16 and 18 carbon length fatty acids, which are transferred from the FAS I complex to Co-enzyme A and used in the synthesis of phospholipids (Bhatt et al., 2007). The C16 acyl-CoA product acts as a substrate for the synthesis of meromycolic acids by FAS II (Bhatt et al., 2007, Takayama et al., 2005). Alternatively, fatty acids may be elongated further by FAS I to form fatty acids of a carbon length of 20 to 26. These are also released as the Co-enzyme A derivatives (Takayama et al., 2005). Hexacosanoyl-CoA (C26) generated by FAS I form the short α chain of the mycolic acids (Bhatt et al., 2007, Takayama et al., 2005).

The FAS II system consists of enzymes that act successively and repeatedly in the elongation of fatty acids for the synthesis of the meromycolic acids in mycobacteria. The condensing enzymes KasA and KasB are the principal enzymes of the mycobacterial FAS II pathway. The enzyme mtFabH forms the link between the FAS I and II systems and initiates the starting reaction of meromycolic acid synthesis by catalysing a

condensation reaction between the C14-CoA primer generated by FAS I and malonyl-AcpM to form β-keto-acyl-AcpM (Bhatt et al., 2007, Schweizer and Hofmann, 2004). The function of AcpM is to shuttle acyl intermediates between enzymes (Bhatt et al., 2007). The elongation condensing enzymes, KasA and KasB catalyse the condensation of β-keto-acyl-AcpM and malonyl-AcpM in a three-step reaction that elongates the growing chain by two carbon units (Bhatt et al., 2007). KasA may catalyse the initial elongation reactions while KasB extends the chain to form the meromycolic acid (Bhatt et al., 2007). The acyl primer generated by mtFabH is transferred to the active site and AcpM is released. Malonyl-AcpM is then bound to the enzyme and decarboxylated to allow the condensation reaction to occur (Bhatt et al., 2007). Functional groups are introduced by a number of cyclopropane synthases and finally, Pks13 catalyses the condensation of the α-branch and the meromycolate to form the mycolic acid (Bhatt et al., 2007, Takayama et al., 2005).

1.2.4.2 Fatty Acid Metabolism

Not only are fatty acids an important component of the mycobacterial cell envelope but there is a growing body of evidence to suggest that *M. tuberculosis* uses fatty acids as a carbon and energy source *in vivo* (Cole et al., 1998, Wheeler and Blanchard, 2005). Segal and Bloch (1956) demonstrated that *M. tuberculosis* isolated from the lungs of infected mice grew preferentially on media in which fatty acid was the major carbon source. More recently, it has been demonstrated that isocitrate lyase 1 (ICL1), an enzyme involved in the metabolism of fatty acids, is essential for the late stage persistence of *M. tuberculosis* in the mouse model (McKinney et al., 2000). Further work revealed that there are two *M. tuberculosis icl* homologues, *icl1* and *icl2*. Again, deletion of *icl1* resulted in a reduction of bacterial load in chronic infection, while deletion of *icl2* had little effect. However, bacteria lacking both genes were unable to grow in mice and were rapidly cleared from the lungs and spleen (Munoz-Elias and McKinney, 2005). Concurrent with the hypothesis that fatty acid is the carbon source *in vivo*, the ICL gene, *icl1*, along with other enzymes of the glyoxylate cycle were upregulated in during *M.*

tuberculosis during infection of macrophages (Schnappinger et al., 2003) and mice (Timm et al., 2003).

The exact source and type of fatty acid utilized by *M. tuberculosis* are unknown; however, there are a number of possibilities (Munoz-Elias and McKinney, 2006). Fatty acids may be acquired from the lipid rich host-cell debris in mature granulomas (Honer zu Bentrup and Russell, 2001). Lung surfactant is also rich in fatty acids and can be internalised by macrophages or *M. tuberculosis* may be able to utilize macrophage triacyglcerol stores mobilized during phagocytosis (Munoz-Elias and McKinney, 2006). In support of this, growth of *M. bovis* BCG in macrophages has been shown to decrease the triacylglycerol (TAG) levels in the host cell (Jackson et al., 1989). Alternatively, *M. tuberculosis* may metabolise fatty acids stored as TAG (Daniel et al., 2004) (This aspect will be discussed at length in Chapters 3 and 7). If this is the case, it is important to understand the means by which mycobacteria metabolise fatty acid.

The β-oxidation cycle is the principle pathway for the degradation of fatty acids in bacteria and eukaryotes. Succesive rounds of β-oxidation yield acetyl-CoA that is channelled into the citric acid cycle (Munoz-Elias and McKinney, 2006). The first step of β-oxidation is the introduction of a *trans* double bond in the hydrocarbon chain of the activated fatty acid, which is catalysed by an acyl-CoA dehydrogenase with FAD as a co-factor (Gurr and James, 1975). *M. tuberculosis* has 36 homologues of the *noc* gene encoding an acyl-CoA dehydrogenase (Cole et al., 1998). Enoyl CoA hydratase catalyses the addition of water across the *trans* double bond of the unsaturated acyl-CoA to form β-hydroxyacyl-CoA (Gurr and James, 1975). There are 21 homologous enzymes belonging to the enoyl-CoA hydratase family encoded by the *M. tuberculosis* genome (Cole et al., 1998). The abundance of *M. tuberculosis* genes devoted to lipid catabolism lends support to the hypothesis that fatty acids are a major carbon source for this pathogen (Cole et al., 1998, Wheeler and Blanchard, 2005).

The next step in the pathway is the dehydrogenation step, which converts the β-hydroxyacyl-CoA into a β-keto fatty acid, the enzyme β-hydroxyacyl-CoA-

dehydrogenase catalyses this step, with NAD^+ as a co-factor. The final step involves a thiolytic cleavage of the keto acid acid in which the –SH group of the CoA displaces an acetyl-CoA moiety, thus resulting in a molecule that is two carbon atoms shorter than the original molecule. The process is repeated until the carbon chain has been reduced to acetyl-CoA groups. Therefore, each cycle generates energy in the form of one molecule of $FADH_2$, NADH and acetyl-CoA (Gurr and James, 1975).

The acetyl-CoA generated in the β-oxidation of fatty acids can be directed into the glyoxylate shunt pathway (Figure 3). This is the first step leading to the flux of carbon into gluconeogenesis, which is the only mechanism by which the organism can acquire and conserve carbon from growth on fatty acid as the limiting carbon source (Russell, 2001). The key enzyme, ICL, converts isocitrate into succinate and glyoxylate, followed by the addition of acetyl-CoA to glyoxylate to form malate by malate synthase (Sharma et al., 2000, Russell, 2001). The glycoxylate shunt pathway thereby bypasses the two decarboxylation steps of the citric acid cycle (the metabolic pathway by which acetate is oxidized to generate ATP), to allow incorporation of two carbon molecules, such as acetate from β-oxidation, into the cycle (Wall et al., 2005). The pathway not only allows the synthesis of carbohydrates from fatty acids but also supplies the citric acid cycle with intermediates (Honer zu Bentrup and Russell, 2001). In addition to mycobacteria, ICL appears to be critical for the survival of other intracellular pathogens. The *Salmonella typimurium* isocitrate lyase is required for persistence in a mouse model of chronic infection (Fang et al., 2005) and deletion of isocitrate lyase in *Rhodococcus equi*, an important foal pathogen, caused the attenuation of the strain (Wall et al., 2005). Therefore, intracellular pathogens may shift their primary carbon source from carbohydrate to fatty acid in the host environment (Honer zu Bentrup and Russell, 2001). These studies demonstrate the discrepancies between the culture conditions used in the laboratory and those that are encountered in the host.

Figure 3: The Glyoxylate Cycle

The glyoxylate shunt pathway is required for carbohydrate synthesis and supply of citric acid cycle intermediates when fatty acid is the principal carbon source (Russell, 2001). Acetate (highlighted by red ovals) is generated from the β-oxidation of fatty acid and is incorporated into the cycle in a step that bypasses the two decarboxylation steps of the citric acid cycle. The net result of the glyoxylate cycle is the consumption of two molecules of acetate to generate one molecule of succinate and one molecule of glyoxylate (Honer zu Bentrup and Russell, 2001). The number of carbon atoms in each molecule is indicated in blue adjacent to the corresponding molecule. Image is adapted from Russell (2001).

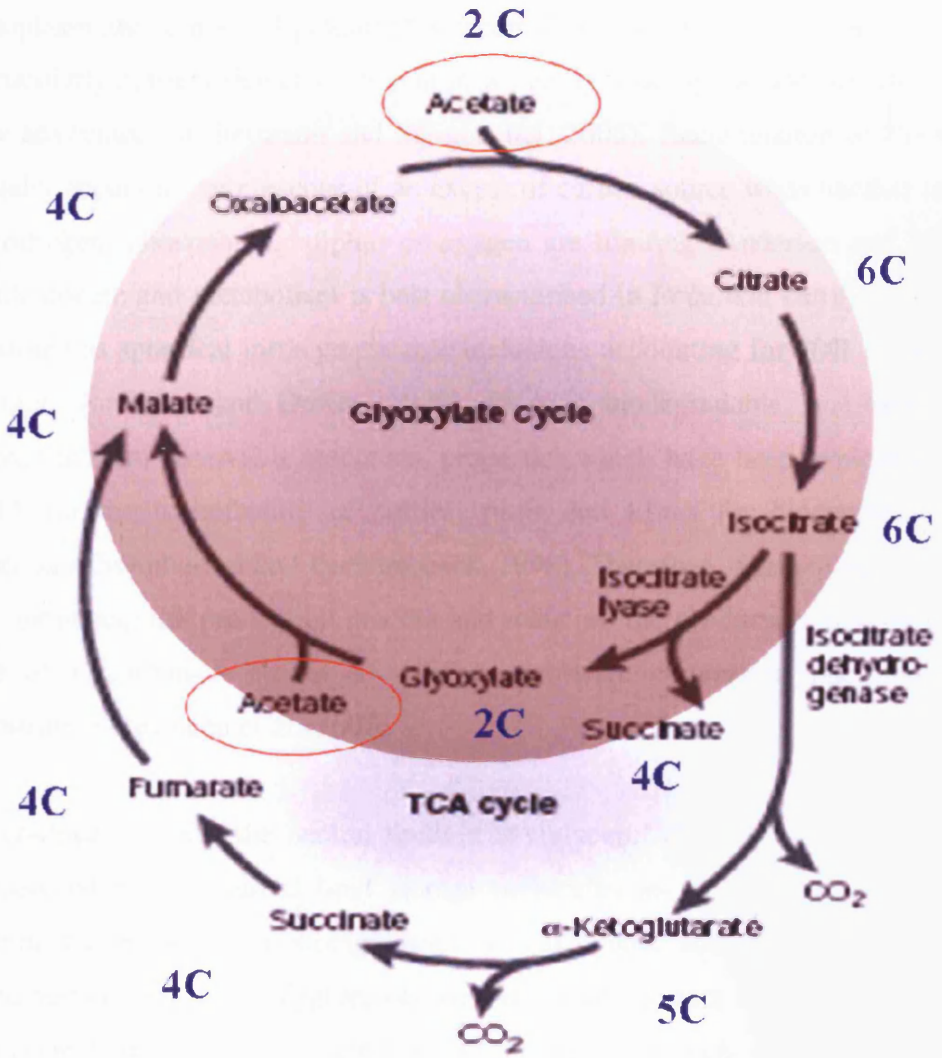

1.2.5 Lipid Storage in Prokaryotes

Lipids, in addition to their role in membranes and envelopes of bacteria can also act as storage materials in prokaryotes. The most common storage molecule is poly-β-hydroxybutyrate (PHB) or other polyhydroxyalkanotes (PHA) (Waltermann and Steinbuchel, 2005), a polyester of the poly-3-hydroxyalkanoate type. PHB is sometimes considered to be a carbohydrate; however, it has solubility characteristics of a lipid (Ratledge and Wilkinson, 1988). These lipids accumulate as inclusion bodies in the cytoplasm and almost all prokaryotes accumulate one type of lipid, unless they inhabit a particularly nutrient rich environment in which lipid storage would not afford the bacteria any advantage (Waltermann and Steinbuchel, 2005). Accumulation of PHA in bacteria usually occurs in the presence of an excess of carbon source when another nutrient, such as nitrogen, phosphorus, sulphur or oxygen are limiting (Anderson and Dawes, 1990). PHA storage and metabolism is best characterised in *Ralstonia eutropha*, in which PHA is stored as spherical intracytoplasmic inclusions accounting for 90% of the cellular dry weight (Anderson and Dawes, 1990). PHA is biodegradable, non-toxic and can be produced from renewable resources, properties which have been exploited in the use of PHA for the manufacture of bottles, films and fibres for biodegrabable packaging materials (Steinbuchel and Fuchtenbusch, 1998). Therefore, research on PHA has centred on optimising the production process and reducing the production cost by exploring the use of recombinant strains to enhance substrate conversion rate and inexpensive substrates (Verlinden et al., 2007).

In contrast to PHB, the neutral lipids triacylglycerol (TAG) and wax esters (WE) are considered to be unusual lipid storage molecules in prokaryotes. However, TAG is commonly found as a storage lipid in eukaryotes and plant seeds (Alvarez and Steinbuchel, 2002). Triacyglycerols are fatty acid triesters of glycerol and represent a convenient and highly efficient form of storing fatty acids (Alvarez and Steinbuchel, 2002). As we have seen, fatty acids can be metabolised by β-oxidation and yield a higher calorific value (weight/weight) than carbohydrates or protein (Gurr and James, 1975,

Alvarez and Steinbuchel, 2002). Until recently TAG biosynthesis had only been demonstrated in a small number of aerobic heterotrophic bacteria and cyanobacteria, however, it has now been shown to be a common feature of the actinomyces group, including *Mycobacterium*, *Streptomyces*, *Nocardia* and *Rhodococcus* and the Gram negative genus, *Acinetobacter* (Alvarez and Steinbuchel, 2002, Waltermann and Steinbuchel, 2005). Research on TAG biosynthesis and storage has been largely carried out in *Rhodococcus opacus* and *Streptomyces lividans* but TAG accumulation in mycobacteria has received renewed interest recently and developments in this field are discussed in the subsequent section of this chapter. In these organisms, TAG is stored in spherical lipid bodies within the cytoplasm and these lipids can contribute up to 70% of the cellular dry weight (Olukoshi and Packter, 1994, Alvarez et al., 2000, Alvarez and Steinbuchel, 2002, Waltermann and Steinbuchel, 2005). For discussion of the ultrastructure and formation of TAG inclusions the reader is referred to Chapter 4 of this thesis.

Accumulation of TAG is stimulated by entry into stationary phase or upon cultivation in media with a low nitrogen to carbon ratio (Olukoshi and Packter, 1994, Alvarez et al., 2000, Alvarez and Steinbuchel, 2002, Waltermann and Steinbuchel, 2005). TAG inclusions in cells grown under these conditions can almost completely fill the cell and are thought to act mainly as energy and carbon storage bodies (Waltermann and Steinbuchel, 2005). However, there have been a number of other functional roles suggested for TAG bodies, such as deposits for toxic or surplus fatty acids from phospholipid biosynthesis (a role which will be discussed in Chapter 3) (Waltermann and Steinbuchel, 2005). TAG bodies may also be utilised to maintain a water supply during periods of dehydration through oxidation of the fatty acid hydrocarbon chains (Waltermann and Steinbuchel, 2005). *R. opacus* has been shown to mobilize stored lipids during prolonged dehydration and under conditions of low carbon. However, there is very little known about the mobilisation and degradation of stored TAG (Waltermann and Steinbuchel, 2005).

Wax esters (WE), which are esters of long chain alcohols and fatty acids, also occur as storage lipids in prokaryotes, predominately in the genus *Acinetobacter* but WE accumulation has also been described in *Moraxella*, *Micrococcus* and *Fundibacter*. WE biosynthesis has also been reported in *Corynebacterium*, *M. tuberculosis* and *Nocardia* (Alvarez and Steinbuchel, 2002, Waltermann and Steinbuchel, 2005). Scott and Finnerty (1976) first demonstrated the accumulation of wax esters as intracellular inclusions in species of *Acinetobacter* grown on hydrocarbons. In *Acinetobacter calcoacetius*, WE can account for up to 25% of the dry weight and are thought to act as carbon storage compounds (Waltermann and Steinbuchel, 2005). WE can be stored as spherical, disk-like or rectangular inclusions, depending on the hydrocarbon source available to the cell (Waltermann and Steinbuchel, 2005).

The identification of a novel wax synthase/ diacyglycerol acyltransferase (WS/DGAT) in *Acinetobacter calcoaceticus* has provided an insight into the synthesis of these neutral lipids. This enzyme catalyses the final step in WE and TAG biosyntheses in which an acyl group from acyl-CoA is esterified to a long chain alcohol or diacylglycerol, respectively (Kalscheuer and Steinbuchel, 2003, Waltermann et al., 2007). The enzyme is active on a broad spectrum of substrates, making it attractive for biotechnological applications (Waltermann et al., 2007). The full TAG biosynthetic pathway is presented in Chapter 3. WS/DGAT actually represents a wide class of bacterial WE and TAG biosynthetic enzymes because all sequenced TAG accumulating strains have homologous genes (Waltermann and Steinbuchel, 2005). The *M. tuberculosis* homologues identified by Daniel et al (2004) are discussed in Chapter 3.

Like PHB, studies of TAG accumulation in bacteria have centred on their application in industrial biosynthesis of lipids (Alvarez and Steinbuchel, 2002); however, the demonstration of TAG accumulation in mycobacteria has attracted the attention of medical researchers. These mycobacterial LBs are discussed below.

1.2.6 Lipid Bodies in Mycobacteria

Although there have been numerous reports of the occurrence of lipid inclusions in mycobacteria the composition of the lipids stored in these bodies remained unknown until recently. The nomenclature of these reported structures has not previously been standardised, however, due to their homology with TAG eukaryotic lipid bodies these structures will now be referred to as Lipid Bodies (LB).

LBs were first reported in mycobacteria by Burdon (1946) by a Sudan black lipid staining method. Further light and electron microscopy studies have demonstrated the presence of these structures in a number of mycobacterial species including, *M. avium* (Knaysi et al., 1950), *M. leprae* (Brieger and Glauert, 1956), *M. kansasii* (Schaefer and Lewis, 1965), *M. smegmatis* (Weir et al., 1972) and *M. tuberculosis* (Barksdale and Kim, 1977). However, these studies were mostly centred on the morphology of these bodies.

Schaefer and Lewis demonstrated that uptake of oleic acid or its ester Tween resulted in the rapid accumulation of LBs and increase in optical density in cultures of *M. kansasii* but the chemical composition of these structures was not elucidated (Schaefer and Lewis, 1965). Two similar studies have provided evidence to suggest that these structures are composed of TAG. Weir et al. (1972) and Garton et al. (2002) have independently demonstrated that the uptake of oleic acid coincides with TAG accumulation and LB formation in *M. smegmatis*. Thin Layer Chromatic (TLC) separation of the non-polar lipid extracts of cells with a high LB content revealed the presence of a lipid component whose mobility was consistent with that of TAG (Garton et al., 2002). Furthermore, TAG was absent in lipid extracts of cells grown in media low in carbon, which had a low LB content. The large amounts of acylglycerols reported to be produced by mycobacteria (Minnikin, 1982) had previously been attributed to the cell envelope (Daffe and Draper, 1998). The identity of these extracted lipids was confirmed by Gas Chromotography Mass Spectrometry (GC-MS) to be TAG (Garton et al., 2002). Concordant with reports

for other TAG accumulating bacteria, *M. smegmatis* formed LBs and TAG in media with low nitrogen content (Garton et al., 2002).

As LBs appeared to be formed under conditions of low nitrogen and utilised during periods of low carbon availability, it has been suggested that LBs act as carbon storage structures. Interestingly, GC analysis of Fatty Acid Methyl Esters (FAME) revealed that the fatty acid profile of TAG from oleic acid supplemented cells, which had previously been subjected to conditions of low carbon, was dominated by oleate but some shorter fatty acids were also present. The oleate had presumably been recently taken up by the cell, while the shorter chains were probably the result of β-oxidation of fatty acids present in the cell prior to low carbon treatment, demonstrating an ability of *M. smegmatis* to metabolise fatty acids in lieu of an available extracellular carbon source (Garton et al., 2002).

McCarthy (1971) has previously suggested that TAG may form to detoxify fatty acids. This hypothesis is supported by the evidence that oleic acid was rapidly and directly incorporated into TAG in *M. smegmatis*, without modification of the chain length (Weir et al., 1972, Garton et al., 2002). Indeed, the cells appeared to actively take up fatty acid, as metabolic inhibition by sodium azide reduced the incorporation of oleate into TAG and phospholipids (Weir et al., 1972) and LB accumulation (Garton et al., 2002). LB accumulation was also inhibited by sodium azide in *M. kansasii* (Schaefer and Lewis, 1965). The proposed pathway for the formation of TAG and the function of LBs in mycobacteria will be discussed further in Chapter 3.

Interestingly, there is some preliminary evidence from work carried out in our laboratory to suggest that LBs in *M. smegmatis* may contribute to survival during antibiotic treatment. However, the role of the LB in survival during antibiotic treatment remains unknown and this issue is addressed in Chapter 6.

Garton et al. (2002) were unable to demonstrate LB formation in *M. tuberculosis in vitro*; however, strikingly LBs were present in acid-fast bacteria (AFB) in human sputum. This

exciting observation lead the authors to suggest that *M. tuberculosis* in sputum may be in a physiological state that is distinct from that of cells grown in culture (Garton et al., 2002). As discussed in relation to fatty acid metabolism above, fatty acids are readily available in the host environment and evidence suggests that lipids are utilised for growth *in vivo* (Garton et al., 2002). These lipids may be stored in a LB structure until they are required for use (Garton et al., 2002).

1.3 Tuberculosis

1.3.1 The origins of *Mycobacterium tuberculosis*

M. tuberculosis is an obligate pathogen (Wayne and Kubica, 1986) and the causative agent of tuberculosis, a disease that has plagued the human race for thousands of years (Tufariello et al., 2003). Isolation of *M. tuberculosis* was first reported by Robert Koch in 1882 and despite continued research into chemotherapy to treat the disease and the development of preventative vaccines, the organism remains a major public health problem (Tufariello et al., 2003).

Before the genome sequence of *M. tuberculosis* was available it was widely believed that the organism evolved from *M. bovis* by specific adaptation of an animal pathogen to the human host as a consequence of the domestication of cattle (Brosch et al., 2002). However, studies of the distribution of a series of genetic deletions (regions of difference, RD) among closely related mycobacteria revealed that this was not the case. *M. tuberculosis* has the fewest deletions and is therefore the most ancestral of the *M. tuberculosis* complex (Brosch et al., 2002, Cosma et al., 2003). *M. bovis* actually has the most deleted regions, indicating that it is the most recently evolved member of the complex. A deletion in RD9 marks the evolutionary divergence of the lineage in which successive deletions have resulted in the evolution of *M. bovis*, with *M. africanum* and *M. microti* as evolutionary intermediates. Furthermore, an *M. tuberculosis* specific deletion, TbD1, marks the evolution of modern strains, such as Beijing, Haarlem and East African from the ancestral strain of *M. tuberculosis* (Brosch et al., 2002).

Until recently, the genome of *M. tuberculosis* was thought to be extremely stable because single polymorphisms in coding regions appeared to be rare events and, therefore, genetic diversity was not considered to be a factor in differences in disease presentation (Sreevatsan et al., 1997, Cosma et al., 2003). However, comparison of the genome of the laboratory strain of *M. tuberculosis*, H37Rv, with the recent clinical isolate, CDC1551,

demonstrated that there were 74 large sequence polymorphisms (LSP; insertions or deletions unique to one strain or relative to another) and over 1000 single nucleotide polymorphisms (Cosma et al., 2003, Fleischmann et al., 2002). In a study examining the occurrence of 17 LSPs in clinical isolates it was shown that there is considerable variation between strains (Cosma et al., 2003, Fleischmann et al., 2002). Microarray and Polymerase Chain Reaction (PCR) analysis of the index isolate, strain CH, of a local tuberculosis outbreak in a Leicester school detected five genomic deletions when compared to *M. tuberculosis* H37Rv (Rajakumar et al., 2004). Therefore, there appears to be extensive genetic heterogeneity among clinical strains (Cosma et al., 2003).

1.3.2 Epidemiology of tuberculosis

Tuberculosis is the leading cause of death from a curable infectious disease due to a single agent (Dye, 2006). It has been estimated through surveys with purified protein derivative (PPD) or tuberculin skin tests that one third of the world's population is infected with *M. tuberculosis* (Dye et al., 1999, Tufariello et al., 2003). Primary infection results in active disease in only approximately 10% of individuals who have been infected, while the remaining 90% become latently infected. In latency the immune system apparently contains the disease and the individual displays no symptoms and remains non-infectious (Tufariello et al., 2003). Many latently infected individuals will never develop disease; however, a disruption of the immune response can cause reactivation tuberculosis. This may include infection by Human Immunodeficiency Virus (HIV), malnutrition or the use of immunosuppressive drugs (Frieden et al., 2003). The estimated lifetime risk of developing reactivation disease is between 2-23% (Tufariello et al., 2003).

There were an estimated 9.2 million new cases of tuberculosis reported in 2006 and 44% of these cases were smear positive, the most infectious form of the disease (Dye et al., 2008). Africa has the highest incidence rate per capita (363 per 100 000 population every year), however, the majority of infected individuals live in the most populous countries of

Asia. India, China and Indonesia are the top three countries in terms of absolute numbers of cases (Dye, 2006, Dye et al., 2008).

The incidence of tuberculosis appears to be growing steadily globally, however, the number of reported cases have decreased in South East Asia, the Western Pacific regions, central Europe, Latin America and the Eastern Mediterranean regions. The global increase seems to be almost entirely attributable to the continued increase in Africa (Dye, 2006). The increase in incidence in Africa is attributed to the high prevalence of HIV, as HIV is the most significant risk factor for reactivation of disease (Corbett et al., 2003). The deadly synergy seen in HIV and *M. tuberculosis* co-infection will be discussed separately.

Currently there are no adequate preventive measures available that may curb the current global increase of tuberculosis. Although the live attenuated *M. bovis* BCG vaccine protects against the development of severe disease in childhood, it does not protect against infection (Russell, 2001). However, even if an effective vaccine was developed, it would not prevent the millions of reactivation cases anticipated to arise from the vast numbers of latently infected individuals. The available chemotherapy is relatively ineffective against latent tuberculosis, therefore, treatment of the latent disease state should be the focus of new research (Parrish et al., 1998).

1.3.3 *M. tuberculosis* and HIV Co-Infection

In 2006, 8% of individuals newly infected with *M. tuberculosis* and an estimated 12% of all deaths caused by tuberculosis were among people infected with HIV (Dye et al., 2008). In fact, one third of the 40 million people infected with HIV/AIDS (Aquired Immuno-Deficiency Syndrome) are co-infected with *M. tuberculosis* and the risk of developing disease in these individuals can be as high as 10% per year (Gandhi et al., 2006, Tufariello et al., 2003). Mortality rates in co-infected individuals are exacerbated by the lack of availability of antiretroviral therapy (ART) to treat HIV. However, the

number of HIV positive tuberculosis patients enrolled on ART in 2006 was more than double that reported in 2005 (Dye et al., 2008, Gandhi et al., 2006). Despite this, the number of TB patients tested for HIV and subsequently enrolled on ART was below the targets set in the World Health Organisation Global Plan for 2006 (Dye et al., 2008). Compliance with anti-TB therapy in South Africa, where HIV is endemic, is poor and the national treatment success rate has been reported to be only 67%, which is significantly below the WHO target of 85%. This poor compliance increases the likelihood of relapse in tuberculosis and the development of drug resistance. Therefore, provision of ART and improvement of tuberculosis programmes are both required if the global burden of tuberculosis is to be reduced (Gandhi et al., 2006).

1.3.4 Multidrug-resistant tuberculosis (MDR-TB)

Multidrug resistant tuberculosis (MDR-TB) is defined as tuberculosis due to bacteria with resistance to both Rifampicin and Isoniazid, with or without resistance to other anti-TB drugs (Ormerod, 2005). In addition to the HIV epidemic, the global burden of tuberculosis has been compounded by the emergence of MDR-TB (Abdel Aziz, Wright, et al 2006). Although globally MDR-TB is not a problem of the same magnitude as that of drug-susceptible tuberculosis, MDR-TB is at critical levels in high prevalence "hotspots" such as Eastern European Countries, Russia and China (Espinal, 2003). MDR-TB is a particular problem because treatment is complex and toxic, more expensive and less successful than conventional treatment of non-resistant strains (Aziz et al., 2006). Loss of response to the frontline bactericidal and sterilizing drugs, Isoniazid and Rifampicin respectively, also results in the patient remaining infectious for a longer period of time (Ormerod, 2005).

MDR-TB is a man-made problem; the countries with the highest prevalence are those which have had a history of poor tuberculosis control. Future control of MDR-TB and prevention of the emergence of new resistant strains relies on the implementation of treatment for the full time course, prevention of transmission and careful introduction of

second line drugs (Espinal, 2003). However, resistance to second line treatment has been reported in extensively drug-resistant strains of tuberculosis (XDR-TB). XDR-TB is defined as the resistance to at least Isoniazid, Rifampicin, fluoroquinolones and either aminoglycosides or capreomycin, or both (Gandhi et al., 2006). Unfortunately, with the currently available drugs, XDR-TB patients are left with very few treatment options. The emergence of drug resistant strains of *M. tuberculosis* places even more need for the development of new drugs (Gandhi et al., 2006).

1.3.5 Clinical Disease

The most common clinical presentation of tuberculosis is pulmonary disease, resulting from primary progression at initial infection or reactivation of latent infection. However tuberculosis may affect any organ of the body as extrapulmonary disease, although this is more common in immunocompromised patients (Frieden et al., 2003). The most common symptom of pulmonary tuberculosis is a persistent cough. The cough may not initially be productive but as the disease progresses and tissue necrosis occurs, sputum is usually produced (Hopewell, 1994). Patients may also cough up blood due to erosion of the bronchial circulation (Hopewell, 1994, Quast and Browning, 2006). In addition, patients may also experience night sweats, weight loss, fever, general malaise, chest pain and shortness of breath; although none of these symptoms is specific to tuberculosis (Frieden et al., 2003, Hopewell, 1994, Quast and Browning, 2006).

Extrapulmonary tuberculosis is due to dissemination of the bacilli via the bloodstream in the early stages of infection (Brandli, 1998). Disseminated or noculat tuberculosis is common in infected HIV positive individuals because it reflects an inability of the immune system to contain the infection (Hopewell, 1994). Failure of immune containment may occur following primary or reactivation infection and result in the proliferation and dissemination of the bacilli throughout the body (Frieden et al., 2003). Miliary TB almost always involves the lungs but multi-organ involvement is also common. Granuloma formation may not be observed due to an inadequate immune

response and in its place is a diffuse pattern of lymphocytic infiltration and edema (Hopewell, 1994). Due to the multisystem involvement, noculat TB is associated with a spectrum of non-specific symptoms including fever, weight loss, anorexia, weakness and wasting (Hopewell, 1994). Prior to the HIV pandemic, lymphatic tuberculosis was the most common form of extrapulomonary tuberculosis, particularly in women and children (Frieden et al., 2003, Hopewell, 1994). This form of the disease usually occurs as painless swelling of one or more lymph nodes (Hopewell, 1994). Other clinical manifestations of tuberculosis include genitourinary tuberculosis, which is caused by the spread of bacteria to the kidney in the initial stages of infection (Hopewell, 1994). Symptoms can include those that are usually associated with urinary infections, such as frequent urination and flank pain, making it difficult to distinguish from other infections. However, many patients are asymptomatic (Frieden et al., 2003, Hopewell, 1994). Skeletal tuberculosis is usually found in older patients. It can affect any bone or joint but it is most commonly associated with the spine (Frieden et al., 2003). Meningeal tuberculosis is the most serious clinical manifestation and usually affects children and HIV positive individuals (Brandli, 1998, Frieden et al., 2003). Tuberculous meningitis involves inflammation of the meninges and lesions in the brain and is frequently associated with disseminated tuberculosis (Frieden et al., 2003, Hopewell, 1994). Symptoms include headache, fever, changed mental status and depending on the positions of the lesions, seizures and motor and sensory defects. Prompt diagnosis is critical as without treatment, meningitis is fatal (Brandli, 1998, Frieden et al., 2003, Hopewell, 1994).

The tests used to diagnose tuberculosis vary according to the setting (Frieden et al., 2003). In developed countries, following a physical examination, a radiographic examination of the chest is carried out (Hopewell, 1994). Pulmonary tuberculosis nearly always causes abnormalities on radiographs and this is the single best predictor of disease (Brandli, 1998, Hopewell, 1994). Primary tuberculosis presents with hilar enlargement and lower or middle lung zone infiltrate and cavities are seen in progressive disease. Reactivation disease typically presents with infiltrates in the upper lung zones, with or without cavitation (Brandli, 1998, Hopewell, 1994). Active disease is confirmed by detection of acid fast bacilli in the sputum and subsequent isolation of the bacteria by

culture (Frieden et al., 2003, Hopewell, 1994). In countries where tuberculosis is prevalent, a positive sputum smear is due to the presence of *M. tuberculosis* in 95% of patients and routine culture is only used where it is practical and affordable (Frieden et al., 2003). In order to culture and isolate the causative organism, sputum must be concentrated and decontaminated and culture is usually carried out on solid and in liquid media. Colony formation on solid media is used to detect mixed populations of bacteria and allow colony morphology to be examined (Frieden et al., 2003). In developed countries, liquid culture is commonly carried out in an automated system (Maartens and Wilkinson, 2007). Rapid detection of *M. tuberculosis* in sputum is achieved by PCR amplification assays of DNA, while DNA fingerprinting techniques may be used to elucidate the epidemiology of a particular strain, particularly during an outbreak (Frieden et al., 2003). Immunological tests are also used to detect tuberculosis. These are based on the detection of released interferon-γ by T-cells in response to the secreted antigens ESAT-6 or culture filtrate protein-10, which are specific to the *M. tuberculosis* complex (Maartens and Wilkinson, 2007).

1.3.6 Pathogenesis and Transmission

The disease states observed during the course of tuberculosis infection are products of both the host and the organism (Honer zu Bentrup and Russell, 2001); the course of disease is shown in Figure 4. *M. tuberculosis* is predominantly transmitted through the inhalation of aerosolised bacteria-containing droplet nuclei of 1-5μm that are taken up by alveolar macrophages in the lung (du Toit et al., 2006, Young and Duncan, 1995). It appears that in the majority of cases, the phagocytosed bacteria are killed by the bactericidal activities of the activated macrophage; these include the release of Reactive Oxygen or Nitrogen Intermediates (ROI and RNI, respectively), lysosomal enzymes and a decrease in pH (Parrish et al., 1998, Smith et al., 2003). However, *M. tuberculosis* possesses specific survival strategies (discussed later) to avoid or resist killing by these bactericidal mechanisms (Young and Duncan, 1995). Surviving bacteria undergo a period of replication in the macrophage and then infect adjacent naïve host cells in the absence

of a specific immune response (Honer zu Bentrup and Russell, 2001, Young and Duncan, 1995). Infected macrophages then spread via the lymphatic system to the hilar lymph nodes (Frieden et al., 2003). The macrophage plays a contradictory role as it is the primary host cell in the defence against infection and yet it provides a key site for bacterial replication and mediates dissemination (Cosma et al., 2003). Macrophage – *M. tuberculosis* interactions will be discussed at length in an ensuing section.

When the host immune response cannot contain this initial replication active disease occurs. This is most common in children under five years old or adults with immunosuppression (Frieden et al., 2003). In the majority of immunocompetent individuals, the immune response contains the infection by the formation of a calcified lesion at the primary site of infection. Infected macrophages induce a localised proinflammatory response by the release of chemokines and Tumour Necrosis Factor (TNF) and this leads to the recruitment of monocytes, lymphocytes and neutrophils to the focal site of infection (Cosma et al., 2003, Russell, 2007, Smith et al., 2003). Natural Killer T cells are the first lymphocytes to be recruited to the site of infection, followed by $CD4^+$ and $CD8^+$ T cells (Russell, 2007). $CD8^+$ cells are able to lyse infected cells and $CD4^+$ cells produce interferon-γ which activates macrophages (Tufariello et al., 2003). In addition, these T-cells then release their own complement of chemokines and cytokines, which amplifies cellular recruitment (Russell, 2007). Release of interferon-γ by these lymphocytes also down regulates this proinflammatory cascade and thereby centralises the response to the centre of infection (Russell, 2007, Tufariello et al., 2003). These cells form the basis of the granuloma around the foci of infection and represent the means by which the immune system limits the dissemination of infection (Honer zu Bentrup and Russell, 2001). However, granuloma formation also benefits the pathogen because the T cells that are capable of activating macrophages are restricted to the periphery of these structures (Honer zu Bentrup and Russell, 2001). The granuloma consists of infected macrophages surrounded by foamy macrophages (macrophages loaded with lipid droplets) and mononuclear phagocytes. These are enclosed by lymphocytes, in association with a fibrous layer of collagen and other extracellular matrix components

which forms the boundary of the structure (Honer zu Bentrup and Russell, 2001, Russell, 2001, Russell, 2007).

The granuloma structure matures and develops a fibrous sheath. The number of blood vessels penetrating the structure diminishes and the centre of the lesion becomes necrotic (Russell, 2007). Mycobacteria are thought to be located in macrophages and the necrotic centres of granulomas. It is within these legions that bacilli in an unknown physiological state are thought to reside during latent infection (Russell, 2007). Histological studies indicate that these granulomas are hypoxic, a characteristic that has formed the basis for *in vitro* studies of bacterial dormancy during latent infection (discussed later) (Russell, 2007). This is a simplistic explanation of host pathology, as there is a great deal of heterogeneity in granuloma structure present in a single host; these can be at various stages of evolution (Cosma et al., 2003, Russell, 2007).

The granuloma structure maintains the "containment" phase of disease during which there are no signs of disease and the infected patient displays a delayed type hypersensitivity response to mycobacterial antigens (Russell, 2007, Tufariello et al., 2003). Many patients will remain latently infected with *M. tuberculosis* for the rest of their life with no clinical presentation of disease. However, a change in immune status of the host, such as old age, malnutrition or HIV infection, may lead to reactivation disease. If the numbers of $CD4^+$ cells become depleted, fewer macrophages are activated and the granuloma is less able to control infection (Tufariello et al., 2003), whereupon the granuloma decays into a structural mass of cellular debris (a process called caseation) and bacteria replicate uncontrollably (Russell, 2007). The granuloma walls break down to form a cavity; releasing viable bacilli into the airways and ultimately resulting in transmission (Russell, 2001, Russell, 2007).

The mechanism by which *M. tuberculosis* cells exit from their proposed dormant state in latency is not known for certain. However, an apparently unrelated study on *Micrococcus luteus* has shed light on the process. *M. luteus* enters a dormant state on prolonged storage in stationary phase. It has been demonstrated that these dormant cells could be stimulated

to re-establish growth by exposure of these cells to non-dormant *M. luteus* (Votyakova et al., 1994). This was shown to be due to the secretion of a protein called resuscitation promoting factor (Rpf) (Mukamolova et al., 1998, Mukamolova et al., 1999). *M. tuberculosis* has 5 *rpf* homologues and mycobacterial Rpfs have been shown to promote the growth of *M. luteus* and *M. bovis* (Mukamolova et al., 2002). Inactivation of individual *rpf* genes had no affect on resuscitation or growth (Downing et al., 2004); however, inactivation of three genes generated mutants that could not resuscitate in culture and that were attenuated in murine infection (Downing et al., 2004). Most recently, Kana et al. have demonstrated that deletion of all 5 Rpf genes from *M. tuberculosis* also results in failure of resuscitation *in vitro* and the mutant strain showed a defect in long term survival in mice (Kana et al., 2008). The Rpf proteins of *M. tuberculosis* appear to act together to promote resuscitation and the observations described above reinforce the view that some form of bacterial dormancy is involved in tuberculosis.

A recent study has demonstrated that the mycobacterial RpfB interacts with a peptidoglycan hydrolase and this complex localises to the septum of dividing bacteria (Hett et al., 2007). Peptidoglycan hydrolases are involved in the final stages of cell division, in which the peptidoglycan layer connecting the daughter cells is cleaved. Further to this, Hett and colleagues have also demonstrated that deletion of the peptidoglycan hydrolase gene *ripA* in *M. smegmatis* resulted in a decrease in growth and the formation of filamentous chains of cells. Therefore it has been suggested that Rpf may be involved in the regulation of the late stages of cell division, perhaps in withdrawal from a dormant or non-growing state (Hett et al., 2008).

Figure 4: Outcomes associated with exposure to *M. tuberculosis*

Uptake of *M. tuberculosis* by macrophages usually results in the elimination of the bacilli by the immune system. However, failure to eliminate the infection results in the multiplication of bacteria in the infected macrophages. In immunocompetent individuals, an immune response is elicited and the site of infection is contained in a granuloma structure. This results in an asymptomatic disease state called latent infection. Latent disease may last a lifetime or reactivation disease may occur. If the immune system is incapable of containing the infection, primary active disease develops in the lungs or in other organ systems if the bacilli are disseminated via the bloodstream. Figure adapted from Parrish et al. (1998).

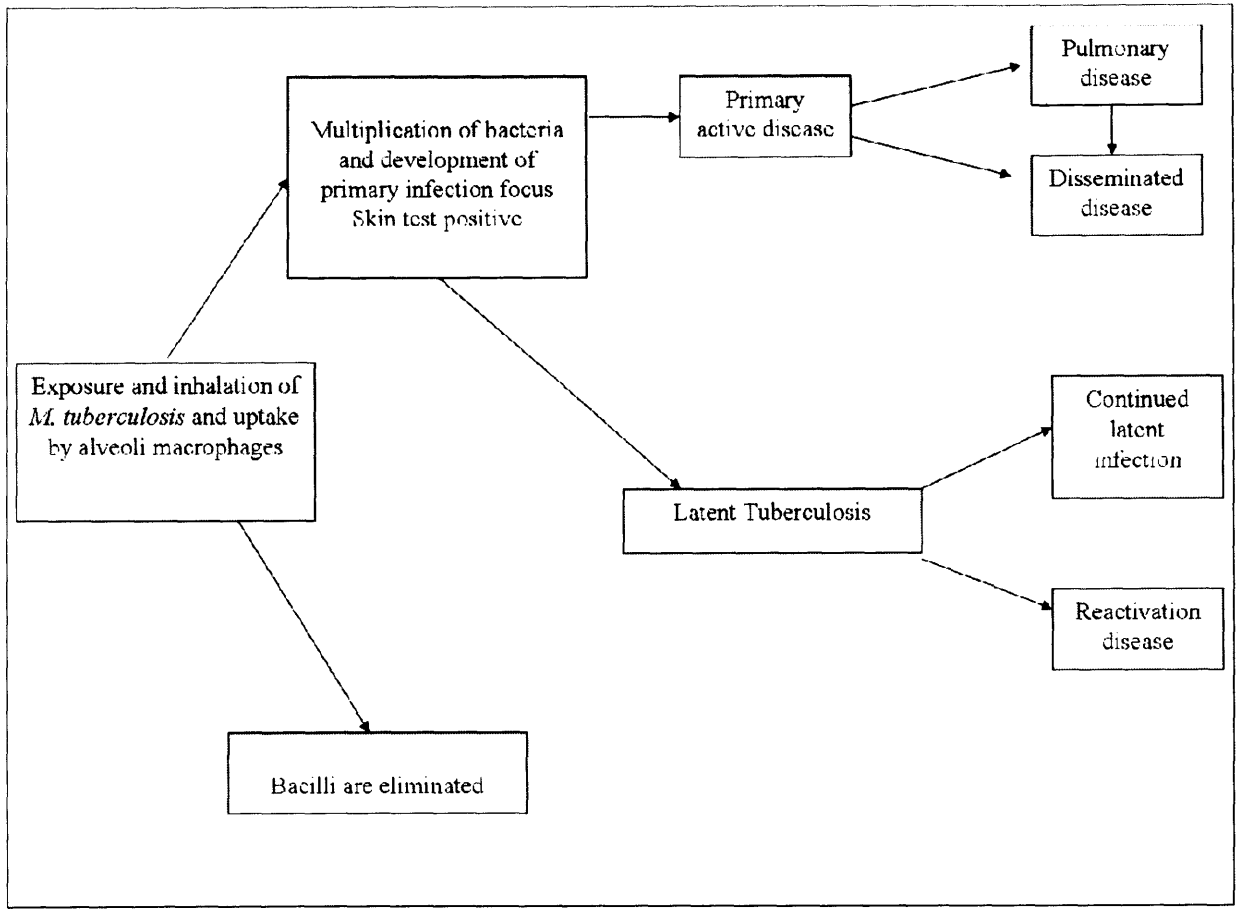

1.3.7 Modulation of the Immune response: *M. tuberculosis* and the macrophage

The macrophage is thought to be the principle location within which pathogenic mycobacteria are able to survive and replicate (Cosma et al., 2003). The immune response plays a central role in regulating this intracellular environment, particularly the activation status of the macrophage. *M. tuberculosis* has adapted strategies to survive in the category macrophage through mechanisms that result in the modulation of the host cell function and prevent macrophage activation by arresting the development of a localised immune response (Russell, 2007). Activation allows the macrophage to overcome survival strategies set in place by *M. tuberculosis*; however, the pathogen has evolved further mechanisms to enable its evasion of the arsenal of antimycobacterial products released by the macrophage (Tufariello et al., 2003).

M. tuberculosis is able to enter the macrophage through a number of different receptors. However, the specificity of the receptor does not appear to be a determining factor in the survival of phagocytosed mycobacteria, as has been shown to be the case for the intracellular pathogens *Leishmania* and *Toxoplasma* (Cosma et al., 2003, Russell, 2007). *M. tuberculosis* cells are engulfed by the macrophage within a phagosome, a membrane bound cytoplasmic vacuole (Amer and Swanson, 2002). The normal maturation process of the phagosome into a digestive, bactericidal organelle involves progressive acidification, accumulation of hydrolytic enzymes and fusion with lysosomal compartments (Amer and Swanson, 2002, Honer zu Bentrup and Russell, 2001). *M. tuberculosis* is able to arrest the maturation of the phagosome and prevent its fusion with lysosomal compartments, thereby maintaining the pH at 6.4 (Cosma et al., 2003, Russell, 2007, Russell et al., 2002). Acidification of the phagosome is achieved through the action of vacuolar ATPases, which are macrophage enzymes that use ATP as an energy source to pump protons into intracellular compartments (Russell, 2001). The limited acidification of the *M. tuberculosis* phagosome has been associated with a reduced level of these enzymes in the vacuole (Cosma et al., 2003, Russell, 2001). While *M. tuberculosis* phagosomes do not fuse with the lysosome they remain fully capable of

fusing with other vesicles, such as early endosomes, facilitating access to nutrients internalised by the host (Cosma et al., 2003, Russell, 2001, Russell et al., 2002, Tufariello et al., 2003).

Investigations regarding the mechanism by which mycobacteria arrest the maturation of the phagosome have largely centred on the identification of host proteins involved in the regulation of intracellular vesicle trafficking and membrane fusion events. Specific membrane fusion is mediated by soluble-*N*-ethylmaleimide-sensitive factor attachment protein receptors (SNAREs, membrane anchored proteins) and GTPases of the Rab family (Mueller and Pieters, 2006, Russell et al., 2002, Tufariello et al., 2003). Rab5 is associated with early endosome fusion and is recruited to newly formed phagosomes (Russell, 2001). Rab5 then recruits the early endosomal antigen 1 (EEA1) that in turn associates with the cytoplasmic face of early endosomes. As EEA1 has two Rab5 binding sites, it has been suggested that it may tether two Rab5 containing membranes (Mueller and Pieters, 2006). EEA1 interacts with syntaxin 13 (a SNARE), leading to membrane fusion and therefore provides a functional link between Rabs and SNARES (Mueller and Pieters, 2006). Rab5 and EEA1 become dissociated from the phagosome as it matures and are replaced by Rab7, a GTPase involved in the fusion of late endosomes and lysosomes, through an unknown mechanism (Sundaramurthy and Pieters, 2007). *M. tuberculosis* subverts this mechanism by retaining Rab5 and releasing EEA1 from the phagosome upon mycobacterial infection. How this is regulated by *M. tuberculosis* remains unclear (Mueller and Pieters, 2006). Phagosomes containing *M. bovis* BCG have been shown to retain Rab5 and remain excluded from the late endosomal compartment, while allowing sustained fusion with early endosomal vesicles (Russell, 2001 Tufariello, 2003 #185).

Another host protein that has been associated with vacuole regulation is the tryptophan aspartate rich coat protein (TACO), which is also known as mouse coronin I. TACO remains associated with the phagosome of viable BCG but is only retained by phagosomes containing live bacteria. TACO rapidly dissociates from phagosomes containing dead bacteria, allowing fusion with lysosomes (Russell, 2001 and Nguyen and

Pieters, 2005). It is thought that TACO forms a protective scaffold around the phagosome, thereby preventing its fusion with the lysosome. However, its exact role in phagosome-lysosome fusion and how this is regulated remains to be established (Mueller and Pieters, 2006).

In addition to host proteins, the mycobacterial cell wall lipopolysaccharide, LAM, has been implicated in the modulation of lysosome fusion. Phagocytosed latex beads coated with mannose capped LAM were shown to recruit less syntaxin 6 (a SNARE involved in trans-Golgi network to phagosome trafficking) and accumulate less lysosomal enzyme precursors than control beads. This suggests that mannose capped LAM obstructs the phagosomal acquisition of lysosomal hydrolases from the trans Golgi network and may account for the diminished accumulation of lysosome markers in mycobacterial phagosomes (Tufariello et al., 2003).

M. tuberculosis is also able to modulate the adaptive immune response by subverting the MHC class II presentation pathway (Tufariello et al., 2003). Antigen presentation allows the infected cell to signal the presence of the pathogen through the display of pathogen derived molecules by histocompatibility antigens, MHC refers to murine antigen presentation and HLA to human. Class I histocompatibility antigens display peptides derived from the cytosol of the infected cell and Class II present peptides present in the endosomal-lysomal vacuoles, where *M. tuberculosis* resides. The Class II molecule is transported to the cell surface where it is presented for detection by the T-cell receptor on specific T cells (Russell, 2001). The ability of *M. tuberculosis* to avoid this response is likely to aid the survival and persistence of *M. tuberculosis* in the macrophage as MHC class II processing and presentation is required for the priming of $CD4^+$ cells (Tufariello et al., 2003). As discussed, $CD4^+$ cells release the macrophage activating molecule interferon-γ and are an important part of the protective immune response (see Pathogenesis section). The mycobacterial vacuole has been shown to contain MHC Class II molecules, however, these molecules are surface derived and already loaded with peptides and are therefore limited in their ability to sample new antigens (Russell et al., 2002). Although, there is only a partial suppression of surface presentation, a 50-70%

reduction, this does appear to generate a discernible reduction in T-cell stimulation (Russell et al., 2002). However, infection of activated macrophages results in the phagosomal recruitment of MHC Class II and its chaperone, which acts by removing peptides blocking the process of antigen loading. These cells are then competent in inducing the T-cell response (Russell et al., 2002).

The mechanism by which *M. tuberculosis* brings about the suppression of macrophage expression of MHC Class II molecules is not fully understood. However, a number of mycobacterial cellular components have been involved in the process. Studies have indicated that mannose capped LAM, a 25 kDa glycolipid and a 19 kDa lipoprotein actively contribute to the inhibition of MHC Class II expression in infected macrophages (Tufariello et al., 2003). In addition, mycobacterial cell wall lipids released by the bacterium stimulate the infected macrophage to release proinflammatory cytokines, such as Inter Leukin 6 (IL6) and TNR that suppress T cell proliferation (Russell, 2001, Russell et al., 2002). This proinflammatory response recruits potential host cells to the granuloma, while T cells are kept at the periphery of the structure (see Pathogenesis section) (Russell, 2001, Russell et al., 2002). Although these mechanisms allow *M. tuberculosis* to minimise the effects of the immune response, such a response will eventually develop and *M. tuberculosis* has evolved alternative strategies to cope with this (Russell, 2001).

Mycobacterial mechanisms set in place to avoid phagosome–lysosome fusion are overcome by the macrophage when it becomes activated by the innate immune response. The macrophage is activated through the release of interferon-γ by stimulated T-cells or through the action of Toll-like receptors (TLRs) (Russell et al., 2002). TLRs are transmembrane proteins that recognise structural motifs in microbial products and are also important in triggering the host defence mechanisms (Russell et al., 2002). TLRs are expressed on the surface of a number of cells involved in the innate immune system, such as macrophages and dendritic cells (Sundaramurthy and Pieters, 2007). Gram negative bacteria are usually recognised through their production of LPS, by the TLR4 receptor, while mycobacteria predominately stimulate TLR2 (Russell et al., 2002). TLR2

recognises a range of mycobacterial cell wall components including, lipoglycan, LAM, PIM and the 19kDa lipoprotein, which are released by the bacilli in the macrophage (Sundaramurthy and Pieters, 2007). The macrophage responds to stimulation by TLRs by upregulating phagocytosis of bacteria, promotion of phagosome maturation and expression of cytokines. Macrophage activation also triggers the release of antimycobacterial products, such Nitric Oxide (NO) and the environment becomes hypoxic and acidic (Sundaramurthy and Pieters, 2007). Interestingly, histological studies of human granulomas have revealed that a significant number of bacteria were contained within macrophages that were localised to the peripheral leukocyte region. If *M. tuberculosis* persists in the activated macrophage during disease latency it must have evolved strategies to adapt to the harsh environment of the activated macrophage (Russell, 2007).

Studies examining the response of *M. tuberculosis* to conditions found in the macrophage and infection of macrophages *in vitro* have provided an insight into how this pathogen is able to alter its metabolism in order to adapt to these changing conditions. How *M. tuberculosis* avoids the toxic effects of reactive nitrogen species (RNI) has been of particular interest because production of these molecules appears to be essential for the containment of infection in murine models and *in vitro* studies of human cells (Tufariello et al., 2003). Alveolar macrophages obtained from healthy individuals produce RNI in response to *M. tuberculosis* infection and its production is associated with a constrained intracellular growth of the bacteria (Rich et al., 1997). In addition, growth of *M. bovis* BCG in human macrophages has been shown to be inhibited by the synthesis of RNI through the activity of Nitric Oxide Synthase 2 (NOS2) but this effect was reversed by treatment with a NOS2 inhibitor (Nozaki et al., 1997) (see Chapter 6 for further discussion of the importance of NO in host defence).

However, *M. tuberculosis* must overcome the bactericidal or bacteriostatic effects of RNI, because immunocompetent human and mouse hosts are not able to completely eliminate the bacterium (Tufariello et al., 2003). Voskuil et al. (2003) have demonstrated that sub-lethal levels of NO can trigger reversible inhibition of aerobic respiration in *M.*

tuberculosis and this was associated with the expression of a set of genes known as "the dormancy regulon". This regulon will be discussed later in relation to other dormancy associated conditions. Global expression profiling has also allowed the identification of genes differentially expressed by *M. tuberculosis* in naïve, interferon-γ activated and NOS2 deficient murine macrophages. These were compared to log grown cultures and cultures exposed to various environmental stresses that *M. tuberculosis* may encounter in the macrophage (Schnappinger et al., 2003). There was overlap between the expression profile of the stressed cultures and that of the mycobacteria in the macrophage, suggesting that these stresses could account for some of the changes in intracellular gene expression (McKinney and Gomez, 2003, Schnappinger et al., 2003). The intracellular expression profile revealed the phagosomal environment to be hypoxic, carbohydrate poor and macro-molecule damaging. The induction of genes involved in β-oxidation of fatty acid and the glyoxylate shunt pathway (see Fatty Acid Metabolism) appears to demonstrate a shift in the diet of *M. tuberculosis* from carbohydrates to lipids *in vivo* (McKinney and Gomez, 2003, Schnappinger et al., 2003). Changes in the transcription profile also demonstrated that *M. tuberculosis* adapts to this environment by the induction of DNA repair proteins, the production of siderophores in order to scavenge iron, modification of cell wall components and induction of the dormancy regulon (Schnappinger et al., 2003). A further set of 68 genes were specifically induced by macrophage activation and these were shown to be dependent on the macrophage's ability to generate NO. This activation specific gene set suggested that the bacterium switched from aerobic to anaerobic respiration and uregulated the expression of the dormancy gene programme (McKinney and Gomez, 2003, Schnappinger et al., 2003). As induction of the dormancy regulon is linked to inhibition of aerobic respiration and cell division, this may characterise the presumed dormant state of the bacilli responsible for latent tuberculosis infection. This suggests that these bacteria may reside in the macrophage during infection. Studies aimed at elucidating the physiology of dormant bacilli will be discussed later in the chapter.

1.3.8 Treatment of Tuberculosis

1.3.8.1 Treatment regimen and DOTS

Streptomycin was the first antibiotic to be used in the treatment of tuberculosis; however, streptomycin monotherapy resulted in the emergence of bacterial resistance and treatment failure (McKinney et al., 2000, Mitchison, 2005). Prior to this, treatment mainly consisted of bed rest for the patient in a sanatorium (Mitchison, 2005). However, a number of attempts had been made to find effective chemotherapeutic agents, notably nicotinamide, of which the current drugs isoniazid and pyrazinamide are analogs (Mitchison, 2005, Zhang and Amzel, 2002). Isoniazid was the first of the modern anti-tuberculosis drugs to be introduced, in 1952 (Mitchison, 2005). One of the most important observations in the early drug development period was that monotherapy resulted in drug resistance (Zhang and Amzel, 2002). In fact, drugs were selected for their ability to prevent the emergence of isoniazid resistance when used in combination (Mitchison, 2005). Pyrazinamide was discovered in 1952 and rifampicin in 1967, both of which were shown to have high sterilizing activity. Ethambutol, while less cidal was also found to be an effective anti-tuberculosis drug (Mitchison, 2005). These four drugs, along with streptomycin are the first line drugs currently used to treat tuberculosis. These are taken daily for two months, followed by a continuation phase of treatment with isoniazid and rifampicin, taken three times a week for four months (Mitchison, 2005, Zhang and Amzel, 2002).

The introduction of these drugs made tuberculosis a curable disease for the first time and reduced its incidence in industrialised countries; an incredible achievement when considered that pulmonary tuberculosis previously resulted in a 50% mortality rate (Mitchison, 2005, Zhang and Amzel, 2002). This success prompted the much quoted Waksman, the pioneer of streptomycin, to proclaim that tuberculosis "is on the way to being reduced to a minor ailment of man...and the complete eradication of the disease is in sight" (Gomez and McKinney, 2004, McKinney, 2000, Zhang and Amzel, 2002). With

the benefit of hindsight this seems like an overly optimistic statement but given the fact that TB is a curable disease why does it remain as a major global health problem?

The answer to this question seems complex and due to a number of factors. However, a major obstacle in eradicating the disease can be related to the extended treatment time; it takes six months of treatment with multiple antibiotics to eliminate active tubercuosis (McKinney et al., 2000). The reasons for this will be discussed below. Extended chemotherapy is expensive and a particular problem for developing countries, where tuberculosis is most prevalent (McKinney et al., 2000). The other major problem associated with long term treatment is poor patient compliance, which frequently results in the development of drug resistant strains or a relapse in infection (Zhang and Amzel, 2002). One of the most common causes for non-compliance is the high incidence of side-effects and high number of tablets that the patient is required to consume (du Toit et al., 2006). In order to combat the problem of patient compliance the WHO introduced Directly Observed Therapy (DOTs) which requires every dose of chemotherapy administered to the patient to be supervised by a health or social worker (McKinney et al., 2000). DOTs is extremely effective, with a cure rate of 95%, but it is clearly expensive and difficult to implement and currently only 1 in 5 tuberculosis patients are supervised in this way (McKinney et al., 2000, Zhang and Amzel, 2002). Therefore, two strategies for reducing the global burden have been suggested. The first is to increase the number of cases to which DOTs can be applied and secondly, to develop drugs that reduce treatment time (McKinney et al., 2000).

The length of treatment time is not so much a result of the inefficacy of drug action but a reflection of the physiology of the bacteria they are used to eliminate *in vivo* (McKinney et al., 2000). It has been noted that drugs used to treat tuberculosis are effective in killing *in vitro* cultures of *M. tuberculosis* within a few days, while it takes six months to achieve the same result in treatment (McKinney et al., 2000). It was suggested that this was due to inefficient penetration of the drugs to the lesions and cavities of the lung. However, this was shown not to be the case when isoniazid, rifampicin and streptomycin were detected in adequate concentrations in lesions in resected lung tissue (Mitchison, 2005). It seems

that the reason behind the delayed drug activity *in vivo* is due to the presence of a number of physiologically heterogeneous populations of bacteria (McKinney, 2000). The actively growing population of bacteria are thought to be eradicated in the first two weeks of chemotherapy, due mainly to the actions of isoniazid, after which the patient is no longer infectious (Zhang and Amzel, 2002). The remainder of the treatment period is required to kill the residual population of slowly metabolising bacteria. Rifampicin is thought to eliminate dormant bacteria with "spurts" of metabolism, while pyrazinamide kills dormant bacilli, as it becomes more effective as bacterial metabolism slows down (Mitchison, 2004) (see discussion in Chapter 7). Therefore, new drug development should be directed at eliminating the persistent population of cells and this can only be achieved through understanding the physiology of *M. tuberculosis in vivo*. New advances in mycobacterial genetics have made it possible to examine this and identify processes that are important for the metabolism of *M. tuberculosis in vivo* that may serve as more relevant drug targets (McKinney, 2000). One example is ICL, which has been shown to be essential for *M. tuberculosis* during infection (see Fatty Acid Metabolism). ICL inhibitors have been shown to have antimycobacterial properties on bacteria grown on fatty acid (McKinney, 2000).

1.3.8.2 Modes of action of anti-tuberculosis drugs

Isoniazid

Isoniazid is a pro-drug that requires activation by the mycobacterial multifunctional catalase-peroxidase enzyme KatG (Somoskovi et al., 2001, Timmins and Deretic, 2006, Zhang and Amzel, 2002). KatG activates isoniazid by peroxidation resulting in the generation of a range of reactive oxygen species and reactive oxygen radicals that act on multiple targets in the mycobacterial cell, including DNA, carbohydrates and lipids (Timmins and Deretic, 2006, Zhang and Amzel, 2002). These reactive species are thought to either oxidise or acylate groups in the protein (Somoskovi et al., 2001). Cidal activity is likely to be due to the effect of isonazid on a combination of these targets (Zhang and Amzel, 2002). One of the major targets is the mycolic acid synthesis

pathway, including the enzymes InhA (enoyl acyl carrier protein reductase) and KasA (β-ketoacyl synthase) (Zhang and Amzel, 2002). A number of mutations have been described that give rise to isoniazid resistance due to its multiple targets. Mutations in the KatG gene are found in 42-58% of isoniazid-resistant mutants. A mutation in Ser315Thr occurs most frequently (Somoskovi et al., 2001). This results in the formation of the enzyme that retains 50% of its catalase-peroxidase activity but loses its ability to activate isoniazid (Somoskovi et al., 2001). This enables the organism to maintain detoxifying activity against host generated radicals (Somoskovi et al., 2001). Other mutations in *katG* have been shown to confer varying degrees of resistance to isoniazid. Mutations have been found in the promoter regions of and, less commonly, in the genes that encode InhA and KasA (Somoskovi et al., 2001). It has also been suggested that overexpression of isoniazid target proteins may also result in resistance (Somoskovi et al., 2001).

Rifampicin

Rifampicin inhibits RNA synthesis by binding to the bacterial DNA-dependent RNA polymerase β-subunit. Monoresistance to rifampicin is rare and rifampicin resitance usually occurs in strains that are also resistant to isoniazid. This is due to the highly specific nature of rifampicin resistant mutations (Somoskovi et al., 2001). More than 90% of resistant strains contain a mutation in a well-defined 81 base pair region of the gene that encodes the RNA polymerase β-subunit. The most common mutations alter codon 526 or codon 531, resulting in high-level resistance to rifampicin (Somoskovi et al., 2001). Mutations in codons 511, 516, 518 and 522 result in low-level resistance and mutations have also been found in the amino-terminal region of RNA polymerase β-subunit, although this is a rare occurrence (Somoskovi et al., 2001).

Pyrazinamide

In common with isoniazid, pyrazinamide is a pro-drug analog of nicotinamide that is thought to target FAS I (Somoskovi et al., 2001, Zhang and Amzel, 2002). Pyrazinamide is converted to its active form, pyrazinoic acid by the mycobacterial enzyme, pyrazinamidase (Somoskovi et al., 2001, Zhang and Amzel, 2002). Pyrazinamide requires an acidic extracellular environment in which to act, in order to facilitate the formation of

uncharged protonated pyrazinoic acid (Zhang and Amzel, 2002). Pyrazinamide passively diffuses into the mycobacterial cell where it is converted into its active form (Somoskovi et al., 2001). Pyrazinoic acid is able to accumulate in the cell due to an inefficient efflux pump mechanism; this activity is decreased in inactive cells and therefore the drug is particularly effectively against non-metabolising bacteria (Mitchison, 2005, Zhang and Amzel, 2002). Proton accumulation results in lowering of the intracellular pH and thereby inhibits vital enzymes, such as FAS I (Somoskovi et al., 2001). Pyrazinoic acid could also de-energize the membrane by collapsing the proton motive force (Zhang and Amzel, 2002). Resistance to pyrazinamide is usually through a mutation in the promoter region or gene encoding pyrazinamidase. A number of mutations have been described that affect the uptake of pyrazinamide or efflux of pyrazinoic acid (Somoskovi et al., 2001).

Ethambutol

Ethambutol acts on the biosynthesis of arabinogalactan. It inhibits arabinosyl transferase, an enzyme involved in the polymerisation of arabinan of arabinogalactan and of lipoarabinomannon and induces the accumulation of β-D-arabinofuranosyl-P-decaprenol, an intermediate in arabinan biosynthesis (du Toit et al., 2006, Zhang and Amzel, 2002). Ethambutol is generally bacteriostatic but can be bacteriocidal at high doses (du Toit et al., 2006, Zhang and Amzel, 2002).

Streptomycin

Streptomycin is an aminoglycoside; these drugs are irreversible inhibitors of protein synthesis. Streptomycin inhibits initiation of mRNA translation and promotes DNA misreading and inefficient proofreading by the ribosome (du Toit et al., 2006, Zhang and Amzel, 2002). The site of streptomycin action is the small 30S subunit of the ribosome, where it specifically binds to the ribosomal protein S12 and the 16S rRNA (du Toit et al., 2006, Zhang and Amzel, 2002).

1.3.9 Latent tuberculosis infection

The success of *M. tuberculosis* as a pathogen is due to its ability to maintain prolonged colonisation of the host, without being eradicated by the immune system. As discussed in previous sections, *M. tuberculosis* infection is usually arrested by the immune response and contained within a granuloma structure without the development of active disease, a period known as disease latency. Infection of this kind is defined by a positive conversion in the tuberculin skin test (Boshoff and Barry, 2005). Latency may last for the patient's lifetime or the patient may develop reactivation disease. In one study, the *IS6110* insertion sequence fingerprint of *M. tuberculosis* isolated from a patient with tuberculosis was matched to an isolate taken from his father over 30 years previously, demonstrating that reactivation disease is due to long term infection and not the acquisition of a new infection (Boshoff and Barry, 2005). Therefore, *M. tuberculosis* resides in the host for decades but is able to maintain the ability to establish active infection given the appropriate conditions. Very little is known about the physiology of *M. tuberculosis* during this stage of infection or even the location it may inhabit. It is thought that the bacteria maintain a non-replicating state, brought about by the growth inhibitory conditions found in the granuloma and the activated macrophage (see previous discussions) (Boshoff and Barry, 2005, Parrish et al., 1998, Wayne and Sohaskey, 2001).

The terminology used to describe the bacteria responsible for latent infection is often used in an ambiguous manner in the literature. This putatively dormant population of cells can be conflated with the slowly metabolising, antibiotic refractory cells that may account for the prolonged treatment time of tuberculosis (see previous section). The latter group will be referred to as "persisters", a term first coined by Bigger (1944) to describe non-resistant mutant *Staphylococcus* spp that had survived antibiotic treatment (Lewis, 2007). The physiology characterising this group of bacteria will be discussed in Chapter 6. The term latency refers only to the disease state and not the responsible bacteria. Given the assumed nature of these bacilli, they will be assigned the designation "dormant". The bacterial context of dormancy has been defined as "a reversible state of low metabolic activity in a unit that maintains viability" (Kaprelyants and Kell, 1993, Keep et al., 2006).

1.3.10 Location and physiological state of *M. tuberculosis* during disease latency

Studies using various techniques have been carried out to determine the location of *M. tuberculosis* during dormancy with the purpose of defining the conditions encountered by these bacilli. Before the introduction of antimycobacterial agents and in cases of antibiotic resistant tuberculosis, surgical intervention was employed to remove sections of affected lung tissue (Boshoff and Barry, 2005). Examination of removed tissue has revealed that in a single specimen the lesion pathology can be extremely heterogeneous (Boshoff and Barry, 2005). Open cavities from patients who tested positive for tubercle bacilli in their sputum (smear positive) yielded positive smears and cultures from bacilli isolated from this location. Closed lesions taken from patients who had recently converted to smear negative status contained bacilli that were detectable by smear but only around 0.1% of these grew back in culture. However, it was not possible to assess whether the bacteria observed were viable or whether they were in altered growth state which rendered them unculturable (Salkin and Wayne, 1956). Other studies demonstrated that homogenates of fibreous, caseous lesions taken from the apex of the lung from cadavers who had died from causes other than tuberculosis were capable of causing tuberculosis in noculated guinea pigs; while homogenates taken from caseous or calcified lesions only rarely caused tuberculosis when noculated into guinea pigs. In addition, almost half of homogenates obtained from apparently normal lung tissue were also found to be infectious to guinea pigs (Gomez and McKinney, 2004, Opie and Aronson, 1927). However, in another study tubercle bacilli were only found in normal lung tissue in a very small number of cases (Feldman and Baggenstoss, 1939, Gomez and McKinney, 2004).

It has been suggested that during infection, *M. tuberculosis* loses its acid-fast staining characteristics, perhaps explaining the low numbers of bacilli detectable in lung tissue taken from latently infected individuals. Non-acid fast bacilli isolated from tuberculosis patients regained this property on culturing in liquid media (Khomenko, 1987). In a

contemporary study of lung tissue samples taken from patients with active, cavitating tuberculosis and latent, non-progressive tuberculosis, it was shown that tissue was often negative for acid fast bacilli but yielded a positive result on culture, especially in tissue taken from latently infected individuals (Ulrichs et al., 2005). This conflicts with some earlier studies which suggested that bacilli in tissues from latently infected individuals could be detected by acid-fast staining but not through culture (Wayne and Sohaskey, 2001). In contrast, caseous cavities with access to the bronchial system contained high numbers of acid-fast bacilli. The authors suggested that loss of acid-fastness may be due to alterations in the cell wall (Ulrichs et al., 2005). As acid-fast staining was an unsuitable method to examine the location of these bacilli, immunohistological staining was used to show that in both active and latent tuberculosis, mycobacteria were found in the cavity wall of the granuloma (latent) or cavity (active), peripheral infiltrations and in small granulomas, located away from the larger granulomas (Ulrichs et al., 2005). Mycobacteria were detected in the necrotic centres and periphery of the lesions examined. There were a higher number of macrophages and lymphocytes associated with latent tuberculosis granulomas than their active counterparts, indicating that sustained immune activity was crucial in containing infection. Overall, this study suggests that *M. tuberculosis* resides and is contained within the granuloma during latent infection (Ulrichs et al., 2005). Other studies have demonstrated that *M. tuberculosis* is contained within macrophages associated with the granuloma peripheral leukocyte infiltrate (Russell, 2007).

Other recent work to detect *M. tuberculosis* in lung tissue has employed the use molecular techniques. Hernández-Pando et al (2000) used *in situ* PCR to detect the *M. tuberculosis IS6110* insertion sequence in lung tissue from patients with tuberculosis. Bacterial DNA was detected in old granulomatous lesions but also normal lung tissue with no pathological signs of disease. However, this technique did not allow the discrimination between live and dead bacteria (Boshoff and Barry, 2005, Gomez and McKinney, 2004). Examination of differential gene expression by quantitative real time PCR of a number of genes in resected lung tissue from patients with active disease compared with broth grown cultures and lung tissue from mice generated variable results

(Timm et al., 2003). As discussed, studies with murine macrophages have indicated that *M. tuberculosis* may switch to fatty acid metabolism *in vivo*. This was reflected by an increase in expression of *icl* in the lung tissue of mice but *icl* expression from various patients samples varied from levels comparable to *in vitro* grown *M. tuberculosis* and those observed for mouse tissue (Timm et al., 2003). The authors suggested that this may be due to tissue variability, as *icl* expression had previously been detected by RNA-RNA *in situ* hybridisation in *M. tuberculosis* located in the peripheral leukocyte region but not the necrotic region (Fenhalls et al., 2002). Expression levels of *hspX*, a hypoxic responsive gene were highly expressed in mouse and human infection but again results were variable in human infection (Timm et al., 2003).

As we can see, reports describing the location and possible physiological state of dormant *M. tuberculosis* are somewhat conflicting. Of course this area of research is limited by the availability of tissue for examination and possible difficulty in detecting bacilli due to loss of acid-fast staining. Although there is conflicting evidence, *M. tuberculosis* appears to reside in the necrotic centres and macrophages of the granuloma. Many *in vitro* studies have attempted to model mycobacterial dormancy through mimicking the conditions that *M. tuberculosis* may encounter in these environments. Another approach has been to use animal models of latent disease. These methods will be discussed in the following section.

The physiological state of the bacteria responsible for latent infection remains largely unclear. However, given that isoniazid, which is only active against replicating cells, is effectively used to treat latent infection, it suggests that these bacteria must be metabolically active (Wayne and Sohaskey, 2001). The prolonged period needed to treat latent tuberculosis suggests that replication is in a state of flux, possibly due to ongoing dynamic interactions with the immune system in which bacteria are constantly being released by macrophages through apoptosis, while at the same times others are taken up by macrophages. This may allow periods of replication, which is arrested upon uptake by activated macrophages (Wayne and Sohaskey, 2001).

1.3.11 *In vivo* modelling of latency: The Cornell Mouse Model

Latent infection has been difficult to study *in vivo* because there are no available small animal models which replicate all aspects of human tuberculosis (Boshoff and Barry, 2005, Gomez and McKinney, 2004). While non-human primate models are the closest representations of tuberculosis in humans, they are too expensive to use routinely (Boshoff and Barry, 2005, Gomez and McKinney, 2004). Of the small animal models, rabbits display the closest disease pathogenesis to that observed in human infection (Gomez and McKinney, 2004). Unlike the guinea pig and mouse models, rabbit infection leads to the liquefaction of caseous granulomas to form cavities, as seen in human disease (Gomez and McKinney, 2004). However, rabbits are not widely used because they are relatively expensive and because the murine model has been more widely researched in the study of infectious disease and chemotherapy (Boshoff and Barry, 2005, Gomez and McKinney, 2004). In addition, a number of genetically defined mice strains are available. While there are similarities in the immune response to tuberculosis in mice and humans, there are some important differences in disease progression (Gomez and McKinney, 2004, Boshoff and Barry, 2005).

Aerosol infection of mice results in granuloma formation throughout the lungs, however, these lack the structure observed in human granulomas. Murine granulomas consist of aggregates of macrophages and lymphocytes that do not progress to caseation (Boshoff and Barry, 2005). Bacterial replication is arrested and controlled by the immune response, however, unlike human disease, the chronic infection stage is characterised by the presence of high numbers of bacteria in the lungs and spleen (Boshoff and Barry, 2005). Examination of tissue taken from autopsies has demonstrated that bacterial numbers are low in chronic human disease (Boshoff and Barry, 2005, Gomez and McKinney, 2004). As discussed previously, the production of RNI has been shown to be important in immune control of this stage of infection. As is suggested by the high tuberculosis infection and reactivation rates in HIV infected individuals, CD4+ and CD8+ cells have been shown to be significant in sustaining infection control in mice (Gomez and McKinney, 2004, Boshoff and Barry, 2005).

The Cornell model, developed by McDermott and colleagues at Cornell University in the 1950s, is the most widely used model of *M. tuberculosis* latent infection (Gomez and McKinney, 2004). In this model, the mouse is infected with a high dose of *M. tuberculosis* then treated with isoniazid and pyrazinamide for an extended period (Cosma et al., 2003, Honer zu Bentrup and Russell, 2001). No bacteria can be recovered from organ homogenates following treatment, a phenomenon called "sterile state" but DNA content remains constant (Boshoff and Barry, 2005, Gomez and McKinney, 2004). However, disease reactivates spontaneously in approximately one third of animals, three months after the discontinuation of treatment (Boshoff and Barry, 2005). This models the latent state in humans when few bacteria can be detected in the lung but unlike human infection, this latent-like state can only be induced by drug treatment (Cosma et al., 2003). Mice are then subjected to immunosuppressive drugs and the infection "reactivates", presumably through renewed growth of a small and undetectable population of bacteria that had survived chemotherapy (Honer zu Bentrup and Russell, 2001). The recovered bacteria are fully susceptible to isoniazid and pyrazinamide, indicating that survival was not dependent on the development of drug resistance (Gomez and McKinney, 2004). Hu et al. (2000) demonstrated that mycobacterial mRNA was present in detectable amounts during the sterile state, indicating that substantial numbers of nonculturable bacteria are present in infected tissues post-chemotherapy. This implies the existence of a phenotypically drug tolerant population; this has clear parallels with drug treatment of human tuberculosis (Hu et al., 2000). This suggests that the development of drug tolerance is not necessarily a response to the conditions found in the granuloma. The Cornell model assumes that this drug tolerant population represents the bacteria that sustain human latent infection; however, the differences in pathology and its dependence on chemotherapy limit the application of this model (Boshoff and Barry, 2005, Gomez and McKinney, 2004, Honer zu Bentrup and Russell, 2001).

1.3.12 *In vitro* modelling of *M. tuberculosis* dormancy

The Wayne Model

The conditions encountered by *M. tuberculosis* in the activated macrophage and granuloma have been discussed previously. Oxygen limitation in the granuloma and activated macrophage has been proposed to be one of the main signals for the switch to *M. tuberculosis* dormancy (Wayne and Sohaskey, 2001). Abrupt depletion of oxygen is lethal to *M. tuberculosis*; however, *M. tuberculosis* is able to adapt to a gradual withdrawal of oxygen and survive anaerobiosis (Wayne and Sohaskey, 2001). One of the most widely studied *in vitro* methods used to study *M. tuberculosis* adaptation to hypoxia was developed by Wayne in the 1970s. Here, slowly stirred cultures are maintained with a limited head-space and they enter a non-replicating persistence (NRP) state (Wayne and Sohaskey, 2001). In developing this model, Wayne examined static cultures of *M. tuberculosis* in sealed tubes of media in which he showed that the bacilli settled to the bottom of the tube through a self-generated oxygen gradient (Wayne and Sohaskey, 2001). The bacilli adapted to hypoxia as they settled through the gradient and the sedimented bacteria were adapted to anaerobiosis. The transition period was characterised by an increase in the expression of ICL and glycine dehydrogenase (Wayne and Sohaskey, 2001). On resuscitation in aerobic conditions, these dormant bacteria were shown to immediately accelerate RNA synthesis and undergo several rounds of synchronous replication, suggesting that growth arrest occurred at a specific stage in the cell cycle (Wayne and Sohaskey, 2001).

The heterogeneity in settling times in the original unstirred model meant that the timing and sequence in adaptive changes could not be established. Therefore, the slowly stirred, limited head space ratio model was developed in order to allow the examination of these changes along a temporal rather than spatial gradient (Wayne and Sohaskey, 2001). In this model, tubes with a calculated head space ratio of air to media of 0.5 are inoculated with low numbers of *M. tuberculosis*, to avoid rapid consumption of oxygen. Tubes are sealed and incubated with stirring at a speed that allows distribution of the bacilli through

the media but does not disturb the surface of the liquid, allowing slow consumption of oxygen (Wayne and Sohaskey, 2001).

Optical density readings have revealed that these cultures progress through three distinct stages of growth (Figure 5). Initially, the bacteria grow exponentially; however, when the dissolved oxygen reaches a microaerophilic level of 0.1% saturation, in respect to air, replication stops abruptly. This stage in *M. tuberculosis* adaptation to depleting oxygen is termed non-replicating persistence stage 1 (NRP1) (Wayne and Sohaskey, 2001). The optical density reading continues to increase at a reduced level during this stage. This has been shown not to be due to cellular replication but a thickening in the outer region of the cell wall. This increase in optical density plateaus as the dissolved oxygen tension is reduced to an anaerobic level of 0.06% and cells enter NRP stage 2 (Wayne and Sohaskey, 2001). On adaptation to NRP, DNA synthesis and protein synthesis are halted and RNA synthesis becomes reduced (Wayne and Sohaskey, 2001). Further metabolic changes must then occur during NRP2 because survival during this stage is dependent on the transition period through NRP1. Aeration of NRP2 cells results in synchronous growth as observed for unstirred NRP cultures (Boshoff and Barry, 2005, Wayne and Sohaskey, 2001).

NRP cells also become less susceptible to antibiotics, although this topic will largely be discussed in Chapter 6. Conversely, NRP cells become sensitive to metronidazole, an antibiotic used to treat anaerobic infections (Boshoff and Barry, 2005, Gomez and McKinney, 2004). However, treatment of infected mice with metronidazole failed to eliminate chronic infection (Boshoff and Barry, 2005, Gomez and McKinney, 2004). This may indicate that environmental factors other than hypoxia are experienced by *M. tuberculosis* during latent infection or may be a reflection of the tissue pathology in mouse infection, in which granulomas do not undergo caseation. Interestingly, there is some evidence to suggest that metronidazole treatment leads to an improvement radiographic response in patients with active disease, high-lighting the difference in pathogenesis observed between mouse and human infection (Boshoff and Barry, 2005). While the Wayne model is reproducible and allows examination of non-replicating *M.*

tuberculosis (gene expression studies using the Wayne model are discussed later), it may over simplify the complex range of environmental stimuli the pathogen is expected to face *in vivo* (Honer zu Bentrup and Russell, 2001).

Figure 5: Optical density growth curve of *M. tuberculosis* during adaptation to hypoxia in the Wayne Model

Line **A** shows growth with aeration and line **B** shows growth in the slowly stirred 0.5 (volume:volume) head space ratio model of hypoxia. Both cultures grow logarithmically in the first 70 hours. In the model, when oxygen is depleted to a microaerophilic level (NRP1-shown in blue), replication stops and the optical density increases due to cell wall thickening. After 200 hours oxygen is depleted to an anaerobic level and cell wall thickening ceases (NRP2-pink). Adapted from Wayne and Sohaskey (2001).

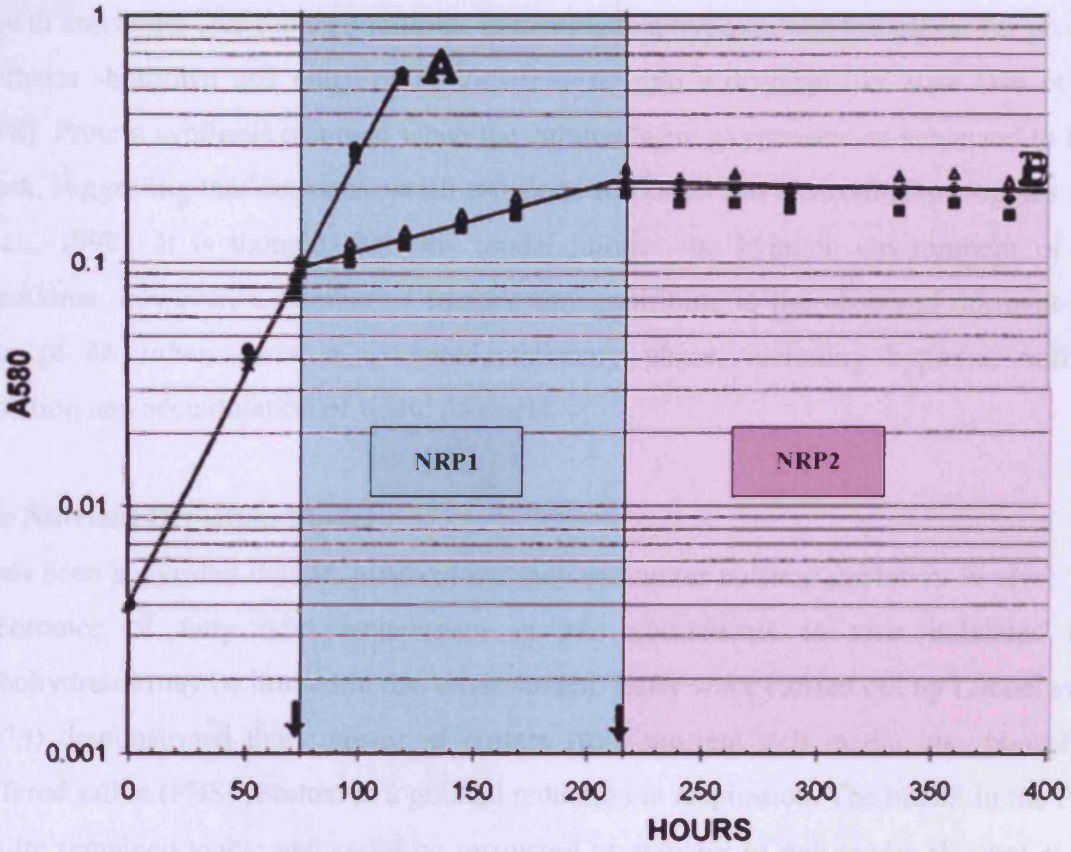

Stationary Phase Models

M. tuberculosis subjected to an extended stationary phase has also been used to model transcriptional changes in mycobacterial dormancy. In this model, unknown factors become limiting, which results in a non-proliferating culture (Voskuil et al., 2004). The disadvantage of this method is that it is difficult to determine the specific signals contributing to changes in gene expression (Voskuil, 2004). Protein synthesis has been shown to gradually decrease over 50 days in a long-term stationary phase static culture of *M. tuberculosis*, which was considered to be microaerophilic (Hu et al., 1998). When the culture was switched to anaerobic conditions, protein synthesis was completely shutdown (Hu et al., 1998). Colony forming unit counts remained constant during stationary phase growth and under anaerobic conditions, indicating that hypoxia was the trigger for protein synthesis shutdown and entry of *M. tuberculosis* into a dormant-like state (Hu et al., 1998). Protein synthesis resumed when the cultures were oxygenated or subjected to heat shock, suggesting that dormant bacilli remained responsive to environmental signals (Hu et al., 1998). It is thought that this model mimics the hypoxic environment of the granuloma; however, a number of factors may contribute to the observed dormant-like state of *M. tuberculosis* in extended stationary phase, including hypoxia, nutrient depletion and accumulation of waste products.

The Nutrient Depletion Model

It has been suggested that *M. tuberculosis* may encounter nutrient depletion *in vivo*. The importance of fatty acid metabolism in *M. tuberculosis in vivo* indicates that carbohydrates may be limited in this environment. Early work carried out by Loebel et al. (1933) demonstrated that transfer of culture from nutrient rich media into phosphate buffered saline (PBS) resulted in a gradual reduction in respiration. The bacilli in the PBS culture remained viable and could be recovered by transfer to rich media (Loebel et al., 1933). Betts et al. (2002) developed a model based on this work, in which a 7 day culture of *M. tuberculosis* was transferred to PBS and incubated statically for six weeks. Oxygen was shown to be depleted after 9 days of incubation of control culture in rich media but not in the nutrient depleted model. Colony forming unit counts of the nutrient depleted cultures remained constant throughout incubation, indicating that unlike NRP cells in the

Wayne model, nutrient depleted cells entered a dormant-like state before oxygen reached a limiting level (Betts et al., 2002). In common with Wayne NRP cells, cells adapted to nutrient depletion displayed tolerance to rifampicin and isoniazid but remained sensitive to metronidazole because metronidazole requires reduction under anaerobic conditions to become active (Betts et al., 2002).

1.3.13 Gene Expression in dormant *M. tuberculosis*: The DosR Regulon

The use of microarray technology has revolutionised the analysis of genome wide gene expression in response to dormancy inducing conditions. Sherman et al. (2001) identified a set of 48 genes that were upregulated in response to short term oxygen depletion. This involved culture flasks which were connected to a supply of oxygen and nitrogen that were subjected to oxygen depletion at less than 1% saturation for 2 hours (Sherman et al., 2001). Among this gene set was the two component response regulator pair Rv3133c/ Rv3132c. Deletion of Rv3133c (the regulator) lead to a reduced expression of the hypoxic response gene α-crystallin, while no phenotype was observed for disruption of Rv3132c (sensor kinase of the two component system) (Sherman et al., 2001).

Using the same hypoxic system, Park et al. (2003) went on to demonstrate that disruption of Rv3133c, termed DosR for dormancy survival regulator, resulted in a dramatic reduction of this transcriptional response. This demonstrated that almost all of the genes that were expressed in response to hypoxia required DosR for their induction and computer analysis revealed that a consensus motif was located upstream of the majority of these genes. In addition, DosR was shown to bind to the copies of this motif upstream of the α-crystallin gene. This study established the role of DosR as the primary mediator of the hypoxic response in *M. tuberculosis* (Park et al., 2003).

Studies of gene expression in response to hypoxia have shown that a subset of genes is highly induced in this condition. This group of genes has been termed the "dormancy regulon" because their expression is upregulated in *M. tuberculosis* in response to

dormancy inducing conditions, although it does not represent a definitive set of genes which are expressed in response to these conditions (this will be discussed below). Of the 48 dormancy regulon genes originally identified by Sherman et al. (2001) 42 and 36 were induced and were continued to be expressed throughout the first month of NRP in cultures in the Wayne model in two independent studies (Voskuil et al., 2004, Muttucumaru et al., 2004, respectively). The dormancy regulon genes were some of the most highly induced genes in this model. In a steady state chemostat culture exposed to hypoxia, 35 of the dormancy regulon genes were induced (Bacon et al., 2004); this system is discussed further in Chapter 3. Dormancy regulon genes were also induced in a stationary phase culture (27 genes) (Voskuil et al., 2004) and in a static culture (which generates a hypoxia gradient) which had been allowed to settle for 30 minutes (31 genes) (Kendall et al., 2004). Oxygen depletion was considered to be the trigger for induction in both of these models. The dormancy regulon genes do appear to play a central role in the response of *M. tuberculosis* to hypoxia; however, additional genes that do not belong to this subset were also induced in different studies of the hypoxic response.

Both studies of gene expression of NRP *M. tuberculosis* followed what was essentially the same method but there were discrepancies between the gene expression data obtained in each. Voskuil et al. (Voskuil et al., 2004) identified an additional 60 genes that were induced in NRP, of which only 17 were found to be induced in NRP in the study carried out by Muttucumaru et al. (2004). Voskuil (2004) commented that this may be due to differences in the performance of the microarray analysis or it could be due to difficulties in reproducing the Wayne model. The dormancy regulon has since been shown to be induced in response to a number of conditions that are thought to inhibit aerobic respiration.

The dormancy regulon was expressed in *M. tuberculosis* in response to a non-toxic level of NO, a condition which reversibly inhibited respiration and growth (Voskuil et al., 2003). Ohno et al. (2003) confirmed the induction of the regulon in response to 4 hour treatment of *M. tuberculosis* with two different NO releasing agents in three independent microarray studies. A number of these genes were shown to respond to NO in a dose

dependent manner (Ohno et al., 2003). Kendall et al. (2004) also demonstrated induction of the dormancy genes on exposure of *M. tuberculosis* to s-nitrosglutathione (GSNO, an NO releasing agent), ethanol and to a lesser extent, hydrogen peroxide but not in response to heat or cold shock. This suggests that *M. tuberculosis* regulates its response to these conditions through overlapping signalling pathways, although this does not necessarily mean that these conditions induce a switch to the same metabolic state (Boshoff and Barry, 2005). The induction of DosR by a number of conditions makes it difficult to interpret the specific contribution of each of these to the host environment, in which mycobacterial genes may be regulated by a number of environmental signals simultaneously (Ohno et al., 2003, Warner and Mizrahi, 2006). As yet, there is little evidence to show that the dormancy gene set is required for *M. tuberculosis* survival during the period of disease latency in humans (Voskuil et al., 2003).

However, there is some evidence to show that DosR or genes of the regulon are important in animal and macrophage infection by *M. tuberculosis*. Five of the dormancy genes were shown by quantitative real time PCR to be highly expressed in infected mouse lung tissue. Expression levels were comparable to those induced by NO exposure (Voskuil et al., 2003). As discussed previously, Schnappinger et al (2003) also demonstrated that members of the DosR regulon were upregulated in the activated murine macrophage and this was dependent on the production of NO. The role of NO in containing infection in the mouse model has been discussed. Genes induced by NO are likely to be important in the immune control in mice infected with *M. tuberculosis* but this may differ from human disease. However, there is some conflicting evidence of the importance of DosR for survival during murine infection. Two groups independently created DosR disrupted mutants; one group demonstrated that disruption of this regulator with a kanamycin resistance gene attenuated *M. tuberculosis* in guinea pigs (Malhotra et al., 2004); while the other group showed that their unmarked mutant was more virulent in mice than the wild type (Parish et al., 2003). This may reflect the differences in methods used to generate the gene disruption but it may also be due to the tissue pathology of the mouse model. As discussed, granuloma formation is limited in the mouse model; therefore, *M. tuberculosis* may not be subjected to all of the environmental conditions shown *in vitro* to

induce the regulon. Interestingly, DosR is required for virulence in the guinea pig model in which infection does progress to granuloma formation (Malhotra et al., 2004).

Significantly, ICL is not a member of the DosR regulon but it is upregulated in *M. tuberculosis* infected murine macrophages (Schnappinger et al., 2003) and is expressed on entry into NRP in the Wayne model (Wayne and Sohaskey, 2001). The importance of ICL during infection has been discussed elsewhere. However, it is clear that while the dormancy regulon may play an important role during adaptation to stress and may act as a marker for dormancy *in vivo*, it does not reflect the full response to the range of conditions *M. tuberculosis* is expected to encounter in the granuloma or activated macrophage. In a recent study, it was demonstrated that a DosR mutant exposed to hypoxia entered bacteriostasis with only a small decrease in viability (Rustad et al., 2008). In both the mutant and wild type strains of *M. tuberculosis*, a core of 230 stably induced genes (termed the Enduring Hypoxic Response genes) were found to be expressed for a much longer period during hypoxia than the dormancy regulon genes (Rustad et al., 2008). The authors suggested that these genes may be involved in regulating and maintaining bacteriostasis and that induction of the DosR regulon may simply prepare *M. tuberculosis* for growth arrest by allowing the sequestering of nutrients and triggering changes that do not require continued regulation (Rustad et al., 2008).

1.3.14 Genes implicated in dormancy

The functions of many of the *M. tuberculosis* genes that are induced in conditions considered to be linked to dormancy, belonging to the DosR regulon or otherwise, are unknown. One of the most highly expressed DosR genes during the hypoxic response in *M. tuberculosis* is *hspX* (otherwise known as *acr*, Rv2031c), which encodes a 16kDa α-crystallin-like protein (Hu et al., 2006, Parrish et al., 1998). The α-crystallin-like protein is an immunodominant antigen and is recognised by the immune response of patients with tuberculosis (Parrish et al., 1998). The α-crystallin protein is a member of the α-crystallin-like heat shock protein family, which act as molecular chaperones that prevent

thermal aggregation of other proteins (Hu et al., 2006). While the α-crystallin protein has been shown to act as a chaperone, there was no effect on survival of an hspX mutant exposed to heat shock and as *M. tuberculosis* has other heat shock proteins, there may be some functional redundancy (Hu et al., 2006). It is unlikely that α-crystallin functions in this role during dormancy and there is some evidence to suggest that it may be an important structural protein during this time. Cunningham and Spreadbury (1998) demonstrated that α-crystallin protein was localised to the cell wall of *M. bovis* BCG cultured under low oxygen tension. This coincided with a thickening of the cell wall layer, consisting of what was presumed to be lipid. This cell wall thickening is thought to account for the increase in optical density at the onset of NRP1 in the Wayne model (Wayne and Sohaskey, 2001). Although there are no data to show that the α-crystallin protein is responsible for the change in cell envelope property, it has been proposed that this protein is involved in stabilising the cell structure during long term survival. It has also been suggested that the α-crystallin protein affects the growth rate of mycobacteria (Hu et al., 2006).

Overexpression of *hspX* leads to a decrease in the logarithmic growth rate of *M. tuberculosis* (Yuan et al., 1996) and the lag phase growth of *M. smegmatis*. An unmarked deletion of *hspX* was shown to increase the growth rate of *M. tuberculosis* in naïve and activated macrophages and during mouse infection, although lung damage was not significantly different, when compared to the wild type parent strain (Hu et al., 2006). Another study using an *M. tuberculosis* mutant in which *hspX* was replaced with a hygromycin resistance gene showed that this strain was attenuated in a macrophage model of infection (Yuan et al., 1998). Again, this may be due to the method by which the mutants were generated. The presence of α-crystallin protein antibody in tuberculosis patients' sera suggests that it is produced and shed by *M. tuberculosis* during infection and that it may have an important role *in vivo*. However, it remains to be seen what role is fulfilled and whether α-crystallin is involved in reducing the growth rate of *M. tuberculosis* during the latent infection period.

In hypoxic environments many bacteria are able to use nitrate as a final electron acceptor in the proton motive force. Nitrate reductase is an alternative respiratory enzyme that is able to accept electrons that are of lower redox potential (Sohaskey and Wayne, 2003). The DosR regulon includes the *narK2- narX* operon, encoding a nitrate reductase and nitrite efflux system. However, the nitrate reductase of this operon is non-functional as deletion of *narX* has no effect on the reduction of nitrate (Sohaskey and Wayne, 2003). The non-DosR regulated *narGHJI* operon is the only nitrate reductase that is active in *M. tuberculosis* (Sohaskey and Wayne, 2003). A *narG M. bovis* BCG mutant was attenuated in severe combined immune deficiency (SCID) mice, while wild type BCG induced an acute progressive infection in these animals (Weber et al., 2000). In addition, Shi et al. (2005) demonstrated that expression of the nitrate transporter *narK2* was upregulated during late state infection of the mouse lung, suggesting that nitrate reduction is increased in *M. tuberculosis* during infection.

As discussed, β-oxidation may provide an important means by which energy is generated and two carbon units are provided for gluconeogenesis. However, this mechanism may be limited by the availability of terminal electron acceptors. Metabolism of fatty acids via the β-oxidation cycle results in the production of the reducing equivalents NADH and $FADH^2$ that must be reoxidized for the cycle to resume (Boshoff and Barry, 2005). It is expected that nitrate is present in the phagosome of activated macrophages and in granulomas, because nitrate can occur as a degradation product of NO (Boshoff and Barry, 2005). *M. tuberculosis* may reduce nitrate via the nitrate reductase encoded by the *narGHJI* operon and remove the resulting nitrite through the nitrite-efflux system encoded by the *narK2* gene, allowing restoration of the redox balance during growth on fatty acids (Boshoff and Barry, 2005). However, it has not been demonstrated that *M. tuberculosis* uses alternative electron acceptors and the enzymes discussed above may only function alongside the terminal oxidases that utilise oxygen in balancing energy generation with growth (Boshoff and Barry, 2005).

Alternate sigma factors are transcriptional regulators that recognise the promoters of large groups of genes involved in adaptation to environmental changes and allow the organism

to adjust their transcription rapidly in response (Gomez et al., 1997). The alternate sigma factor, SigF, is not a member of the DosR regulon but it is thought that it may play a role in gene regulation in response to stress. Only the slow growing, pathogenic mycobacteria possess a *sigF* gene, suggesting that SigF may be important during infection or adaptation to slow growth (Gomez et al., 1997). In support of this hypothesis, transcription of *sigF* has been shown to be induced in stationary phase cultures of *M. tuberculosis* but was undetectable in exponential growth (Gomez et al., 1997). In addition, a *sigF* mutant exhibited a three fold higher growth rate in stationary phase, in comparison to the wild type strain (Chen et al., 2000). Microarray studies have shown that *sigF* is induced in response to nutrient starvation (Betts et al, 2002), hypoxia (Sherman et al., 2001), anaerobiosis, cold shock, hydrogen peroxide treatment and exposure to the antibiotics rifampicin, ethambutol and metronidazole (under anaerobiosis) (Michele et al., 1999). Studies of mutants with disrupted or deleted *sigF* genes revealed that *sigF* is important during late stage disease. An *M. tuberculosis* mutant in which *sigF* was disrupted by a hygromycin resistance gene was shown to be less virulent in mice by time to death assessment (Chen et al., 2000). Geiman et al. (2004) showed that an *M. tuberculosis sigF* deleted mutant was unable to reach the same bacterial load as the wild type strain in infected mouse lungs during late stage infection and this was accompanied by the formation of fewer lesions. Expression of genes involved in the structure and the mycobacterial cell wall was reduced in the *sigF* mutant, indicating that cell wall adaptation is important in late stage disease. This may form part of the stress response controlled by *sigF*, as the cell wall is thought to protect *M. tuberculosis* against the action of chemicals, dehydration and certain antibiotics (Geiman et al., 2004).

ICL and RelA are considered to form an important part of adaptation to a number of stresses. The reader is referred to the Fatty Acid Metabolism section of this chapter for discussion of ICL and its importance *in vivo* and Chapter 6 for discussion about RelA.

Many of the genes, including the DosR regulon, that have been shown to be responsive to what are considered to be dormancy inducing conditions have been identified through microarray expression analysis. The disadvantage of this method is that it sometimes

creates more questions than it answers because the majority of these genes have unknown functions. Functional studies of these genes need to be carried out in order to elucidate their possible roles during infection. The relevance of *M. tuberculosis* gene expression studies of these conditions to the physiology of *M. tuberculosis* during latent infection is yet to be clarified.

1.4 Aims and Objectives of this study

The overall aims of this study were to examine the formation and occurrence of LBs in mycobacteria, with particular emphasis on the role of LBs in *M. tuberculosis* in sputum. The specific aims were:

- To determine the extent to which LBs occur in acid fast bacilli in sputum
- Define conditions required for LB promotion in *M. tuberculosis in vitro*
- Dependent on the demonstration of above, assess the association of LBs with mycobacterial tolerance of antibiotics, as it has been previously shown that LB positive *M. smegmatis* were more tolerant of antibiotic treatment than their LB negative counterparts.
- To examine whether LB formation in mycobacteria is consistent with that observed in *Rhodococcus* spp. by examining morphological details of mycobacterial LBs that may indicate the mechanism of formation including:
    - Whether they are connected to the cell surface and if so are they connected at all times
    - The presence of a membrane boundary
    - Association of LBs with the cell membrane

Chapter 2

General Materials and Methods

2.1 Bacterial Strains and Plasmids

Table 1: Strains and plasmids used in this study.

Strain	Description	Source
E. coli DH5α	*E. coli* with high transformation phenotype.	Laboratory stocks
E. coli α *select*	Chemically competent *E. coli*	Bioline
M. smegmatis mc^2155	Strain with high transformation efficiency	Laboratory stocks
M. tuberculosis H37Rv	Virulent laboratory strain	Laboratory stocks
M. tuberculosis H37Rv *devR* (3132c/ 3133c) unmarked disrupted mutant strain	447-bp *Bal*I deletion in regulator	Neil Stoker (Parish et al., 2003)
M. tuberculosis H37Rv *devR* (3132c/ 3133c) complemented strain	Contains integrating plasmid carrying *devR*	Neil Stoker (Parish et al., 2003)
M. tuberculosis CH	Index isolate from tuberculosis outbreak	Laboratory stocks

Plasmid	Description	Source
pSD26	Mycobacterial, *E. coli* overexpression shuttle vector. Contains a hygromycin resistance gene for selection and an acetamide inducible promoter.	Natalie Garton

pSD26:3130c	Plasmid psD26 with an insert of the 3130c (*tgs1*)	Natalie Garton
pJFX4	Plasmid identical to JFX2 with GFP under the control of the *M. fortuitum* β-lactamase promoter. Kan^r	(Rollinson, 2003) (Triccas et al., 1999)
JFX2	Promoter probe vector. Carries promoterless copy of *gfp*. Kan^r	(Rollinson, 2003) (Triccas et al., 1999)
JFX2:ftsZ	pJFX2 with *gfp* under control of the promoter of *ftsZ*	This study
JFX2:whiB2	As above with *whiB2* promoter sequence insert.	This study
JFX2:sigB	As above with *sigB* promoter sequence insert.	This study

2.2 Laboratory Reagents and Culture Media

2.2.1 Chemicals and Media

All chemicals were obtained from Sigma-Aldrich Company Limited (Poole, Dorset, UK) or Fisher Scientific (Loughborough, Leicestershire, UK), unless otherwise stated. Media were obtained from Difco Laboratories (Detroit, USA), unless otherwise stated. Media were sterilised at 120°C for 20 minutes unless otherwise stated.

2.2.2 Growth Media

Middlebrook 7H9 Broth with Tween

Middlebrook broth was prepared by dissolving 4.7g broth powder in 900ml double distilled water containing 2.5g glycerol and 0.5g Tween 80. This was autoclaved at 121°C for 17 minutes. Broth was supplemented with Albumin-dextrose-catalase (ADC) at a concentration of 10% (v/v) prior to use.

Middlebrook 7H9 Broth with Tyloxapol

Middlebrook broth was prepared as above, replacing the Tween with 0.5g Tyloxapol.

Middlebrook 7H10 Agar

Middlebrook agar was prepared by dissolving 19g of agar powder in 900ml distilled water containing 6.25g glycerol. The agar was boiled for 30 minutes to allow the powder to dissolve and then kept at 50°C until sterilisation by autoclaving at 121°C for 17 minutes. Agar was supplemented with oleic acid dextrose complex (OADC) at a concentration of 10% (v/v) prior to use.

ADC Supplement

ADC was prepared from the following reagents in 150ml distilled water:

Bovine Serum Albumin fraction V (BSA)	7.50 g
D-Glucose	3.00g
Sodium Chloride	1.28g
Catalase	6.0mg

The solution was centrifuged at 6371 x g for 30mins in a Beckman Coulter Avanti J-E refrigerated superspeed centrifuge. The supplement was then filter sterilised (0.2µm filter, Nalgene, USA) and stored at 4°C.

OADC Supplement

The supplement was prepared as above (ADC), with the addition of 8.63ml Oleic Acid solution (1% (w/v) in 0.2M sodium hydroxide). Before centrifugation the solution was sonicated (Decon FS 100, Ultrasound Ltd, UK) for 30min to allow emulsification of the oleic acid.

Sautons Broth

Sautons Broth was prepared from the following reagents in 900 ml distilled water:

Potassium dihydrogen orthophosphate	0.5g
Magnesium sulphate	0.5g
L-Asparagine	4.0g
Glycerol	75.0g
Ferric ammonium citrate	50.0mg
Citric acid	2.0g
1% (w/v) zinc sulphate	0.1ml
Tween 80	0.5g

The pH was adjusted to 7.0 and the solution was made up to a final volume of 1 litre. Sautons agar was prepared by adding Bactoagar to a final concentration of 1.5% (w/v) (Rollinson, 2003).

Youmans Broth

Youmans broth was prepared from the following reagents in 900 ml distilled water:

Potassium dihydrogen orthophosphate	5.0g
Magnesium sulphate	0.5g
L-Asparagine	5.0g
Glycerol	40.0g
Ferric ammonium citrate	50.0mg
Sodium citrate	2.5g

The pH was adjusted to 7.0 and the solution was made up to a final volume of 1 litre.

Low Nitrogen Youmans Broth (LNYB)

LNYB was prepared as above with 1.25g L-Asparagine.

Low Carbon Youmans Broth (LCYB)

LCYB was prepared in the same manner as Youmans Broth, excluding all glycerol and with the replacement of L-Asparagine with 2g Ammonium chloride.

BSA and Oleic Acid Supplement

BSA (5g) was dissolved in 100ml of distilled water. Once this had been completely solubilised, 200µl oleic acid was added to give a stock concentration of 6.3mM. The mixture was sonicated for 1 hour. The solution was filter sterilised and stored at 4°C.

40% Glycerol solution

Glycerol (40g) was dissolved in 100ml distilled water and sterilised by autoclaving.

Luria-Butani (LB) Broth and agar

The following reagents were dissolved in 900ml of distilled water:

1% (w/v) Bacto-tryptone

0.5% (w/v) Bacto-yeast extract

0.5% (w/v) NaCl

The pH was adjusted to 7.4 and the volume was made up to 1 litre with distilled water. For LB agar, 1.5% (w/v) bactoagar was added to the reagents above.

Phosphate buffered saline (PBS)

Phosphate buffered saline (PBS) was prepared using PBS tablets (Sigma-Aldrich). One tablet was dissolved in 200ml distilled water to give a solution of 0.01M phosphate buffer, 0.002M potassium chloride and 0.137M sodium chloride at pH7.4.

Mineral Salts Medium (MSM)

Mineral Salts Medium was prepared from the following reagents in 900 ml distilled water:

Disodium hydrogen orthophosphate dodecahydrate	9.0g
Potassium dihydrogen orthophosphate	1.5g
Ammonium chloride	1.0g
Magnesium sulphate 7-hydrate	0.2g
Ferric ammonium citrate	1.2mg
Calcium chloride	20mg
Hoagland number 2 basal salts mixture (Sigma)	2ml

The pH was adjusted to 7.0 and the solution was made up to a final volume of 1 litre. 0.5g of sodium barcarbonate (0.5g/ml solution, filter sterilised) was added prior to use (Schlegel et al., 1961). Media to promote the formation of wax esters in *M. smegmatis* contained 1% glucose (filter sterilised) in addition to 0.3% (w/v) hexadeconol.

Addition of Antibiotics

Antibiotics were added to broth or agar in order to maintain plasmids. Stocks of antibiotics were prepared in distilled water, filter sterilised and stored at 4°C. Antibiotics were used at the following concentrations; kanamycin 25μg/ml and hygromycin 50μg/ml.

N-acetyl-L-cysteine (NALC)

A 50mM solution of sodium citrate in distilled water was prepared. Immediately before use, 0.5g NALC powder was added to 50ml sodium citrate solution (Summers and Good, 1985).

Phosphate buffer

Phosphate buffer was prepared by combining 134mM NaH_2PO_4 and 134mM Na_2HPO_4 at a ratio of 51:49 to give a 67mM solution at pH6.8 (Summers and Good, 1985).

2.3 Cultivation of Bacteria

2.3.1 Stock Cultures

Stocks of *M. smegmatis* and *M. tuberculosis* were prepared by mixing 500µl exponentially growing culture (doubling every 3 or 24 hours, respectively, as assessed by optical density readings) and 500µl 50% sterile Glycerol solution (in distilled water). These 1ml aliquots were stored in 1.5ml Cryovials at -80°C (NUNC, USA).

2.3.2 Cultivation of M. smegmatis

2.3.2.1 Standard Culture Techniques

M. smegmatis was grown on solid media by streaking a loop of glycerol stock or a single colony from a previous plate onto a 7H10 plate. Plates were incubated at 37 °C for 2-3 days, when single colonies became visible. A liquid culture was prepared by emulsifying colony growth in the appropriate broth. The optical density at 580nm (OD_{580}) of the cell suspension was adjusted to 0.5 and 5ml of this was used to inoculate 100ml broth (7H9 with ADC, Youmans Broth or Sautons), to give a final OD_{580} of 0.025. Cultures were incubated at 37°C with shaking for 1-2 days.

2.3.2.2 Preparation of Low Nitrogen treated M. smegmatis

A culture of *M. smegmatis* was prepared as above, using LNYB as a growth medium. The culture was incubated at 37°C with shaking for a week.

2.3.2.3 Preparation of Low Carbon treated M. smegmatis

A culture of *M. smegmatis* in 7H9 with Tyloxapol was prepared as outlined above (2.3.2.1). This was incubated overnight at 37°C with shaking. The culture was washed by harvesting the cells by centrifugation at 3000 x g for 10 minutes. The supernatant was removed and the resulting pellet was resuspended in fresh LCYB broth. The cells were washed three times in this manner and finally resuspended in 100ml LCYB broth. This culture was incubated for 3 days- 1 week at 37°C.

2.3.2.4 Preparation of M. smegmatis in media to promote wax ester formation

A culture of *M. smegmatis* was prepared as described (2.3.2.1), using MSM containing hexadecanol as a growth medium. The culture was incubated at 37°C with shaking for 3 days. Control cultures were grown in MSM without hexadecanol.

2.3.3 Cultivation of M. tuberculosis

2.3.3.1 Standard culture techniques

M. tuberculosis is an ACDP category 3 hazardous pathogen and all work with this bacterium was carried out in a Class 1 or Class 2 microbiological safety cabinet, within the Containment laboratory suite and in accordance with the suite Code of Practice. All liquid and solid cultures were double bagged when under incubation.

Starter cultures of *M. tuberculosis* were prepared by thawing a stock aliquot and adding this to 5ml 7H9 broth. This was incubated for 7 days at 37° C with shaking at 100rpm. Starter cultures were then used to inoculate 50-100ml 7H9 broth in polycarbonate flasks, which were incubated for 5-7 days. These cultures were used to inoculate 100-200ml media at a calculated OD_{580} of 0.05 in roller bottles (Greiner). Roller bottles were incubated at 37° C with rolling for 4-7 days.

2.3.3.2 Preparation of Lawn Growth of M. tuberculosis

Lawn growth was prepared by spreading 100µl exponential (see definition in 2.3.1) *M. tuberculosis* culture on OADC supplemented Middlebrook 7H10 agar plates. Plates were sealed, double bagged and incubated for 5 days, until a thin film of growth was observed.

2.3.3.3 Enumeration of Colony Forming Units

Colony counts were carried out by the drop plate method, which is a modified version of the Miles and Misra method (Hoben and Somasegaran, 1982). Ten-fold serial dilutions of broth culture or cell suspension were made in aliquots of 7H9 containing Tween (without ADC supplementation). Three 20µl drops were plated out from each dilution on duplicate 7H10 agar plates. The plates were sealed with laboratory sealing film (Nescofilm, Osaka, Japan), inverted and incubated in double bags at 37° C. Colonies were counted using a dissection microscope at x4 magnification. The plates were counted weekly until the counts stabilised. Final counts of 10-100 colonies were used for the final calculation of colony forming units (CFUs), shown below:

CFU/ml = (average colony count per 20µl spot) x (dilution factor) x 50

2.3.3.4 Measuring Optical Density

The absorbance of a culture was measured at a wavelength of 580nm using a SANYO SP75 UV/Vis spectrophotometer in the main lab or a Jenway 6300 spectrophotometer in the containment suite. 1ml volumes were transferred into 1.5ml cuvettes and these were sealed with autoclave tape and laboratory film. Thick cultures (OD greater than 0.5) were diluted 1:10 before measurement.

2.3.3.5 Decontamination of sputum and preparation of sputum smears

Clinical sputum samples were decontaminated and homogenised through treatment with N-acetyl-L-cysteine (NALC). NALC (2.2.2) was freshly prepared prior to use as it is readily inactivated by oxidation. An equal volume of digestant was added to the sputum

and gently mixed fro no longer than 30 seconds. The mixture was allowed to stand for 15 minutes with occasional agitation. Following this, the liquefied sample was transferred to 50ml Falcon centrifuge tube. Phosphate buffer (67mM) was added to within 5ml of the top of the tube and centrifuged 2000 x g for 20 minutes (Summers and Good, 1985). The supernatant was removed and the pellet was resuspended in 500µl and stored at 4°C. Slides of digested material for microscopy were prepared as outlined in 2.4.3.3.

2.4 Staining, labelling and sample preparation for fluorescence light microscopy

2.4.1 Preparation of Fluorescent Probes, staining solutions and reagents

2.4.1.1 Nile Red

A stock solution of Nile Red (Molecular Probes, Invitrogen) was prepared at 0.5mg/ml in ethanol. This was filtered using a syringe and filter (2µm, Acrodisc) to remove any crystals in the solution. The bottle was wrapped in foil and stored at -20°C (Ch. The stock was diluted in ethanol to make a 10µg/ml solution for staining slides directly. This was stored in an amber bottle at room temperature (Garton et al., 2002).

2.4.1.2 Auramine O

Auramine O staining solution was prepared as detailed below:

Solution 1: 0.1g of Auramine O was dissolved in 10ml 95% ethanol.

Solution 2: 3.0g of phenol crystals were dissolved in 87ml distilled water.

The two solutions were mixed and stored in a tightly stoppered amber bottle (Weyer et al., 1999 - http://www.sahealthinfo.org/tb/microacid.htm).

2.4.1.3 Acid Alcohol

Acid Alcohol was made by adding 0.5ml concentrated hydrochloric acid to 100ml 70% ethanol (Summers and Good, 1985).

2.4.1.4 Potassium Permanganate

A 0.5% aqueous solution was prepared by dissolving 5.0g of potassium permanganate in 1L distilled water.

2.4.1.5 Sudan Black

Sudan Black (Sigma) powder (0.3g) was dissolved in 100ml 70% ethanol.

2.4.2 Labelling and Staining Protocols

2.4.2.1 Formaldehyde treatment of coverslips and slides

Slides and coverslips of immobilised *M. tuberculosis* were treated with formaldehyde to allow their safe removal from the containment suite. These were placed inside a glass slide box alongside a tissue soaked in 23% (w/v) formaldehyde and sealed. This was placed inside another box and sealed. The slides were fixed overnight and removed from the microbiological safety cabinet inside a clean slide box.

2.4.2.2 Labelling of Mycobacterial cells with Nile Red

Mycobacteria culture or cell suspension (200-1000µl) were washed by pelleting cells in 1.5ml micro-centrifuge tubes at a speed of 16 000 x g (in an Eppendorf 5415 D centrifuge, Helena Biosciences, Sunderland, UK). Cell pellets were resuspended in equal volumes of PBS and the process was repeated three times. 1µl Nile Red stock solution (0.5mg/ml in ethanol) was added for every 50µl cell suspension to give a final staining concentration of 10µg/ml. Labelled suspensions were incubated at 37°C for 10 minutes in the dark. The labelled cells were washed a further three times to remove Nile Red crystals from the solution and then immobilised on coverslips (2.4.3.2). Nile red-labelled cells were stored for future use at -20° C (Christensen et al., 1999).

When simultaneous Nile Red staining of a large number of samples was required it was more suitable to immobilise cells on coverslips prior to staining (2.4.3.2). Coverslips were placed in foil wrapped Petri dishes and covered in three changes of PBS. The

coverslips were then covered in a 10μg/ml solution of Nile Red in PBS for 10 minutes and finally washed in three further changes of PBS.

2.4.2.3 Auramine/Nile Red Dual staining of *M. tuberculosis*

Smears of digested sputum were prepared as described in 2.4.3.3. Slides were flooded with Auramine O solution for 15 minutes, washed in tap water and decolourised by flooding with Acid Alcohol for 15 minutes. The slides were washed with tap water and covered with 10μg/ml Nile Red solution in ethanol for 10 minutes and subsequently washed in tap water (Garton et al., 2002). Finally, the slides were covered in 0.5% potassium permanganate solution for no longer than 1 minute to reduce non-specific background staining, washed, blotted and allowed to dry. Glass coverslips were applied to the stained slides, which were mounted in PBS and sealed with colourless nail varnish.

2.4.2.4 Sudan Black/Ziehl Neilson Dual staining of *M. tuberculosis*

Fixed smears of decontaminated sputum or culture were flooded with 0.3% Sudan black and left for 15 minutes and rinsed in tap water. The slides were then flooded in xylene, left for 10 minutes and washed in tap water. Slides were then covered in Ziehl's carbol fuchsin (Beckton Dickinson), gently heated from underneath with a bunsen burner and allowed to steam for 5 minutes. Slides were washed in tap water and then washed with ZN decolourisation solution (Becton Dickinson) until the wash off ran clear. Finally, the slides were flooded with methylene blue for 30seconds, rinsed and allowed to dry. Glass coverslips were applied to the stained slides and mounted in PBS and sealed with colourless nail varnish. Slides were examined under ×100 oil immersion objective with bright field illumination (Method adapted from Burdon, 1946).

2.4.3 Preparation of slides and fluorescence microscopy

2.4.3.1 Preparation of APS coated coverslips

Coverslips were coated with 3'Aminopropyltriethoxysilane (APS) (Sigma-Alrich) in order to render the surface more suitable for immobilisation of bacteria. APS reacts with free hydroxyl groups on the glass resulting in a positively charged surface at a physiological pH (Wilkinson and Schut, 1998). Coverslips were passed through acetone to remove any contamination and laid out in a shallow glass tank. A solution of 2% (v/v) APS in acetone was prepared. A sufficient volume of APS solution to cover the coverslips was gently poured into the tank to prevent floatation of the slips. The tank lid was replaced and sealed with vacuum grease to prevent the evaporation of acetone and subsequent precipitation of APS. The coverslips were left in solution overnight and then washed in acetone to remove excess APS. Coverslips were then washed in water followed by acetone to prevent smearing. The coated surface was marked with a permanent marker pen to allow identification.

2.4.3.2 Immobilisation of bacteria on glass coverslips

Bacteria were immobilised on APS coated glass coverslips (2.4.3.1) using the Bellco slide microchamber systems developed by Walker et al (1994) and outlined in Figure 6 and Figure 7. The chamber system was constructed as demonstrated (Figure 6 and Figure 7) and 50µl volumes of cell suspension were dispensed into the wells. The slides were centrifuged at 1000 x g for 10 minutes in a IEC Centra-4X centrifuge (International Equipment Company, Dunstable, Bedfordshire, UK). The sealed chamber shown in Figure 7 was specifically used in the Containment laboratory and these were centrifuged at 1000 x g for 10 minutes (Mistral 3000L centrifuge), thereby avoiding the need for fixation prior to immobilisation of category 3 hazard organisms. The supernatant was removed from the wells using a pipette before the block was dismantled. The position of the spot was marked with a permanent marker pen on the underside for ease of

identification. Coverslips of immobilised *M. tuberculosis* samples were subjected to formaldehyde fixation prior to removal from the suite (see above). The coverslips were allowed to dry, mounted on a glass slide in PBS and sealed with colourless nail varnish (Barer, 1991).

Figure 6: Assembly of rectangular Bellco slide silicone chamber system for the immobilisation of bacteria on coverslips.

The system was assembled as indicated by dashed arrows and 50µl cell suspension was dispensed into each well.

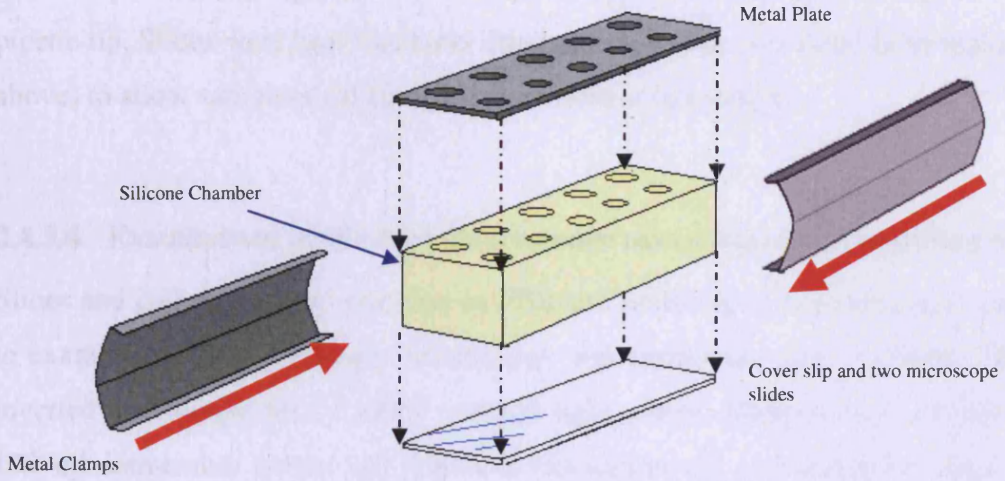

Figure 7: Assembly of universal tube silicone chamber system for the immobilisation of *M. tuberculosis* on coverslips.

The system was assembled as indicated by aqua arrow and 50µl cell suspension was dispensed into each well.

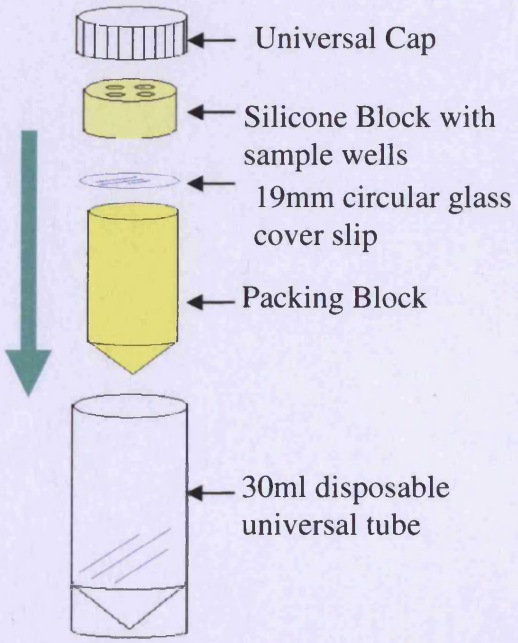

2.4.3.3 Preparation of sputum smears

Slides of decontaminated sputum samples (see above) were prepared for examination by microscopy. To make a smear, 10µl of digested material was deposited on a clean microscope slide and spread over an area of approximately $2cm^2$ using the side of the pipette tip. Slides were heat fixed and dried on a hot plate and fixed in formaldehyde (see above) to allow safe removal from the containment laboratory.

2.4.3.4 Examination of slides by fluorescence microscopy and recording of images

Slides and coverslips were mounted in PBS and sealed with colourless nail varnish prior to examination by microscopy. Microscopy was carried out using a Nikon Diaphot 300 inverted microscope with a 100W mercury light source. Bacteria were viewed under a × 100 oil immersion lenses and Citifluor immersion oil. A number of filter sets were employed for epifluorescence and are shown in Table 2. Images were obtained via a 12/10 bit, high speed Peltier-cooled CCD camera (FDI, Photonic Science, East Sussex, UK) and recorded using Image Pro Plus software (Media Cybernetics, U.S.A) (Cooney, 2000).

Table 2: Filter sets used for fluorescence microscopy.

Filter sets used are shown alongside the emission and excitation filter band widths and the dye or stain the filter was used to visualise.

Filter set	Excitation wavelength (nm)	Emission wavelength (nm)	Fluorescent dye or stain
11001V2 Blue (Chroma Technology Corp.)	470±40	>515	Auramine-O
G-2A (Nikon)	510-560	590±10	Nile Red
FITC (Nikon)	480±40	535±50	Green Fluorescent Protein, HAF

Chapter 3

Factors Affecting the Occurrence of Lipid Bodies in Mycobacteria

3.1 Introduction

Lipid Body (LB) formation in *M. smegmatis* has been shown to be environmentally regulated through previous work within this group (Garton et al., 2002). The formation of LBs by *M. smegmatis* cultivated in low nitrogen broth and their subsequent utilisation during carbon starvation supports the suggestion that these structures act as long term carbon storage depots. However, Barer and Garton (unpublished work) have proposed a dynamic role for LBs in regulating the Long Chain Fatty Acid-coenzyme A (LCFA-coA) pool in mycobacteria (Figure 8). The mycobacteria have an extraordinary requirement for LCFA because of the unusual high lipid content of the cell envelope; which consists largely of mycolic acids, unique LCFA derivatives of approximately 90 carbons in length (Reviewed by Minnikin et al., 2002). While the cell is actively growing, large amounts of LCFA must be acquired in order to synthesise new cell envelope components (discussed in the Introduction Chapter). An exogenous fatty acid source would therefore be extremely advantageous to the growing mycobacterium; however, LCFA is potentially toxic to mycobacteria due to its detergent like action (Kondo and Kanai, 1972). Therefore, storage of LCFA as triacylglycerol (TAG) within a LB structure may act as a buffer against LCFA toxicity and provide a source of fatty acids for biosynthesis of essential cellular components (Figure 8).

The proposed flow of LCFA through the cell is summarised in Figure 8 and described below.

LCFA may be taken up by the cell via a fatty acid transport system or may enter the cell by passive diffusion and is activated by the addition of coenzyme A (CoA) via the action of a fatty acid CoA synthase enzyme (Garton and Barer, personal communication). Depending on the requirements of the cell, the LCFA may be immediately utilised for the biosynthesis of complex cell envelope lipids. LCFA taken up by the cell are elongated via the actions of enzymes of the Fatty Acid Synthase (FAS) type II system (Reviewed in Chapter 1) to form fatty acids with chain lengths of up to 56 carbons in length (Cole et

al., 1998). Environmentally acquired LCFA, in addition to fatty acid (FA) formed through the *de novo* FAS I pathway, may also be channelled into phospholipid synthesis during periods of growth (Schweizer and Hofmann, 2004). When bacterial growth becomes arrested due to nutrient limitation or unfavourable changes in environmental conditions the biosynthesis of phospholipids and cell envelope lipids is likely to cease. As a consequence, surplus LCFA that would have been utilised in these processes is incorporated into TAG to form a carbon and LCFA source that may be exploited by the cell when environmental conditions become more favourable for growth (Walterman and Steinbuchel, 2005). TAG may initially be located in the cell envelope, where it may be utilised but saturation of the envelope with TAG may then lead to LB formation. TAG formation may also serve to detoxify the exogenous and endogenous cellular environment by incorporating LCFA into this inert storage molecule (McCarthy, 1971). The TAG biosynthetic pathway is outlined in Figure 9.

TAG is formed by the addition of a fatty acid chain to the biosynthetic precursor, diacylglycerol (DAG), via catalysis by a diacylglycerol acyl transferase enzyme (DGAT). Fourteen mycobacterial genes have been identified through their shared homology with a dual-function WS/DGAT enzyme from *Acinetobacter calcoaceticus* (Daniel et al., 2004). When cloned and expressed in *Escherichia coli*, these gene products showed DGAT/ triacylglycerol synthase (TGS) activity, with the gene product of *3130c* displaying the highest activity (Daniel et al., 2004). The gene products showed wax ester synthase activity at much lower levels and were therefore termed triacylglycerol synthases (TGS) and the most active gene, *3130c*, was designated *tgs1* (Daniel et al., 2004).

LCFA incorporated into TAG may be utilised in the biosynthesis of cell wall and membrane lipids or in the absence of a carbohydrate carbon source, used to generate energy in the form of ATP through catabolism by β-oxidation (see Chapter 1 for description). However, this is dependent on the release of stored fatty acid through the hydrolysis of TAG by a lipase (Deb et al., 2006). There are 21 putative lipase genes annotated on the *M. tuberculosis* genome (Cole et al., 1998). While none of the gene products have been shown to have TAG hydrolase activity, three more lipase genes have

been identified through their homology with a putative lipase from *M. tuberculosis* strain W17 (Deb et al., 2006). Expression of these genes in *E. coli* revealed that one of the gene products (designated LIPY) possessed TAG hydrolase activity. In addition, TAG utilisation during starvation was greatly diminished in a *M. tuberculosis* LIPY mutant (Deb et al., 2006)).

The recent studies of TAG metabolism, summarized above, lend some support to the proposed model of LB formation in *M. smegmatis*. However, application of this model of LB formation to *M. tuberculosis* has been impeded because little work has been carried out to characterise the conditions under which LBs form in *M. tuberculosis*. This is due to the fact that LBs have only been demonstrated anecdotally in *M. tuberculosis* isolated from sputum and have not been convincingly demonstrated in *M. tuberculosis* cultured *in vitro* (Garton et al., 2002).

LBs were first demonstrated in Acid-Fast Bacilli (AFB) in sputum from a patient suffering from TB in The Gambia (Garton et al., 2002). One third of tuberculosis cases in The Gambia are caused by *M. africanum* as opposed to *M. tuberculosis* (de Jong et al., 2007). Furthermore, acid-fast staining does not discriminate *M. tuberculosis* from other acid-fast mycobacteria. Therefore, a survey examining the occurrence of LBs in AFB in sputum samples taken from patients in Leicester (where infection with *M. africanum* is unusual) and The Gambia was undertaken in order to confirm whether this phenomenon was confined to one particular centre of infection and species or is a widespread observation.

During the course of the sputum survey it was contemporaneously demonstrated by microarray and quantitative real-time PCR analysis that the dormancy transcription regulatory gene, *dosR*, and *tgs1*, a gene linked to TAG accumulation and LB formation, are upregulated in *M. tuberculosis* cells in sputum (Garton et al., 2008). As a member of the DosR regulon (see Chapter 1), expression of *tgs1* has been linked to adaptation to non-replicating persistence (NRP) in the hypoxic shift-down model (Park et al., 2003) and in response to Nitric Oxide (NO) (Voskuil et al., 2003). Induction of several *tgs*

genes, accompanied by TAG accumulation, was also demonstrated in *M. tuberculosis* subjected to both the slow withdrawal of oxygen and NO exposure. Of these, *tgs1* showed the highest induction by both treatments (Daniel et al., 2004). The association of both hypoxia and NO exposure with LB formation have been examined.

Schnappinger et al. (2003) demonstrated that *M. tuberculosis* transcription is modified upon infection of murine macrophages. Gene expression of *dosR* and *tgs1* was up-regulated upon infection and increased further in response to macrophage activation. The conditions encountered by *M. tuberculosis* within the macrophage are discussed further elsewhere (Chapter 1); however, it is clear that the intracellular environment is an important factor for *M. tuberculosis in vivo*. A number of experiments were conducted using both a monocyte cell line and monocytes isolated from blood to determine the effect of macrophage internalisation on *M. tuberculosis* LB formation.

Drawing on all the evidence outlined above, which has characterised *tgs1* as an important "dormancy" related gene, it seems likely that *M. tuberculosis* forms LBs in response to DosR activating conditions. However, although they share the common ability to activate the DosR regulon there may be some important differences in the metabolic states induced by these conditions. Boshoff and Barry (2005) comment that while there is some overlap between the gene expression patterns induced by NO and hypoxia their effects on redox processes are expected to be different. In short, exposure to depleted oxygen or NO may result in two different metabolic states which share some common phenotypic characteristics. One such characteristic may be growth arrest. As described in previous sections (Chapter 1), cells subjected to the Wayne model of hypoxia become growth arrested upon the slow depletion of oxygen and Voskuil et al. (2003) have shown that NO reversibly inhibits respiration in *M. tuberculosis*. This raises the possibility that LB formation in response to these conditions is actually a result of growth arrest and may occur following exposure to stimuli that exert a DosR independent response in *M. tuberculosis*. To address this, the effect on LB formation in *M. tuberculosis* of a number of conditions which do not induce the DosR regulon was investigated.

The experiments described below were designed to examine the factors associated with LB formation in *M. tuberculosis*. The results were considered in relation to the proposed model of LB formation in *M. smegmatis* and the wider implications of *M. tuberculosis* physiology *in vivo*.

Figure 8: Proposed model for LBs in regulating the LCFA-coA pool in mycobacteria

It has been proposed that LBs may play a role in the regulation of long chain fatty acid (LCFA) flux through the myobacterial cell (Garton and Barer, unpublished results). LCFA are stored as triacylglycerol (TAG), via the pathway set out in Figure 9. TAG may be mobilized during periods of starvation by lipase degradation and β-oxidation of released fatty acids to yield energy in the form of ATP (Gurr and James, 1975). If environmental conditions are permissive for cellular replication, the activated long chain fatty acid may be elongated via the Fatty Acid Synthase system 2 (FAS2) and utilised in the formation of mycolic acid and other LCFA derivatives (Takayama et al., 2005). LCFA may also be utilised in phospholipid turnover during active growth, via the formation of the biosynthetic intermediate, Phosphatidic acid (PA). Acetyl- Co enzyme A (CoA) is the primer molecule for *de novo* synthesis of short chain fatty acids; which occurs via the FAS 1 system. Fatty acids are formed through condensation of acetyl-CoA and malonyl-CoA and may be used in cell envelope lipid or phospholipid biosynthesis (Takayama et al., 2005). LBs are formed depending on the environmental balance of availability of LCFA and conditions favourable for cell growth. If cell growth is rapid, the LCFA flux through the cell may be rapid due to cell wall lipid and phospholipid turnover. If the cell growth becomes arrested, LCFA that may have been utilised in these processes is diverted to TAG synthesis for storage. TAG may be present in the cell envelope, until it becomes saturated, whereupon it is stored in LBs. In addition, if LCFA is in excess it may be removed into TAG storage to avoid intra- and extra-cellular toxicity.

TAG synthesis is indicated by black arrows, other lipid biosynthetic pathways are indicated by blue arrows. Lipid degradation is shown in green. Enzymes are italicised and shown in red. Metabolic pools are enclosed in oval shapes.

Figure adapted from proposed model by Garton and Barer (unpublished results).

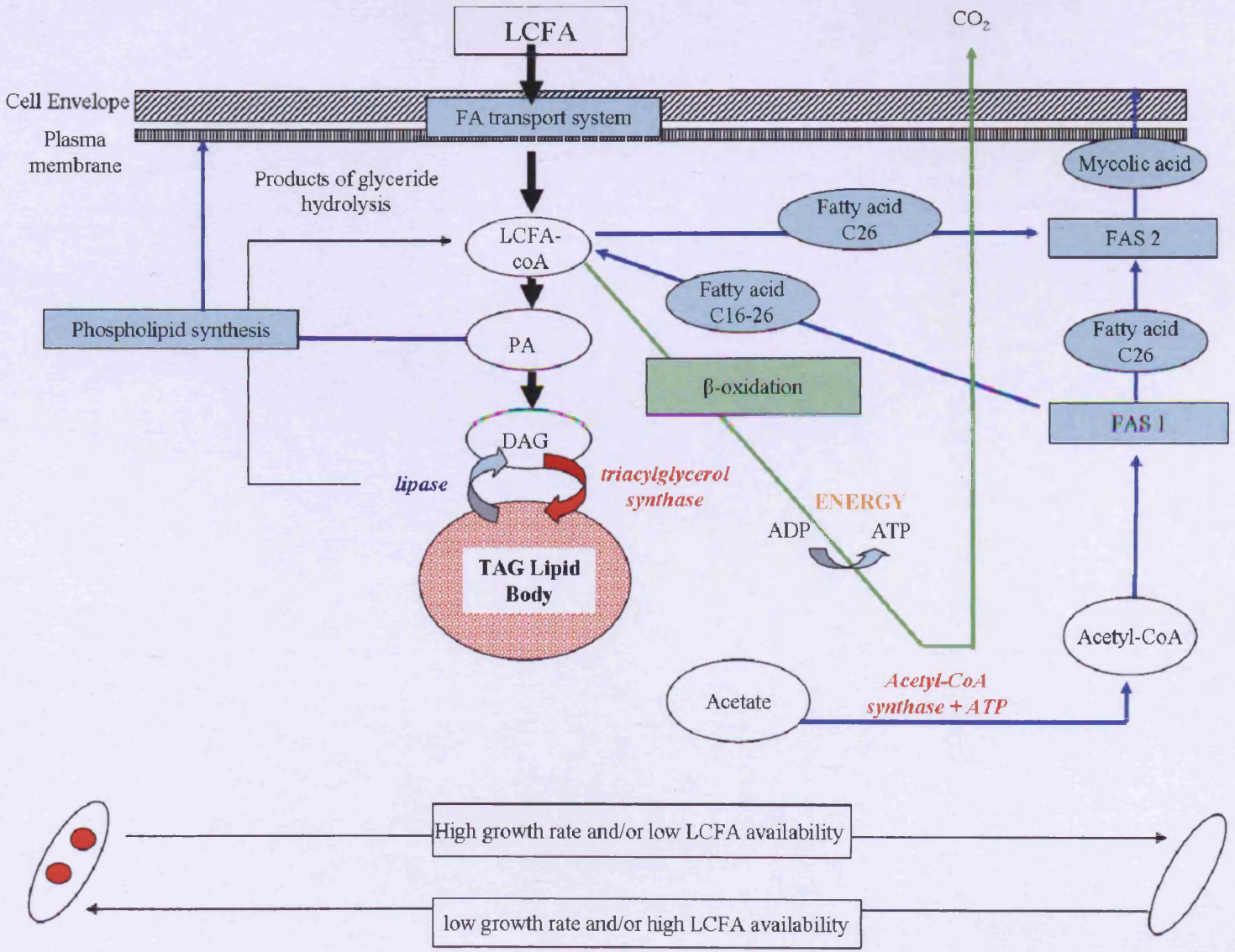
LCFA
CO_2
Cell Envelope
Plasma membrane
FA transport system
Products of glyceride hydrolysis
Mycolic acid
Fatty acid C26
LCFA-coA
FAS 2
Fatty acid C16-26
Phospholipid synthesis
PA
Fatty acid C26
β-oxidation
FAS 1
DAG
lipase
triacylglycerol synthase
ENERGY
ADP
ATP
TAG Lipid Body
Acetyl-CoA
Acetate
Acetyl-CoA synthase + ATP
High growth rate and/or low LCFA availability
low growth rate and/or high LCFA availability

Figure 9: Proposed model for the metabolic pathway of TAG formation in mycobacteria

The system shows a proposed scheme for the uptake and incorporation of long chain fatty acids (LCFA) into triacylglycerol (TAG). Fatty acids are activated by coenzyme-A (acetyl-coA), an ATP dependent reaction which is catalysed by a fatty acid CoA synthase (Gurr and James, 1975). If LCFA availability exceeds the requirements of the cell it may be esterified to diacylglycerol (DAG) to form TAG via the action of a triacylglycerol synthase enzyme (such as *tgs1*). The DAG pool may form from the result of acylation of existing monoglyceride or from dephosphoration of Phosphatidic acid (PA). PA is derived from acylation of glycerol phosphate to form lysophosphatidic acid, which is acylated further by lysophosphatidate to yield PA (Gurr and James, 1975). This reaction is represented in a simplified form in the diagram. TAG and DAG may be subsequently broken down by a lipase to replenish the LCFA-coA pool. Deb et al. (2006) identified a mycobacterial lipase with TAG hydrolase activity. As the pool of TAG increases the lipid collects in a LB structure (discussed further in Chapter 4).

Enzymes are shown in italics. Forward reactions are shown in red and reverse are shown in blue. Figure adapted from proposed model by Garton and Barer (Unpublished Results).

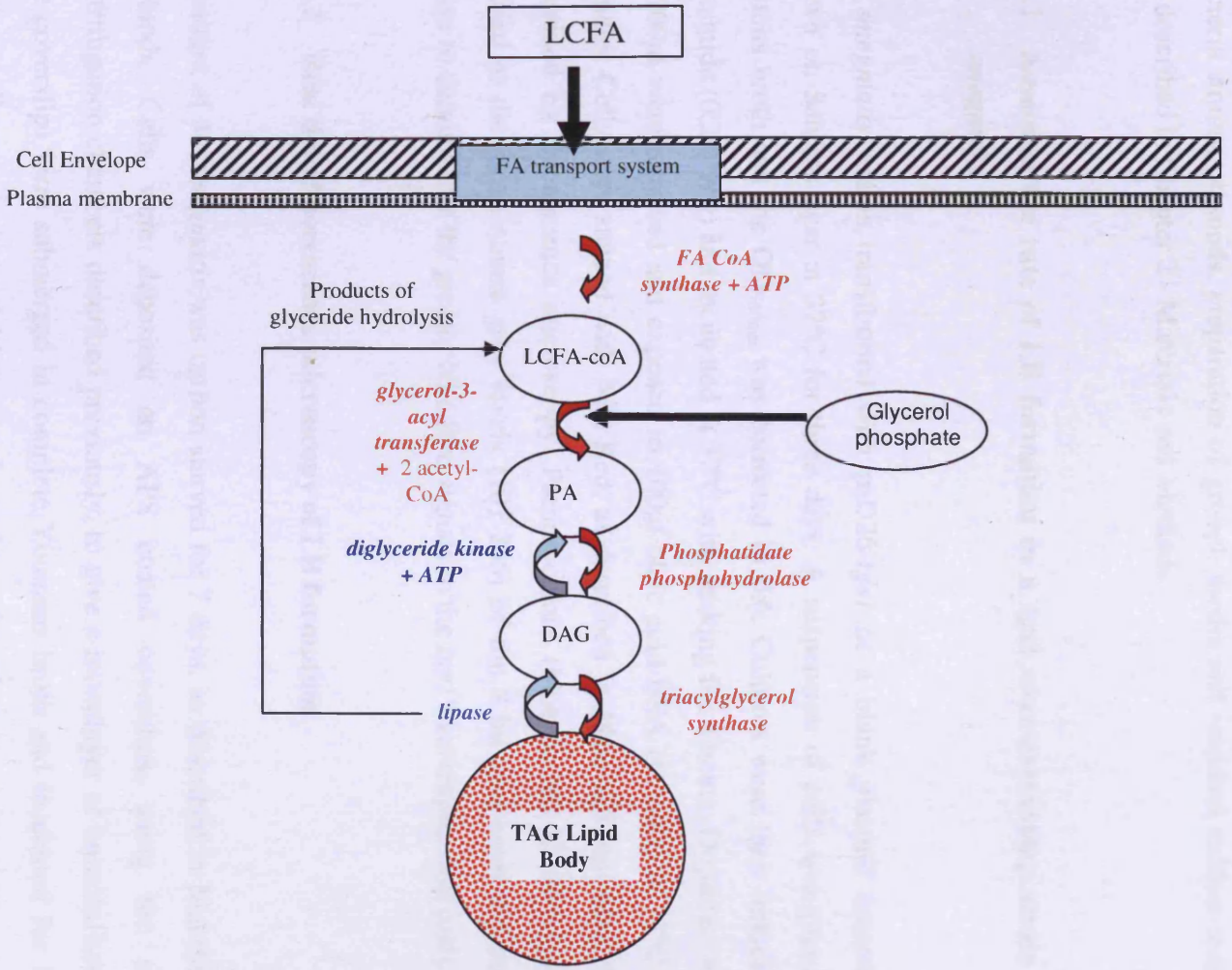
LCFA
Cell Envelope
Plasma membrane
FA transport system
FA CoA synthase + ATP
Products of glyceride hydrolysis
LCFA-coA
glycerol-3-acyl transferase + 2 acetyl-CoA
Glycerol phosphate
PA
diglyceride kinase + ATP
Phosphatidate phosphohydrolase
DAG
lipase
triacylglycerol synthase
TAG Lipid Body

3.2 Methods

Bacteria strains, plasmids, preparation of growth media and standard culture techniques are described in Chapter 2 - Materials and Methods.

3.2.1 Assessing the rate of LB formation in a tgs1 over-expressing strain of *M. smegmatis*

M. smegmatis strains transformed with psD26-*tgs1* or a blank plasmid control were grown on Sautons agar at 37°C for three days. A suspension of cells was prepared in Sautons broth and the OD_{580nm} was corrected to 0.6. Cultures were then induced with acetamide (0.2% v/w) and incubated at 37°C with shaking for 4 hours. Duplicate samples of 900µl were removed and exposed to 100µl oleic acid-BSA (6.3mM) at 37°C for 10 minutes. Cells were stained with Nile Red, as described in Materials and Methods and examined by fluorescence microscopy. Pseudo-colour (blue to red-10 divisions) was applied to the most intense grey levels (101-255) of the 8-bit grey-scale fluorescence image to demonstrate the greater Nile Red signals in the *tgs1* over-expressing cells.

3.2.2 Real time fluorescence microscopy of LB formation

A culture of *M. smegmatis* was carbon starved for 7 days, as described in Materials and Methods. Cells were deposited on APS coated coverslips, using the silicone centrifugation chambers described previously, to give a monolayer of immobilised cells. The coverslips were submerged in complete Youmans broth and incubated for 1 hour. The coverslips were removed, blotted to dry and transferred to a heated microscope stage, set at 37°C. Cells were located by phase contrast microscopy and focussed using the Image Pro Plus preview function. A 20µl drop of complete Youmans broth containing 630µM oleic acid and 0.5µg/ml Nile Red was placed on top of the cell monolayer. Fluorescence images were taken every 2 minutes, avoiding exposure in between time

points in order to reduce photobleaching. Pseudo-colour was applied to the 8-bit fluorescence image as described above.

3.2.3 Generation of LBs in *Mycobacterium tuberculosis*

M. tuberculosis was exposed to a number of conditions to assess their affect on LB formation. The general experimental design is outlined in Figure 10 and any variations are detailed in the appropriate section.

Figure 10: Standard procedure for assessing the effects of different conditions on LB formation in *M. tuberculosis*

A roller bottle culture of *M. tuberculosis* was prepared as described in Materials and Methods. This was incubated with rolling at 37°C for 4-5 days and growth was monitored by measurement of optical density. An exponentially growing (doubling over 24 hours) culture at an OD_{580nm} of 0.4-0.6 was exposed to the test or control condition for the appropriate time. Following this, samples for LB assessment were removed and frozen at -20 °C. All samples from a single experiment were thawed together and batch stained with Nile Red.

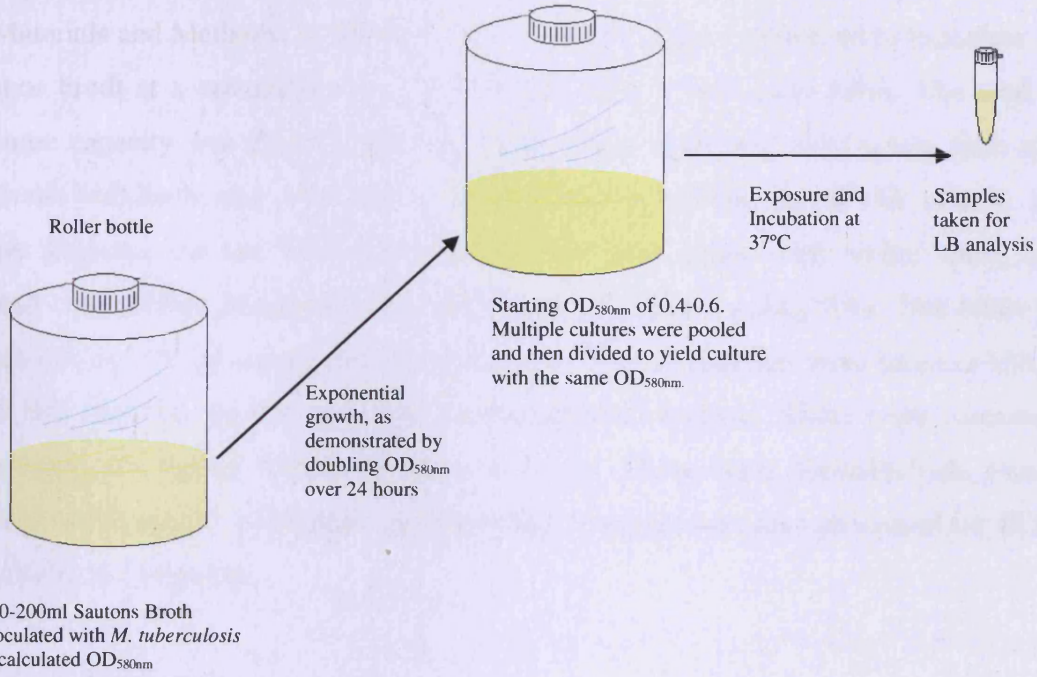

3.2.4 Conditions examined for their influence on LB formation

Low oxygen:

Cultures of *M. tuberculosis* were exposed to hypoxia as described.

The Wayne Model:

This experiment was carried out in collaboration with Claire Senner, St George's University of London, according to the method described by Wayne and Hayes (1996).

Cultures of *M. tuberculosis* strains H37Rv and CH were prepared as described (Chapter 2-Materials and Methods) in Middlebrook 7H9 broth. These were used to inoculate 17ml Dubos broth at a calculated OD_{580} of 0.004 in 20x125 mm glass tubes. The total tube volume capacity was 25.5ml, therefore there was a calculated head space ratio of 0.5 (8.5ml/17ml).Each tube contained a sterile magnetic stirring bar (PTFE coated, 1.5 x 8mm magnetic stir bar, Fisher Scientific).Tubes were sealed with rubber lined, screw thread caps (Fisher Scientific) and sealed with laboratory sealing film. The tubes were incubated at 37°C on a magnetic stir plate set at 120rpm. Samples were taken at 168, 288 and 504 hours by sacrificing a tube for microscopic analysis. Slides were prepared by spreading of 10µl of culture to make a smear. These were formaldehyde fixed as described (Chapter 2 – Materials and Methods). Samples were also processed for TEM as described in Chapter 4.

Hypoxic Incubator:

A culture was prepared as described. 25 ml of culture was placed in two $75cm^3$ cell culture flasks with gas permeable tops (NUNC, USA). One was transferred to the static hypoxic incubator and the other to a static CO_2 incubator, as a control. A further 25ml of culture was incubated in a 50ml culture flask with shaking and all were incubated at 37°C. The oxygen concentration inside the hypoxic incubator was adjusted to 19% and the culture was allowed to equilibrate to this concentration for 2 days. Following this, the oxygen concentration was adjusted daily to the following concentrations: 15%, 10%, 5%

and 1%. Cultures were removed from the incubators after a total of 6 days and slides were prepared for microscopic examination.

Anaerobiosis:

Evenly inoculated, 5 day old lawn plates of *M. tuberculosis* were prepared as described in Chapter 2. Test plates were placed inside air tight bags (AnaeroGen plastic pouches, Oxoid) (3 to a bag) with an anaerobic generating envelope (AnaeroGen compact foil sachet, Oxoid) and sealed. Anaerobic indicator strips (Oxoid) were included in the plastic pouches to visually confirm that anaerobic conditions were achieved. Control plates were double bagged, to comply with the Containment Lab Code of Practice. Test and control plates were incubated for 4 or 24 hours at 37°C. Lawn growth was harvested by disruption of the layer with a sterile cell spreader and emulsification in 5ml Middlebrook 7H9 broth. Antibiotic tolerance assays were prepared (Chapter 6) and samples were taken for microscopic examination.

3.2.5 Subjection of a chemostat grown culture of *M. tuberculosis* to low oxygen conditions

Chemostat cultures of *M. tuberculosis* H37Rv were kindly provided by Joanna Bacon (Health Protection Agency, Porton Down). Cultures were grown to steady state conditions in 1 litre chemostat vessels. The system was subject to a constant flow rate of 15ml/hour to give a working culture volume of 500ml and a mean generation time of 24 hours. Cultures were propagated at a dissolved oxygen tension (DOT) of 50% and maintained at 37°C for 8 days. Following this, culture was transferred to fresh vessels and the DOT was adjusted to 20% and allowed to stabilise for 2-3 days. Cultures were subjected to low oxygen concentration by a stepwise reduction of the DOT from 20% to 1% over a period of 5-7 days. Cultures at a DOT of 1% were allowed to achieve steady state growth before samples were taken (Bacon et al., 2004). Samples were received as frozen pellets of culture and were immediately transferred to a freezer at -80 °C. Specimens for microscopic analysis were taken by aspiration of frozen stocks in PBS.

3.2.6 pH Shock

Acid:

Duplicate cultures of *M. tuberculosis* were prepared as indicated in Figure 10 and described in Chapter 2. Samples (20ml) of culture were removed to 50ml Falcon centrifuge tubes and pelleted at 2000 x g for 30 mins at 37°C. Pellets were resuspended in 20ml Sautons broth at a range of pH: 4.5, 5.5 and 7. Culture was separated into volumes of 500µl in screw top micro-centrifuge tubes and incubated in a hot block at 37°C with occasional agitation. Duplicate samples were removed every 5 minutes within a 30 minute period and placed on ice. Samples were then stored at -20 °C prior to the preparation of slides for microscopic examination.

Alkali:

Duplicate cultures of *M. tuberculosis* (Figure 10) were subjected to alkaline conditions as outlined above. Pellets of culture were resuspended in Sautons broth at a range of pH: 9.5, 8.5 and 7. Culture was separated and incubated as described above.

3.2.7 Temperature Shock

Heat shock:

Duplicate cultures of *M. tuberculosis* (Figure 10) were divided into volumes of 500µl in screw top micro-centrifuge tubes and incubated in hot block at 50°C, with occasional agitation. Control samples were incubated at 37 °C. Duplicate samples were removed every 5 minutes within a 30 minute period and placed on ice. Samples were then stored at -20 °C prior to the preparation of slides for microscopic examination.

Cold shock:

Duplicate cultures of *M. tuberculosis* (Figure 10) were subjected to cold shock as described above, with incubation at 30 °C.

Duplicate cultures of *M. tuberculosis* (Figure 10) were divided into 20ml volumes in Universal tubes (Sterilin). These were sealed with laboratory sealing film (Nesco, Osaka, Japan) and double bagged individually. Tubes and bags were swabbed before transfer to a shaking water-bath at 20 °C. Control cultures were incubated with shaking at 37 °C. 1ml samples were taken hourly over a 24 hour period and frozen at -20 °C prior to preparation of slides for microscopy.

3.2.8 Nitric Oxide Exposure

A volume of 10mM solution of the nitric oxide donor, Spermine NONOate (SPER/NO), or the control compound, Spermine tetrahydrochloride (SPER.4HCL) in sterile distilled water, was added to an exponential culture of *M. tuberculosis* to give a final concentration of 100µM. SPER/NO powder was handled under a flow of nitrogen gas due to its oxygen sensitive nature. All NO experiments were carried out with culture grown in Sautons Broth, using a final concentration of 100µM of SPER.4HCL or SPER/NO to match the conditions used by Daniel *et al* (2004).

3.2.9 Exposure of *M. tuberculosis* to Nitric oxide over a time course of 24 hours

Following the addition of SPER/NO or the control compound the culture was immediately divided into 500µl aliquots in sealed micro-centrifuge tubes inside Falcon 50ml centrifuge tubes and incubated with rolling at 37°C. An aliquot was removed every 30 minutes, for a period of 24 hours. Cells were deposited on coverslips, stained with Nile Red and examined microscopically. The numbers of cells with and without LBs were enumerated.

3.2.10 Exposure of *M. tuberculosis* to Nitric oxide over a time course of 30 minutes

An exponentially growing culture was exposed to NO as described above and divided into 11ml aliquots in 50ml Falcon centrifuge tubes. These were sealed, swabbed and incubated with manual shaking in a 37°C waterbath. A tube was removed every 5 minutes, for 30 minutes, and immediately placed on ice. Cells were deposited on coverslips, stained with Nile Red and examined microscopically.

3.2.11 Infection of Monomac 6 macrophage cell line with *M. tuberculosis*

Non- adherent Monomac 6 (MM6) macrophages were infected with *M. tuberculosis* strains H37Rv and CH. Cultures of both strains in Middlebrook 7H9 were grown as described (Chapter 2) to an OD_{580nm} of 0.4 and washed twice in PBS to remove any Tween residues that may lyse the macrophage cells. MM6 cells were kindly provided by Bernard Burke (Leicester University) and were enumerated using a haemocytometer. 5ml of MM6 cells at a concentration of 5 x 10^6/ml were mixed with 5ml *M. tuberculosis* culture in RPMI cell medium to give an overall concentration of 2.5 x 10^6/ml MM6 and an OD_{580nm} 0.2 for *M. tuberculosis*. *M. tuberculosis* cells were not enumerated in this experiment as the primary objective was to examine the formation of LBs during the course of infection and not any changes in bacteria numbers. MM6 cells were infected for 4 hours and then washed 5 times in 5ml Hanks salt solution with 2% fecal calf serum (FCS) by centrifugation at 100 x g for 5 minutes and gentle resuspension. The infected cells were resuspended in a final volume of 10ml RPMI media containing 1% FCS and labelled "Monomac". The washings were saved and pelleted at 2000 x g for 15 minutes. The resulting pellets were resuspended in 10ml RPMI and 1% FCS and labelled "extracellular". Cultures of *M. tuberculosis* H37Rv and CH were also incubated directly in RPMI with or without 1% FCS as a control. After 24 hours of infection 2ml of infected MM6 cells or 1ml "extracellular" bacilli were treated with NALC by the method described (Chapter 2) to disrupt the macrophages and release intracellular bacteria. The pellet obtained after NALC treatment was washed 3 times in PBS and resuspended in 100µl PBS, 20µl of which was used to prepare slides for microscopy. Examination of

these slides revealed that background staining due to cell debris was still very high and few individual bacteria were present. Therefore, 1-2ml samples taken at 48 hours and 5 days after infection were pelleted at 16 000 x g for 2 minutes and resuspended in an equal volume 0.07% SDS. Samples were then washed in 3 times PBS and used to make slides. The remainder of all samples were stored at -20°C.

3.2.12 Infection of Primary Blood Monocytes with *M. tuberculosis*

This work was carried out in collaboration with Bernard Burke and Natalie Garton.

Primary Blood Monocytes (PBMC) were isolated from blood and enumerated by Bernard Burke. These were dispensed into 24 well tissue culture plates (Corning) in 1ml volumes and incubated with CO_2 at 37 °C for 5 days to allow maturation of monocytes to macrophages. Sterile coverslips were placed in a number of wells to allow direct examination of *M. tuberculosis* within the macrophage. On the fifth day of maturation macrophages were adherent to the bottom of the plate wells and coverslips. Antibiotic containing RPMI was removed from these cultures, followed by 2 washes in antibiotic free RPMI. Cultures of *M. tuberculosis* had previously been grown and enumerated by CFU prior to storing at -80 °C. Macrophages were infected with *M. tuberculosis* H37Rv and CH at a Multiplicity of Infection (MOI) of 0.1. After 4 hours of infection, the medium was removed and the macrophage cultures were washed with two medium changes in order to remove extracellular bacteria. Plates were incubated at 37 °C with CO_2 with or without hypoxia. Samples for LB analysis were removed on d0, d3, d6 and d9 of infection by the addition of 200µl of 0.25% SDS to wells in order to lyse macrophages. These samples were used to prepare slides for the examination of released intracellular bacteria and their LB content. Coverslips were also removed at these time points. Coverslips were treated in two ways:

1. The medium was removed and replaced with 1.5% Glutaraldehyde for 5 minutes and then washed 3 times in PBS.
2. The medium was removed and monolayers were fixed in formaldehyde vapour.

Fixed coverslips were stained with Auramine and Nile Red as described previously.

3.2.13 Mycobacterial RNA extraction and manipulation

All RNA manipulations were carried out using precautions to minimise the degradation of RNA by Ribonuclease (RNase) contamination. To this end, gloves were worn at all times and were changed frequently. RNase free filter pipette tips were used and all equipment and work areas were treated with RNaseZap (Ambion) to remove surface RNase decontamination. All reagents used were dedicated RNA work stocks and were kept separately from other laboratory reagents. In addition, all work was carried out on ice to reduce RNase activity and prevent degradation of RNA.

Preparation of Guanidine thiocyanate (GTC) solution

Guanidine thiocyanate (GTC) solution was prepared by mixing the following reagents in 200ml distilled water:

GTC	295.4g
Sodium N-lauroyl sarcosine	2.5g
1M sodium citrate (pH 7.0)	12.5ml
Tween-80	5ml

The solution was incubated overnight at 37°C with shaking to allow the GTC to dissolve fully. The solution was made up to a volume of 500ml with distilled water. Immediately prior to use, 7µl/ml β-mercaptoethanol was added to the GTC solution (Lee, 2007).

3.2.14 RNA extraction from *M. tuberculosis* H37Rv

M. tuberculosis culture samples (5ml) were taken for RNA extraction. GTC solution was added in four parts to one part culture volume to stabilise the RNA. The cells were pelleted at 2000 x g for 30 minutes and the supernatant was removed. The pellet was

resupended in 200µl GTC solution and transferred to a screw cap micro-centrifuge tube. The suspension was pelleted by centrifugation and the supernatant was removed using fine-tipped filter pipette tips. The pellet was overlaid with 1ml TriReagent/Trizol (Sigma) and the samples were frozen at -80°C prior to further extraction steps.

Prior to lysis, ceramic beads (Lysing matrix A, Qbiogene, UK) were added to the Trizol and cells. In addition to the physical disruption of the cells, Trizol also maintains the integrity of the RNA. The bacteria were lysed using a reciprocal shaker (Ribolyser, FastPrep FP120, ThermoSavant) set at 6.5m/s (vertically) for 45 seconds. Samples were then allowed to cool at room temperature for 10 minutes before the addition of 200µl of chloroform. The samples were mixed by vortexing and centrifuged at 16 000 x g for 3 minutes (in a Heraeus FRESCO 17 centrifuge, Thermo Electron Corporation) at 4°C to separate the aqueous and phenolic phases. The aqueous phase was transferred to a new tube and care was taken to avoid carry over of interphase material. The aqueous phase was re-extracted with the addition of an equal volume of chloroform. The tubes were centrifuged as before to separate the phases. The aqueous phase was removed to a new tube and an equal volume of isopropanol was added to this and mixed by inversion. Glycoblue co-precipitant was added to each tube to a final concentration of 150µg/ml and mixed by inversion. RNA was allowed to precipitate overnight at -20°C.

The tubes were centrifuged at 16 000 x g at 4°C for 10 minutes to reveal blue pellets of RNA. The supernatant was removed and discarded and the pellets were washed twice in 70% (v/v) ethanol. Ethanol was removed and the pellets were allowed to completely air-dry before resuspension in 100µl RNase-free water.

The extracted RNA was purified using an RNeasy Mini Column, including the optional on-column DNase-free DNase set (Qiagen) and following the manufacturer's instructions. Buffer RLT (350µl) was added to each 100µl sample of RNA. To this, 250µl ethanol was added and mixed by pipetting. The samples were placed in an RNeasy Mini column inside a collection tube. Tubes were centrifuged for 15 seconds at 9600 x g and both the collection tube and flow through were discarded. The columns were then

transferred to new collection tubes and 350µl buffer RW1 was applied to each column. Tubes were centrifuged for 15 seconds at 9600 x g and the flow through was discarded. On column digestion was performed by adding a mixture of 10µl DNase1 and 70µl RD1 to each column. This was incubated at room temperature for 15 minutes, following which, the columns were washed with the addition of 350µl buffer RPE. Tubes were centrifuged and the flow through was discarded. The columns were washed in the same manner, with the addition of 350µl buffer RPE to each tube but with centrifugation for 2 minutes. The flow through was discarded and the tubes were centrifuged for a further 1 minute to remove excess buffer. The columns were transferred to fresh collection tubes and 50µl RNase free water was applied to each column to elute the bound RNA. The tubes were incubated at room temperature for 5 minutes prior to centrifugation for 1 minute at 9600 x g (Lee, 2007).

3.2.15 RNA quantification by spectroscopy

A crude estimate of extracted RNA concentration was made by spectroscopy. RNA (1µl) was diluted in 50µl RNase free water in a UV cuvette (Eppendorf). RNase free water was used as a blank. Absorbance of RNA was measured at 260nm in a spectrophotometer.

The concentration of RNA was calculated using the equation below, assuming that an absorbance of 1 is equivalent to 40µg/µl RNA (Lee, 2007).

$$C = \frac{A \times 40 \times D}{1000}$$

Where: C = concentration (µg/µl)
A = absorbance at 260nm
D = dilution factor
1000 = converts ml to µl

3.2.16 Reverse-transcription Polymerase chain Reaction (RT-PCR) using genome directed primers

Extracted RNA was reverse-transcribed to yield cDNA. Reverse-transcription was carried out using SuperScript II Reverse Transcriptase (Invitrogen) and Mycobacterial genome directed primers (mtGDPs) (Rachman et al., 2006 - Primers listed in Appendix 1). Genome directed primers were designed to amplify all the known open reading frames of the *M. tuberculosis* H37Rv genome. These mtGDPs consist of 37 heptamers and octamers and are used to prime first strand cDNA synthesis. The following reagents were used in each 18µl reaction inside an RNase free PCR tube:

dNTPs (10mM)	1.5µl
mtGDPs (10pmol/µl)	1.5µl
RNA	0.5µg*
Water	to 18µl

*the volume of RNA suspension varied between samples according to concentration extracted. Where possible, 0.5µg of RNA was used in the reaction but if the concentration of extracted RNA was less than this, half the available RNA was used. The concentration of extracted RNA was divided by 0.5 to give the volume in µl to be added to the reaction.

The reactions were heated to 65°C in a PCR machine for 5 minutes and then immediately snapped cooled on ice to disrupt the secondary structure of the RNA. The following reagents were then added to the reaction:

5x Superscript II reaction buffer (Invitrogen)	6µl
DTT 0.1M	3µl
RNasin Ribonuclease inhibitor (20 units/µl) (Promega)	1.5µl

The tubes were incubated at 25°C for 2 minutes inside a PCR machine to allow primer annealing, the reaction was subsequently quenched on ice. Finally, 1.5µl Superscript II reverse transcriptase was added to each sample before two further incubation steps in the PCR machine. Duplicate tubes were set up for each sample without the addition of

reverse-transcriptase. These acted as "no-RT" controls to monitor non-specific amplification of DNA contamination. Tubes were incubated at 25°C for 10 minutes and reverse transcription was carried out at 42°C for 50 minutes, following this, the reaction was quenched by incubation at 70°C for 15 minutes (Lee, 2007).

3.2.17 Real-time Quantitative PCR using Taqman probes

Real-time quantitative PCR was performed using Taqman probes and Absolute QPCR Master-mix (ABgene).This master-mix contained reaction buffer, dNTPs, $MgCl_2$ and a hot start DNA polymerase.

Reagents were aliquoted into 0.1ml Rotor-gene tubes (Corbett Research):

Template cDNA	1µl
Forward primer (6.25µM)	1µl
Reverse primer (6.25µM)	1µl
Taqman probe (3.75µM)	1µl
qPCR master mix	12.5µl
Nanopure water	8.5µl

Tubes containing ten-fold dilutions of a known concentration of *M. tuberculosis* CDC1551 genomic DNA (10^7-10^2 and $5x10^6$) were run in parallel and acted as known standards. A standard curve of gene copy number was generated by Rotor-gene software and this was used to calculate the test gene copy number. DNA contamination of test samples was estimated including a set of tubes containing the cDNA from the no-RT controls generated from each sample. The results from these controls were subtracted from the test results. Therefore, for each sample there were 3 test tubes and 3 no-RT control tubes.

The PCR was carried out in a Rotor-gene 6000 (Corbett Research) Real-time quantitative PCR machine using the conditions set out below:

Temperature hold for activation of hot-start Taq polymerase	95°C	15 minutes
Cycling (40 cycles):		
	95°C	15 seconds
Primer annealing	56-60°C	60 seconds
Fluorescence acquisition	72°C	60 seconds

Table 3 shows the primer annealing temperatures and the fluorescence signal acquired during PCR cycling.

Table 3: Annealing temperatures and fluorescence signal acquisition for RT-PCR Taqman assays.

Temperatures and parameters for RT-PCR were taken from Lee (2007). Fluorescence was acquired for FAM (carboxyfluorescein) or JOE (6-carboxy-4',5'-dichloro-2',7'-dimethoxyfluorescein) at a temperature of 72°C.

Assay	Primer Annealing temperature	Fluorescence signal acquired
16S	56°C	FAM
sigA	60°C	JOE
tgs1	56°C	FAM

3.2.18 Statistical analysis

All statistical analysis was carried out using Minitab 14 statistical software. Sets of data were compared using a Paired Two Sample t-test. Anderson Darling normality and variance ratio tests were preformed to confirm that t-test assumptions of normal distribution and equal variance were not violated. P values are shown at 95% confidence. The symbol ± indicates the above and below the average value of duplicate data sets.

For expression data, the value obtained for DNA contamination was subtracted from that of the triplicate values obtained for gene copy number. As the DNA controls were not specific to any one of the samples, every permutation to control for DNA contamination was calculated. The expression of *tgs1* was divided by that of *sigA* to normalise. Every possible combination was calculated and averages and standard deviations were taken of this set of values.

3.3 Results

3.3.1 LB formation in *M. smegmatis*

Garton et al. (2002) have previously demonstrated LB accumulation in *M. smegmatis* by fluorescence microscopy. Variations of the defined medium, Youmans broth (YB) were used to manipulate the occurrence and pattern of cell labelling by the neutral lipid dye, Nile Red. Cells grown in a low carbon YB showed an annular pattern of labelling with Nile Red, while a low Nitrogen YB yielded cells with large intracellular LBs. Addition of exogenous oleic acid to carbon starved cells led to LB formation in these cells after 10 minutes.

This work was repeated in order to confirm the observations set out above and to establish a set of defined conditions for promotion of LBs in *M. smegmatis* to be used in subsequent studies. In addition, wax ester storage was examined in *M. smegmatis*. The Acinetobacter TGS1 homologue, WS/DGAT, is know to possess wax ester synthase properties, however, wax ester storage has not previously been observed in *M. smegmatis*.

For full details of cultivation of *M. smegmatis* the reader is referred to Chapter 2, however, for simplicity methods are described briefly here. Cell mass for low carbon treatment was generated from an overnight culture of *M. smegmatis* grown in Middlebrook 7H9 with Tyloxapol in place of Tween. The LB content of *M. smegmatis* grown in broth with Tyloxapol is much reduced in comparison to cells grown in the presence of Tween (NJ Garton, Personal Communication). This prevents large initial LB numbers in the innoculum that is to be subject to conditions of low carbon. Cell mass was then incubated in Low-Carbon Youmans Broth (LCYB) for 7 days. To examine LB formation in *M. smegmatis*, low carbon culture was amended with glycerol and incubated for 1 hour prior to the addition of BSA emulsified oleic acid (OA) and incubated for a further hour.

A time course of LB formation in *M. smegmatis* was examined by a simple real time fluorescence microscopy method. Slides of immobilised low carbon cells were incubated in complete Youmans Broth, following which, uptake of Nile Red labelled oleic acid was observed by fluorescence microscopy.

LB formation was examined after culture of *M. smegmatis* in Low Nitrogen Youmans Broth (LNYB) and in Mineral Salts Medium containing hexadecanol for wax ester promotion.

Characteristic labelling patterns were observed for each growth condition, corresponding to the observations made by Garton et al. (2002). Nile Red labelling was restricted to the cell envelope and peripheral deposits in low carbon cells. Upon addition of exogenous long chain fatty acids to the culture medium, these low carbon cells formed large LBs, indicated by strong intracellular signals of Nile Red labelling, with very little labelling of the cell envelope. Cells from cultures which were grown with low nitrogen or in the presence of hexadecanol formed large LBs, which were also readily observed under phase microscopy (Figure 11).

Real time observation of LB formation proved to be challenging due to the difficulty in keeping the image in focus and rapid fading of the Nile Red dye. This problem prevented the capture of images of initial labelling by Nile Red or observations of LB formation over a prolonged period of time. However, fluorescence images taken over a time course of LB formation in *M. smegmatis* did reveal that LBs are formed at the cell periphery and the increase in label intensity, together with the growth in size of the body, suggests that the lipid concentration is increasing at these sites (Figure 13).

LB formation was also examined in strains of *M. smegmatis* transformed with the acetamide inducible plasmid psD26 with and without a *tgs1* insert. Enhanced LB formation, demonstrated by an increase in Nile Red signal, was clearly demonstrated in the TGS1 overexpressing strain in comparison to the control strain following oleic acid

supplementation (Figure 12). This work was carried out in collaboration with Natalie Garton. Enhanced TAG accumulation was also demonstrated in the overexpressing strain in the experiment (carried out by NJ Garton) (Garton et al., 2008).

Figure 11: LB formation in *M. smegmatis* is dependent on growth condition

M. smegmatis was grown under various growth conditions: **a)** low carbon, **b)** low carbon followed by oleic acid supplementation, **c)** low nitrogen and **d)** with hexadecanol. Top panels show phase contrast images and bottom panels show Nile Red fluorescence signals. Bar is equal 2μm. Images are representative of observations carried out on samples taken in numerous experiments, except for panel (d) which represents one experiment.

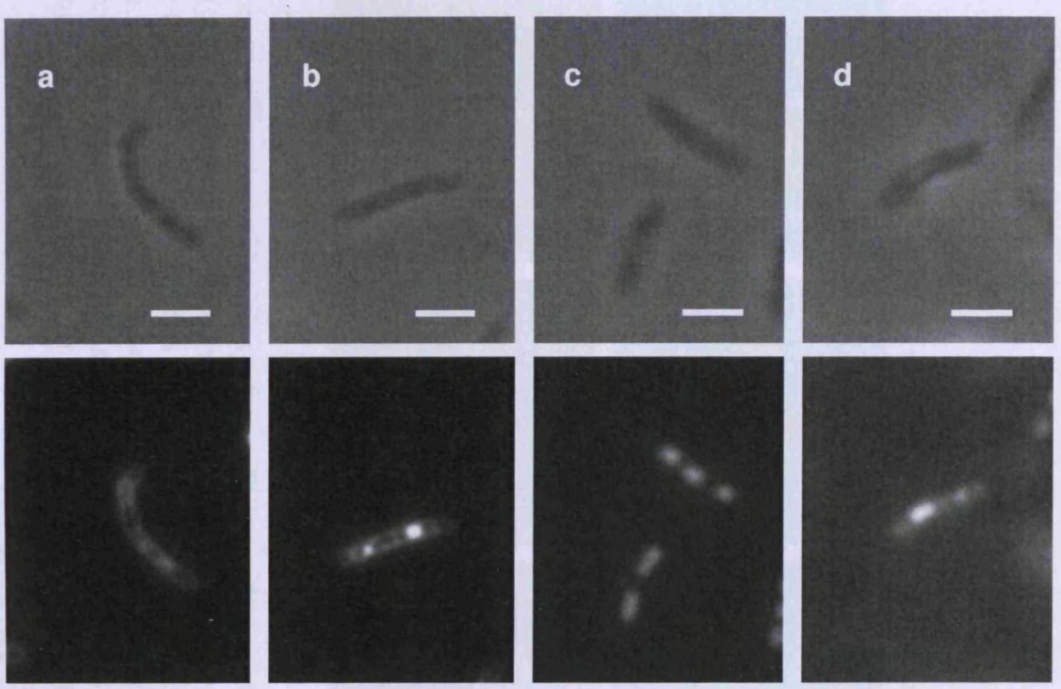

Figure 12: Overexpression of tgs1 in *M. smegmatis* leads to enhanced LB formation

M. smegmatis psD26 and psD26-*tgs1* were induced with 0.2% (w/v) acetamide for 4 hours and then exposed to 630μM OA for 10 minutes. Cells were labelled with Nile Red and examined by fluorescence microscopy. Pseudo-colour (blue to red 10 divisions) was applied to the most intense levels (101-255) of the 8-bit grey-scale fluorescence image to demonstrate the greater Nile Red signals in the TGS over-expressing cells. Scale bar is equal to 2μm. Images represent one experiment.

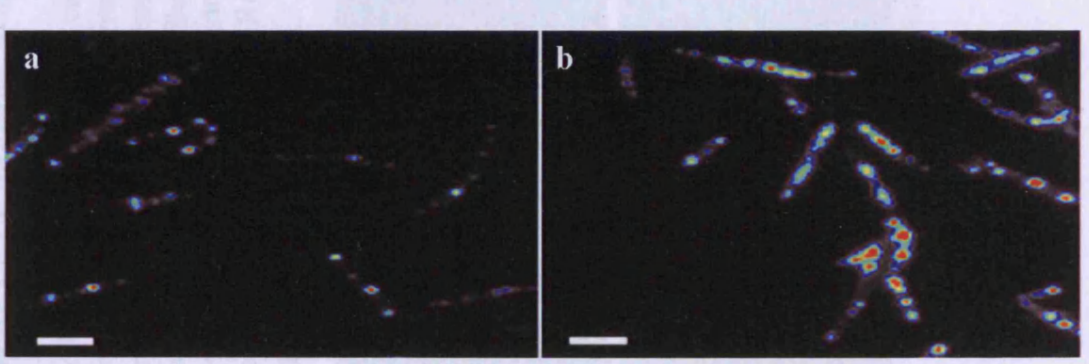

Figure 13: LB formation in *M. smegmatis* occurs at the cell periphery

Cells grown in media low in carbon were immobilised on coverslips and incubated in complete Youmans Broth for 1 hour. Coverslips were blotted dry and transferred to a heated microscope stage set at 37°C. Cells were located by phase microscopy and 20µl Youmans Broth with 10% OA supplementation was placed on top on the immobilised cells. Nile Red was added to the broth to a final concentration of 0.5µg/ml. Fluorescence images were taken every 2 minutes and were not exposed between time points in order to avoid photo-bleaching. Pseudo colour was applied in 10 divisions to the most intense grey levels (101-255) of the 8 bit image to demonstrate increasing Nile Red signals. Scale bar is equal to 2µM. Images of cells are representative of observations made over two replica experiments.

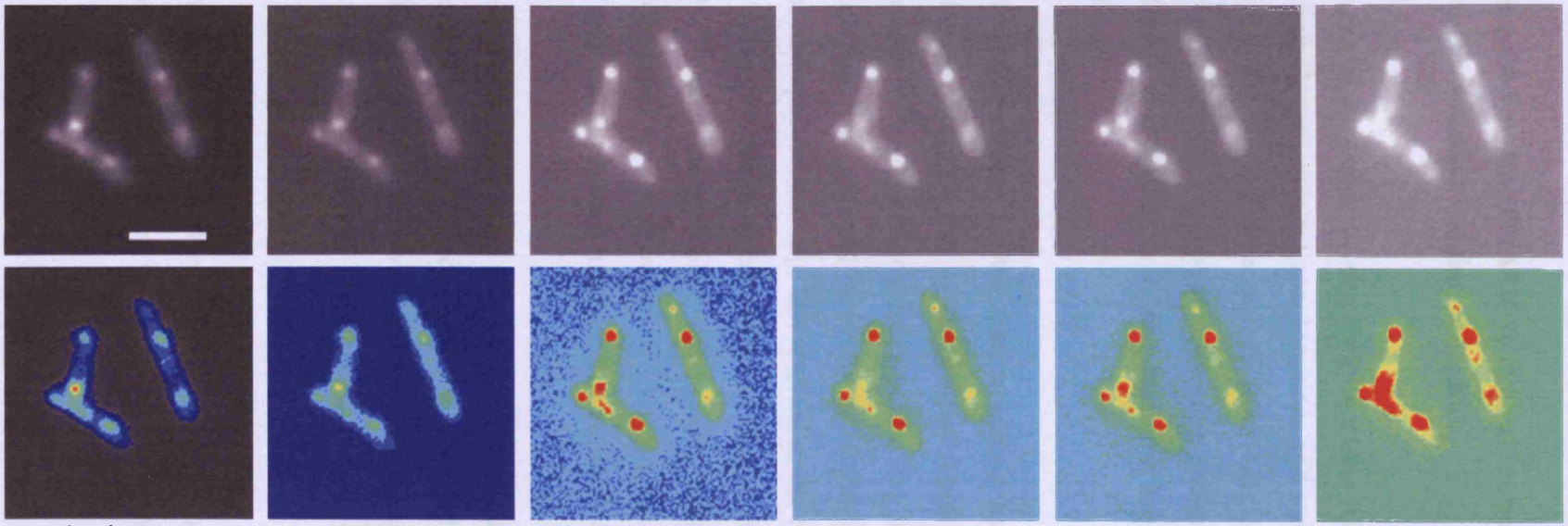

3.3.2 LB demonstration in Acid-Fast Bacilli (AFB) in clinical sputum specimens using a dual Nile Red-Auramine-O staining procedure

A simple dual staining method was developed to identify LBs within AFB in sputum. A number of staining solution formulations, reagent concentrations and staining times were examined in order to optimise the fluorescence signals from LBs and AFB, while maintaining minimal background staining. The optimum staining method remained very similar to that described by Garton et al. (2002), with the addition of methods to decrease background staining of specimens.

Background staining of cell debris present in the sputum sample by Nile Red was extremely variable despite attempts to reduce this by digestion of sputum with N-acetyl-L-cysteine (NALC) and treatment with potassium permanganate. In a number of cases, high background staining with Nile Red obscured intracellular LB fluorescence signals. Depending on the severity of non-specific staining, this resulted in the examination of a greater number of fields of view in order to obtain sufficient data or occasionally this rendered the slide unreadable. Numbers of AFB also varied greatly between samples. A minimum of 100 cells were assessed for the presence of LBs and this population was expressed as a percentage of total cells examined in which LBs could be observed.

LBs were almost universally present in AFB in all sputum specimens examined. The only specimens in which LBs were not observed had contained very few AFB. In these cases the presence of LBs would be undetectable if it was a feature of less than 10% of cells. The observed number of LB positive cells and LB numbers per cell varied between samples (Figure 14).

LBs were observed in sputum specimens collected from patients with symptoms of tuberculosis both in The Gambia and Leicester. Although the numbers of LB positive

cells appeared to be greater in Gambian samples (Figure 15), there was no significant difference (P=0.180) between the means of the two sets of results.[1]

[1]Statistical tests are described in the Materials and Methods section of this chapter.

Figure 14: The number of LB positive cells and LB per cell are heterogeneous in dual stained sputum specimens

Smears of digested sputum were stained with the Auramine O for 15 minutes, followed by decolourisation in acid-alcohol for 10 minutes, staining with Nile Red 10μg/ml for 10 minutes and treatment with 0.5% potassium permanganate solution for 1 minute to reduce non-specific background staining. Smears were examined for LB positive AFB.

The number of LB positive cells varied substantially from 3-80% of the population of AFB in sputum samples collected from patients in The Gambia and Leicester. The bottom panel shows fields of view with AFB with high (e) or low LB (f) positivity, respectively. Top panels (a-d) show the wide variation in LB numbers observed per cell, from 0-8, respectively. Images show Nile Red fluorescence in cells confirmed as Acid Fast Bacilli by dual labelling with Auramine-O. Bar is equal to 2μm. See also Garton et al. (2008).

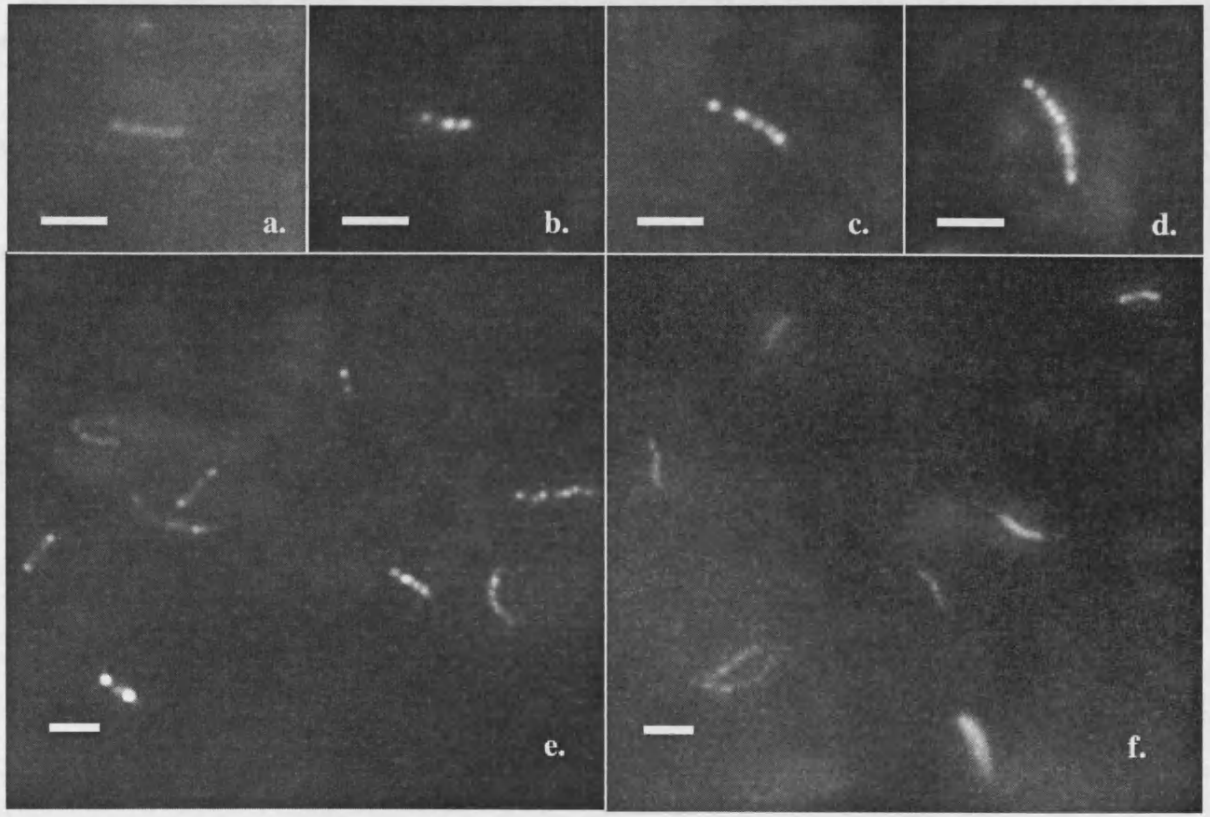

Figure 15: Numbers of LB positive AFB demonstrated by dual staining of sputum samples collected from patients in The Gambia and Leicester.

Sputum samples were collected from patients in The Gambia and Leicester. Smears of samples were dual stained with Auramine and Nile Red and examined for LB positive AFB. The LB positive population is expressed as a percentage of the total population examined. The graph shows the distribution of LB numbers in samples taken from both centres of infection.

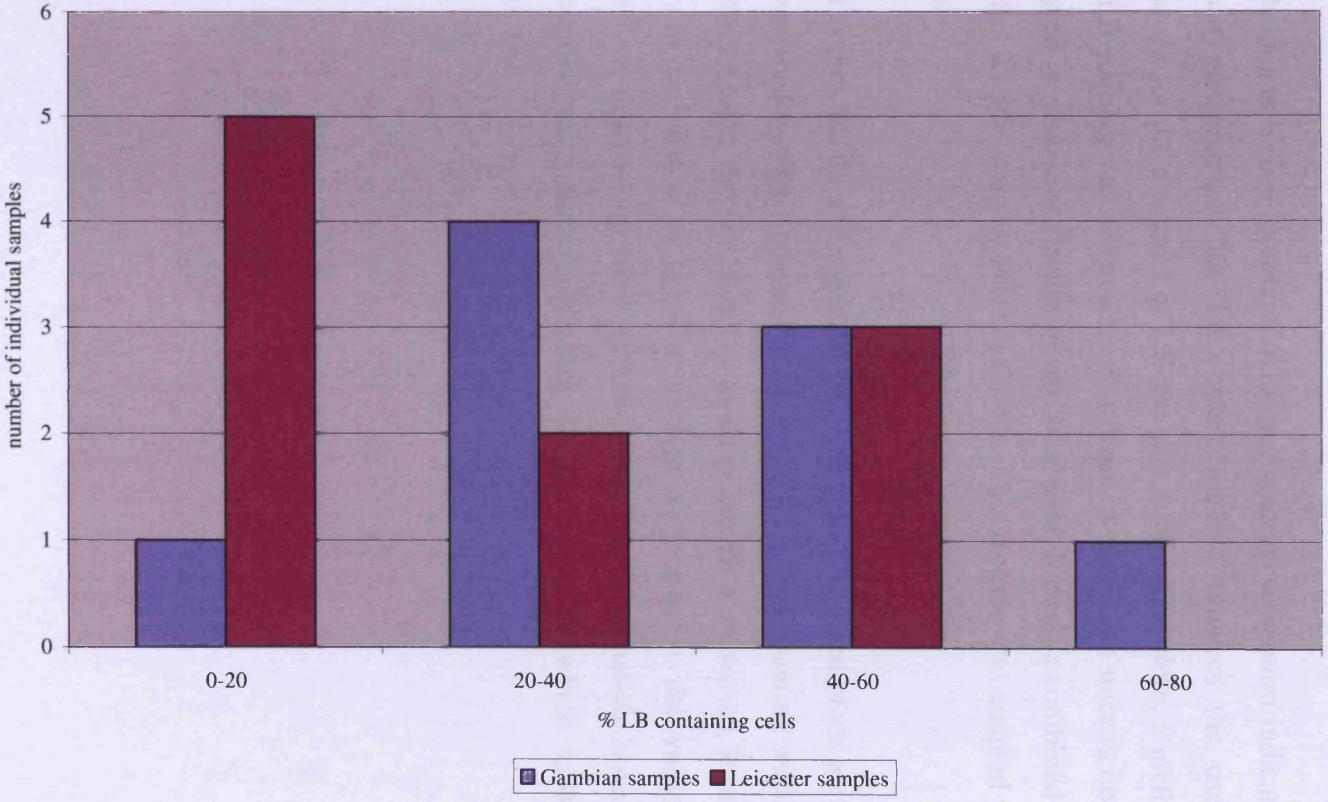

3.3.3 LB demonstration in AFB in clinical sputum specimens using a combined Sudan black-Zeihl Neelsen stain

The presence of LBs as a universal feature of AFB populations in sputum indicates that this is a widespread phenomenon but the current method requires the use of a fluorescence microscope for the detection of LB positive AFB. Therefore, a method for dual Acid-fast and LB staining was devised for examination with light microscopy. LBs were first demonstrated in numerous species of mycobacteria through a combined Sudan Black and Zeihl carbol fuchsin stain by Burdon (1946). This method was adapted for use with sputum smears.

AFB were observed as pink bacilli and a number of these cells contained black inclusions in sputum smears examined by this method (Figure 16). Background staining with Sudan black was still relatively high, despite attempts to keep this to a minimum level. This resulted in difficulty in the location of Acid-fast cells in comparison to the Auramine-O acid-fast stain. Therefore, this method was not adopted for LB examination; however, it was successfully applied to sputum specimens in Malaysia, in which LBs were demonstrated (Figure 16).

Figure 16: Demonstration of LBs in sputum specimens by a combined Sudan Black and Ziehl Neelsen stain.

Image was kindly provided by Eddy Cheah and shows a Sudan Black stained sputum specimen taken from a patient in Malaysia. The arrow indicates an example of a LB and the bar is equal to 10μm.

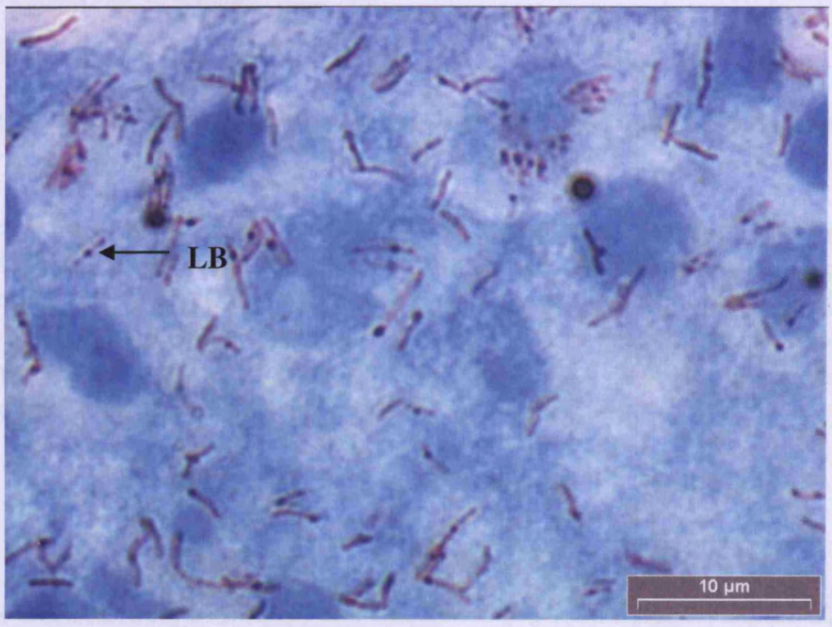

3.3.4 LB formation in Wayne dormant *M. tuberculosis*

M. tuberculosis H37Rv and CH, a clinical strain responsible for a large outbreak of TB (Rajakumar et al., 2004), were subjected to Wayne's hypoxic shift down model of non replicating persistence. Nile Red labelling demonstrated LB formation in both strains during non-replicating persistence phase 1 (NRP1), with increasing numbers observed in NRP2 (Table 4). This work was carried out in collaboration with Claire Senner of St George's, University of London.

Table 4: LBs are formed in *M. tuberculosis* subjected to Wayne's shift-down model of hypoxia

M. tuberculosis strains H37Rv and CH were exposed to hypoxia through careful replication of Wayne's hypoxic shift down model. At each time point, one tube was sacrificed for the preparation and Nile Red staining of slides for microscopic analysis. The number of LB positive cells observed is expressed as a percentage of the overall cell number counted. The average number of LBs per cell is also shown, with the range shown in brackets. Data represents results from one experiment.

Strain	168 hours		288 hours		504 hours	
	% LB	Av. LB/cell	% LB	Av. LB/cell	% LB	Av. LB/cell
H37Rv	29	1 (1-3)	50	2 (1-3)	41	2 (1-5)
CH	42	1 (1-6)	65	2 (1-4)	56	2 (1-4)

3.3.5 LB formation in *M. tuberculosis* under conditions of reduced oxygen

Wayne's Shift-down system of hypoxia is perhaps the most widely used and characterised approach for generating hypoxia in mycobacteriology. LBs have been shown to form in Wayne NRP cells following exposure to hypoxia in this model (3.3.4). The aim of these experiments was to evaluate the use of alternate hypoxic conditions stimulating the formation of LBs and to confirm that this event is a general response to

hypoxic conditions and not specific to NRP cells. *M. tuberculosis* was subjected to two additional methods to generate hypoxia.

For one method, a culture was placed within a static hypoxic incubator. Controls were grown with and without shaking at atmospheric oxygen. The other method involved the incubation of solid *M. tuberculosis* culture inside air-tight pouches with an anaerobic generation envelope.

LBs were formed in *M. tuberculosis* subjected to both conditions (Table 5). However, LBs were also observed in control cultures for the first time. This will be addressed in the discussion section.

Table 5: LBs are formed in *M. tuberculosis* in response to two models of hypoxia

Cultures incubated in a static hypoxic incubator subjected to a step-wise reduction in oxygen concentration from 20-1% over 5-7 days. Plates of *M. tuberculosis* lawn growth were incubated within sealed pouches, alongside anaerobic generating sachets for 4, 24 and 48 hours. Samples were stained with Nile Red and examined by microscopy. The number of LB positive cells is expressed as a percentage of the overall cell population examined. Data was obtained for single replicas.

Hypoxic Model	**LB%**	
	Test	**Control**
1% oxygen, static hypoxic incubator	50	-
Shaking control 6 days	-	11
Standing control 6 days	-	47
Anaerobic envelopes 4 hours	42	15
Anaerobic envelopes 24 hours	41	15
Anaerobic envelopes 48 hours	21	12

3.3.6 LB formation in *M. tuberculosis* in response to NO exposure

M. tuberculosis was subjected to NO exposure over a 7 hour period to determine its ability to stimulate the formation of LBs and identify a time course of LB formation.

LBs were formed after 30 minutes of NO exposure and peak LB accumulation occurred after 4-4.5 hours (Figure 17a). LB numbers subsequently declined over time and assessment at 24 hours revealed that the number of cells with LBs had halved, compared to peak exposure levels. Interestingly, further experiments revealed that the LB content of cultures exposed to NO for 4 hours (see Chapter 6) had approximately halved upon examination after 24 hours of exposure (Table 6).

Following demonstration of LB formation in *M. tuberculosis* subjected to 30 minutes of Nitric Oxide treatment, a short-term exposure experiment was carried out to determine the start of LB accumulation within that period. LBs were observed in *M. tuberculosis* after only 5 minutes of NO exposure (Figure 17b) and these numbers continued to increase to similar levels observed in previous experiments after 30 minutes of exposure. LBs were not observed in control samples.

Figure 17: Time course of LB formation in response to NO

Culture was exposed to a single dose of the NO donor, Spermine NONOate (SPER/NO), or the control compound, Spermine tetrahydrochloride (SPER.4HCL) to a final concentration of 100μM. Exposed culture was divided into 500μl aliquots and incubated with rolling at 37°C. One tube was removed for microscopic analysis every 30 minute. For short course of LB formation in response to NO, culture was divided into 11ml aliquots. Tubes incubated in a 37°C water-bath, with manual shaking. Samples were taken every 5 minutes. The number of LB positive cells is expressed as a percentage (LB%) of the total cell population counted. LB % formation is shown over a time period of 7 hours **(a)** and 30 minutes (as an average of 2 values) **(b)**.

a)

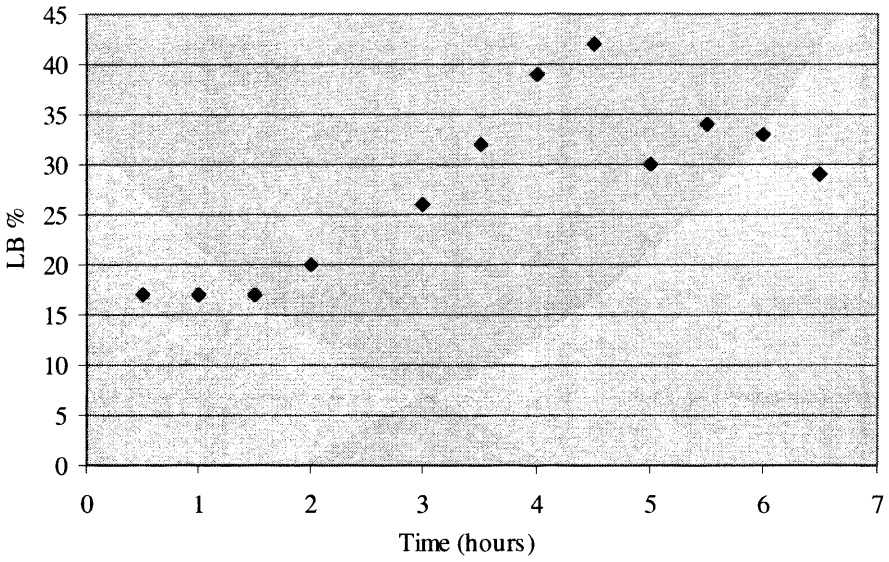

b)

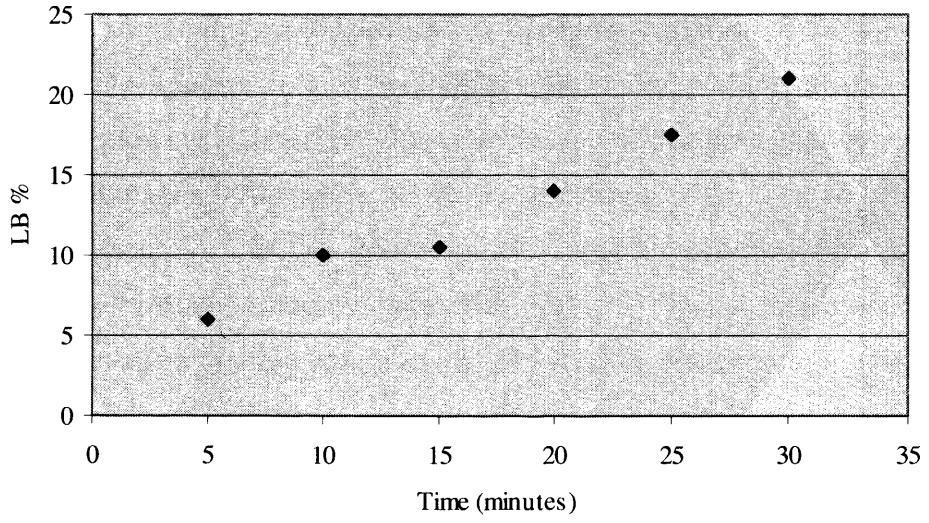

Table 6: LB positive populations of *M. tuberculosis* halve following 24 hour incubation

Cultures (200ml) of *M. tuberculosis* were exposed to 100μM SPER/NO or the control compound and incubated. The LB content of these cultures was assessed after 4 and 24 hours exposure. In one experiment LB content was assessed after 48 hours (*experiments in which this sample was not taken) The LB content of populations of cells exposed to NO for 4 hours approximately halved when examined after 24 hours exposure. No LBs were observed in the control cultures. Single LB counts were taken.

	LB %		
	4	24	48
Replica 1	64	29	*
Replica 2	47	23	*
Replica 3	46	17	7

3.3.7 Gene expression in Lipid Body positive populations of *M. tuberculosis* following NO exposure

LB formation in *M. tuberculosis* was shown to peak after 4-4.5 hours of NO exposure. Daniel et al. (2004) had previously demonstrated that expression of *tgs1* is induced by NO treatment, with maximum levels of expression occurring after a concurrent time of 4 hours of exposure. The expression of *tgs1* has also been implicated in LB formation in *M. smegmatis* and *M. tuberculosis* isolated from sputum, indicating a likely role for TGS1 in LB accumulation following NO treatment. In order to analyse the gene expression of *tgs1* in relation to LB formation, RNA was extracted from cultures of *M. tuberculosis* treated with NO donor or control compound. Extracted RNA was reverse transcribed and gene copy numbers were evaluated using real time PCR (Table 7). The average expression of *tgs1* in duplicate cultures was up-regulated by 245 fold in comparison to the control value.

Table 7: tgs1 is expressed by *M. tuberculosis* in response to Nitric Oxide exposure

RNA was extracted from duplicate *M. tuberculosis* cultures exposed to NO donor or control compound. Gene copy numbers were quantified using a Real-time quantitative Taqman assay. Gene copy numbers were normalised to *sigA* and average values taken from two replica cultures are shown. Standard deviation was calculated as indicated in Materials and Methods of this Chapter. Corresponding LB counts are expressed as a percentage of the total cell population taken.

Time following NO exposure (hours)	Control		NO	
	tgs1	LB%	*tgs1*	LB%
0	0.11 (SD 0.14)	0	0.15 (SD 0.19)	0
4	0.22 (SD 0.27)	0	49 (SD 22)	46
24	0.24 (SD 0.63)	0	2.2 (SD 2.07)	17

3.3.8 LB formation in *M. tuberculosis* DosR mutant and complemented strains following NO exposure

The formation of LBs have been shown to correspond to *tgs1* expression following NO treatment (see above) and in this study a DosR deleted mutant strain was used to determine the role of DosR in regulating this phenotypic response. DosR mutant and complemented strains were exposed to NO donor or control and LB formation was assessed by microscopic analysis after 4 hours of treatment. LB formation was shown to occur in duplicate cultures of the DosR disrupted mutant strain (mean LB%= 18 range = ± 1.5), all be it at a diminished level in comparison to the complemented strain (mean LB%= 35 range = ± 2). Cultures exposed to the control compound did not contain LBs.

3.3.9 LB formation in the presence and absence of Tween-80

Tween 80 is used in media to improve dispersal of *M. tuberculosis* cells. Tween 80 is a polyethylene sorbitol ester with oleic acid as the principle fatty acid constituent.

M. tuberculosis may hydrolyse Tween 80 to release fatty acids for LB formation. *M. smegmatis* grown in media containing Tween readily form LBs but not to the same extent when Tween is replaced with the detergent Tyloxapol. The aim of this experiment was to ascertain the importance of Tween as a fatty acid source in LB formation in *M. tuberculosis* during NO exposure.

The cultures were grown in Sautons broth with Tween. Prior to treatment with NO, the cultures were pelleted and resuspended in either Sautons with Tween or Tyloxapol. Cultures were exposed to NO donor or control, as before and LB formation was assessed after 4 hours treatment. LBs were formed in NO treated cells in duplicate cultures incubated in both media containing Tween (mean LB%=20 range = ± 3) and Tyloxapol (mean LB%=31 range = ± 1). The number of LBs was lower than expected within the Tween incubated group but correspondence between duplicate cultures was good under both conditions. No LBs were observed in control cultures.

3.3.10 LB formation in *M. tuberculosis* isolated from monocytes

Non-adherent Monomac 6 macrophages were infected with *M. tuberculosis* strains H37Rv and CH and samples were taken over the course of infection for examination of isolated bacilli and their LB content. No LBs were observed in either strain of *M. tuberculosis* isolated from macrophages at 24, 48 or 120 hours after infection or in control cells incubated in RPMI cell culture medium.

LB formation was also examined in Primary Blood Monocytes. As these cells were directly isolated from blood, it was felt that they provided a more relevant comparison to alveolar macrophages encountered by *M. tuberculosis* during infection. Activated and naïve macrophages were infected with *M. tuberculosis* H37Rv and CH and incubated with or without hypoxia. The results were technically unsatisfactory, as few bacteria were harvested from infected cells. Intracellular bacteria released following 3 days of infection were not numerous enough to form a conclusion regarding the LB content of cells within

the population. However, there were sufficient numbers of *M. tuberculosis* H37Rv bacilli isolated to evaluate LB formation on day 6 but not day 9 of infection. LB formation appeared to occur in naïve and activated macrophages incubated at ambient oxygen concentrations. Growth of bacteria was assessed by CFU by Bernard Burke and data is presented in Appendix 2. The numbers of LB positive cells increased in macrophages incubated initially under normoxia for 3 days followed by hypoxia for a further 3 days (Table 8). Interestingly, the growth of bacteria in this culture of *M. tuberculosis* H37Rv and *M. tuberculosis* H37Rv in activated macrophages had begun to decline at day 6 of infection. However, growth of *M. tuberculosis* in naïve macrophages cultured at ambient oxygen concentrations continued to increase at this time point. Therefore, it is difficult to say whether LB formation coincided with a decrease in growth rate. Control cells incubated in RPMI did not contain LBs but there were insufficient numbers recovered for a confident comparison.

Macrophages were also allowed to adhere to sterile coverslips prior to infection with *M. tuberculosis*. Coverslips were removed at the times outlined above and were stained with Auramine-O, for the location of intracellular bacilli and Nile Red, to examine LB formation in intracellular bacteria. Intracellular *M. tuberculosis* bacilli were visualised through Auramine staining, however, Nile Red staining of macrophage lipid material obscured any signals localised to the bacteria.

Table 8: LBs may form in *M. tuberculosis* H37Rv following infection of Primary Blood Monocytes

Primary macrophages isolated from blood were infected with *M. tuberculosis* for 4 hours. Infected cells were incubated with CO_2 at atmospheric O_2 or within a hypoxic incubator. Macrophages were lysed with SDS treatment and released bacilli were stained with Nile Red and examined microscopically. The number of LB positive cells is expressed as a percentage of the total population examined. Results are shown for bacteria isolated after 6 days of infection and represent data from a single replica experiment.

Condition	LB%
Normoxia	14
Normoxia and IFN-γ activation	12
Normoxia→Hypoxia	23

3.3.11 LB promotion in *M. tuberculosis* by non-DosR activating stimuli

The capacity of *M. tuberculosis* to form LBs in response to heat, cold, acid and alkali shock was examined. Culture was exposed to shock treatment for 30 minutes and samples were taken for microscopic analysis. LBs were demonstrated in all treated cultures of *M. tuberculosis* (Table 9). Again, LBs were observed in the control samples. This may be due to experimental design and this will be considered in the discussion. In a separate experiment, *M. tuberculosis* was subjected to 20°C cold shock, however, no LBs were observed in the control or test samples.

3.3.12 LB formation in Chemostat cultures in hypoxic or nutrient limited conditions

Steady state chemostat cultures of *M. tuberculosis* were subjected to low oxygen, low phosphate and low iron. Cultures were exposed to a low oxygen concentration by a stepwise reduction of the dissolved oxygen tension (DOT) from 20% to 1% over a period of 5-7 days. The control cultures was grown at steady state at a DOT of 50% in an iron and phosphate replete medium. LBs were demonstrated in all test cultures (Table 10).

Table 9: LBs are formed in *M. tuberculosis* in response to growth arresting stimuli

Cultures of *M. tuberculosis* H37Rv were subjected to various shock treatments for 30 minutes. For pH shock, cultures were pelleted, resuspended in Sautons broth at the appropriate pH and divided into micro-centrifuge tubes. Cultures for temperature shock were divided into micro-centrifuge tubes and incubated at the appropriate temperature. Tubes were incubated in a hot block with manual agitation. Samples were stained with Nile Red and examined microscopically. The number of LB positive cells is expressed as a percentage of the total population observed and represents the average of data collected from 2 replica samples. * no duplicate

Treatment	Mean LB %	Range	Av. LB number/cell
pH 7 control	11	1	4
Acid pH 4.5	40	2	3
Acid pH 5.5	29	*	4
Alkali pH 8.5	29	5	4
Alkali pH 9.5	34	7	3
Temperature control 37°C	12	10	4
Cold shock 30°C	38	10	4
Heat shock 50°C	25	5	3

Table 10: LBs are formed in response to hypoxic and nutrient limiting conditions in chemostat cultures of *M. tuberculosis*

Culture material was pelleted and frozen. Samples for microscopy were removed by aspirating frozen material in PBS. Samples were stained with Nile Red and examined by microscopy. The number of LB positive cells is expressed as a percentage of the total population observed for single samples.

Chemostat growth condition	LB%	Av. LB number/cell
Low phosphate	56	3
Low Iron	17	2
Low oxygen	34	3
Low iron and low oxygen	34	2
Control	<1	-

3.4 Discussion

3.4.1 Fluorescence microscopy of Nile Red stained cells revealed characteristic staining patterns in *M. smegmatis* grown under different growth conditions

These results confirm the findings reported by Garton et al. (2002) that manipulation of the growth condition affects the occurrence of LBs in *M. smegmatis*. Cultivation in low nitrogen broth leads to the formation of large globular LBs (see Chapter 4). This formation of LBs may coincide with the depletion of available nitrogen, whereupon the cells may "stockpile" any excess carbon source, as observed in other TAG accumulating bacteria (Waltermann and Steinbuchel, 2005). This stored lipid may be available for utilisation when conditions become more favourable for growth. Exposure to an exogenous source of long chain fatty acid leads to the rapid formation of LBs in *M. smegmatis*. As LB formation has been demonstrated to coincide with TAG accumulation in *M. smegmatis* in response to fatty acid exposure, it has been suggested that free fatty acid may be incorporated into TAG in order to detoxify the cellular environment (Garton et al., 2002).

M. smegmatis forms LBs under standard culture conditions, perhaps because it is able to hydrolyse the Tween component of the media to release fatty acids for incorporation into TAG. Schaefer and Lewis (1965) have previously demonstrated through Sudan Black staining that *M. kansasii* forms LBs in cells grown in the presence of Tween 80 but not in cells grown without. These LBs are mobilised upon carbon starvation, suggesting that the lipids stored in the LB are broken down and catabolised by β-oxidation during periods of low carbon availability. *R. opacus* has previously been shown to mobilise stored TAG in the absence of a carbon source (Waltermann and Steinbuchel, 2005). Only peripheral lipid deposits are visible following carbon starvation. Real time observation of oleic acid uptake by carbon starved *M. smegmatis* revealed that lipid accumulates at these peripheral LB sites, where presumably the LB continues to grow in size before release into the cytoplasm. LB formation has been demonstrated to occur at the Rhodococcus cell

membrane through ultra-structural studies that have demonstrated LB and WS/DGAT association with the cell membrane (Waltermann and Steinbuchel, 2005). The mechanism of LB formation in *M. smegmatis* has not previously been elucidated and the investigation of this process is described in Chapter 4.

TAG accumulation has previously been shown to coincide with expression of the triacylglycerol synthase gene, *tgs1*, in *M. tuberculosis* exposed to hypoxia or NO, however, expression of *tgs1* has not been inextricably linked to LB formation. The demonstration that overexpression of this gene in *M. smegmatis* leads to enhanced LB production in comparison to the blank plasmid control is the first evidence that the activity of the *tgs1* gene product is directly involved in LB formation. This discovery raised the possibility that LBs are formed in conditions in which the expression of *tgs1* is induced. The ability of these conditions to promote LB formation in mycobacteria is the subject of the remainder of this chapter.

3.4.2 LBs are a universal feature of AFB in sputum

Strikingly, LBs were present in a sub-population of AFB in all but specimens with extremely scanty numbers of AFB, collected from two geographical locations. LBs had previously been reported anecdotally in 4-5 sputum specimens (Garton et al., 2002) and this further evidence now confirms the presence of heterogeneous populations of tubercle bacilli in human infection. The implications of such a mixed population of tubercle bacilli *in vivo* are discussed, in relation to additional findings, elsewhere (Chapter 7 – General Discussion).

Sudan black staining proved to be a useful tool for examination of LBs in AFB in situations where a fluorescence microscope is not available for use. However, a full comparison of this method with the sensitive Auramine and Nile Red staining protocol would be needed to fully validate this method as a suitable alternative.

3.4.3 LBs are formed in *M. tuberculosis* response to hypoxia

LBs were demonstrated in *M. tuberculosis* subjected to the shift-down hypoxic model of non-replicating persistence and three other models of hypoxia. This suggests that the occurrence of LBs is not specific to a particular method used and is a general response to hypoxic conditions. The formation of LBs in the standing control for cultures subjected to lowered oxygen in a hypoxic incubator is perhaps not surprising considering that the expression of *tgs1*, as part of the DosR regulon, is upregulated in cultures that have been allowed to stand for just 30 minutes (Kendall et al., 2004). Furthermore, Sirakova et al. (2006) demonstrated that *M. tuberculosis* accumulated TAG when subjected to static growth conditions for 1 week. The small number of LB positive cells observed in the shaking control may be a result of an extended stationary phase, a condition which has been shown to induce the expression of *dosR*. The examination of LBs during prolonged cultivation of *M. tuberculosis* should be included in future studies.

The base-line LB formation in solid growth *M. tuberculosis* controls for the anaerobic generation envelope model may be as a result of excess LCFA in the form of the oleic acid supplementation present in the agar. The presence of LBs in cells grown on agar without the inclusion of oleic acid should be examined to determine whether this is the case.

3.4.4 LBs are formed in *M. tuberculosis* response to NO exposure

LB formation was demonstrated in *M. tuberculosis* exposed to NO. LB accumulation was rapid, with low levels of LBs observed after 5 minutes of NO exposure. This is consistent with the induction of NO-responsive genes, which was detectable by microarray within 5 minutes of exposure (Voskuil et al., 2003). The subsequent peak in LB accumulation corresponds to the maximal expression levels of *tgs1* after 4 hours of NO treatment (Daniel et al., 2004).Within this thesis, the upregulation of *tgs1* was also shown to

correlate to LB formation, providing further confirmation that TGS1 plays a central role in LB formation.

The NO releasing agent SPER/NO has a half-life of 39 minutes at 37°C, with 2 moles of NO released per mole of donor molecule (Aga and Hughes, 2008). Presumably, the observed decline in numbers was due to the dissipation of NO; however, it is likely that cells *in vivo* would be constantly exposed to NO (Daniel et al., 2004).

Interestingly, the LB content of populations of *M. tuberculosis* exposed to NO for 4 hours halved after 24 hours of exposure. This may indicate that the non-LB positive population has undergone one round of division, thereby diluting the number of LB positive cells by half. This suggests that LB positive cells are growth arrested, however, it is not direct evidence of such and this issue is addressed in Chapter 5.

Preliminary results showed that a DosR deleted mutant strain of *M. tuberculosis* was impaired in LB formation, suggesting that DosR is largely responsible for the regulation of the expression of *tgs1*. However, a small subset of cells were found to be LB positive after NO treatment. These LBs could have been formed either through the activity of *tgs1*, acting independently of DosR, or that of a *tgs* homologue. There are 13 other *tgs* genes encoded by the *M. tuberculosis* genome (Daniel et al., 2004) which are not part of the DosR regulon (Park et al., 2003) and two of these, *tgs2* and *4*, were induced on exposure to NO (Daniel et al., 2004) It is possible that one or more of these genes was induced by a DosR independent, NO-responsive pathway. Interestingly, in a study of a *tgs1* disrupted mutant, the expression levels of other *tgs* genes were higher than those in the wild type and complemented strain during treatment with NO (Sirakova et al., 2006). This suggests that these gene products may be able to compensate for loss of activity of TGS1. Quantitative PCR could be used to investigate the expression of these *tgs* genes in the DosR mutant during NO exposure, in order to determine which gene product is responsible for LB formation in the absence of DosR regulation.

The effect of the availability of an exogenous source of fatty acid on LB formation in *M. tuberculosis* during NO exposure was also assessed. A preliminary experiment showed that cells incubated with the Tween substitute, Tyloxapol, during NO exposure are able to form LBs. The cells used in this experiment were grown in media containing Tween because previous attempts to grow cultures in Sautons broth with a Tyloxapol replacement were unsuccessful. The cells were then resuspended in media with Tyloxapol prior to the addition of NO.

Christensen et al. (1999) demonstrated reduced HAF labelling in *M. smegmatis* after treatment with Tween and suggested that Tween may compete with HAF for insertion into the outer lipid layer of the envelope. Therefore, Tween could have been present in the cell envelope and utilised later for LB formation. However, this does not explain why the Tween incubated cells had fewer LBs. Sautons broth was selected as a growth medium for these experiments in order to replicate the conditions used by Daniel et al. (2004) to demonstrate TAG accumulation in *M. tuberculosis* exposed to NO. It may have been more suitable to have cultivated the cell mass for the experiment in Middlebrook 7H9 with Tyloxapol in place of Tween, as this has been shown to support the growth of *M. tuberculosis*.

3.4.5 LB formation in intracellular *M. tuberculosis* requires further investigation

There is no definitive evidence to suggest that *M. tuberculosis* forms LBs during infection of macrophages. LBs were not observed in *M. tuberculosis* infection of cells from a macrophage cell line. This may be due to active replication of the bacilli or the activation status of the macrophage. Upon activation the macrophage releases NO and the intracellular environment becomes hypoxic (Honer zu Bentrup and Russell, 2001), conditions now known to induce LB formation. Infection studies of blood-derived primary macrophages were carried out in order to further investigate the effect of macrophage activation on LB formation in intracellular *M. tuberculosis*.

Unfortunately, these studies were technically unsatisfactory because insufficient numbers of bacilli were recovered from infected macrophage. The small numbers of LBs observed in bacteria that were isolated from macrophages were similar to the base levels observed in some control samples in other experiments. Therefore, there is little evidence provided by this experiment to show that this is a genuine result. In addition, attempts to stain infected macrophages with Nile Red to demonstrate LBs in phagacytosed bacilli were unsuccessful due to the high lipid content of the macrophage. This is a disappointing result, especially in light of the recent evidence that *M. tuberculosis* may enter a dormant-like state in macrophages (Biketov et al., 2000). Cells of the avirulent *M. tuberculosis* strain, Academia, recovered from murine peritoneal macrophage lysates showed enhanced viability when measured using Most Probable Number (MPN) counts in liquid medium when compared to CFU counts on solid medium. This was further enhanced by the addition of the *Micococcus luteus* resuscitation promoting factor (Rpf) protein (see Chapter 1). This may indicate that *M. tuberculosis* enters a dormant-like programme in response to the macrophage environment that renders cells unable to form a colony on solid medium (see Chapter 7) and these cells may be recovered or resuscitated using Rpf (Biketov et al., 2000). Therefore, it would be of great interest to carry out further studies of macrophage infection, perhaps with a higher MOI in order to ensure the isolation of enough cells to carry out cytological assays.

3.4.6 LBs are formed in *M. tuberculosis* in response to growth arresting stimuli

Inhibition of growth, regardless of the mechanism involved, may be the common link between the physiological responses to the DosR activating stimuli examined. *M. tuberculosis* was subjected to a number of treatments that are not thought to elicit a DosR regulated response and that may reduce the bacterial growth rate. Chapman and Bernard (1962) demonstrated that *M. tuberculosis* has a narrow pH range for growth between pH 6.2 and 7.3. Heat, cold and pH shock do not induce the expression of *dosR* (Kendall et al., 2004, Fisher et al., 2002) but were shown to stimulate LB formation after 30 minutes of treatment. Sirakova et al. (2006) demonstrated that *M. tuberculosis* accumulates TAG

when incubated in acidic conditions (pH5). However, this was over a three week period. Alternatively, LB formation may be a response to increased sensitivity to LCFA present in the media in the form of Tween because oleate has been shown to be more toxic to *M. tuberculosis* in acidic conditions (Tummon, 1975).

Caution should be taken in describing heat shock at 50°C as a LB promoting condition because the LB numbers generated by this condition were not a great deal higher that those observed in the control. The low level of LB formation observed in control samples may have been due to the small head space of air in the micro-centrifuge tube or the lack of continuous agitation, both of which may lead to the rapid induction of the DosR regulon and therefore upregulation of *tgs1* (Kendall et al., 2004). The experiments should be repeated in tubes with a larger head space ratio and these should be incubated with continuous agitation, in order to validate the observation that LBs are formed in response to these conditions.

Presumably, the observed LB formation coincides with growth arrest. The association of LB formation with growth phase is examined elsewhere within this study.

3.4.7 Chemostat cultures of *M. tuberculosis* form LBs in response to hypoxia and nutrient limitation

The presence of LBs in steady-state cultures of *M. tuberculosis* grown under nutrient deprivation or hypoxia in a chemostat vessel is hard to reconcile with the hypothesis that LB positive cells are growth arrested because replication must be constant in this system in order to maintain cell mass. Results in this thesis indicate that LB formation in response to an environmental trigger is rapid, within 5 minutes in the case of NO exposure. It is possible that non-replicating, LB positive cells are generated at a constant rate in steady state culture and when these cells are removed by dilution they are replaced by cells from the next generation. These results high-lighted the need to characterise the

growth status of the LB cell and this subject is addressed by studies detailed later within this thesis.

Figure 18: Proposed scheme for the regulation of LB formation in mycobacteria

The system shows a proposed scheme for the regulation of LB formation in mycobacteria through a balance of environmental signals and growth rate. The incorporation of Long chain Fatty Acids (LCFA) into diacylglycerol (DAG) to form triacylglycerol (TAG) LBs is catalysed by the enzymes of the TGS family. LB formation has been shown to coincide with expression of *tgs1* in *M. smegmatis* and *M. tuberculosis* in studies presented in this thesis. Control of the gene *tgs1* is likely to be under two or more regulatory pathways which are induced according to environmental stimuli that are not permissive for bacterial growth. A reduction in growth rate also increases the accumulation of LBs, because lipids that would otherwise be utilised in the production of phospholipids and cell envelope lipids in the replicating cells are employed in TAG formation and stored in a LB structure. Active growth requires a high amount of LCFA for mycolic acid and phospholipid synthesis. Therefore, LCFA is rapidly incorporated into biosynthesis of these products and bypasses TAG synthesis. The model below is a simplified version of lipid synthesis in mycobacteria; see Figure 8 for overview of LCFA and its role in lipid biosynthesis.

The synthesis of phospholipid and mycolic acid and LCFA derivatives by FAS I and II is indicated by blue arrows. Factors affecting LB formation are boxed and metabolic pools are shown in oval shapes. Factors affecting growth rate are shown in green.

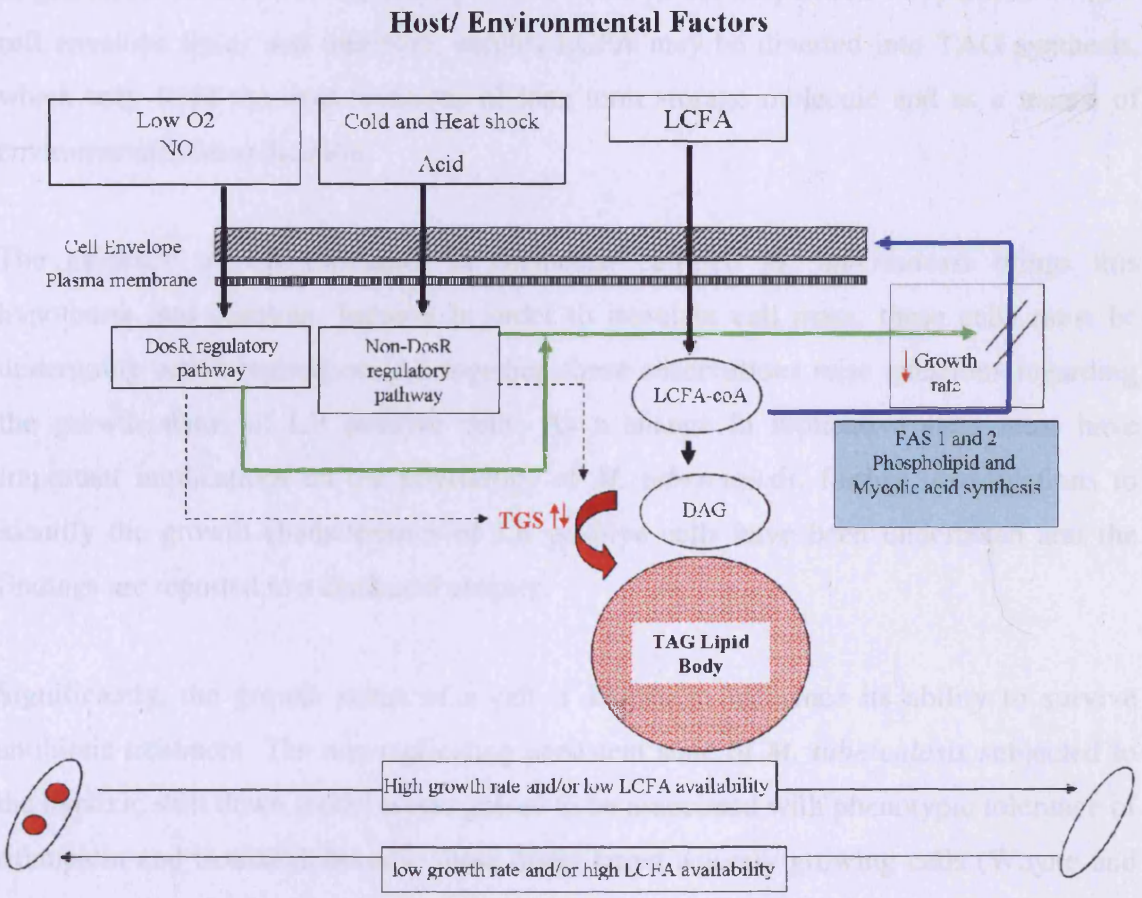

3.5 Conclusions

If all the evidence of LB accumulation in *M. smegmatis* and *M. tuberculosis* is drawn together, it is possible to build on the model previously proposed for *M. smegmatis*. The model is summarised in Figure 18. The balance of LB formation/utilisation appears to be influenced by environmental signals and the availability of exogenous LCFA. Exposure to hypoxia and NO, both DosR activating conditions, results in the expression of *tgs1* and LB formation in *M. tuberculosis*. As discussed, growth arrest may be an important physiological outcome common to the response to both treatments (Wayne and Hayes, 1996, Voskuil et al., 2003). And since LB formation occurs in cells exposed to non-DosR activating conditions it is feasible that LB formation is a general response to growth arresting conditions; although this requires further investigation. The effect of these conditions on expression of the *tgs* genes remains unknown and this requires assessment. In general, a cessation of replication would result in the suspension of synthesis of new cell envelope lipids and therefore, surplus LCFA may be diverted into TAG synthesis, which may fulfil the dual functions of long term storage molecule and as a means of environmental detoxification.

The evidence of LB formation in chemostat cultured *M. tuberculosis* brings this hypothesis into question, because in order to maintain cell mass, these cells must be undergoing active replication. All together, these observations raise questions regarding the growth status of LB positive cells. As a change in replicative state must have important implications on the physiology of *M. tuberculosis*, further investigations to identify the growth characteristics of LB positive cells have been undertaken and the findings are reported in a dedicated chapter.

Significantly, the growth status of a cell is known to influence its ability to survive antibiotic treatment. The non-replicating persistent state of *M. tuberculosis* subjected to the hypoxic shift down model is recognised to be associated with phenotypic tolerance of rifampicin and isoniazid, because these drugs target actively growing cells (Wayne and

Hayes, 1996). Since LBs have been observed in tubercle bacilli subjected to the Wayne model and appear to be associated with growth arrest, it raises the possibility that LBs are in fact markers of phenotypic antibiotic tolerant cells. Given that LBs can be readily demonstrated in AFB isolated from sputum samples it is evidently crucial to establish whether such a relationship exists. This is the focus of the work presented in Chapter 6.

Chapter 4

An Electron Microscopic Investigation of Lipid Bodies in Mycobacteria

4.1 Introduction

Fluorescence microscopy of *M. smegmatis* revealed a set of distinctive LB profiles, characterised by their position in the cell and the apparent difference in size and shape, with clear distinctions demonstrated between growth conditions. Transmission Electron Microscopy (TEM) provided a method for examination of these cytological differences in closer detail, with the aim of establishing how LBs are formed. Electron micrographs were specifically examined for structural details, such as the presence of LB boundary membranes or LB attachment to the cell membrane, which may provide an indication of the physical mechanisms involved in LB formation. *M. smegmatis* cells cultured under different growth conditions were also examined by the freeze fracture replication method, in order to further characterise the structure and organisation of the LB and in particular, to demonstrate the presence of a limiting membrane.

4.1.1 Transmission Electron Microscopy

The high resolving power of the electron microscope is due to the short wavelength of the electron; which, depending on the velocity of the electrons, allows a theoretical resolution of as low as 0.002nm. The actual resolution is closer to 1nm for biological specimens due to limitation by factors such as specimen thickness, contrast and radiation damage (Alberts et al., 1994). This is compared to the highest possible resolving power of the light microscope, which is 0.2μm (Alberts et al., 1994). The electron beam is generated by a cathode set at the top of the microscope chamber and then accelerated by the anode through the aperture. The electrons are focussed by magnetic lenses, which are set within a vacuum to avoid scattering of the electrons by air molecules. The specimen is placed in a holder that is in the path of the electrons. Specimens to be examined by TEM must be dehydrated and embedded in resin in order for the material to be thin enough to allow the transmission of electrons. The sections are stained with heavy metals, which scatter electrons and areas stained with these appear as electron dense. Electrons passing through

the specimen are focussed to form an image on a phosphorescent screen (Alberts et al., 1994).

TEM has previously been used to examine a range of carbon storage inclusions in a number of bacterial species (Reviewed by Shively, 1974). Prokaryotic inclusions have formally been divided in to two groups depending on the demonstration of a limiting membrane in thin sections by TEM (Shively, 1974). The barrier surrounding all of these inclusions (summarised in Table 11) is thought to consist of a single layer of membrane, around 2-4nm in thickness (Shively, 1974).

PHB is the best-characterised storage lipid and it has been demonstrated that the boundary surrounding these inclusions consists of a phospholipid monolayer with enzymes involved in PHB synthesis, mobilization and structural function embedded in this layer. Proteins called phasins are associated with PHB granules; these are thought to be structural proteins, and together with the phospholipid boundary, they separate the PHB core from the cytoplasm and prevent coalescence with other granules (Waltermann and Steinbuchel, 2005).

Until recently, triacylglycerol (TAG) was considered to be an unusual storage compound in prokaryotes; however, TAG accumulation appears to be common feature of the actinomycetes (Alvarez and Steinbuchel, 2002). Single unit membranes, with a similar morphology to those observed bordering other carbon storage structures, have been demonstrated by TEM in association with TAG LBs in *Streptomyces* sp. (Packter and Olukoshi, 1995) and *Rhodococcus opacus* (Waltermann and Steinbuchel, 2005).

Although LBs have been demonstrated in numerous species of mycobacteria, including *M. tuberculosis* and *M. smegmatis*, by TEM studies (Garton et al., 2002), their association with TAG accumulation in *M. smegmatis* has only recently been elucidated (Garton et al., 2002). Prior to this discovery, it was believed that all the TAG produced in the mycobacterial cell was located in the cell envelope (Daffe and Draper, 1998). There is some conflicting evidence as to whether mycobacterial LBs are membrane limited. A

single unit membrane was noted surrounding the LBs of *M. smegmatis* (Barksdale and Kim, 1977, Gale and McLain, 1963)and *M. tuberculosis* (Barksdale and Kim, 1977) but there was little indication made of how frequently this structure was observed. LBs observed by TEM in *M. kansasii* (Schaefer and Lewis, 1965) and *M. lepraemurium* (Whitehouse et al., 1971) were not bound by a limiting structure.

The presence of a limiting membrane structure may play a role in the stabilisation of the LB during formation and prevent coalescence of the bodies (Waltermann and Steinbuchel, 2005). Therefore, such an observation in ultrathin sections of LB positive *M. smegmatis* may provide some insight into how the structure is formed and maintained in the cell.

Table 11: Membrane limited inclusions have previously been demonstrated in numerous species of bacteria by Transmission Electron Microscopy (TEM)

Inclusions consisting of various storage compounds have been demonstrated to be enclosed by a single unit membrane by TEM of ultrathin sections of numerous species of bacteria.

Species of bacteria	Storage compound	Reference
Acinetobacter species H01-N	Hexadecane inclusions	(Scott and Finnerty, 1976)
Bacillus cereus (partially lysed cells)	Poly-β-hydroxyoctanoate	(Dunlop and Robards, 1973)
Clostridium spp.	Polyglucoside granules	(Reviewed by Shively, 1974)
Thiobacillus ferrooxidans	Poly-β-hydroxybutyrate (PHB)	(Reviewed by Shively, 1974)
Chromatium weissi	Sulphur granules	(Reviewed by Shively, 1974)
Thiobacillus spp.	Polyhedral bodies	(Reviewed by Shively, 1974)

4.1.2 Freeze Fracture Replication

Freeze fracture and freeze etching has been used as a tool for the examination of lipid inclusions in a number of studies (Scott and Finnerty, 1976, Dunlop and Robards, 1973). The freeze fracture technique involves striking a frozen sample with a cold microtome knife to introduce a fracture or break in the specimen. Fracturing occurs along the line of least resistance within the cell and therefore, the fracture plane preferentially cleaves the biological membrane along the centre of the phospholipid layer. The structure of the membrane bilayer is due to the hydrophobic phospholipid fatty acid tails, which avoid contact with the aqueous environment by facing inside the membrane. During freeze fracture, the water molecules are immobilised by freezing and therefore, these forces of interaction are absent, allowing membrane cleavage (Shotton and Severs, 1995).

Following specimen cleavage, the fracture face is freeze etched. Freeze etching involves the removal of ice from the surface of the fracture face by vacuum sublimation, thereby exposing membrane surfaces and structural features of the cell. A replica of the fractured and etched specimen is made by deposition of platinum, followed by a carbon coat. Once the biological material has been removed by treatment with bleach, the replica may be viewed in a standard TEM (Shotton and Severs, 1995).

These techniques have been employed to demonstrate the structure of lipid inclusions and in particular the presence of a limiting membrane. Fracturing along a membrane, followed by etching, produces fracture faces with a distinctive morphology. The phospholipid fatty acid tails of the membrane are interrupted by inter-membrane proteins (IMPs), which predominately partition with the protoplasmic half of the membrane on fracturing. The other half of the membrane has complementary pits where the proteins had crossed through the membrane (Shotton and Severs, 1995). The fracture plane may cleave the outer membrane of a cell or may pass through a cross section of a cell. Depending on the line of fracturing, an entire lipid inclusion along with one half of the lipid bilayer may be removed to reveal the inner surface of the membrane. The concave

face of the membrane surrounding a freeze fractured Hexadecane inclusion isolated from Acinetobacter species HO1-N was demonstrated in such a way (Scott and Finnerty, 1976).

Alternatively, the fracture may travel through a cross section of the inclusion, removing part of the membrane. In such cases, the surrounding ice may be sublimed to expose part of the surrounding membrane, which is characterised by a lip-like protrusion. The coat and limiting membrane of a poly-β-hydroxybutyrate (PHB) granule within a freeze fractured and etched *Bacillus cereus* cell was observed using this technique (Dunlop and Robards, 1973). The possible fracture pathways to reveal a membrane limited inclusion are detailed in Figure 19.

The TEM study of *M. smegmatis* was performed prior to the development of LB inducing conditions in *M. tuberculosis*. Therefore, *M. smegmatis* has been used as a model system for LB formation in mycobacteria because LB manipulation is straightforward in this organism. After the discovery that LB formation could be promoted by certain environmental conditions in *M. tuberculosis*, cells exposed to a number of these conditions were examined by TEM. At the time of this particular electron microscopic study, only Wayne dormancy and certain chemostat growth conditions had been examined by fluorescence microscopy and therefore, only these cultures were included in the analysis. The advantage of using cultures generated in a chemostat is that a large culture volume is generated and TEM preparation requires a large pellet of cells because of the inevitable loss of material due to the high number of washes.

Figure 19: Possible freeze fracture planes that may reveal membrane limited inclusions

A freeze fracture plane may cleave a specimen containing a membrane limited body in a number of ways. Firstly, the fracture may cleave the cellular membrane (not shown), or the fracture plane may travel through a cross section of a cell. Panel a shows an intact cell (embedded in ice) containing an inclusion surrounded by a double membrane, the outer leaflet of which is shown in red. Scheme b-c demonstrates how the fracture plane can travel through the cell to remove the inclusion, while leaving the outer leaflet embedded in the specimen. Alternatively, a small part of the inclusion membrane may be removed from the fracture plane. Sublimation of the surrounding ice reveals the structure surrounding the membrane (d-f).

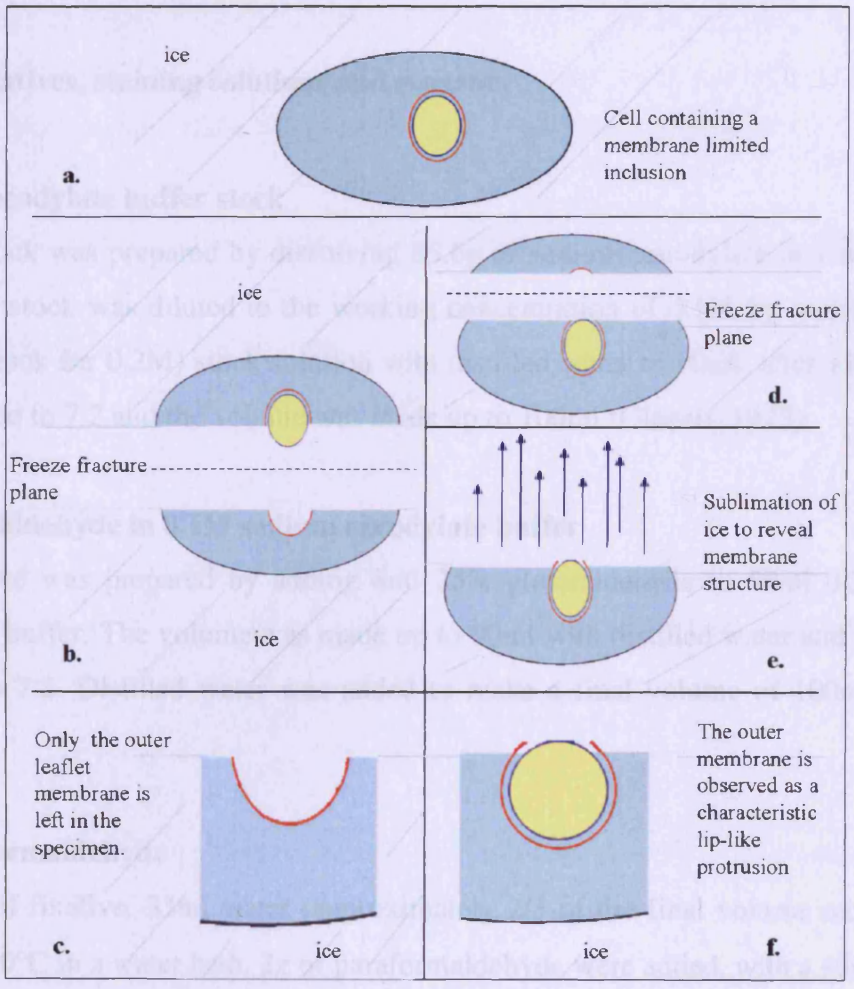

4.2 Materials and Methods

4.2.1 Electron Microscopy

Preparation and use of fixatives and stains during specimen processing was carried out in dedicated fume hoods and in accordance with the COSHH guidelines, due to the hazardous nature of many of the chemicals used.

4.2.2 Fixatives, staining solutions and reagents

Sodium cacodylate buffer stock

A 0.4M stock was prepared by dissolving 85.6g of sodium cacodylate in 1 litre distilled water. The stock was diluted to the working concentration of 0.1M by combining 25ml (or 50ml stock for 0.2M) stock solution with distilled water to 90ml, after which the pH was adjusted to 7.2 and the volume was made up to 100ml (Glauert, 1975).

2% glutaraldehyde in 0.1M sodium cacodylate buffer

This fixative was prepared by adding 8ml 25% glutaraldehyde to 50ml 0.2M sodium cacodylate buffer. The volume was made up to 90ml with distilled water and the pH was adjusted to 7.2. Distilled water was added to make a final volume of 100ml (Glauert, 1975).

4% paraformaldehyde

For 50ml of fixative, 33ml water (approximately 2/3 of the final volume required) was heated to 60°C in a water bath. 2g of paraformaldehyde were added, with a stir bar, to the water. The solution was shaken and returned to the water bath. A drop of 2M NaOH was added to the solution, which should rapidly clear. 10ml of 3xPBS was added and the pH of the solution was adjusted to 7.2 with hydrochloric acid. The volume was adjusted to

50ml and finally, the solution was filtered (0.2μm Acrodisc syringe filter) to remove crystals (Cooney, 2000).

2% osmium tetroxide

To prepare a 2% solution, an ampoule of 1.0g of osmium tetroxide was broken and placed in a clean brown glass bottle. 50ml distilled water was added and the mixture was shaken to mix. The solution was kept in a fume cupboard (Glauert, 1975).

2% potassium ferricyanide

Potassium ferrocyanide (2g) was dissolved in 90ml 0.2M sodium cacodylate buffer. The pH was adjusted to 7.4 and the volume was made up to 100ml with 0.2M cacodylate buffer. The solution was left to mature for 7 days before use (Glauert, 1975).

1% osmium tetroxide and 1% potassium ferricyanide in 0.1M sodium cacodylate buffer

Osmium tetroxide (2%) solution (w/v) was combined in a 1:1 ratio with 2% potassium ferricyanide (w/v) in sodium cacodylate buffer (Glauert, 1975).

5% Uranyl acetate

Uranyl acetate (5g) was dissolved in 90ml distilled water with gentle heating at 60°C. The solution was cooled and the volume was adjusted to 100ml with distilled water and stored in a foil covered jar at 4 °C (Lewis and Knight, 1980).

Spurr resin

Spurr resin (Spurr, 1969) was made by cumulatively adding the following reagents:

Nonenyl succinic anhydride	26g
ERL 4206	10g
D.E.R. 736	4g
S-1	0.4g

TAAB resin

TAAB resin was made in a polyethylene graduated pot by cumulatively adding the following components:

TAAB resin	53g
DDSA	43g
MNA	6g
DMP-30	2ml

The resin was mixed by shaking or gentle rolling and left in a warm place to allow the dispersal of bubbles.

Lead citrate (Reynolds)

The following solutions were prepared:

Stock A: 8.86g Lead nitrate was dissolved in 100ml distilled water.

Stock B: 11.53g of Tri sodium citrate was dissolved in 100ml distilled water.

Reynolds solution: 30ml of stock A was combined with 30ml stock B and mixed for 30 minutes. 16ml freshly prepared and filtered 1M sodium hydroxide and 24ml distilled water was added. The solution was aliquoted into micro-centrifuge tubes and stored at 4°C (Lewis and Knight, 1980).

4.2.3 Procedure for processing Mycobacteria for electron microscopy

Methods adapted from Glauert (1975)

Primary fixation

1-5ml of cell suspension or culture was harvested in a micro-centrifuge tube by centrifugation (16 000 x g) and washed in 0.1M sodium cacodylate buffer or PBS three times. The pellets were resuspended in 1ml 2% glutaraldehyde and left for 1 hour. Following this, the pellets were washed a further three times in buffer. *M. tuberculosis* samples were fixed in 4% paraformaldehyde prior to primary fixation to ensure complete fixation and safe removal from the containment suite. These samples were washed in

buffer three times before resuspension in 1ml paraformaldehyde and left overnight. Primary fixation was then carried out as outlined above.

Secondary fixation

The glutaraldehyde fixed samples were pelleted by centrifugation (16 000 x g) and the supernatant was removed and replaced with 1ml 1% osmium tetroxide for 1.5 hours. The pellet was washed once in buffer and a further 2 times in distilled water.

En bloc staining with uranyl acetate

Following primary and secondary fixation, pellets were resuspended in 5% uranyl acetate and left overnight. Pellets were then washed 3 times in distilled water.

Embedding of pellets in agar

Small or friable specimen pellets were embedded in agar, following fixation, to reduce loss of material. Micro-centrifuge tubes containing the specimens were transferred to a warm water bath. A small drop of molten agar was added to the bottom of each micro-centrifuge tube and mixed with the specimen, using a cocktail stick. The specimens were once again centrifuged (16 000 x g) to form a tight pellet. Once the agar was set, the specimens were removed from the micro-centrifuge tubes, using a razor blade to cut the plastic away. The embedded specimens were divided into two pieces and placed in small glass vials, ready for dehydration.

Dehydration

The specimens were dehydrated through a graded ethanol series. The fixed samples were resuspended (agar pieces were transferred to vials of ethanol) in 70% ethanol for 30 minutes. This process was repeated in 90% ethanol and two changes of 100% ethanol. The 100% ethanol was replaced with propylene oxide (PO) for 5 minutes and then transferred through two changes of 50:50 PO and resin mix. Finally, the micro-centrifuge tubes/vials were filled with 50:50 PO and resin mix and sealed with a foil lid. At the end of the day, holes were pierced in the foil lid to allow evaporation of PO over night. The resin was changed two times the following day to remove any traces of PO.

Embedding in resin

Agar embedded specimens were transferred to individual polyethylene capsules (BEEM, New York) using a pair of fine forceps. The specimen area was placed at the bottom of the tube for ease of trimming. Paper labels were placed inside the capsules or micro-centrifuge tubes (specimens without agar embedding) and the tubes were filled with fresh resin. The resin was polymerised in an oven set to 60°C for 16 hours.

Preparation of glass knives for use in sectioning

Glass knives were prepared using a LKB Knifemaker as described by Reid (1975). A plate glass strip was cleaned with ethanol and placed rough face down on the Knifemaker table. The glass was scored and broken into squares by clamping the glass between two sets of pins located on the clamping head and the table. A scoring wheel was drawn across the glass and the breaking knob was turned to slowly raise the lower set of pins until the glass was broken. The square was turned around and pinned by two corners. The glass was scored again to create two triangle shapes. The pins were raised with very gentle turning of the breaking knob to ensure a slow break and therefore, a good knife. The knife edges were warmed on a metal plate and water troughs were attached using molten dental wax. The edges were then sealed with wax to prevent water leakage.

Preparation of specimen for ultramicrotomy

The specimen to be sectioned was removed from the micro-centrifuge tube or BEEM capsule with a razor blade. Remnant resin was removed with a saw and the remainder was shaped to fit the ultramicrotome specimen holder. The specimen was secured in the specimen holder and placed in the viewing position on the ultramicrotome stage (Reichert-Jung Ultracut E). Resin was carefully trimmed away from the specimen to create a large surface area of exposed material. A trapezoid face was then cut into the specimen area to allow good ribbon formation of sections.

The specimen holder was placed in the horizontal position for sectioning and the knife was secured in the knife holder. The knife water trough was filled with water, the surface

of which was levelled with a pump to give a smooth surface for floating sections. The knife was positioned close to the block face by eye. The specimen was orientated with the longest of the parallel sides at the knife edge, which was angled to match that of the specimen. The cutting window was set to allow the specimen to pass the knife slowly and then make a quick return. The knife was carefully brought closer to the specimen through very small movements on the dial controlling the specimen position. The knife was judged to be very close to the specimen face when diffraction of light was observed through the gap between specimen and knife. The instrument arm was then set to cut sections of 1μm thickness. Once the knife reached the specimen face, ribbons of thick sections were floated onto the water and rounded together with an eyelash tool. The sections were collected on a drop of water on a metal loop and deposited on a microscope slide. The slide was dried on a hot plate to prevent wrinkling of the sections and then flooded with toluidine blue for 30 seconds. The stain was drained off and the slide blotted dry. The stained sections were examined on a light microscope under a ×50 objective for large areas of specimen concentration. The specimen face was then trimmed further, as small block faces make superior ultra thin sections. Areas shown by light microscopy to contain only small areas of material were cut away, leaving a block face with a high concentration of specimen (Method adapted from Reid, 1975).

Production of Ultrathin sections

The knife was changed and advanced by eye to the block face. The specimen was set up as outlined above and the instrument arm was set to cut with an advancement of 90nm for the production of ultrathin sections. Thin sections were observed as gold in colour until the knife became blunt, which became apparent when silver-blue sections were formed. If more sections were required the blade was moved to a new area. Ribbons were smoothed out on the surface of the water trough by passing a chloroform soaked cotton wool bud over them. The sections were collected on 200 mesh copper grids, using a fine pair of forceps. The grids were immersed in the water trough, matt side down, and brought up under the ribbon. The grids were dried under a lamp (Method adapted from Reid, 1975).

Staining of grid mounted ultrathin sections with uranyl acetate

Sections immobilised on grids were stained with uranyl acetate and lead citrate (both heavy metal stains) to provide greater contrast for viewing by TEM. A drop of 5% uranyl acetate was placed on each grid and left for 15 minutes and then washed in 3 changes of freshly distilled water (Lewis and Knight, 1980).

Staining of grid mounted ultrathin sections with Lead Citrate

Staining with lead citrate was carried out under conditions excluding CO_2 to prevent the precipitation of insoluble lead citrate onto the sections. The lead citrate solution was kept in a sealed syringe at 4°C. When used, a small amount of lead citrate was released from the syringe onto a piece of filter paper to remove any solution that may have reacted with the air and formed crystals. A piece of laboratory sealing film (Nesco, Osaka, Japan) was placed at the bottom of a glass Petri-dish; this was surrounded by moistened pellets of sodium hydroxide in order to remove CO_2 from the atmosphere. The dish was transferred to a nitrogen tank and small drops of lead citrate were placed on the film. The grids to be stained were immersed under the drops, using fine forceps and, left for 2 minutes. The grids were then washed in three changes of freshly distilled water (to exclude CO_2) to remove any crystals and allowed to dry on filter paper (Lewis and Knight, 1980).

4.2.4 Freeze Fracture Replication

Freeze fracture work was carried out at the Electron Microscopy Unit at the University of Manchester with the technical assistance of Roger Meadows.

M. smegmatis that had been cultured with media low in nitrogen, low carbon and low carbon and oleic acid supplemented were prepared as described previously (Chapter 2). Cultures were fixed in glutaraldehyde and washed in PBS, as described above. The fixed culture was harvested by centrifugation and the resulting pellet was resuspended in a very small amount of PBS to make a thick paste. A small amount of cell paste was transferred with the end of a pipette tip into a specimen holder. The material was rapidly frozen by

contact with stage that had been pre-cooled with liquid nitrogen. The freeze-fracture and etching procedure was carried out in a Cressington CFE-50B freeze-fracture unit. The fracture chamber had been pre-cooled to -170°C by the addition of liquid nitrogen into the cooling unit. The frozen specimen mounted on the cooled table was introduced into the evacuated chamber through an air lock and clamped into position under the cold ultra-microtome knife. The microtome knife was manually lowered and the specimen was struck to produce a fracture face. In order to freeze etch the surface, the temperature was elevated to -80°C and etching was allowed to proceed for 15 minutes. Following this, the temperature was lowered to -170°C to stabilise the fracture face. A replica was formed by rotary shadowing by deposition of a thin layer of evaporated platinum, set at an angle of 45°, followed by a backing of carbon at 90°. The specimen was removed from the chamber and placed in bleach to remove the biological material from the replica. The replica floated to the surface of the bleach, where it should have been left to remove the attached cells. However, the replica sections were very fragile and began to break up, therefore, the sections were immediately picked up on copper mesh grids. Grids were left overnight on filter papers soaked in distilled water to remove the bleach and then allowed to dry. Examination of grids by TEM revealed that biological material had not been removed and cells appeared to be intact and not fractured (data not shown) (Method adapted from Shotton and Severs, 1995)

The method was modified to allow better cleavage of the specimen and to provide a larger section surface area for stability. A thin layer of fixed cell paste was frozen between mica sheets and these were pulled apart to fracture within the chamber, as before and etched. The resulting fracture replicas still showed intact cells. The difficulty in fracturing the cells may be due to the thickness of the mycobacterial cell wall.

4.3 Results

4.3.1 Examination of the ultrastructural of LBs in *M. smegmatis* by Transmission Electron Microscopy

Cultures of low carbon, low nitrogen and OA supplemented *M. smegmatis* were prepared as described in Chapter 2. Samples were also taken from exponential cultures of *M. smegmatis* grown in the rich medium, Middlebrook 7H9 broth with Tween 80, and the defined medium, complete Youmans broth with glucose. Samples were prepared for electron microscopy following the protocol set out in the Materials and Methods section of this chapter.

TEM demonstrated distinct ultrastructural features for each growth condition examined. LBs appeared as discrete electron opaque globules located within the cytoplasm or at the cell periphery. No structures were apparent within the LB, however, mesosome-like structures were observed within 10% cells cultured in rich medium (Middlebrook 7H9) or with oleic acid supplementation but not in cells cultured in minimal media (LCYB and Youmans broth with glucose). The majority of these structures were observed in LB positive cells and occasionally appeared to be in close association with the LB (Figure 20c).

The morphology and pattern of LB occurrence varied according to the conditions under which the cells were cultured. Cells exposed to an exogenous source of fatty acid, in the form of oleic acid or Tween, contained between 1-6 individual, discrete LBs (Figure 20 and Figure 21), with some evidence of a single unit membrane boundary (Figure 20b and Figure 21b-c). Boundary membranes were observed in association with 46% of the LBs examined in cells grown in the presence of an exogenous fatty acid source. These LBs were characteristically rounded in shape and located within the cytoplasm of the cell. The corresponding carbon starved cells (Figure 22 and Figure 23) and cells grown in Youmans broth (Figure 24) had few intracellular LBs and these were confined to the cell

periphery. Peripheral deposits appeared to be surrounded by a double membrane (Figure 23) and were often associated with a collection of electron transparent material (Figure 23 and Figure 24b). It was unclear whether this material had collected between the leaflets of the cell membrane or within the cytoplasm immediately adjacent to the membrane, although in (Figure 24b) it appears to be located in the cytoplasm, adjacent to the cell membrane. Collection of lipid and formation of peripheral bodies has previously been observed in TEM images of *R. opacus*. This suggests that LB formation occurs at the cell membrane and may follow the scheme laid out by Wälterman et al. (2005) based on *in vitro* and *in vivo* analysis of LB formation in *Rhodococcus opacus* (see discussion section).

Cells grown under low nitrogen conditions contained large, globular and irregularly shaped LBs (Figure 25). These structures were electron transparent but black deposits were frequently observed on the surface of the exposed LB. This may be due to some unspecific precipitation of lead citrate or osmium staining of exposed unsaturated lipid. The number of LBs per cell appears to be lower than cells exposed to oleic acid; 1-2 large LBs frequently occupied a large proportion of the cytoplasm.

Disc-like LB structures were observed in *M. smegmatis* grown in media containing hexadecanol (Figure 26). These LBs were similar to those observed in the wax ester accumulating *Acinetobacter* sp strain M-1 (Ishige et al., 2002).

Figure 20: *M. smegmatis* grown in the presence of Tween 80 form intracellular Lipid Bodies

Images **a-c** show *M. smegmatis* from an exponential culture grown in Middlebrook 7H9 and Tween and subsequently prepared for Transmission Electron Microscopy (TEM). Electron opaque intracellular Lipid Bodies (LBs) are indicated by arrows. Limiting membranes were occasionally observed as single unit boundaries surrounding the LB, as indicated in Image **b**. Membranous structures, putatively identified as mesosomes, were observed in association with the Lipid Body structures. Strikingly, the LB shown in Image **c** appears to be connected to the cell membrane through a membranous structure. This suggests a role in these structures in LB formation. Scale bars are shown in the right hand corner.

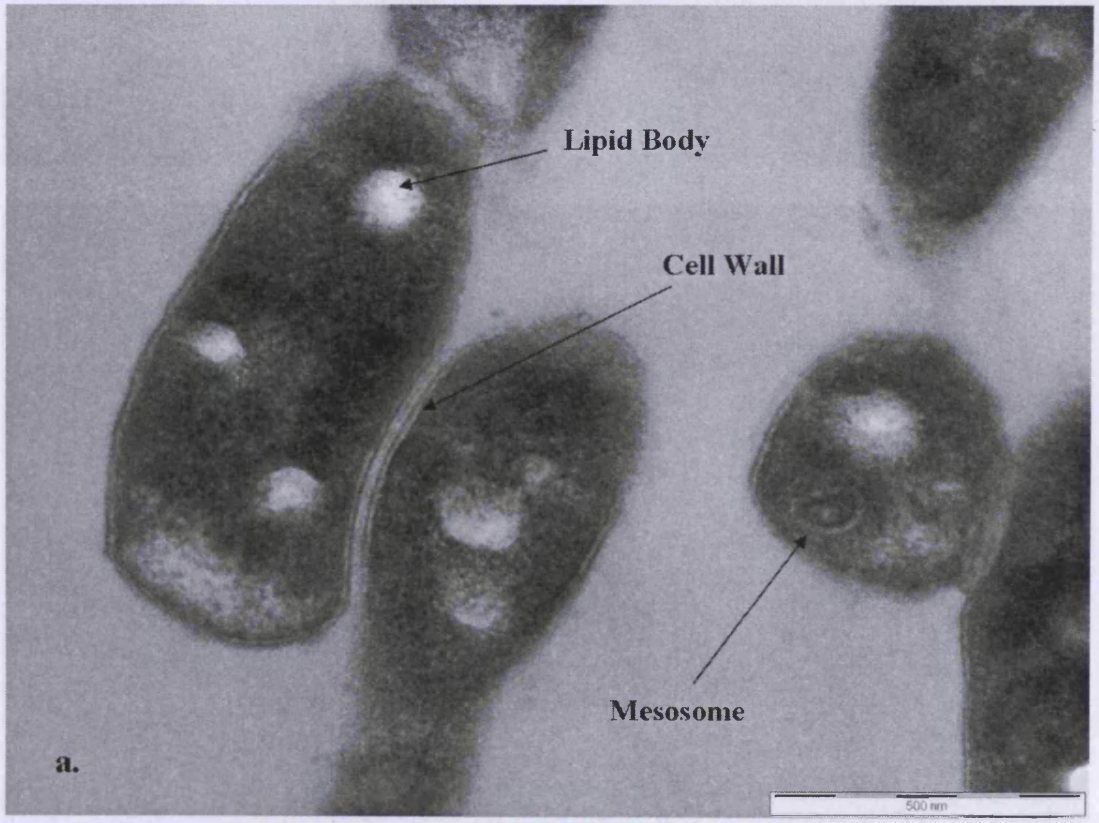

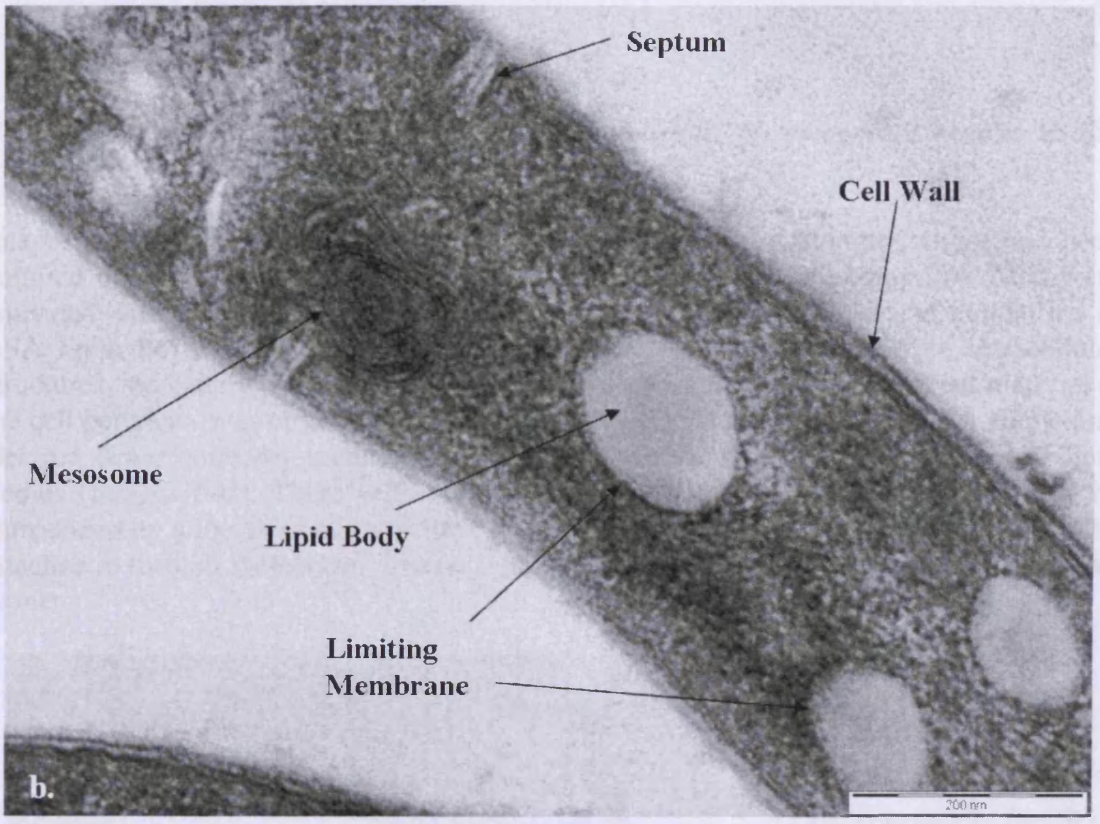
Septum
Cell Wall
Mesosome
Lipid Body
Limiting
Membrane
b.
200 nm

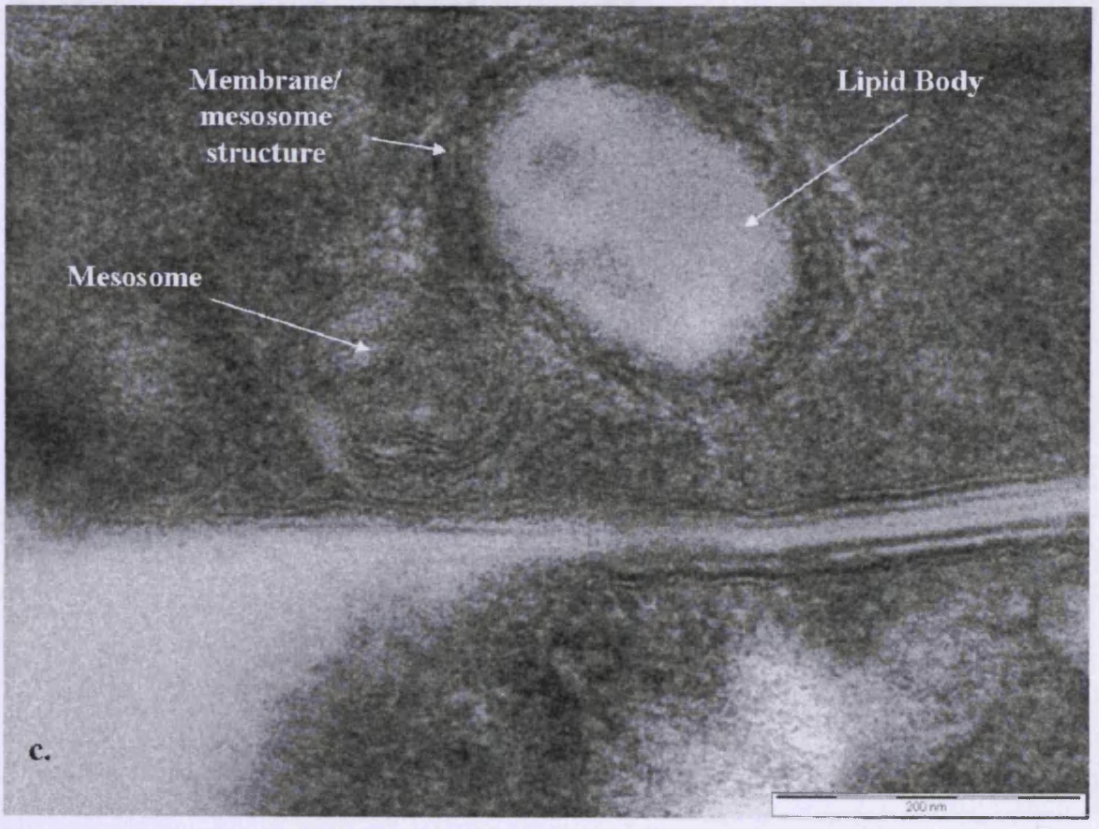
Membrane/
mesosome
structure
Lipid Body
Mesosome
c.
200 nm

Figure 21: Oleic acid supplementation of low carbon *M. smegmatis* results in the formation of intracellular Lipid Bodies

Images **a-f** show transmission electron micrographs of *M. smegmatis* which had been cultured in Low Carbon Youmans Broth (LCYB) for 7 days. Following this, cells were amended with glycerol for 1 hour and then exposed to 630μM oleic acid emulsified in BSA for a further hour. Lipid Bodies were observed as electron opaque intracellular structures, indicated by arrows. In addition, a collection of electron transparent material at the cell periphery was observed in a small number of cells (Images **b** and **e**). A single unit electron dense boundary membrane was observed in association with a number of lipid bodies (Images **b-d**). There were two instances in which the LB was observed to be surrounded by a membranous structure, possibly a mesosome, which did not appear to be attached to the cell membrane (Images **e** and **f**). Scale bars are indicated in the right hand corner.

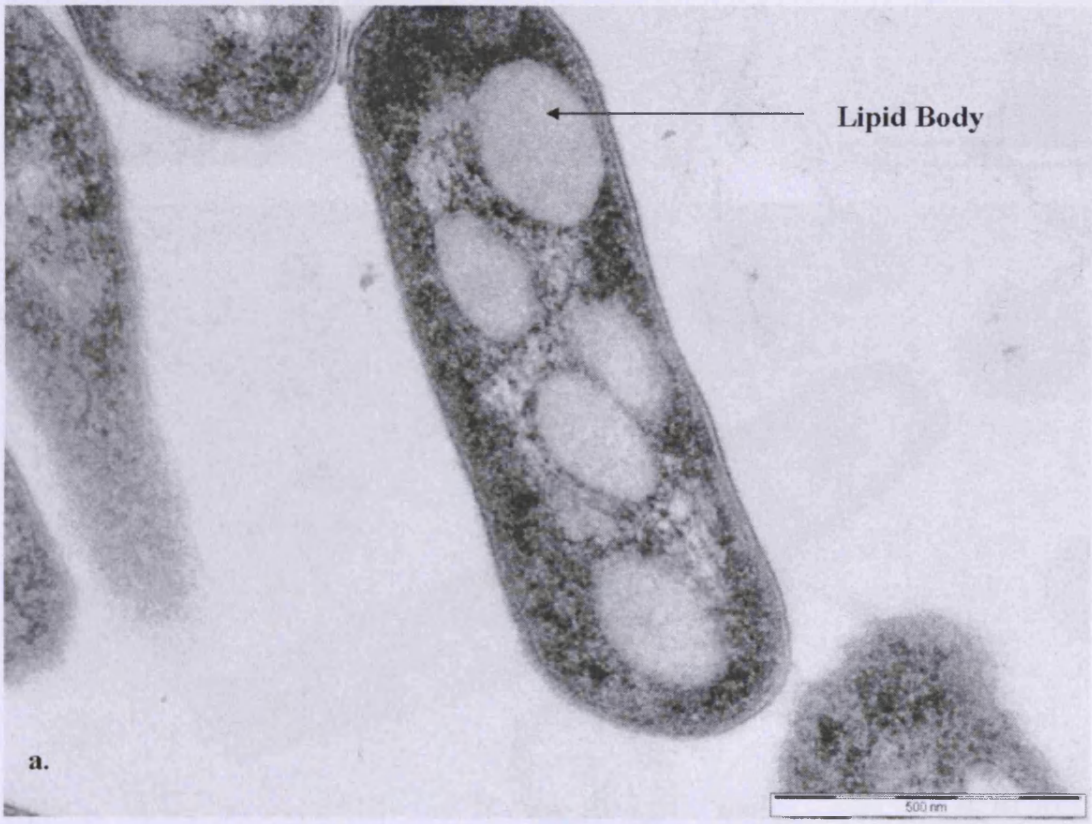

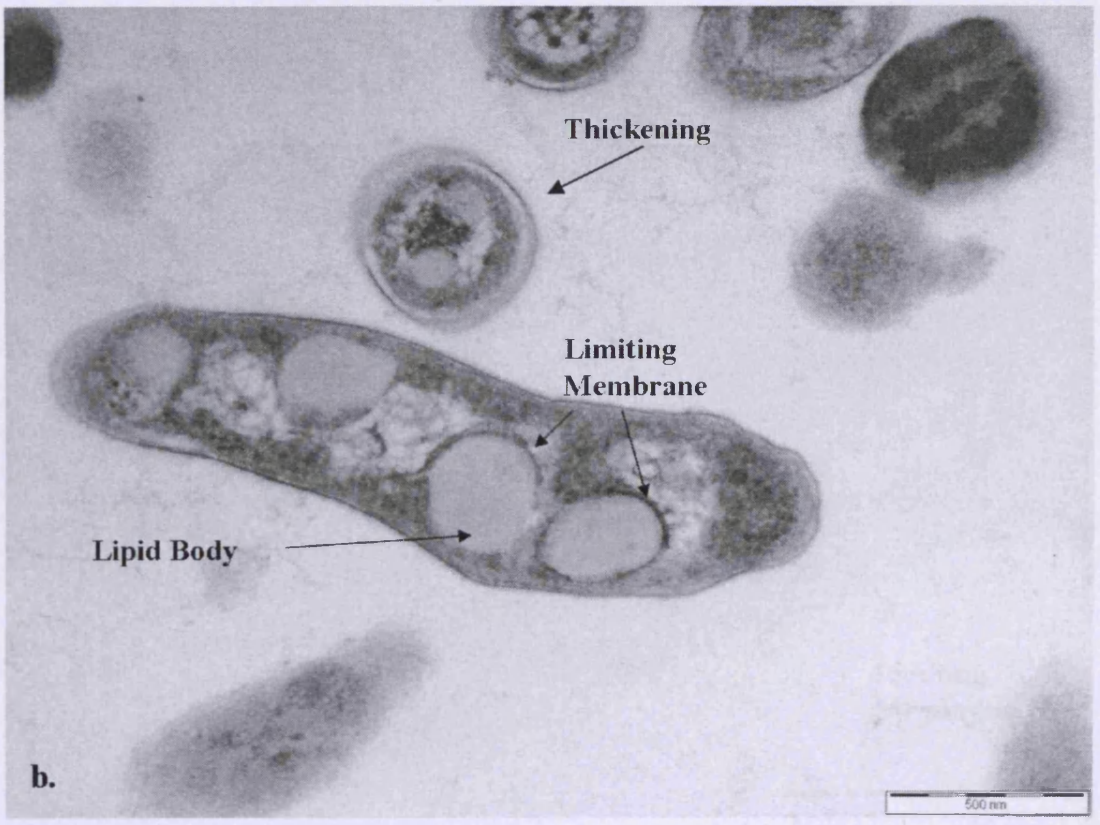
Thickening
Limiting
Membrane
Lipid Body
b.
500 nm

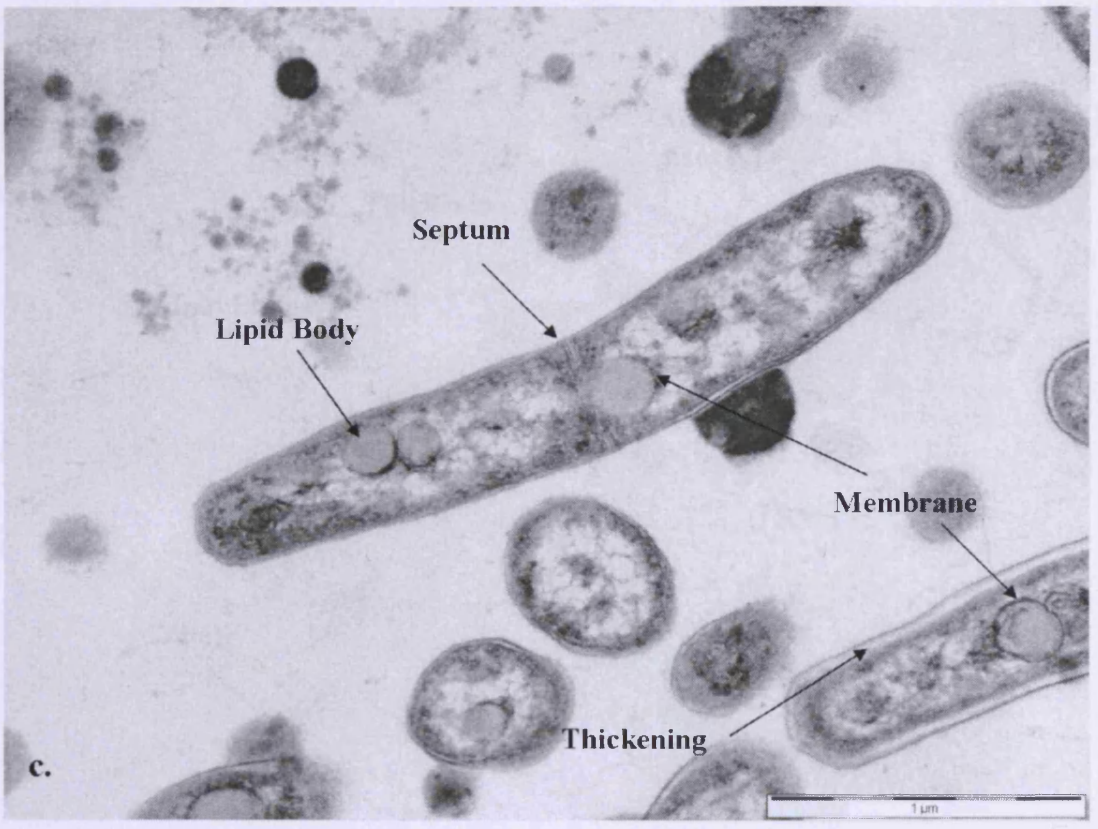
Septum
Lipid Body
Membrane
Thickening
c.
1 µm

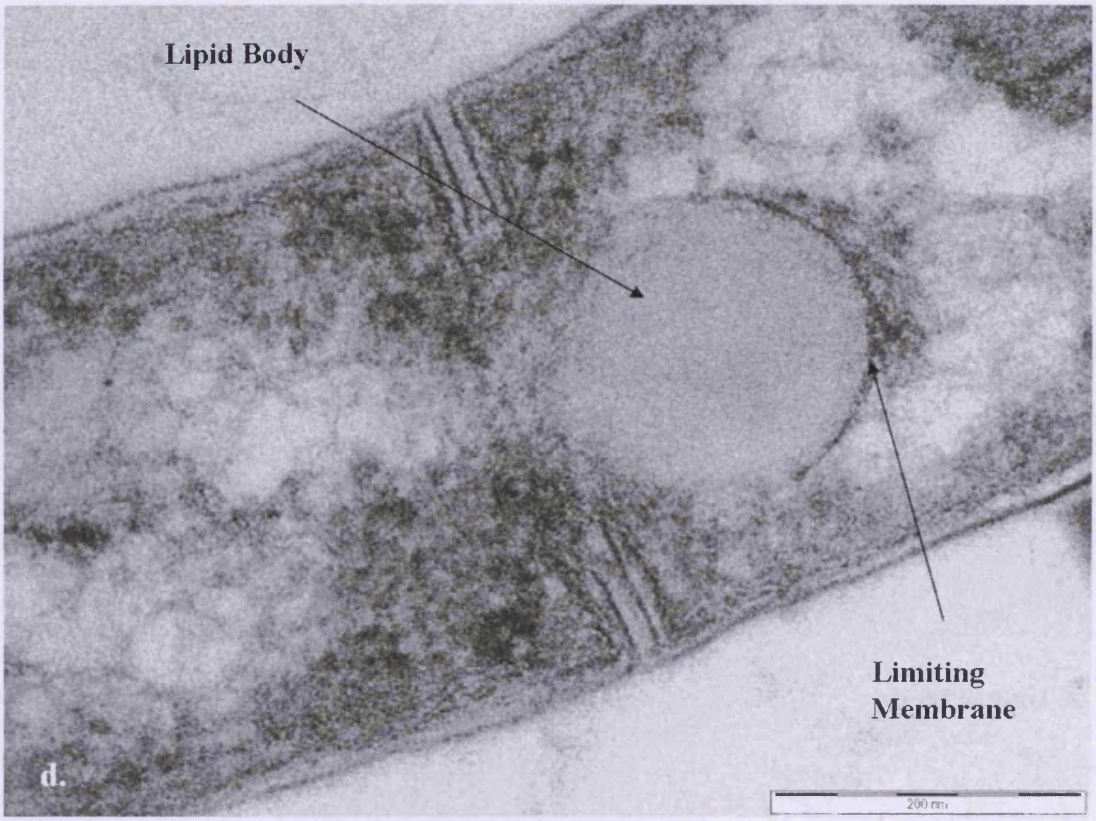
Lipid Body
Limiting
Membrane
d.
200 nm

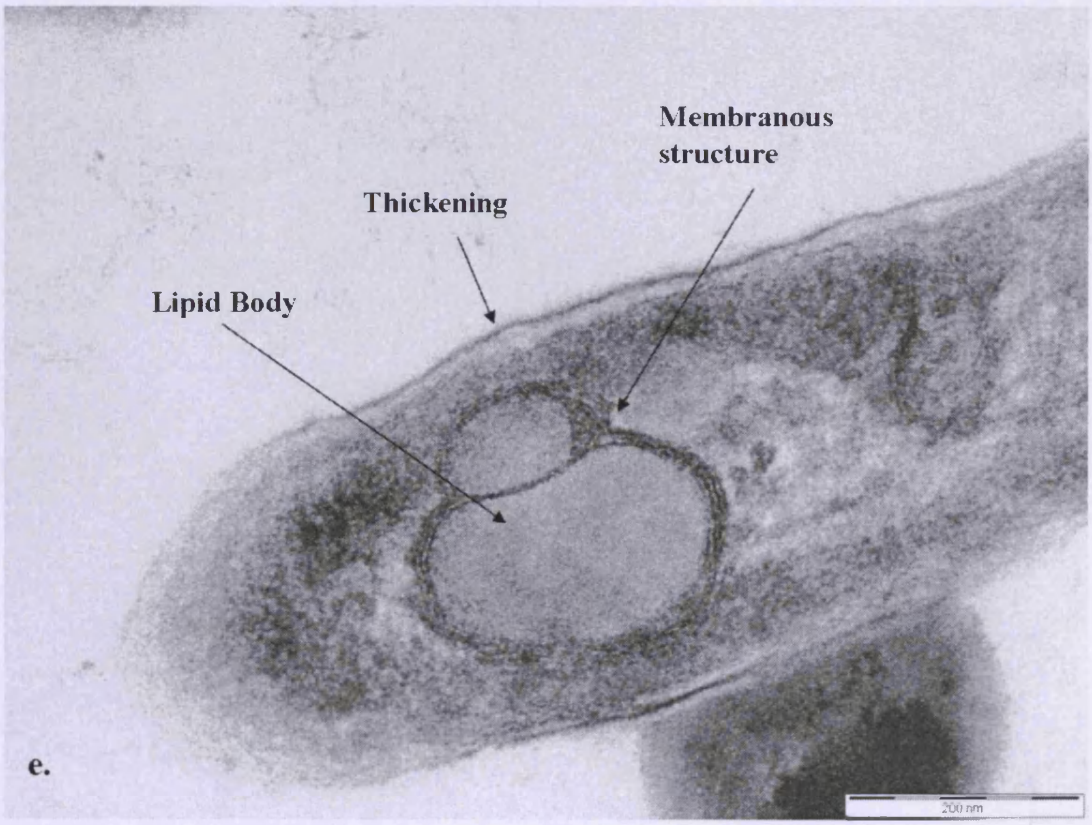
Membranous
structure
Thickening
Lipid Body
e.
200 nm

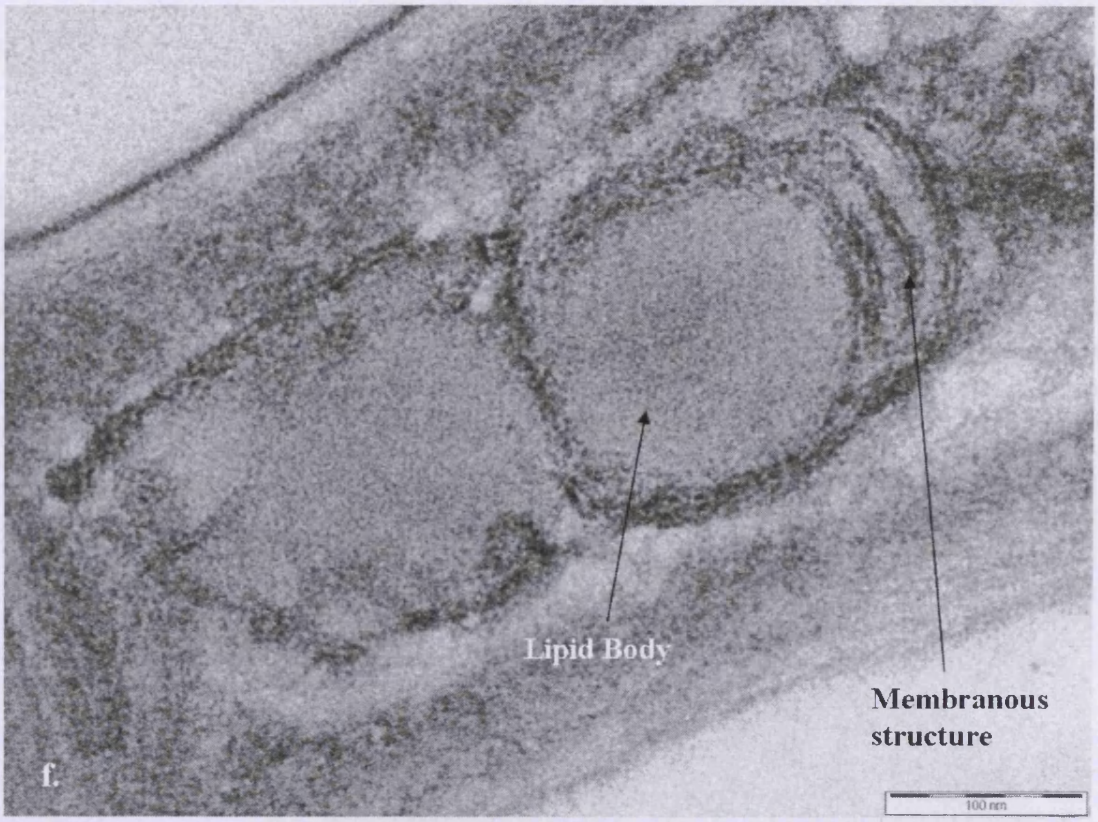
Lipid Body
Membranous structure
f.
100 nm

Figure 22: *M. smegmatis* grown under low carbon conditions contain peripheral Lipid Bodies

Image shows electron micrographs of *M. smegmatis* grown under conditions of low carbon. Lipid Bodies were associated with the cell periphery and are therefore referred to as peripheral Lipid Bodies (indicated by arrows). A thickening/collection of electron transparent material was also frequently observed at the cell periphery. A scale bar is indicated in the right hand corner.

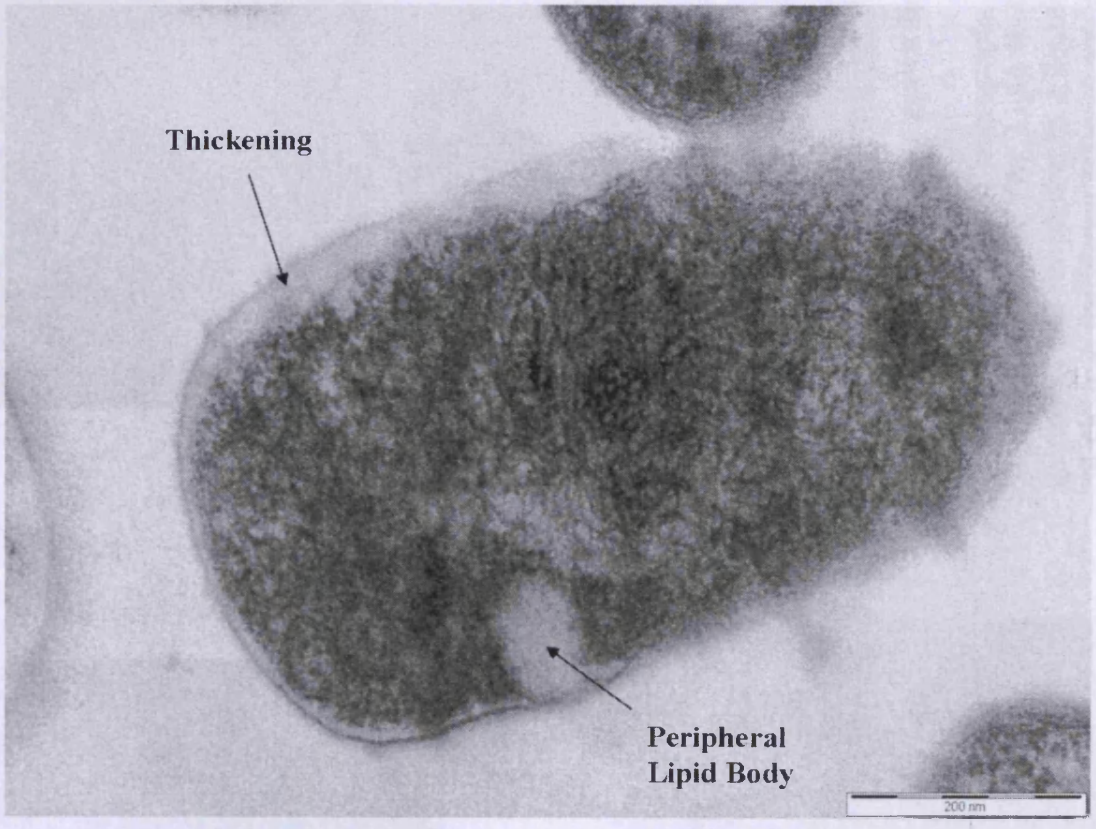

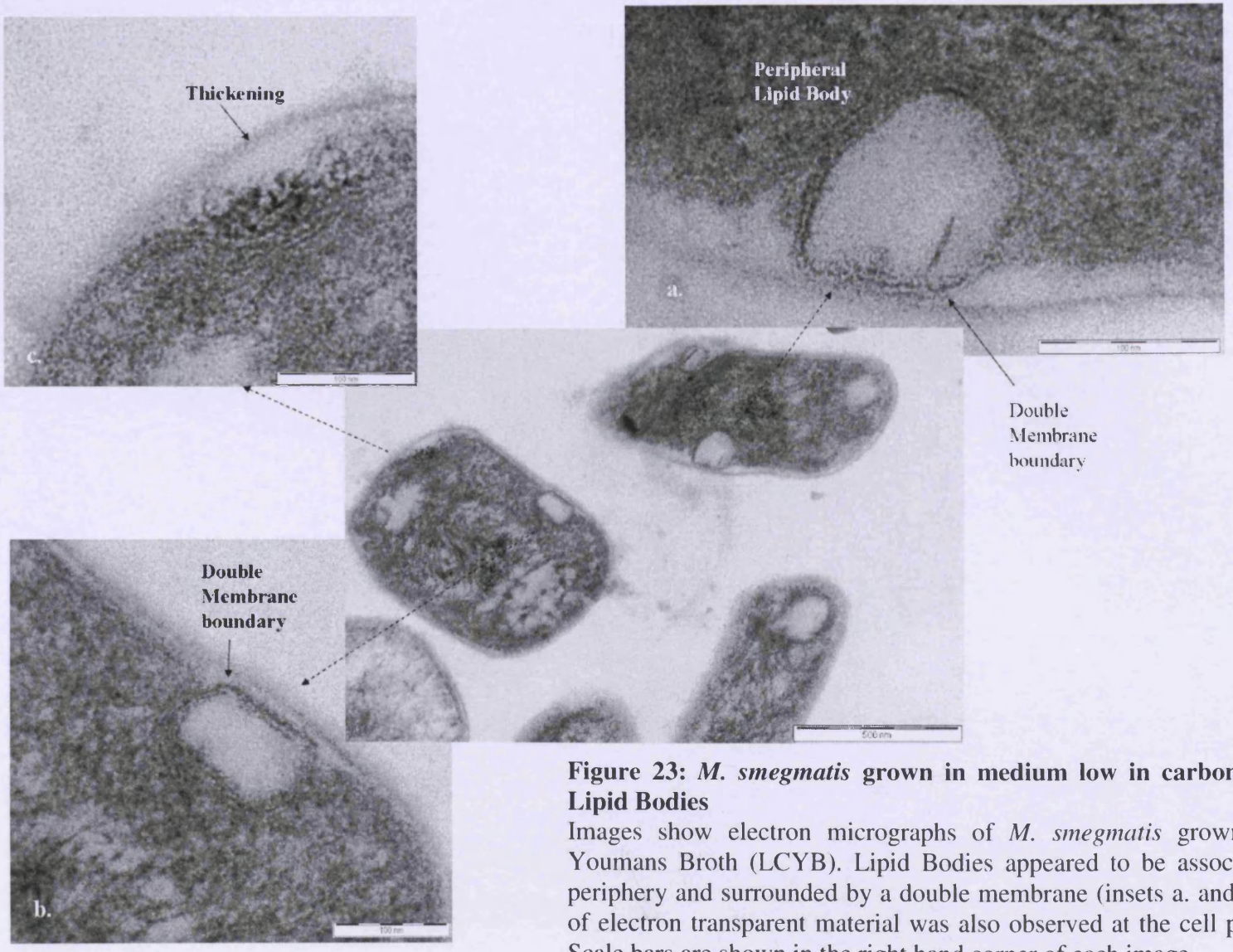

Figure 23: *M. smegmatis* grown in medium low in carbon form peripheral Lipid Bodies

Images show electron micrographs of *M. smegmatis* grown in Low Carbon Youmans Broth (LCYB). Lipid Bodies appeared to be associated with the cell periphery and surrounded by a double membrane (insets a. and b.). Accumulation of electron transparent material was also observed at the cell periphery (inset c.). Scale bars are shown in the right hand corner of each image

Figure 24: *M. smegmatis* cultured in a defined medium contains peripheral Lipid Bodies

Images **a-b** show electron micrographs of *M. smegmatis* grown in Youmans broth with glucose as a carbon source. Peripheral Lipid Bodies and thickening with comparable morphology to low carbon cells were also observed in cells grown in this medium. Scale bars are indicated in the right hand corner.

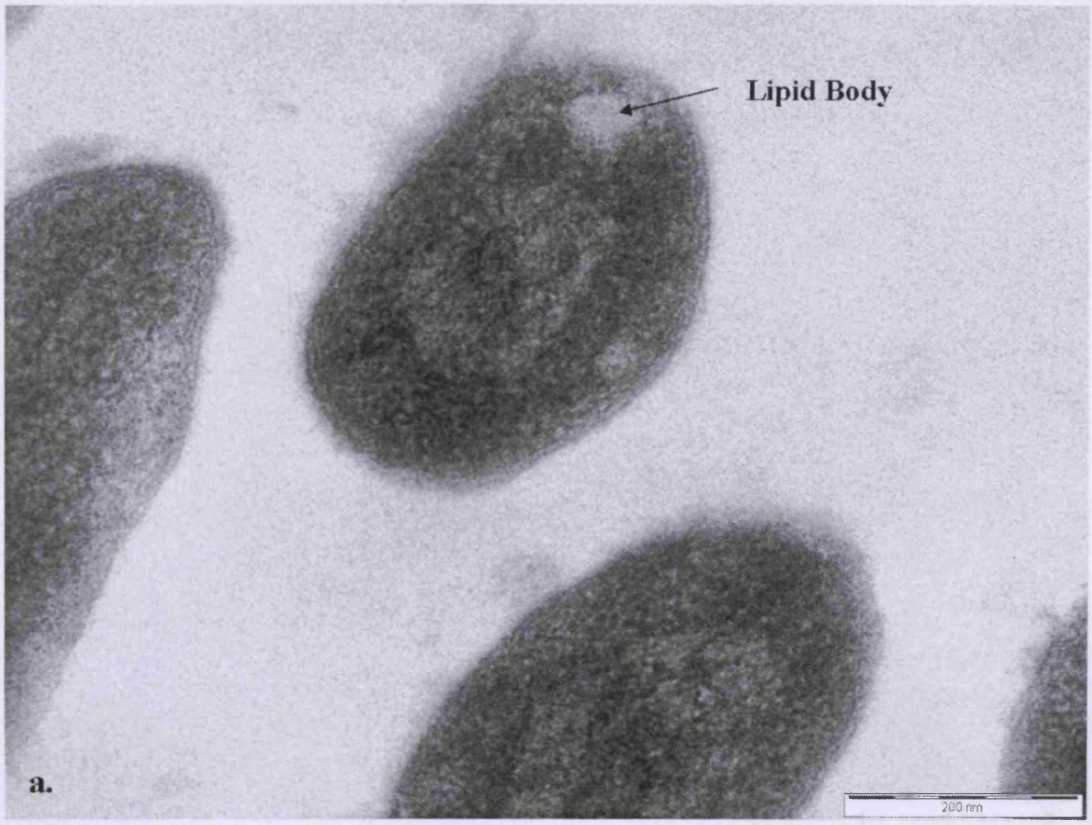
Lipid Body
a.
200 nm

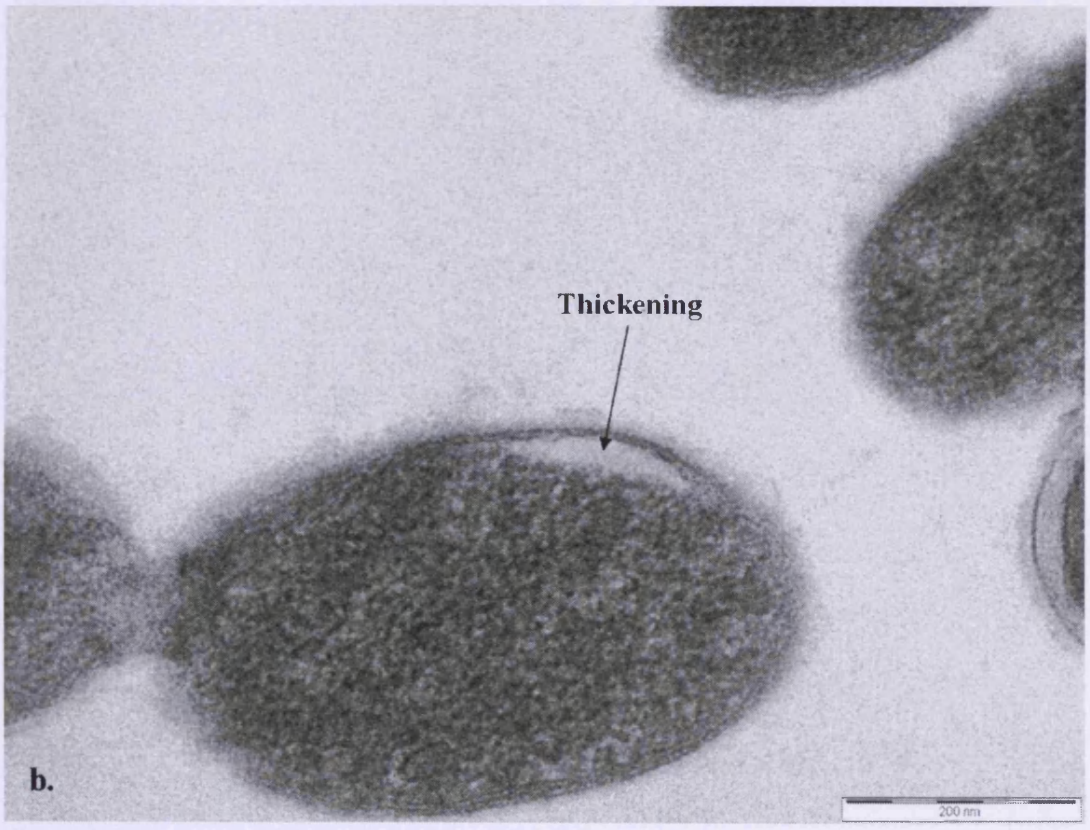
Thickening
b.
200 nm

Figure 25: *M. smegmatis* grown under low nitrogen conditions form large globular lipid bodies

Images **a-b** show electron micrographs of *M. smegmatis* grown in Low Nitrogen Youmans Broth (LNYB) for 7 days. Large, electron transparent, globular Lipid Bodies occupied a large volume of the cell and these structures were frequently associated with irregularly shaped black deposits. No evidence of a limiting membrane was observed. Scale bars are indicated in the right hand corner.

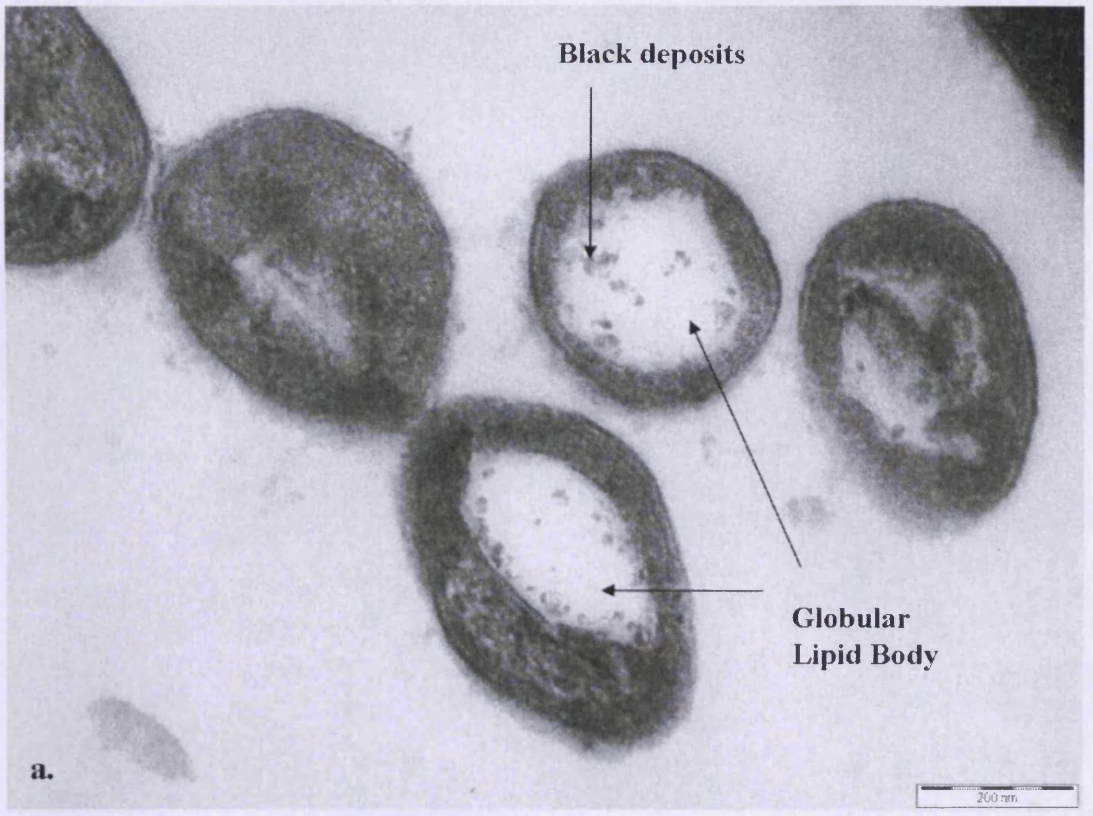
Black deposits
Globular
Lipid Body
a.
200 nm

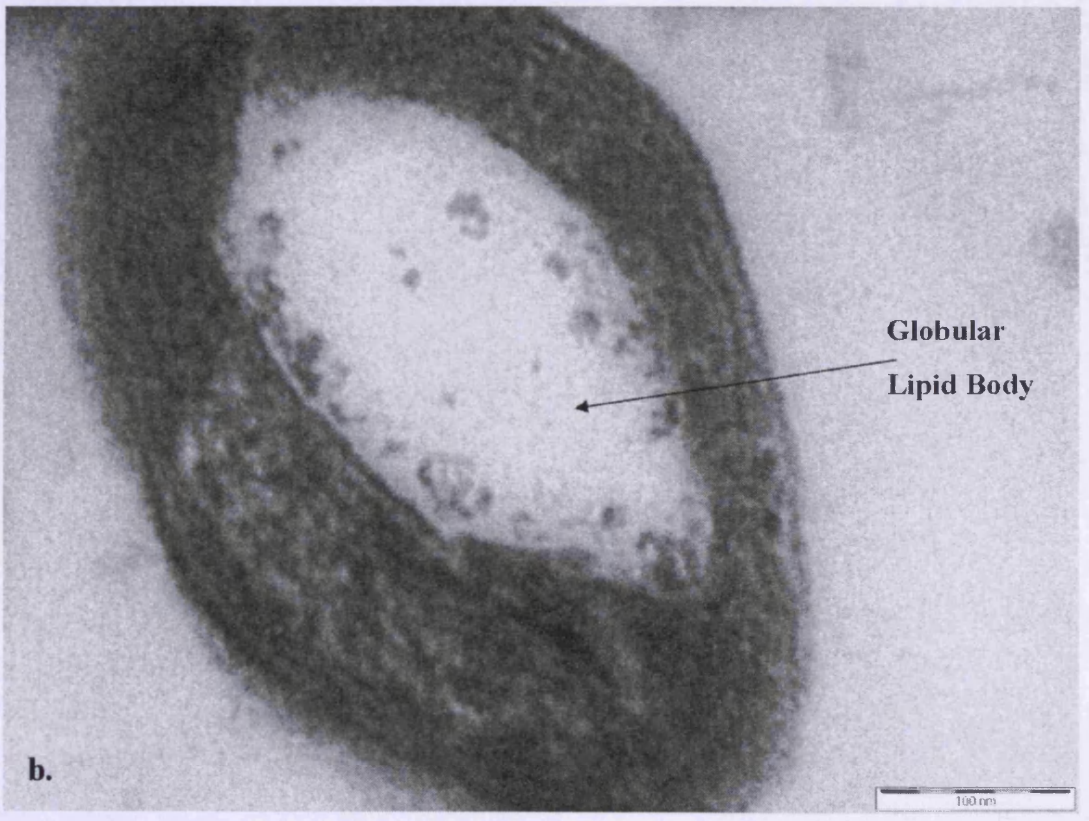
Globular
Lipid Body
b.
100 nm

Figure 26: *M. smegmatis* grown in the presence of hexadecanol form disc-like Lipid Bodies

Images **a-b** show electron micrographs of *M. smegmatis* grown in Mineral Salts Medium with 0.3% hexadecanol for 3 days. Cells contained Lipid Bodies with a disc shaped morphology (indicated by arrows). Image **a** shows a longitudinal section of a cell, while image **b** shows a horizontal section of a cell.

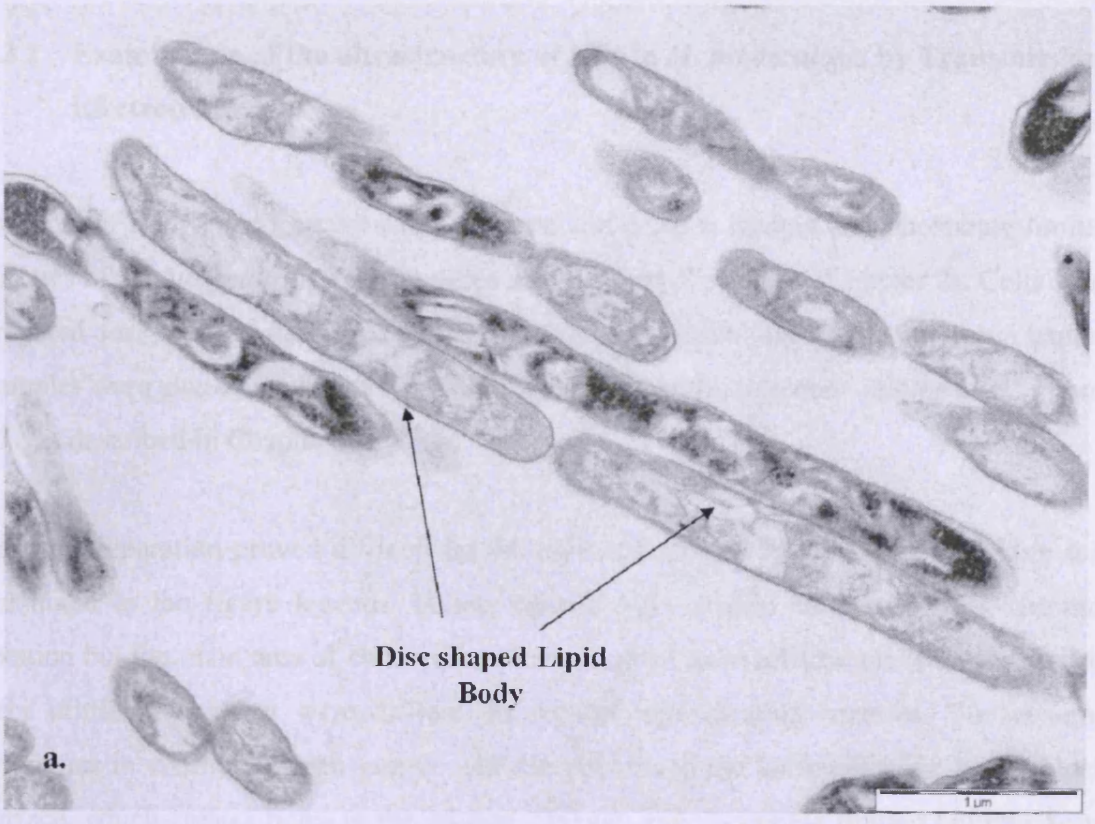
Disc shaped Lipid Body
a.
1 µm

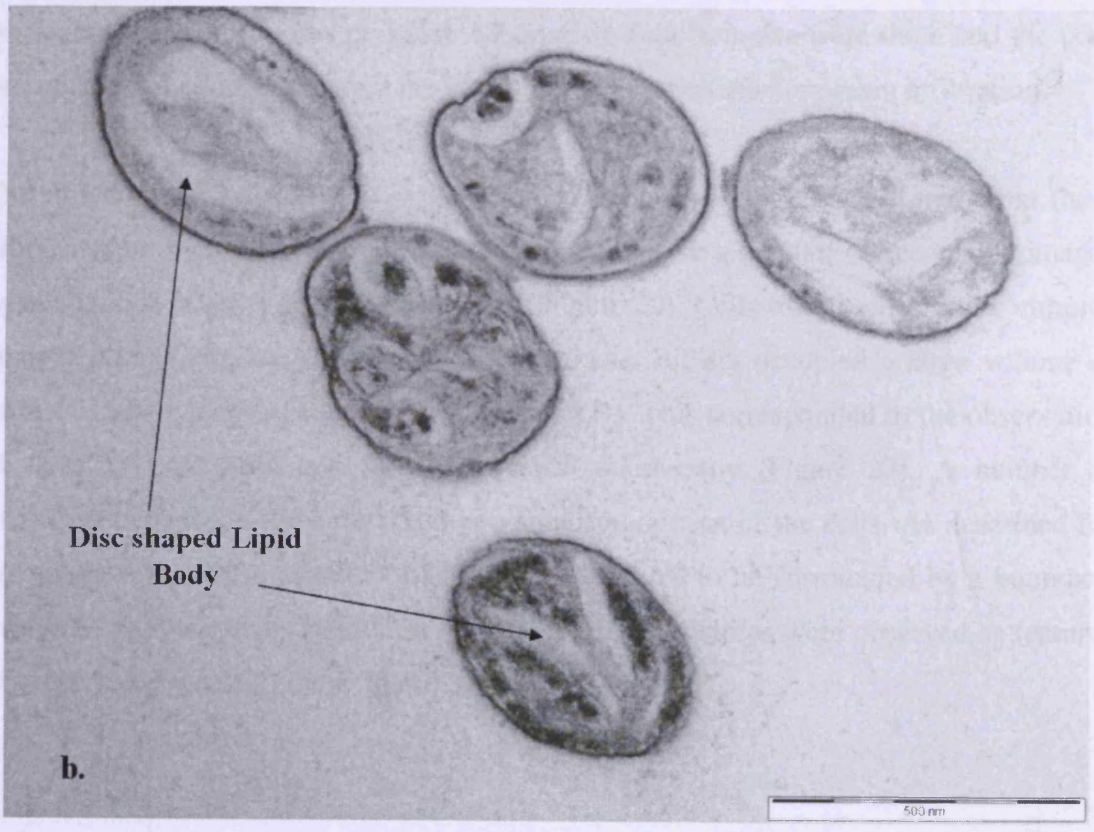
Disc shaped Lipid Body
b.
500 nm

4.3.2 Examination of the ultrastructure of LBs in *M. tuberculosis* by Transmission Electron Microscopy

Cultures of iron limited, oxygen limited, iron and oxygen limited and phosphate limited cultures of *M. tuberculosis* were prepared as described previously (Chapter 2). Cells were prepared for TEM as described in the Materials and Methods section of this chapter. Samples were also stained with Nile Red and viewed by fluorescence microscopy (Figure 27), as described in Chapter 2.

Sample preparation proved difficult for *M. tuberculosis* and features resulting from this are noted in the figure legends. Pellets became very friable after secondary osmium fixation but the main area of concern was unsuccessful resin infiltration. This resulted in very brittle blocks that were difficult to section into ultrathin sections. The ensuing difference in texture between sample and resin results in the knife catching on the block surface, which creates holes in the section. Oxygen and phosphate limited cultures were particularly affected by this problem. Sections of these samples were thick and the poor preservation of cellular structure is clear evidence of unsatisfactory resin infiltration.

The iron limited and iron and oxygen limited culture preparations suffered from these problems but to a much less severe degree and therefore a number of acceptable images were obtained of these cells (Figure 28 and Figure 29). Cells from both of these cultures contained large electron opaque LBs that characteristically occupied a large volume of the cell. Cells typically contained 1-4 of these LBs. This corresponded to the observation of large LBs in these cells by fluorescence microscopy (Figure 27). A number of membranous features were observed in a small proportion of the cells. As described for *M. smegmatis*, a small number of LBs (10%) appeared to be surrounded by a boundary membrane (Figure 29b). In addition, mesosome-like structures were observed as features of some of these cells (Figure 30a-d).

Figure 27: *M. tuberculosis* grown under different conditions in a chemostat contain morphologically distinct Lipid Bodies

M. tuberculosis grown in a chemostat under conditions of **a)** low iron **b)** low phosphate **c)** low oxygen and **d)** low iron and low oxygen and samples were stained with Nile Red and viewed by fluorescence microscopy. Large globular LBs were observed for cells grown under each condition. Scale is equal to 2μM.

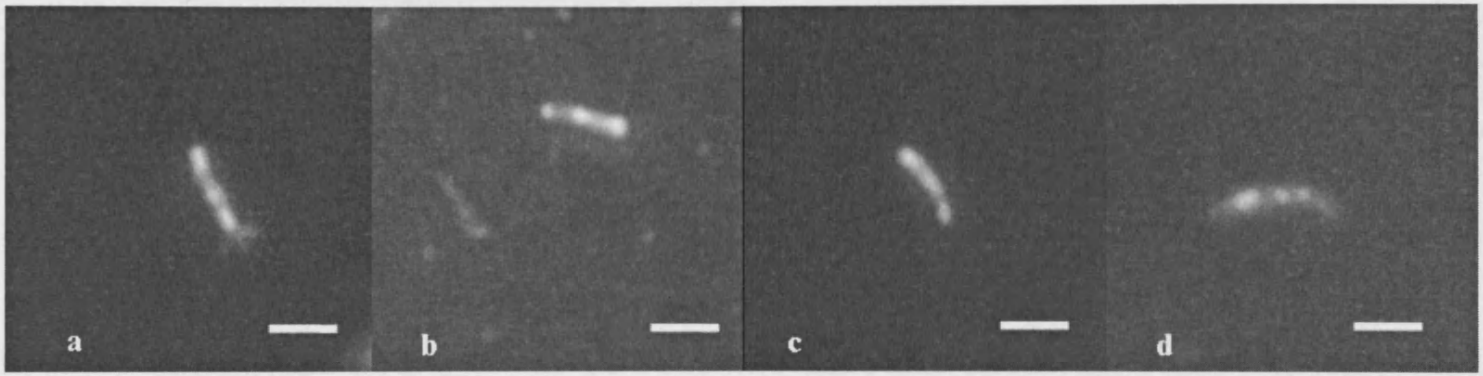

Figure 28: *M. tuberculosis* grown under conditions of low iron form large Lipid Bodies

Images **a-d** show electron micrographs taken of *M. tuberculosis* grown in a low iron medium in a chemostat vessel. Large intracellular Lipid Bodies were observed in these cells, indicated by arrows. Mesosome-like structures were present in a small number of cells. Image **b** shows the cell featured in **a** but taken at a higher magnification. A mesosome in contact with the cell membrane can be clearly seen in this image. Again, image **d** shows the cells in **c** but at higher magnification. Mesosomes were observed in both cells and these appeared to be associated with the cell membrane. Scale bars are indicated in the right hand corner.

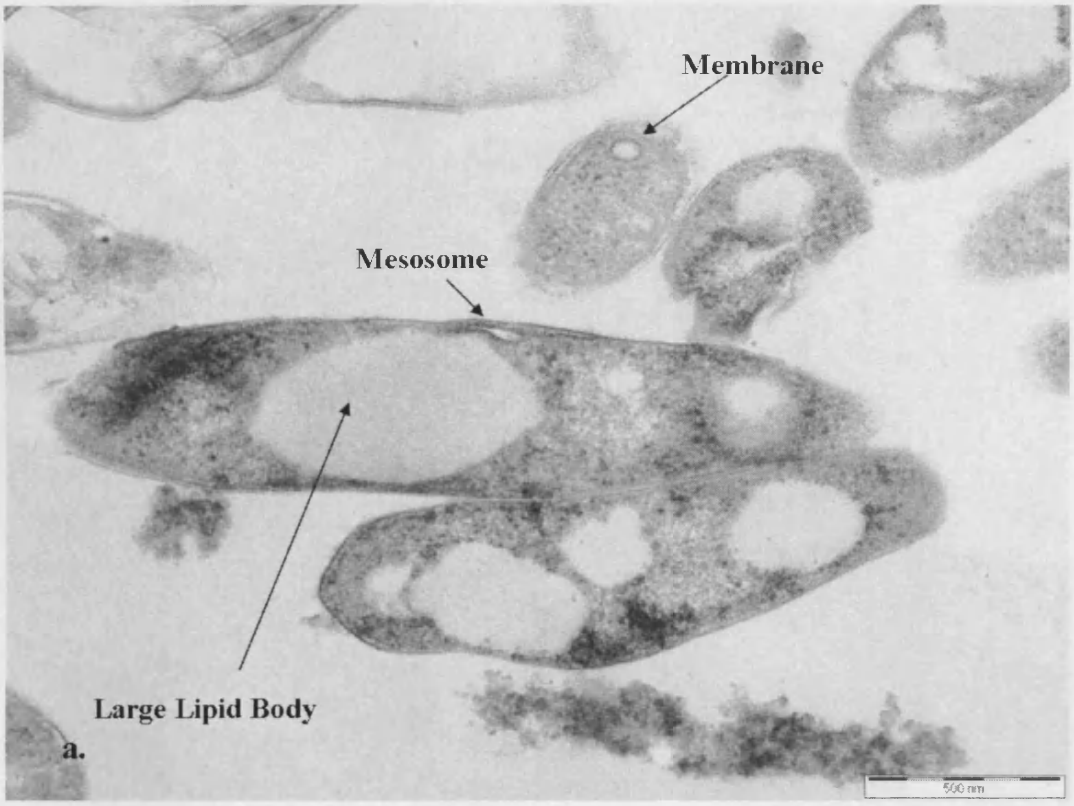
Membrane
Mesosome
Large Lipid Body
a.
500 nm

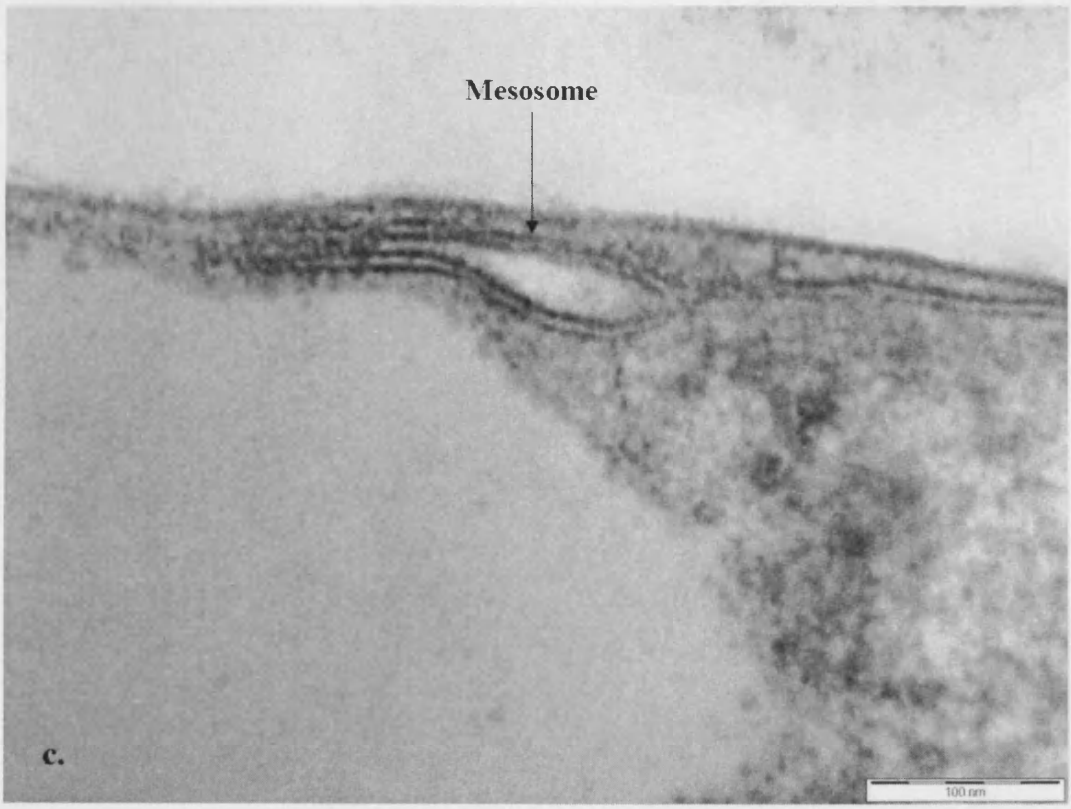
Mesosome
c.
100 nm

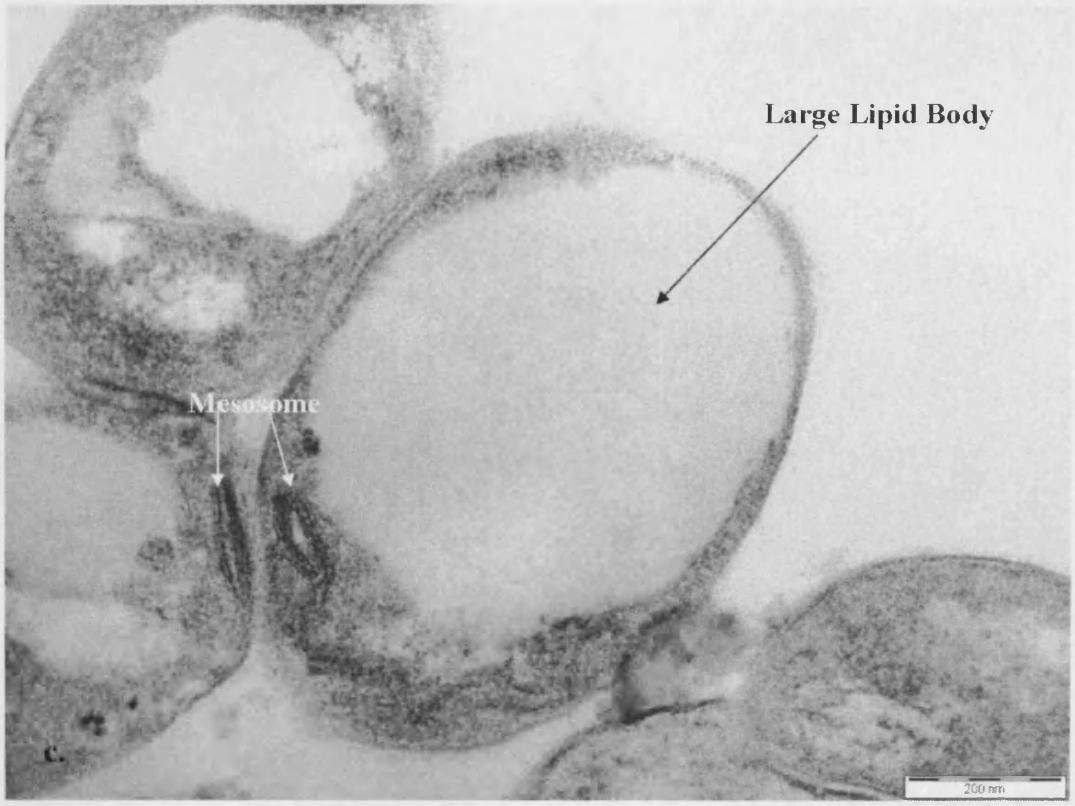
Large Lipid Body
Mesosome
c.
250 nm

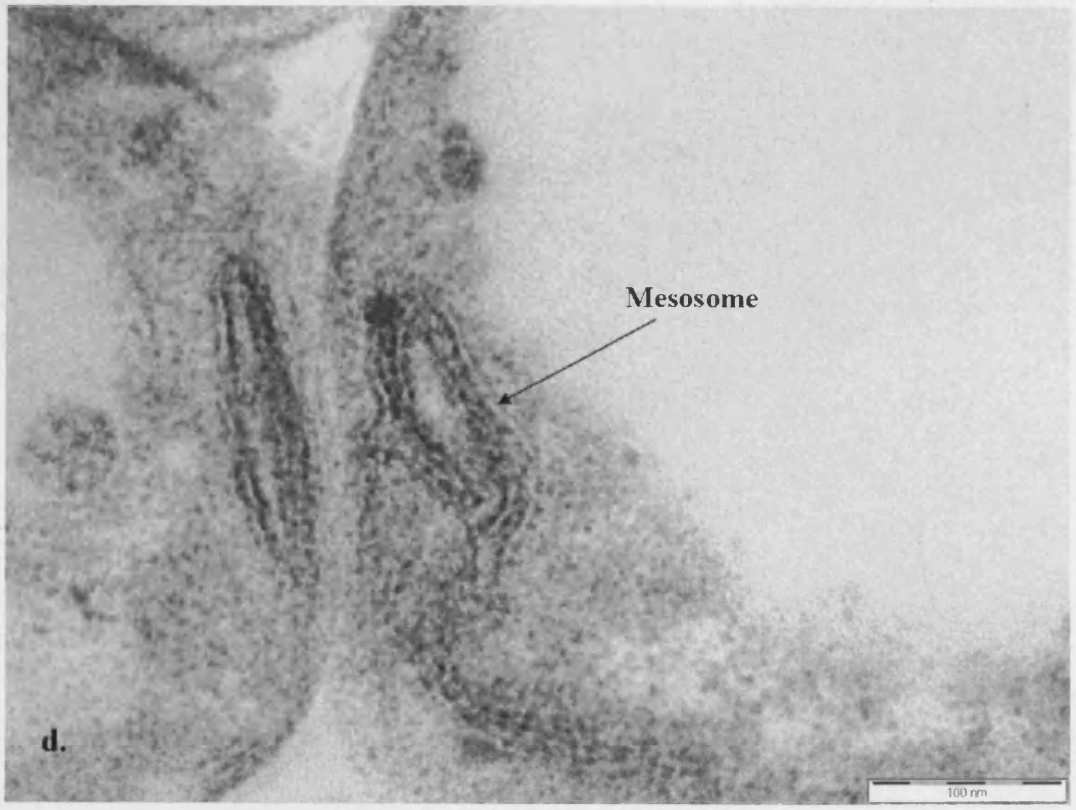
Mesosome
d.
100 nm

Figure 29: *M. tuberculosis* grown under conditions of low iron and low oxygen form globular Lipid Bodies

Images **a-b** show electron micrographs of *M. tuberculosis* grown in low iron medium and under hypoxia. Large and small Lipid Bodies were observed in these cells, indicated by arrows. These were morphologically similar to the Lipid Bodies observed in *M. tuberculosis* grown in low iron medium. Single unit membranes were observed in a small number of cells (image **b**) and were most frequently observed in association with small LBs. Scales are indicated in the right hand corner.

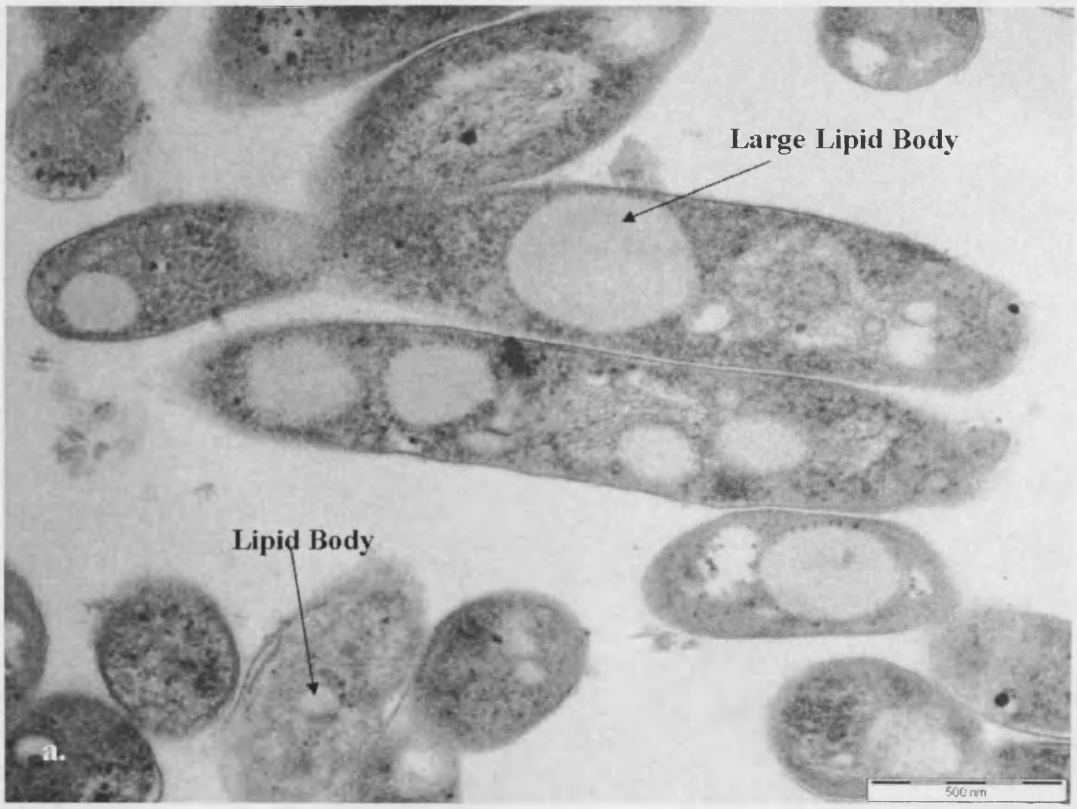
Large Lipid Body
Lipid Body
a.
500 nm

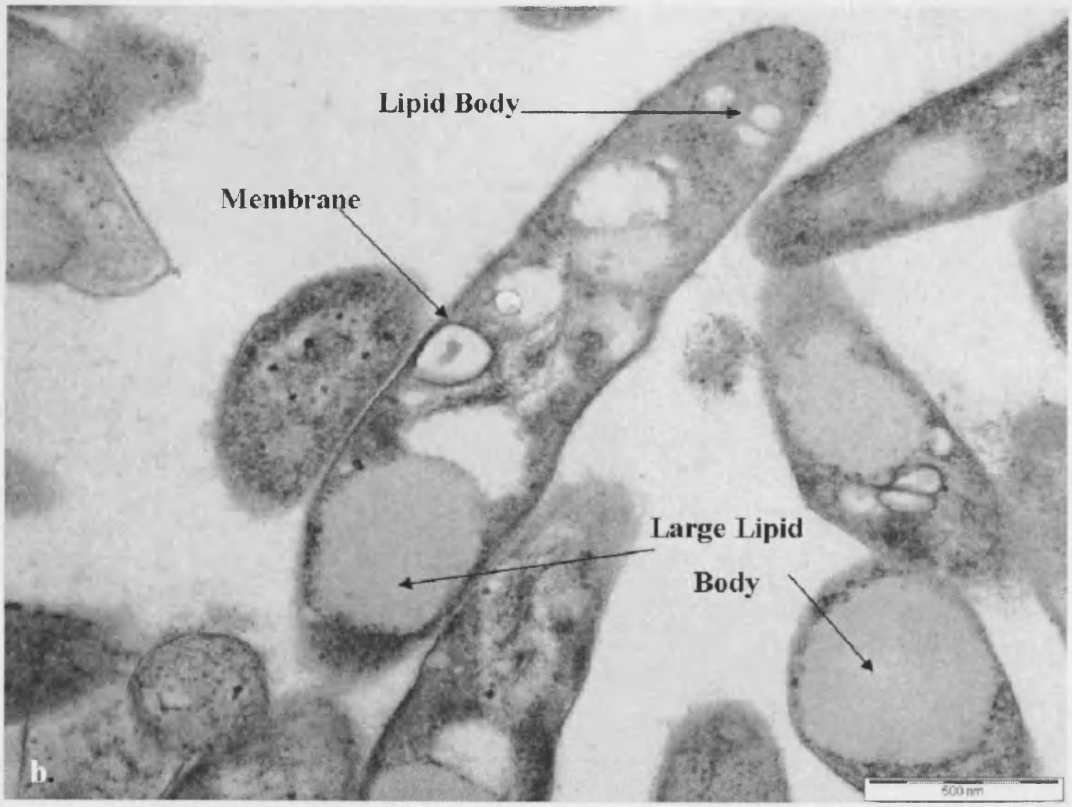
Lipid Body
Membrane
Large Lipid
Body
b.
500 nm

Figure 30: *M. tuberculosis* grown under hypoxia contain Lipid Bodies

Images **a-b** show electron micrographs of *M. tuberculosis* grown under hypoxia within a chemostat vessel. Although specimen preservation was poor, it was possible to observe Lipid Bodies in these cells. Lipid Bodies (LB) resembled those observed in *M. smegmatis* supplemented with fatty acid rather than the large LBs described in *M. tuberculosis* grown under low iron and a combination of low iron and low oxygen. Scales are indicated in the right hand corner.

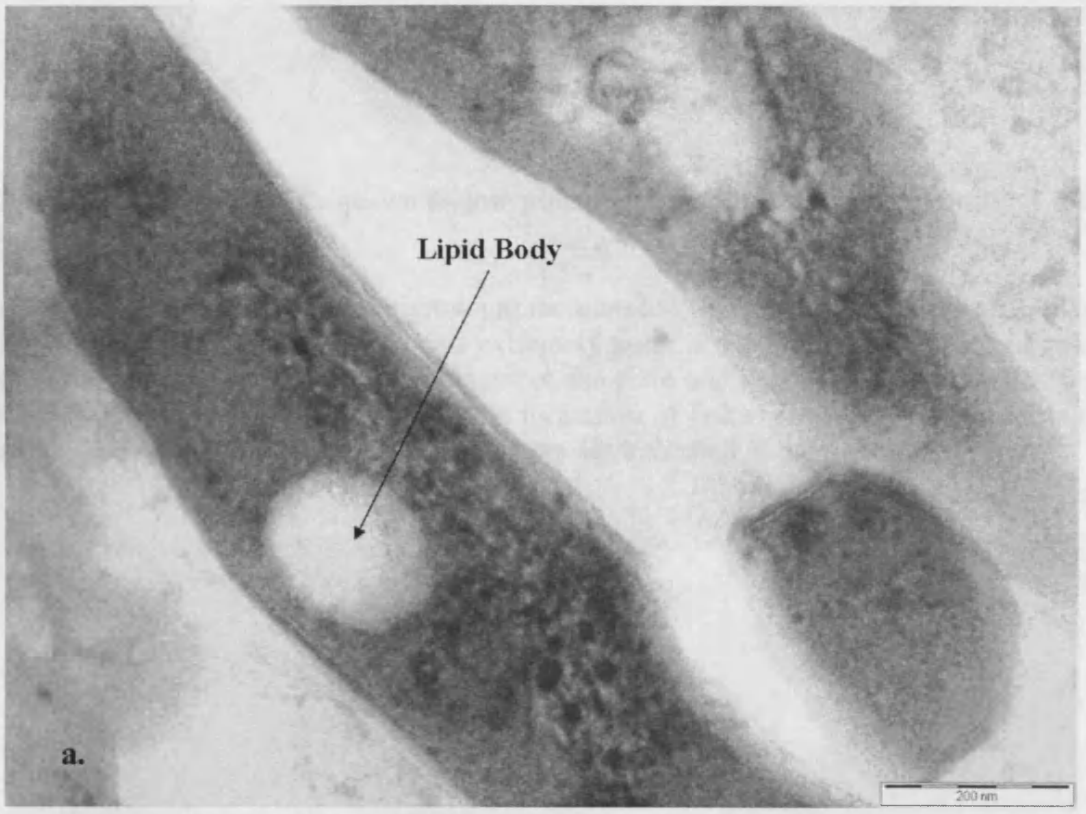
Lipid Body
a.
200 nm

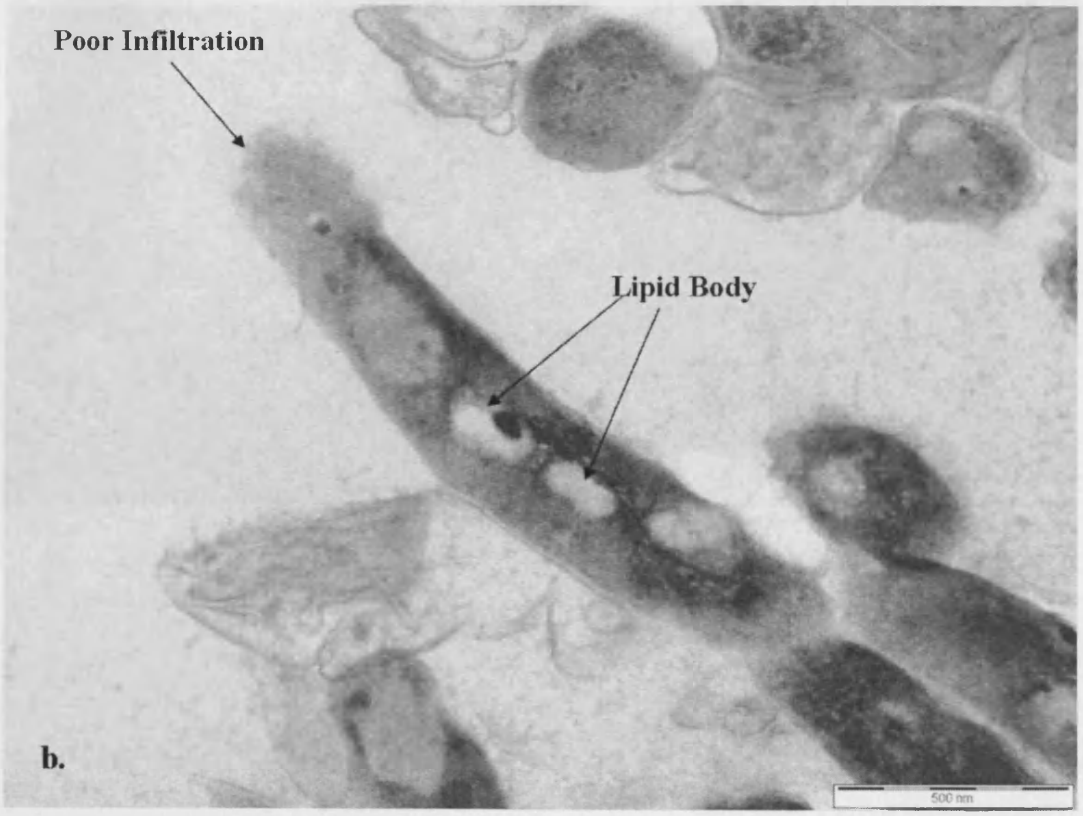
Poor Infiltration
Lipid Body
b.
500 nm

Figure 31: *M. tuberculosis* grown in low phosphate medium contains globular Lipid Bodies

The image shows *M. tuberculosis* grown in medium low in phosphate within a chemostat vessel. The specimen preservation was extremely poor, possibly due to insufficient resin infiltration. The difference in texture between the resin and specimen lead to difficulties in sectioning the material, resulting in the formation of holes. However, it is possible to see large Lipid Bodies in these cells. Scale bars are indicated in the right hand corner.

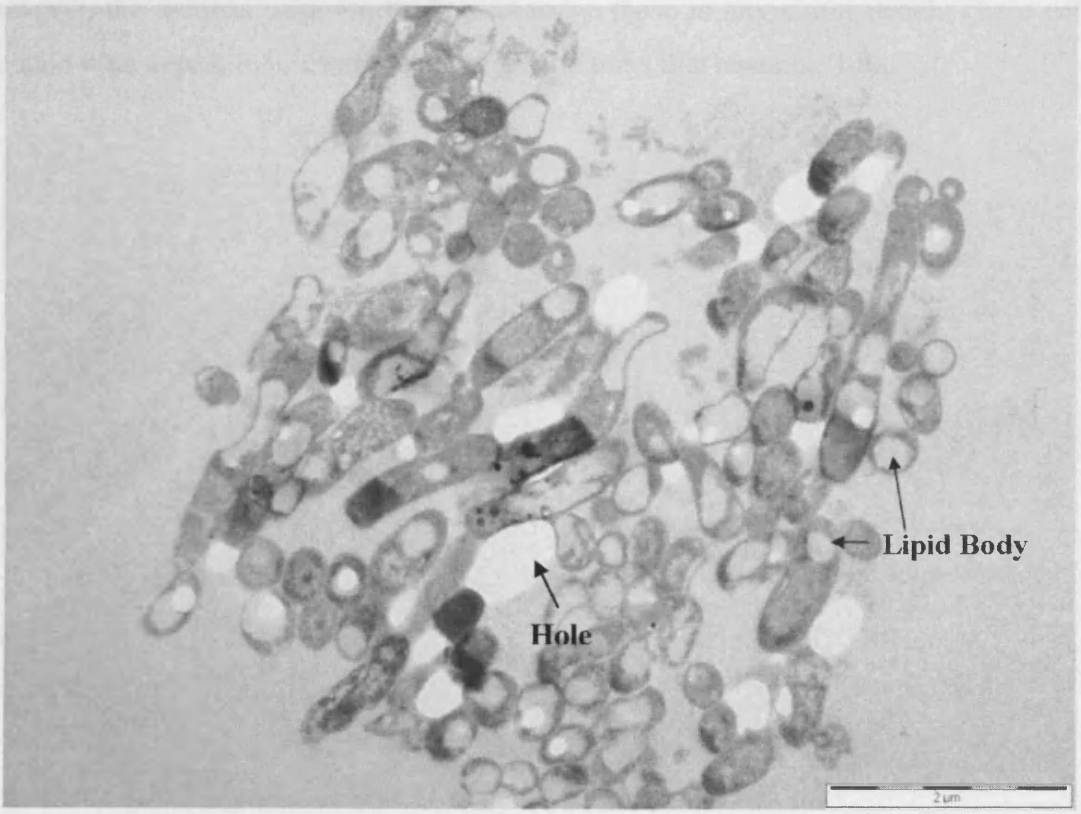

4.3.3 Freeze fracture and freeze etch of *M. smegmatis*

M. smegmatis was cultured in medium low in nitrogen, low in carbon or low in carbon followed by oleic acid supplementation, as described previously. A thin layer of fixed cells was frozen between mica sheets and fractured, as described in Materials and Methods of this chapter. The resulting sections of replica freeze fractured and etched specimen faces were examined by TEM. What appeared to be intact cells were observed on all the sections, indicating that the cells had not fractured fully (Figure 32). Some intracellular structure seems to have been revealed in low carbon and low nitrogen cells, however, the sections were too thick to examine these in any closer detail. These cells contain what appear to be clearly delineated structures that resemble LBs.

Figure 32: Freeze fracture and etch of *M. smegmatis* failed to produce a fracture plane through the cell.

Cultures of *M. smegmatis* were grown in medium low in carbon followed by oleic acid supplementation (a), low in carbon (b) or low in nitrogen (c). Intact cells or thick cell fragments were observed on the section, demonstrating that the cells had not fractured fully. Possible LB structures are indicated by arrows in each image and discussed alongside. However, the quality of the preparation is too poor to draw any firm conclusions. Scale bars are shown for each image.

Image shows a fractured *M. smegmatis* cell grown under conditions of low carbon and then exposed to oleic acid. There is no visible internal structure

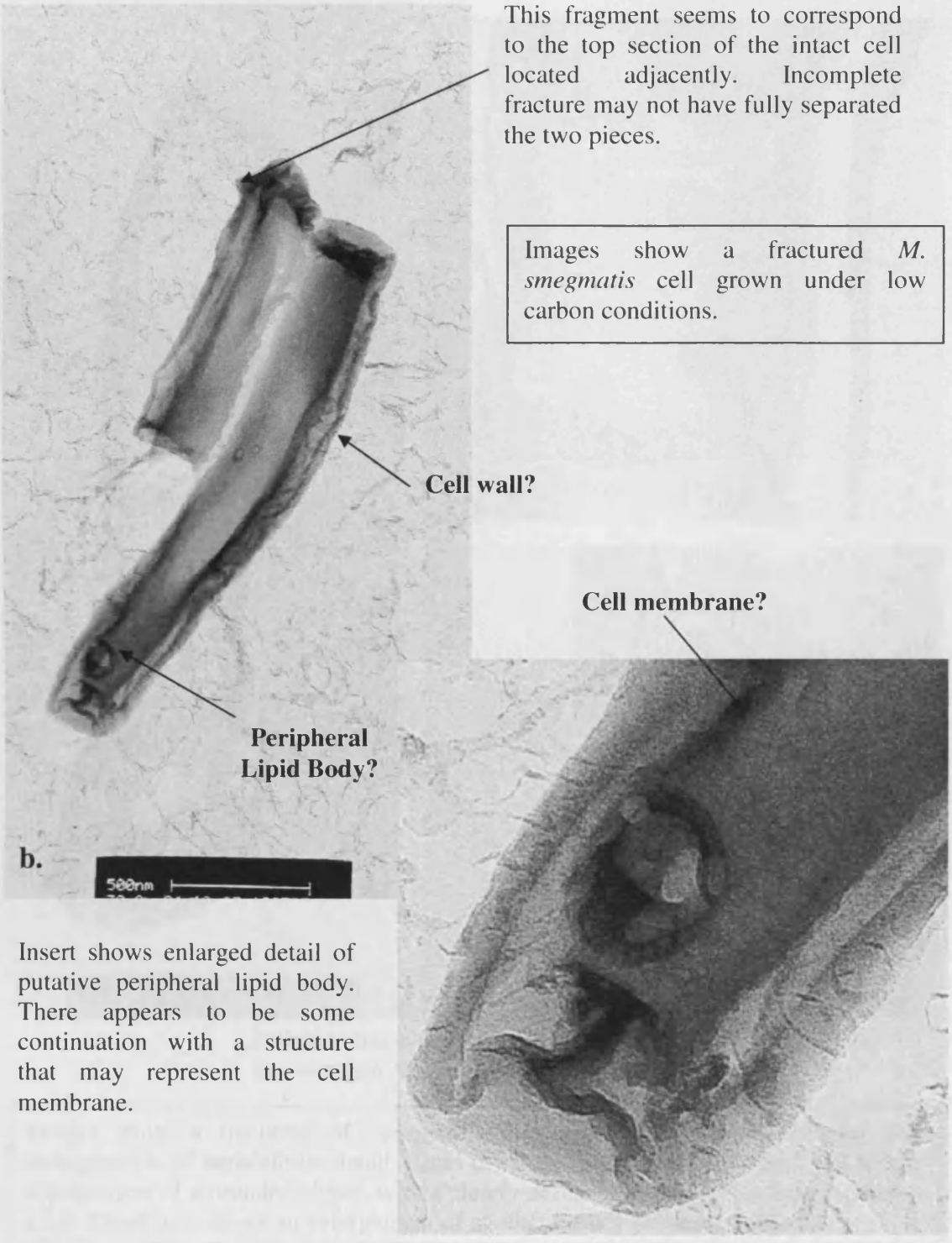
This fragment seems to correspond to the top section of the intact cell located adjacently. Incomplete fracture may not have fully separated the two pieces.
Images show a fractured *M. smegmatis* cell grown under low carbon conditions.
Cell wall?
Cell membrane?
Peripheral Lipid Body?
b.
500nm
Insert shows enlarged detail of putative peripheral lipid body. There appears to be some continuation with a structure that may represent the cell membrane.

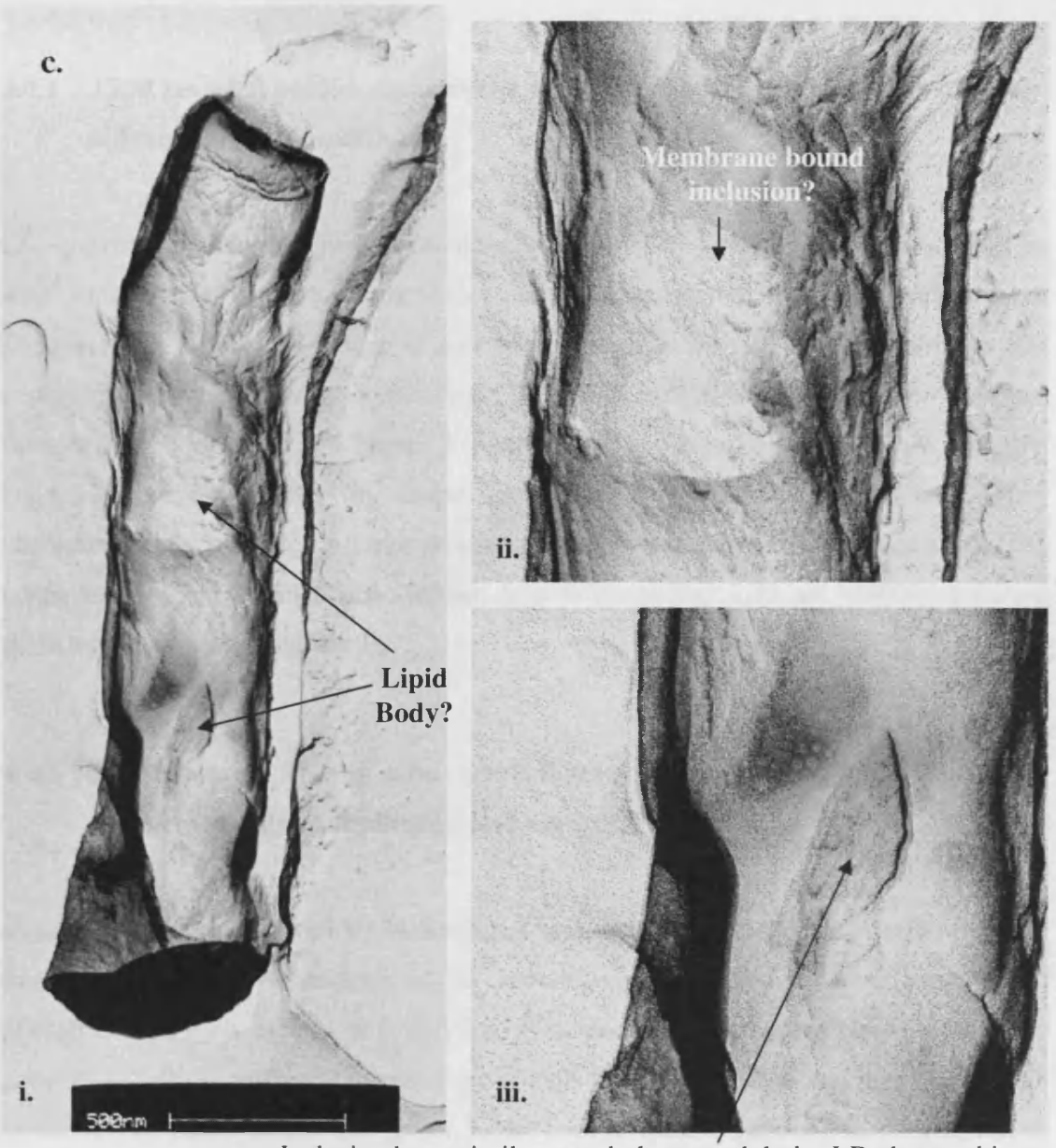

Inclusion has a similar morphology to globular LB observed in low nitrogen *M. smegmatis.*

Images show a fractured *M. smegmatis* cell grown under low nitrogen and enlargements of intracellular detail. Panel (i.) shows the entire cell. Panel (ii.) shows enlargement of a rounded object, with a clearly defined boundary; this may represent a LB. Panel (iii.) shows an enlargement of another clearly delineated object.

4.4 Discussion

4.4.1 TEM revealed unique ultrastructural features in *M. smegmatis* grown under different growth conditions.

LBs appeared as electron opaque, round inclusions in oleic acid supplemented cells. LBs with similar ultrastructure have previously been demonstrated in *Mycobacterium kansasii* (Schaefer and Lewis, 1965) and *M. smegmatis* (Weir et al., 1972). This confirms that exposure to fatty acid is associated with LB accumulation in *M. smegmatis* and was discussed in more detail in Chapter 3. In contrast, the LBs formed under low nitrogen conditions were irregular in shape and were limited to 1-3 per cell. They characteristically occupied a large proportion of the cell volume. Carbon starved cells contained few intracellular LBs, further demonstrating that LBs are mobilized during periods of starvation (Chapter 3).

4.4.2 TEM revealed that *M. tuberculosis* forms large intracellular lipid bodies in response to nutrient limitation and low oxygen tension.

Lipid bodies were observed by fluorescence and electron microscopy in cells obtained from chemostat grown cultures of *M. tuberculosis* subjected to iron, oxygen and phosphate limitation. Due to what appeared to be poor specimen preservation it was only possible to fully examine the morphology of cells grown under iron and iron and oxygen limitation. *M. tuberculosis* cells grown under both of these conditions were observed to have characteristically large LBs and these occupied a considerable amount of the cell volume. The size of these LBs was comparable to LBs formed by *M. smegmatis* grown in low nitrogen broth. This may reflect a similarity in lipid composition (see below for discussion).

Although structural preservation of *M. tuberculosis* cells grown in media with low phosphate or at a low oxygen tension was poor, it was possible to observe LBs in cells grown under both conditions. The phosphate limited cells each appeared to contain one very large LB that occupied the majority of the cell volume, while LBs in the oxygen limited cells seemed to be small, discrete structures. The problems arising in processing these samples for electron microscopy may be due to a thickening of the cell wall in response to the culture conditions. Cunningham and Spreadbury (1998) demonstrated that microaerobically and anaerobically cultured *M. tuberculosis* and *M. bovis* BCG developed a thickened, electron dense cell wall outer layer. The sections taken of the low phosphate and low oxygen cultures were not of sufficient quality to examine the cell wall morphology, however, the presence of a thick cell wall would explain the poor resin infiltration observed in these samples.

4.4.3 Changes in Lipid Body morphology may be due to a change in lipid composition

The difference in ultrastructure between LBs in OA supplemented and low nitrogen cells may reflect differences in lipid composition. As discussed in Chapter 1, Garton *et al* (2002) found that *M. smegmatis* grown under low nitrogen conditions had incorporated fatty acids with various chain lengths, including fatty acids with chain lengths of C24 into TAG reserves. While, the fatty acid profile of TAG extracted from low carbon *M. smegmatis* that had then been supplemented with oleic acid was dominated by oleate. McCarthy (1971) noted that nitrogen limited *Mycobacterium avium* cultures formed 5 times more material with a chain length of C24 in comparison to exponentially growing cells, which contained mostly oleate. Long chain fatty acids are less water soluble than short chain fatty acids (Gurr and James, 1975) and have a higher melting point due to the physical properties of the long hydrocarbon chain. Therefore, TAG composed of long chain fatty acids may have an altered consistency and interact differently with the surrounding cytoplasm, leading to a modified LB form.

M. smegmatis grown in the presence of hexadecanol contained disc-like inclusions with a similar ultrastructure to inclusions formed in *Acinetobacter* sp strain M-1 (Ishige et al., 2002) grown in the presence of hexadecane. Formation of these disc shaped LBs coincided with high levels of wax ester accumulation in this strain of *Acinetobacter* (Ishige et al., 2002). Attempts were made to perform a lipid extraction on *M. smegmatis* cells from this culture. The extracted lipids were separated by Thin Layer Chromatography (TLC) but unfortunately staining of the TLC plate was unsuccessful.

Of the *M. tuberculosis* samples processed for TEM, only an assessment of the LBs within iron limited cells was possible due to poor preservation in the other samples. These LBs resembled the globular LBs observed in *M. smegmatis* grown under low nitrogen conditions more closely than those demonstrated in oleic acid supplemented cells. Cultures of Iron limited *M. tuberculosis*, grown under the same conditions within a chemostat, have been shown to accumulate a novel wax ester and TAG when compared to an iron replete control (Bacon et al., 2007). The structure of LBs formed in *M. tuberculosis* cells subjected to both iron and oxygen limitation resembled those formed under iron limitation rather then low oxygen conditions. Although there were a number of small LBs in these cells that were similar to LBs seen in oxygen limited cells. This change in composition suggests that the cellular location of the novel wax ester produced in response to low iron is within the LB structure.

In addition, the morphology of the LBs within iron limited cells did not match the disc like structures observed in the hexadecanol supplemented *M. smegmatis* cultures and other wax ester accumulating bacteria. This indicates that both the TAG and wax ester accumulated under this condition are stored in the LB, explaining the closer resemblance to the low nitrogen LBs of *M. smegmatis*.

4.4.4 Lipid Bodies are associated with membrane-like structures.

A number of LBs observed in samples of *M. smegmatis*, especially in cells grown in the presence of an exogenous fatty acid source, appeared to be surrounded by a membrane like structure. This seemed to be restricted to a single unit membrane in intracytoplasmic LBs but was observed as a double membrane in peripheral bodies in carbon starved cells. There was also some evidence of unit membrane enclosed LBs in iron and oxygen limited cultures of *M. tuberculosis*. The boundary membranes observed in these cells was most frequently found in association with smaller LBs. This suggests that the membrane structure may play a part in controlling the size of the LB. It is unclear why such large LBs have formed in these cells but it is possible that phospholipid synthesis could not be sustained at a rate that would allow all LBs to be surrounded by a unit membrane. Alternatively, if these LBs consist of a mixture of lipids they may have been formed by a different mechanism to TAG LBs.

The morphology of mycobacterial LB boundaries correspond to that of the single unit membranes that have previously been demonstrated in association with TAG LBs in *Streptomyces lividans* (Packter and Olukoshi, 1995) and *R. opacus* PD630, in addition to other membrane limited carbon storage structures (Table 11). It has been suggested that lipid inclusion limiting membranes consist of only one unit because the membrane is only in contact with an aqueous environment on one side, while the other is in contact with the hydrophobic lipid (Scott and Finnerty, 1976). The presence of a monolayer membrane may also reflect the manner in which the LB is formed (see section 4.4.6 for further discussion). Previous studies of TAG LBs in prokaryotes did not detail whether every LB observed was bordered by a membrane. It is possible that boundary membranes were not observed in association with all LBs examined in this study because poor specimen resolution made it impossible to view the structure in some cases or chemical fixation may not have preserved this feature. Therefore, further evidence of the presence of a limiting membrane in mycobacterial LBs will need to be provided. *M. smegmatis* TAG LBs have not yet been isolated and studies of this kind may reveal the presence of LB associated proteins and phospholipids and verify the existence of such a structure.

In addition to TAG, Rhodococcus LBs were shown to contain phospholipids and proteins (Alvarez et al., 1996) that may be components of the limiting membrane. Kalscheuer et al. (2001) isolated inclusions from *R. opacus* and *R. ruber* and were able to purify TAG body associated proteins. A small portion of these were highly bound and were thought to play a role in the structure and formation of TAG inclusions. Some of the genes encoding these LB associated proteins have been identified as outer membrane porins (Reviewed by Waltermann and Steinbuchel, 2005). These associated proteins and phospholipids may insert into the lipid to form the single unit membrane observed in both *Rhodococcus* and now, *Mycobacterium* species.

The presence of a membrane may prevent coalescence of LBs or alternatively LB integrity may be maintained through hydrophobic interactions of the lipid with the aqueous cytoplasm.

4.4.5 Mesosomes may be involved in the formation of Lipid Bodies

Mesosome-like structures were observed in a small number of *M. smegmatis* and *M. tuberculosis* cells. No definitive ultrastructural profile was observed but generally these structures occurred as collections or invaginations of intra-cytoplasmic membranes. These bodies appeared to be divided into 4 groups; (i.) an invagination of the cell membrane, (ii.) association with septum formation, (iii.) located within the cytoplasm and (iv.) association with LB structures. Mesosomes have classically been defined as invaginations of the plasma membrane or collections of membranous components and may be associated with septum formation, chromosome replication, sporulation or hydrolytic activities (Greenawalt and Whiteside, 1975). Structures with ultrastructural similarities to mesosomes with little further characterisation have been reported in a range of Gram positive and negative bacteria (Greenawalt and Whiteside, 1975).

There has been some debate as to whether the mesosome is in fact an artefact brought about by changes in the cell membrane in response to conventional fixation for the preparation for electron microscopy (Higgins et al., 1976, Ebersold et al., 1981). This has been shown to be the case in *Bacillus cereus*, in which mesosomes were only shown to occur in cells fixed in glutaraldehyde and not in cryofixed cells. This was thought to occur because chemical fixation does not lead to an immediate immobilisation of the membrane (Ebersold et al., 1981).

However, interest in the mesosome has been renewed recently with several examples of mesosome formation in bacteria following treatment with antibiotics and antimicrobial peptides (Santhana Raj et al., 2007, Friedrich et al., 2000). In samples of *Staphylococcus aureus* processed for TEM with short fixation periods, mesosome formation was shown to be confined to antibiotic treated *S. aureus* and was not detected in the control group (Santhana Raj et al., 2007). Mesosomes were formed in response to treatment with a number of antimicrobials with various sites of action (Santhana Raj et al., 2007, Friedrich et al., 2000); therefore, it has now been suggested that mesosomes should be regarded as being indicative of cytoplasmic membrane alterations.

The description of any membranous structure must therefore be approached with caution and the structure should not be present in control groups of cells. As the structures observed in *M. smegmatis* have not been investigated further they will be referred to as "mesosome-like" and described in only physical terms. It is interesting to speculate on the role of these structures in regard to LB formation. However, dedicated ultrastructural studies, beyond the scope of this project, would need to be carried out to determine whether these structures are genuine features of the myocbacterial cell. For example, mycobacterial mesosomes should be present in chemically and cryofixed cells to demonstrate that they are not artefacts.

Before questions were raised regarding the authenticity of the mesosome as a cellular feature there was much speculation over the role of such a structure. While the existence of mesosomes has been disproved in a number of species of bacteria, there have been

accounts in the literature of many morphologically different structures in numerous bacterial species that have been assigned the putative label of "mesosome" (Greenawalt and Whiteside, 1975) but that have not been investigated further. It is possible that if some of these mesosome-like structures are confirmed then they may have a number of roles depending on the species of bacterium and the cellular location or the structure. While no specific role can be definitively assigned to the mesosome, the structure may simply act to concentrate and localise membrane-associated biochemical functions at specific sites within the cell ((Greenawalt and Whiteside, 1975).

Association of a membranous structure with mycobacterial LBs may indicate a putative role of this structure in TAG and LB formation. In support of this mesosomes were mainly observed in cells with LBs and only in cultures with an exogenous fatty acid source. As enzymes involved in the biosynthesis of lipids such as PIMs and aminophospholipids are compartmentalized in the plasma membrane of mycobacteria (Morita et al., 2005), it seems likely that enzymes involved in the synthesis of other lipids are also located here. Since the mesosome is a collection of membranes, it may provide a focus for lipid biosynthesis. Mesosome formation may begin by a collection of Long Chain Fatty Acids (LCFA) at the cell membrane, perhaps represented by the accumulation of electron transparent material observed at the periphery of *M. smegmatis* cells (Figure 24b).

Cell wall thickening was associated with mesosome formation and an increase in glycerol uptake in *Streptococcus faecalis* (Higgins and Daneo-Moore, 1972). This thickening was correlated to growth arrest, a condition which may promote LBs in mycobacteria (Chapter 3 and 5), provided that enough exogenous LCFA is available.

Figure 33 provides a hypothetical model of "mesosome" involvement in LB formation in *M. smegmatis* based on ultrastructural observations. Long chain fatty acid accumulation may cause local disruption of the existing cell membrane, resulting in the formation of a membranous invagination (Figure 28b), or alternatively the mesosome may represent a site of unbalanced phospholipid and membrane biosynthesis (Reviewed by Greenawalt

and Whiteside, 1975), resulting in additional membrane. The collection of lipid may provide the source for the synthesis of LCFA derived lipids, such as phospholipids and mycolic acid.

If the availability of LCFA exceeds the cells demand for lipid synthesis, surplus LCFA may be utilised for TAG formation to avoid further membrane disruption. TAG may initially be localised in the cell envelope in the thickened areas at the cell periphery; which may consist of a mixture of LCFA and TAG. Upon saturation of the cell envelope, large amounts of TAG may be "packaged" into a LB structure for long term storage. The mesosome may begin to protrude into the cytoplasmic space and enclose the lipid in a double membrane-like structure (Figure 23), supporting the growing LB.

Once the LB has reached an unknown critical size, the mesosome may begin to unravel to release the LB into the cytoplasm. The LB shown in Figure 20c is associated with a membranous structure that is connected to the cell membrane. This may represent this step in formation. Finally, the mesosome may detach from the plasma membrane, leaving one leaflet surrounding the LB to form a boundary membrane. LBs in Figure 21e and f appear to be associated with a membranous structure that is not connected to the membrane. Lipases located in the boundary membrane may be responsible for TAG utilisation. PHA inclusions are mobilised by intracellular PHA depolymerises localised to the PHA body during conditions of carbon and energy deficiency (Waltermann and Steinbuchel, 2005). A time course of oleic acid supplementation of *M. smegmatis* would reveal whether mesosome-like structures are involved in LB formation.

Alternatively, the LB may stay connected to the cell membrane through association with the mesosome. Although there is no evidence to support this, the mesosome could also be involved in the mechanism of LB utilisation. During periods of nutrient stress, the mesosome could coil around the LB structure in order to "pull" it back to the cell membrane, where lipases could act on the TAG to be utilised for lipid synthesis or β-oxidation. This would explain why LBs are associated with the cell periphery in cells subjected to low carbon conditions (Figure 33).

Figure 33: Mesosomes may be involved in the formation and utilisation of LBs in mycobacteria.

Panels **(i-v.)** show how mesosome-like structures may be involved in LB formation in mycobacteria. The cell membrane is shown in red, while mesosomes are black and LBs are blue. **(i.)** Lipid collects within a membrane surrounded invagination, **(ii.)** further lipid collection leads to the formation of a peripheral LB, **(iii.)** the mesosome encloses the LB, which is released from the cell membrane, **(iv-v.)** the mesosome becomes detached from the cell membrane and unravels to leave the LB with a single unit membrane. The mesosome is eventually broken down by cytoplasmic enzymes. Alternatively, the mesosome may stay attached to the cell membrane **(vi.)**. The mesosome may then coil around the LB to draw it back to the cell membrane, where lipases can release LCFA for lipid synthesis or β-oxidation **(vii-x)**.

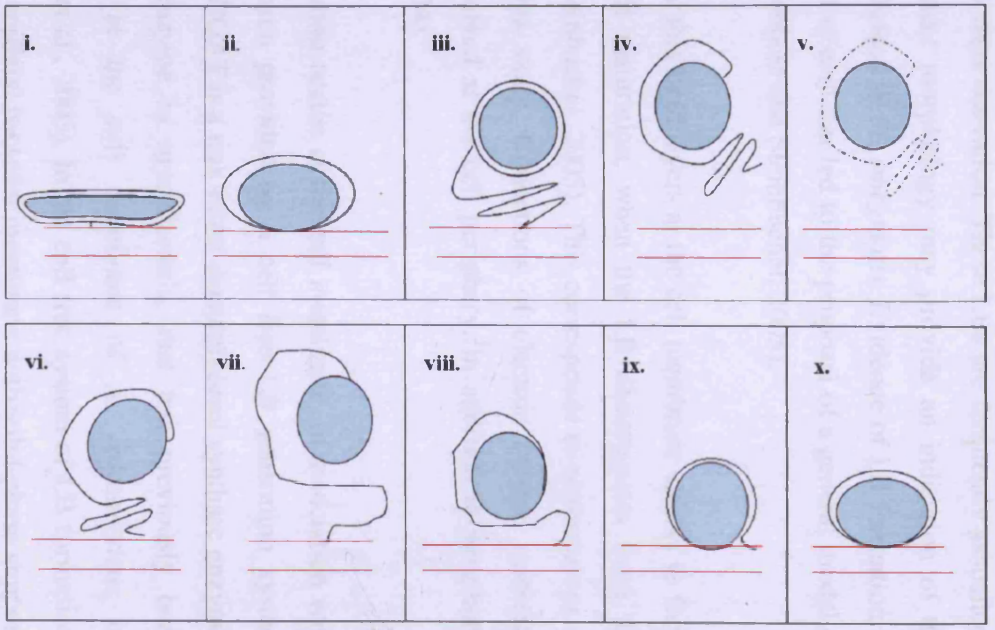

4.4.6 Lipid Body formation in mycobacteria may follow the scheme proposed by Wälterman and Steinbüchel

Carbon starvation is the only condition examined thus far that results in minimal LB content within the *M. smegmatis* cell. Fluorescence and electron microscopy studies have demonstrated that LBs are mobilized during periods of starvation but a number of LBs remain in the cell after 7 days starvation. These LBs are frequently associated with the cell membrane and their morphology may provide an indication of the mechanism by which LBs are formed in *M. smegmatis*. Evidence of LB formation in *R. opacus* and an *in vitro* model system has led to the proposal of a general model of LB formation in bacteria (Waltermann and Steinbuchel, 2005).

TEM images of *R .opacus* show that lipid layers at the cell membrane collect to form LBs at the cell periphery until maturation, when the LB disassociates from the membrane (Waltermann and Steinbuchel, 2005). This corresponds to observations of *M. smegmatis* made within this study. Collections of electron opaque material, expected to be lipid, were observed at the cell periphery, in addition to peripheral bodies of various sizes (Figure 24).

Further evidence that LB formation occurs at the cell membrane, in association with the WS/DGAT enzyme, has been provided by a cell free LB generation system (Waltermann et al., 2005). WS/DGAT is a wax ester/ diacylglycerol synthase enzyme, a homologue of the TGS1 enzyme in mycobacteria, that has previously been demonstrated to be present at the cell membrane of *A. calcoaceticus* by immunolocalisation (Stoveken et al., 2005). In the cell free system of LB formation, WS/DGAT was adsorbed to an artificial bacterial membrane with solid-phase support. Quartz crystal measurements demonstrated that upon addition of a long chain fatty acid-acetyl coenzyme A substrate, lipid pre-bodies were formed at the membrane. The shape of this coalesced lipid was examined further by atomic force microscopy of lipid formation on membrane bound WS/DGAT supported by mica sheets. Small lipid droplets formed at the surface of the mica sheet, comparable to the lipid layer observed at the membrane of *A. calcoaceticus* and now *M. smegmatis*. These small

lipid droplets were shown to coalesce to form spherical structures that corresponded to pre-bodies observed by TEM (Waltermann et al., 2005).

LB formation within the cell is expected to follow a similar pathway. An oleagenous layer of small lipid droplets form at the appropriate membrane bound enzyme and instabilities in this layer leads to coalescence of the lipid droplets at certain parts of the cell to form peripheral lipid body structures. Membrane associated LBs grow until they reach a critical size whereupon they disassociate from the membrane giving rise to mature cytoplasmic LBs. It is possible that the peripheral LB structure is stabilised by the recruitment of phospholipids and proteins that may give the appearance of a membrane like boundary (Waltermann et al., 2005). This model system of bacterial LB formation is summarized in Figure 34.

Also outlined in Figure 34 is a scheme describing LB formation in plant seeds. LBs form via the budding model which consists of lipid droplets formed between the membrane leaflets of the endoplasmic reticulum (ER). The LB buds from the membrane, surrounded by a boundary derived from the outer ER leaflet (Reviewed by Waltermann and Steinbuchel, 2005).

It remains to be seen whether LB formation in *M. smegmatis* follows the Wälterman and Steinbüchel scheme suggested for bacterial LB formation, the system demonstrated in plants or a unique system with elements similar to both pathways. It was unclear whether the oleogenous layer observed in *M. smegmatis* formed at the surface of the membrane or between the membrane leaflets and since LBs have not been isolated from mycobacteria it remains unknown whether the LB is surrounded by any stabilising phospholipids or proteins. It is likely that LB formation in *M. smegmatis* is similar to that demonstrated in *Acinetobacter* due to the homology of the principle enzymes involved in both. To confirm this hypothesis, the cellular location of TGS1 could be identified through immunolocalisation. If the enzyme proves to be membrane bound, LB formation may be demonstrated using a similar cell free system.

Figure 34: Proposed models for LB formation in bacteria and plants

Panels **1-4** show Wälterman and Steinbüchel (2005) model for LB formation in bacteria. **(1.)** Small lipid droplets are formed at membrane docked wax synthase/diacylgylcerol acyltransferase (WS/DGAT) enzyme and remain associated with the enzyme, **(2.)**These small lipid droplets form an oleogenous layer into which phospholipids are inserted, **(3.)**Small lipid droplets are released from the enzyme and conglomerate to form a membrane bound prebody, **(4.)** LB loses contact with the membrane and is released into the cytoplasm.

Panels i-iii show the budding membrane model based on plant seed LB formation (Reviewd by Waltermann and Steinbuchel, 2005). **(i.)** Lipid is formed between the leaflets of the plasma membrane, **(ii.)** LB buds out and becomes surrounded by a phospholipid monolayer derived from the plasma membrane, **(iii.)** The mature LB buds away from the membrane into the cytoplasm. Figure is adapted from Wälterman and Steinbüchel (2005).

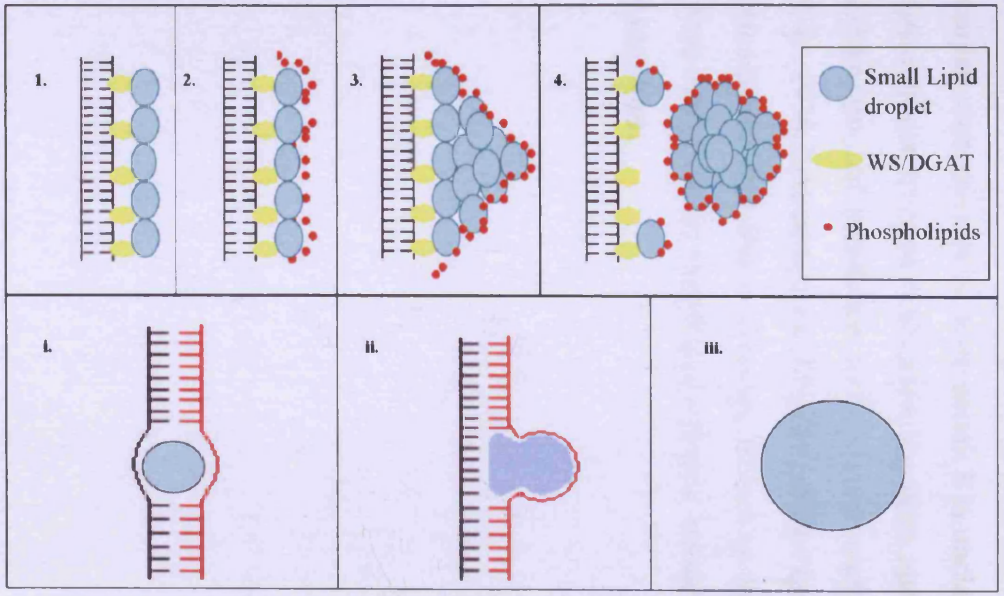

4.4.7 Freeze Fracture Replication of mycobacteria was unsuccessful

Fracture cleavage of mycobacterial cells to reveal cell membrane or intracellular structure was unsuccessful, as demonstrated by the observation of intact cells in the resulting replica sections. Some internal structure was visible in a small number of cells. Structures that resembled LBs were observed in low carbon and low nitrogen treated *M. smegmatis* but the specimen was too thick to examine ultrastructure in more detail. It is unclear why this procedure was unsuccessful because freeze fracture replication has been applied to the study of the mycobacterial cell envelope and membrane using similar methods to those employed in this thesis (Kim et al., 1976, Lounatmaa and Brander, 1989, Nguyen et al., 1979). Nguyen *et al* (1979) demonstrated that freeze cleavage occurs at different levels of the mycobacterial cell envelope and produces four fracture planes, revealing the three dimensional organisation of the envelope.

4.5 Conclusions and Future Work

The morphology of LBs in mycobacteria appears to reflect the composition of the storage lipid; however, this needs to be confirmed by lipid extraction. Although a number of LBs were observed to be surrounded by a boundary membrane there was insufficient evidence to indicate that this is a general feature of LBs in mycobacteria. Isolation of mycobacterial LBs and characterisation of bound proteins and lipids could support the hypothesis that a phospholipid membrane surrounds these structures. There is currently little known about the mobilisation and degradation of TAG stored in LBs. It would be of great interest to examine the mechanism by which mycobacteria utilise this carbon source and this may be examined over a time course of growth in media low in carbon or during starvation in PBS. The enzyme LIPY has been implicated in the degradation of TAG in mycobacteria (Deb et al., 2006) and immunolocalisation of this enzyme may also indicate the mechanism by which lipids stored in LBs are released and made available to the cell. It was also unclear whether the LB remains attached to the membrane. It is unfortunate that freeze fracture replication of *M. smegmatis* was unsuccessful, as this method has the potential to reveal intracellular membrane structures associated with the LB.

There appears to be some similarity in ultrastructural features of LB formation in mycobacteria and *Rhodococcus* spp. As discussed, immunolocalisation of TGS1 may indicate the site of LB formation. Further work may involve ultrastructural studies of LB formation in response to fatty acid exposure over time.

Chapter 5

Are Lipid Body Positive *Mycobacterium tuberculosis* Cells Growth Arrested?

5.1 Introduction

In the studies presented in Chapter 3 of this thesis it was demonstrated that *M. tuberculosis* formed LBs in response to a number of conditions, including hypoxia and Nitric Oxide (NO). It has been shown that gradual depletion of oxygen brings about a reversible growth arrest (Wayne and Sohaskey, 2001) and NO reversibly inhibits respiration in *M. tuberculosis* (Voskuil et al., 2003). Therefore, it was hypothesised that LBs formation may coincide with growth arrest. Only a subpopulation of cells exposed to LB promoting conditions formed LBs, suggesting that the population as a whole was physiologically heterogeneous. Therefore, a number of strategies were employed to identify the growth status of individual LB positive *M. tuberculosis* cells.

Differential fluorescence staining of growing and non-growing cells allows the direct identification of growth status at the individual cell level. A conjugate of vancomycin and the fluorescent stain, BODIPY, (vanBODIPY) has been used in previous studies of *Bacillus subtilis* to label areas of nascent peptidoglycan synthesis (Daniel and Errington, 2003). Localisation of the probe is due to the ability of vancomycin to inhibit transglycosylation of the disaccharide pentapeptide peptidoglycan precursor to the existing peptidoglycan which occurs through the actions of penicillin binding proteins. The mechanism by which vancomycin exerts this inhibition is unknown; however, vancomycin is known to bind the terminal D-Ala-D-Ala chain of the peptidoglycan precursor (Reviewed by Daniel and Errington, 2003). Peptidoglycan synthesis in mycobacteria has been shown to occur at the cell poles and sites of division through vanBODIPY labelling (Thanky et al., 2007). This differs from peptidoglycan synthesis in *B. subtilis*, which occurs in a helical pattern through the cylindrical part of the cell to allow exponential cell elongation (Daniel and Errington, 2003). Cell elongation in mycobacteria may only occur at the restricted points of the cell pole in order to allow for the synthesis of new cell envelope lipids (Daniel and Errington, 2003). Labelling of mycobacteria with vanBODIPY was explored as a method for detecting dividing cells within a population of LB positive mycobacteria.

The fluorescent dye Carboxyfluorescein diacetate, succinimidyl ester (CFDA/SE) has been used to assess bacterial growth rate and distribution in environments as diverse as the mouse gut (Lee et al., 2004) and groundwater systems (Mailloux and Fuller, 2003). CFDA/SE is a non-fluorescent precursor that is able to permeate the cell membrane and is then converted to the fluorescent derivative by non-specific intracellular esterases. The CFDA/SE derivative becomes covalently linked to intracellular proteins through the succinimidyl group of the probe (Lee, 2004). The dye divides equally between daughter cells upon cell division, therefore, the intensity of cellular staining halves at each cell division event (Mailloux and Fuller, 2003). Mycobacteria were labelled with CFDA/SE in order to assess the value of the dye in monitoring mycobacterial cell division.

A further approach used to examine the growth status of mycobacteria was to design a series of cell division Green Fluorescent Protein (GFP) reporter vectors. GFP is a chemiluminescent protein from the jellyfish, *Aequorea victoria*. No specific jellyfish genes are needed for the post-translational modification of GFP, making this protein an invaluable tool in examining the localisation of gene products and in monitoring gene expression in both eukaryotes and prokaryotes (Reviewed by Tsien, 1998). GFP can be used to monitor gene expression by construction of a vector with GFP transcription under the control of the promoter of the gene of interest. A GFP reporter vector has been successfully used to monitor gene expression of *M. tuberculosis* in macrophages (Triccas et al., 1999). This study made use of the *E. coli*/mycobacterial shuttle vector, pJFX2, containing a promoterless mutant version of the GFP gene, which had been designed to exhibit enhanced fluorescence and greater solubility (Triccas et al., 1999). In addition, a transcription terminator placed downstream of *gfp* ensures that expression of the reporter gene is controlled by the inserted promoter of interest and not plasmid promoters (Triccas et al., 1999). The *gfp* gene of pJFX2 was placed under the control of the β-lactamase promoter of *Mycobacterium fortuitum* to make the control plasmid pJFX4 (Triccas et al., 1999). The plasmids pJFX2 and pJFX4 have also been used in previous studies within this laboratory group to examine the expression of the resuscitation promoter factors (*rpf*)

of *M. tuberculosis* (Rollinson, 2003) and form the basis of the constructs used in the studies detailed in this thesis.

Figure 35: Map of the GFP reporter vector, pJFX2

The plasmid pJFX2, constructed by Triccas *et al*, (1999) contains the unique BamHI and ScaI sites for cloning of promoter fragments directly upstream of the *gfp/sacB* operon. A kanamycin resistance gene is included for selection.

t: transcriptional terminator of coliphage T4, **oriE:** *E. coli* origin of replication, **gfp:** green fluorescence protein, **sacB:** *B. subtilis* sucrose sensitivity gene.

Image taken from Triccas *et al* (1999).

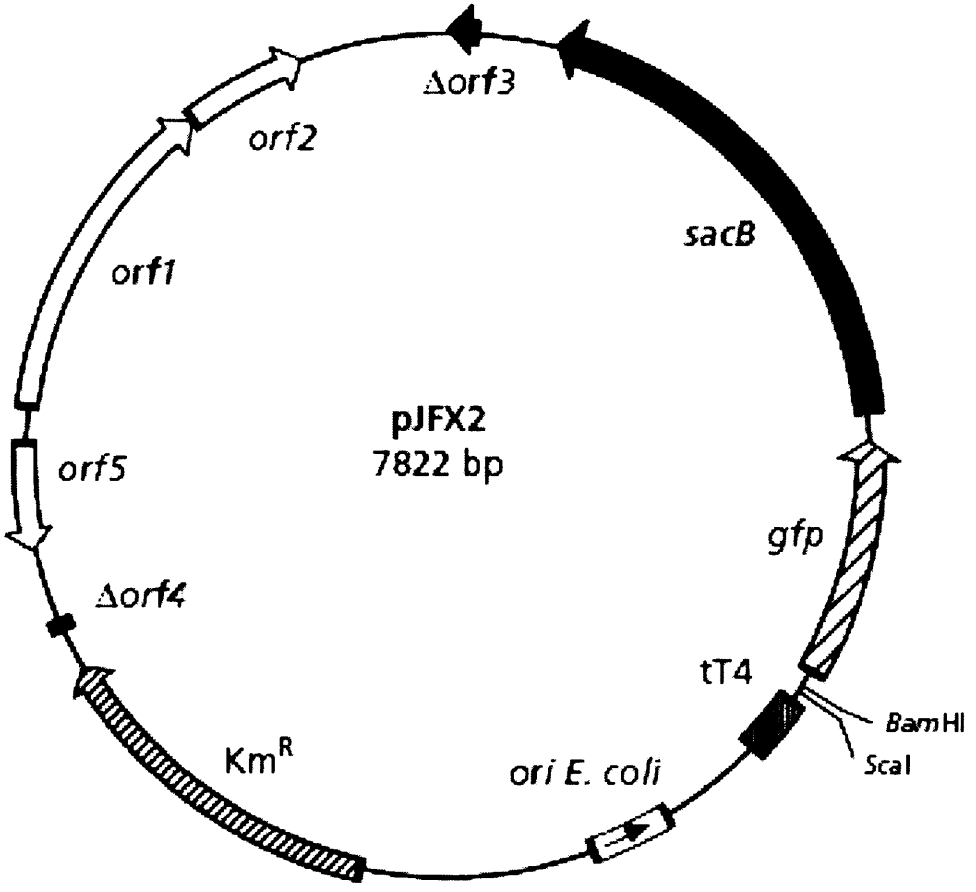

The expression data and literature available for genes identified as belonging to transcription, RNA and DNA synthesis and cell division functional gene classes (Cole et al., 1998) were reviewed in order to identify genes that might serve as reporters for different stages of cell division. In addition to their differential expression in cell growth, the putative promoter regions for three of these genes of interest, *ftsz*, *whiB2* and *sigB*, had previously been identified (Manganelli et al., 2002, Raghunand and Bishai, 2006b, Roy and Ajitkumar, 2005).

In order to ensure that each daughter cell is of equal size and contains a complete chromosome, the mechanism of cell division is closely connected to cell growth, chromosome replication and segregation (Feucht and Errington, 2005). The first step in cell division is septum formation, which is initiated by the cell division protein, FtsZ (Reviewed by Dziadek et al., 2003). FtsZ is a homologue of the eukaryotic polypeptide, tubulin and like tubulin, FtsZ polymerizes in a GFP dependent manner (Lowe and Amos, 1999). The FtsZ protein localises to the site of division in the form of a contractile ring, called a Z ring (Reviewed by Slayden et al., 2006, Dziadek et al., 2003). Septation is orchestrated by the recruitment of other cell division proteins important in septum formation to the site of division through their interaction with FtsZ (Reviewed by Dziadek et al., 2003). *M. tuberculosis* has an FtsZ homologue that is similar to other prokaryotic FtsZ genes in sequence and structure (Slayden et al., 2006). Dziadek *et al* (2003) demonstrated that the cell division process and viability in mycobacteria is sensitive to the intracellular levels of FtsZ. In addition, the FtsZ protein of *M. tuberculosis* can act as a functional substitute in *M. smegmatis*, demonstrating that initiation of septum formation is equivalent in fast and slow growing mycobacteria. Since FtsZ is one of the principle cell division proteins, expression of *ftsZ* has been used as a reporter gene for active cell division within this thesis. Indeed, in actively growing cells, FtsZ protein accounts for 2% of the total soluble protein (Dziadek et al., 2003).

Like *ftsZ*, the *M. smegmatis* cell division gene *whmD* and the *M. tuberculosis* functional homologue, *whiB2* are essential for septation and cell division (Gomez and Bishai, 2000, Raghunand and Bishai, 2006a, Raghunand and Bishai, 2006b). A conditional *whmD M.*

smegmatis mutant showed immediate filamentous growth and an altered frequency and positioning of septa upon depletion of WhmD levels (Gomez and Bishai, 2000). Overexpression of *whmD* resulted in hyperseptation and growth retardation. Since the affect of WhmD depletion on cell division in *M. smegmatis* was immediate, WhmD and WhiB2 have been implicated in the regulation of early stages of mycobacterial cell division (Gomez and Bishai, 2000). The structure of WhiB2–like proteins strongly suggests that these proteins are DNA binding proteins (Raghunand and Bishai, 2006a). In addition, *M. smegmatis* transformants carrying a *whmD-gfp* fusion plasmid showed a diffuse pattern of fluorescence, consistent with its proposed role as a transcriptional regulator (Raghunand and Bishai, 2006b). The WhmD protein and mRNA are present throughout exponential growth and early stationary phase (Gomez and Bishai, 2000), and given this and its importance as a cell division gene, *whiB2* expression was selected as a marker for active cell growth for this study.

Transcription in bacteria is carried out by a 4 subunit RNA polymerase holoenzyme. The core complex of this enzyme carries out the polymerase reaction, while the sigma subunit of this enzyme is required for promoter specific DNA binding (Reviewed by Gomez et al., 1997). The essential principle sigma factor, of the sigma 70 family, recognises the promoters of genes involved in vegetative growth, while alternate sigma factors bring about conditional gene expression. Therefore, activation of alternate sigma factors allows rapid adaptation to environmental changes (Reviewed by Gomez et al., 1997). There are at least 14 different sigma factors in *M. tuberculosis* (Hu and Coates, 1999). The mycobacterial sigma factor, sigA, is growth rate independent and is unresponsive to environmental stresses and as such is considered to be the principle sigma factor (Hu and Coates, 1999). The sigma factor sigB has been described as an alternate sigma factor, because the *sigB* gene can be insertionally inactivated in *M. smegmatis* (Doukhan et al., 1995). The expression of *sigB* is upregulated during stationary phase (Hu and Coates, 1999, Manganelli et al., 1999) and in response to nutrient starvation (Betts et al., 2002, Hu and Coates, 1999), heat shock (Manganelli et al., 1999, Hu and Coates, 1999), SDS treatment (Manganelli et al., 1999), low aeration (Manganelli et al., 1999) and hydrogen peroxide exposure (Hu and Coates, 1999). Therefore, it has been suggested that *sigB*

controls the regulons of stationary phase and general stress resistance (Hu and Coates, 1999). Furthermore, the expression of *sigB* has also been shown to be upregulated in a hollow fibre murine granuloma model (Karakousis et al., 2004) and sputum AFB (Garton et al., 2008). Altogether, this evidence suggests that *sigB* is upregulated in cells in which growth has decreased. Therefore, the expression of *sigB* has been used as a reporter for growth arrest within this thesis.

Three GFP reporter plasmids were constructed to monitor the expression of *ftsZ*, *whiB2* and *sigB* in NO exposed *M. tuberculosis*. It was expected that LB negative populations of cells exposed to NO or the control compound would be actively growing and therefore, expressing high levels of *ftsZ* and *whiB2* but not *sigB*. Whereas, the LB positive cells are hypothesised to be growth arrested and therefore, expression of cell division genes should decrease but expression of the stationary phase sigma factor B should increase.

5.2 Materials and Methods

5.2.1 Preparation of fluorescence probes

Vancomycin, BODIPY FL conjugate (VanBODIPY)

Vancomycin labelled with the BODIPY fluorophore was purchased from Molecular Probes (Invitrogen) in 100µg units. Distilled water (1ml) was added to the 100µg of powder to give a stock concentration of 100µg/ml. The stock container was covered with foil and stored at -20°C.

Carboxyfluorescein diacetate, succinimidyl ester (CFDA/SE)

CFDA/SE was purchased as a Cell Tracer Kit from Molecular Probes (Invitrogen) containing 500µg powder aliquots. The contents of one vial was solubilised in 90µl DMSO (provided with kit) to make a stock solution of 10mM. This stock was diluted in PBS to make working stocks of 20 and 40µM concentrations.

5.2.2 Labelling of *Bacillus* subtilis with vanBODIPY

Method adapted from Daniel and Errington (2003).

A solid culture of *Bacillus subtilis* was kindly supplied by Sarah Glenn (University of Leicester). An overnight culture of *B. subtilis* was prepared by resuspending a single colony in 10ml of LB broth in a sterile universal tube (Sterilin). The culture was diluted 1:10 the following day and incubated for 3 hours to re-establish exponential growth. Tubes were covered in foil and VanBODIPY and unlabelled vancomycin were added at an overall concentration of 1µg/ml. Cells were labelled for 15minutes and samples were removed for microscopic analysis. Stained cells were washed 3 times in PBS and spun

onto coverslips. Coverslips were mounted onto slides in PBS, sealed with nail varnish and examined by phase and fluorescence microscopy.

5.2.3 Labelling of mycobacteria with vanBODIPY

Method adapted from Thanky et al (2007).

A culture of *M. smegmatis* was grown in Middlebrook 7H9 broth. Culture (5ml) was removed during exponential (doubling in optical density over 3 hours) and stationary phase growth (no change in optical density over 3 hours) and transferred to foil covered 32ml sterile universal tubes (Sterilin). VanBODIPY and non-labelled Vancomycin were added to a final concentration of 1μg/ml and labelled for 6 hours. Duplicate samples were taken and one of these was stained with Nile Red, as described. Cells were immobilised on coverslips and examined by microscopy.

5.2.4 Labelling of mycobacteria with CFDA/SE

A culture of *M. smegmatis* was prepared as described (Chapter 2) in Sautons broth to an optical density at 580nm of 0.5. Duplicate samples of culture (1ml) were placed in 1.5ml microcentrifuge tubes and pelleted for 1.5 minutes at 16 000 x g. The supernatant was removed and replaced with 1ml 20 or 40μM CFDA/SE in PBS. Control samples were resuspended in PBS. Tubes were incubated in a hot block for 15 minutes and centrifuged for 1.5 minutes at 16 000 x g. Pellets were resuspended in 1ml Sautons broth and transferred to foil wrapped 32ml sterile universal tubes (Sterilin). Samples (100μl) were taken immediately for OD measurements (diluted 1:10) and microscopic analysis. Tubes were incubated at 37°C and further samples were taken approximately every 3 hours.

5.2.5 Manipulation of DNA

5.2.5.1 Construction of GFP promoter fusion plasmids

Known promoter sequences of genes involved in different phases of the cell division cycle were incorporated into the GFP reporter plasmid, pJFX2. Primers were designed to include the sequence directly upstream of the promoter region for each gene, along with a *BamH1* site and a *Sca1* site in the forward and reverse primers, respectively. The regions of interest were amplified by PCR, using *M. tuberculosis* H37Rv genomic DNA as a template. The size of PCR product was predicted using an online *in silico* PCR programme (*http://insilico.ehu.es/* supplied by the University of the Basque Country). PCR products were separated by agarose gel electrophoresis and products of the correct size were gel purified. Both vector and PCR products were digested with the appropriate enzymes and gel extracted and purified. These digested products were ligated and plasmid constructs were transformed into *E. coli* DH5α. Transformed cells were selected by kanamycin resistance and colonies were cultured and plasmid extracted. Extracted plasmids were digested to confirm the presence of inserted DNA. Purified plasmids were then sequenced (both forward and reverse) across the cloning region, using gene specific primers to confirm the insertion of the correct DNA. Plasmids were then transformed into mycobacteria (Rollinson, 2003).

5.2.6 Reagents

5.2.6.1 Preparation of Primers

Primers were prepared by adding an appropriate volume of water (specified in the MWG synthesis report) to the synthesised oligonucleotide to give a concentration of 100pmol/ml. This stock was left to stand at room temperature for 30 minutes to allow the primer to dissolve fully. A working stock of 10pmol/ml was made by the addition of 10µl primer to 90µl sterile nanopure water.

5.2.6.2 Preparation of dNTP stocks

Stocks of dNTP (100mM) were thawed on ice. Using gloves, 10µl of each dNTP (dATP, dCTP, dGTP and dTTP) were deposited into a clear micro-centrifuge tube to give a volume of 40µl. The volume was adjusted to 100µl with the addition of 60µl sterile nanopure water. This stock of 10mM dNTPs was separated into 20µl aliquots in micro-centrifuge tubes and stored at -20°C.

5.2.6.3 Preparation of TAE buffer

TAE buffer was made in batch. A solution of 40mM Tris-acetate and 2mM Na_2EDTA was prepared and the pH was adjusted to 7.6 (Rollinson, 2003).

5.2.6.4 Preparation of STET buffer

STET buffer was prepared using the following reagents in distilled water:

8% (w/v) sucrose

50mM EDTA pH 8.0

50mM Tris-HCl pH 8.0

0.5% Triton x100

Prior to use, 1mg/ml lysozyme was added. 2µl 100mg/ml stock of lysozyme in distilled water was added to each 200µl STET buffer used (Rollinson, 2003).

5.2.7 Primer Design

Primers were designed to amplify the region of interest and devised to incorporate a clamp region and restriction site. A clamp region was included in order to give the primer stability; the clamp in mycobacterial primers consists of a poly-Adenosine chain because the genome is GC rich. Restriction sites to match the plasmid restriction sites were also included in the primer design. The required restriction cutting site sequences were identified using DNAStar software (DNASTAR, Inc.). The sequence of the gene of

interest was found using the Tuberculist database (Pasteur Institute) and sequence upstream and downstream (at the start of the gene) of this was used in the design. A stretch of the same base or a sequence with complementary bases at each end was avoided to prevent the formation of loops and primer dimers. The gene sequence was also checked for the absence of the required restriction sites using the DNAStar map draw function. The forward primer was a direct reproduction of the upstream sense strand of DNA (5' to 3') whereas; the reverse primer was the complement of the downstream sequence. Each pair of primers were tested in an online *in silico* PCR programme (*http://insilico.ehu.es/* supplied by the University of the Basque Country) to confirm amplification of the correct product. Finally, the primers were matched to the *M. tuberculosis* H377Rv genome using BLAST Nucleotide (short sequence match) in order to confirm that no other genes matched the sequence. Oligonucleotides were purchased from MWG AG Biotech (Germany).

5.2.8 Polymerase Chain Reaction (PCR)

PCR was used to amplify the specific sequence of interest. For each 25µl PCR reaction the following reagents were included in the PCR tube:

10 x PCR buffer	2.5µl
10mM dNTP	0.5µl
Magnesium (Mg^{2+})	1.5µl
Taq polymerase (Abgene)	2.0µl
Forward primer (10pmole/µl)	2.0µl
Reverse primer (10pmole/µl)	2.0µl
M. tuberculosis genome DNA (1ng/µl)	1.0µl
Nanopure water	15µl

Tubes without the addition of DNA acted as no template controls.

The PCR reaction was carried out as follows. A temperature gradient was chosen to incorporate the melting temperatures (T_m) of all of the primers. The lowest T_m was used for each pair of primers and an annealing temperature was selected to be 1°C less than this value, these are shown below:

ftsZ: 56 °C

whiB2: 57 °C

*sig*B: 60 °C

The PCR machine lid was heated to 100°C to avoid evaporation of the sample. The DNA was denatured at 95°C for 2 minutes. This was followed by 40 cycles of denaturation, primer annealing and elongation, beginning with incubation at 94°C for 1 minute. Annealing was carried out at the appropriate temperatures selected for the primers (see above) for 1 minute, followed by elongation at 72°C for 0.5 minutes. Cycling was followed by a final elongation step consisting of incubation at 72°C for 10 minutes. Amplified products were stored at 4°C prior to separation by gel electrophoresis.

5.2.9 Gel Electrophoresis

Agarose gel was prepared at 1.5-2.0% in TAE buffer, with the addition of 0.5μg/ml ethidium bromide for staining DNA. The gel was placed inside an electrophoresis tank and covered with TAE buffer. DNA ladder was loaded into one well for fragment size comparison. 1μl 6x loading buffer (0.25% (w/v) orange G and 30% (w/v) glycerol) was added for each 5μl of DNA in order to monitor the progress of the DNA through the gel. DNA was loaded into the wells and the power unit was set to run at 400mA and 60v. DNA bands were visualised by UV illumination and gel photography was performed using a gel documentation system and imaging software (Kodak) (Rollinson, 2003).

5.2.10 Purification of DNA from agarose gel

Plasmids and PCR products were gel extracted and purified using the YorkBio Gel/PCR DNA purification kit. The manufacturer's instructions were followed for DNA extraction

from agarose gel. Bands of DNA were visualised by UV light and carefully removed with a scalpel into pre-weighted micro-centrifuge tubes. An image of the gel was taken after this to confirm that no primer dimmer bands had also been removed. The gel fragments were weighted and 100µl of binding buffer was added per 100mg of gel slice accordingly. This volume was doubled for agarose gel in concentrations greater than 1.5%. The tubes were floated in a 50°C waterbath with occasional vortex mixing for 5-10 minutes or until the gel was completely solubilised. This mixture was added to a kit spin column and left to stand at room temperature for 2 minutes. The spin columns were centrifuged at 16 000 x g for 1 minute and the flow through solution was discarded. The DNA was washed twice by adding 500µl wash solution to the columns, which were centrifuged for 15 seconds. The flow through solution was discarded. Spin columns were then centrifuged for 1 minute to remove residual wash solution. The columns were then inserted in to clean micro-centrifuge tubes and 40µl elution buffer was applied to the central part of the filter membrane within the spin column and incubated at room temperature for 2 minutes. The column was centrifuged for 1 minute and the eluted DNA was transferred into a clean micro-centrifuge tube. Eluted DNA was stored at -20°C.

5.2.11 Restriction Digest

Plasmids and PCR products were digested with *BamH1* and *Sca1* to provide the correct sticky ends for ligation. Extracted plasmids were also double digested to confirm the insertion of DNA. Enzymes and buffers were supplied by NEB Lifesciences. Restriction digest reactions were carried out in 20µl volumes. The final volume of enzyme was 10% or less to avoid unspecific cutting (star activity). Typical reactions are shown below:

Plasmid Digest:	
Plasmid DNA	5µl
10x Buffer 2	2µl
BamH1	1µl
Sca1	1µl
Nanopure water	1µl

DNA Digest:	
PCR product	10µl
10x Buffer 2	2µl
BamH1	1µl
Sca1	1µl
Nanopure water	6µl

The reaction was carried out for 2 hours and incubated at 37°C in a hotblock.

5.2.12 Ligation of DNA

Digested PCR products and plasmids were joined through the activity of DNA ligase. The reaction was set up in 10µl volumes in 0.2ml PCR tubes, as shown below. Tubes were sealed with laboratory sealing film (Nesco, Osaka, Japan) and incubated at 4°C for a mimimum of 24 hours:

Plasmid DNA	2µl
Insert DNA	2µl
T4 DNA ligase (Promega)	1µl
2X rapid ligation buffer (Promega)	5µl

5.2.13 Preparation of electrocompetent *E. coli* DH5α

A 5ml volume of LB broth was inoculated with a single colony of *E. coli* DH5α and grown overnight at 37°C with shaking. 5ml of this starter culture was used to inoculate a sterile conical flask containing 500ml pre-incubated LB broth. Due to the sensitivity of electrocompetent cells it was important to ensure that the culture flask contained no residual detergent, therefore a dedicated flask, washed without detergent was used. The culture was incubated at 37°C with shaking until the culture reached an OD_{600} of 0.5, approximately 2 hours after inoculation. The flask was placed on ice for 20 minutes and all subsequent steps were carried out on ice. Therefore, all containers, reagents and equipment were pre-chilled. The cells were harvested by centrifugation at 4000g for 15 minutes at 4°C. The supernatant was removed with a pipette to avoid loss of cell pellet. The cells were gently resuspended in 500ml ice-cold sterile 10% glycerol and harvested by centrifugation at 4000g for 15 minutes at 4°C. The supernatant was removed as before and the cells were resuspended in 250ml ice-cold sterile 10% glycerol. The cells were harvested by centrifugation and resupended in 20ml ice-cold sterile 10% glycerol. After pelleting by centrifugation, the cells were finally resuspended in 2ml ice-cold sterile 10%

glycerol. Electrocompetent cells were divided into 50µl aliquots and snap-frozen in a dry ice/ ethanol bath. Cells were stored at -80°C for 6 months (Rollinson, 2003).

5.2.14 Preparation of electrocompetent *M. smegmatis*

An overnight culture of *M. smegmatis* was prepared in 100ml Middlebrook 7H9 broth (as described in Chapter 2). This culture was grown to mid log phase (OD_{580} 0.5-1.0) and incubated on ice for 10 minutes. As for the preparation of electrocompetent *E. coli*, all reagents and equipment were pre-chilled and manipulations were carried out on ice. The cells were harvested at 2000g at 4°C for 10 minutes. The pellet was resupended in 100ml ice-cold 10% glycerol and harvested by centrifugation. The cells were resupended in 50ml ice-cold 10% glycerol and pelleted by centrifugation. The cells were finally resuspended in 5ml ice-cold 10% glycerol and divided into 400µl aliquots and snap-frozen in a bath of dry ice and ethanol. Cells were stored at -80°C for 6 months (Rollinson, 2003).

5.2.15 Preparation of electrocompetent of *M. tuberculosis*

A 100ml culture of *M. tuberculosis* in Middlebrook 7H9 broth was prepared as described (Chapter 2) and grown to mid-log phase, OD_{580} 0.5-1.0 with doubling over a 24 hour period. Cells were harvested by centrifugation at 2000 x g for 15 minutes and washed with an equal volume of 10% glycerol at room temperature. The cells were washed a further 2 times in this manner before resuspension in 10% glycerol at $1/100^{th}$ the original culture volume. The electrocompetent cells were divided into 200µl aliquots ready for transformation. Electrocompetent *M.tuberculosis* was prepared fresh prior to each transformation (Rollinson, 2003).

5.2.16 Transformation of electrocompetent *E. coli* DH5α and *M. smegmatis*

Aliquots of electrocompetent cells were thawed on ice. Plasmid (1-5µl) DNA was added to the cells and incubated on ice for 1 minute. The cells were transferred to a pre-chilled 0.2cm gap electroporation cuvette. The cuvette was wiped clean to remove condensation and care was taken not to touch the metal contacts to avoid the possibility of salt deposition and arching. The following settings were used for electroporation:

Resistance	200Ω (1000 Ω for *M. smegmatis*)
Capacitance	25µFD
Voltage	2.5v

Cells were immediately diluted in warm media (1ml LB broth for *E. coli* and 2ml Middlebrook 7H9 broth for *M. smegmatis*) and transferred to a Universal tube. Transformed cells were incubated at 37°C, with shaking for 90 or 120 minutes, for *E. coli* and *M. smegmatis*, respectively. This allowed the cells to recover and start to express antibiotic resistance. Following this, 200µl volumes of transformed cells were spread on plates of selective media (kanamycin 25µg/ml in LB agar or Middlebrook 7H10 OADC agar). Plates of transformed *E. coli* were incubated overnight at 37°C, while *M. smegmatis* plates were incubated for 3-4 days (Method adapted for Rollinson, 2003).

5.2.17 Transformation of α–select chemically competent *E. coli*

Transformation of ligated products was carried out in chemically competent cells because the high salt in this preparation increased the likelihood of arching during electroporation. The manufacturer's instructions were followed, with some alterations, for the transformation of commercially available α –select chemically competent *E. coli* (Bioline). Aliquots of cells were thawed on ice and 5µl plasmid DNA was added to each. The cell suspension was mixed with slight flicking and incubated on ice for 30 minutes. The microcentrifuge tubes were then placed in a waterbath set exactly at 42°C for 45

seconds. Following this, the tubes were placed on ice for 2 minutes. The transformation reaction was diluted to 1ml with the addition of 950µl LB broth. The tubes were placed inside a 50ml Falcon centrifuge tube and incubated at 37°C, with shaking for 90 minutes. The transformed cells were spread onto selective agar as described in section 5.2.16.

5.2.18 Transformation of electrocompetent *M. tuberculosis* H37Rv

Competent cells were mixed with 5µl plasmid DNA and incubated at room temperature for 10 minutes. Cells were then transferred to a 0.2cm gap electroporation cuvette. Electroporation was carried out in a Biorad Gene Pulser Excel electroporator using the same parameters as those used for *M. smegmatis* (see above). Cells were immediately diluted in 1ml Middlebrook 7H9 broth, which was added to a further 4ml of broth in a 50ml Falcon centrifuge tube. This was sealed, bagged and incubated with shaking at 37°C overnight. Transformed cells were spread onto selective media (Middlebrook 7H10 OADC agar containing 25µg/ml Kanamycin) and incubated at 37°C for 3-4 weeks.

5.2.19 Confirmation of the presence of plasmid DNA in Mycobacteria by the "Zap-Zap" method

Method taken from Rollinson (2003).

Extraction of plasmids from mycobacteria is difficult because the thick cell wall resists lysis by the typical reagents used for plasmid preparation. Therefore, to confirm that transformed mycobacteria contained plasmid constructs, these plasmids were transformed into *E. coli* using electroporation. A small amount of growth from a plate of transformed mycobacteria was emulsified in a thawed aliquot of electrocompetent *E. coli* DH5α. This was incubated on ice for 10 minutes and cells were transferred to a pre-chilled cuvette. The electroporation was carried out with the settings used for the electroporation of *E. coli* (see above). The transformed cells were diluted in 1ml LB broth and incubated for 60 minutes. Cells were then plated onto selective agar (LB containing 25µg/ml kanamycin)

and incubated overnight. Colonies displaying antibiotic resistance were used in crude plasmid preparations.

5.2.20 Crude Triton/boil plasmid preparation

Small scale crude plasmid isolation was carried out to confirm the presence of plasmid constructs in transformed *E. coli*. This was carried out on at least 6 colonies for each plasmid construct. A volume of 5ml of LB broth containing 25µg/ml kanamycin was inoculated with transformed *E. coli* growth and grown overnight at 37°C, with shaking. 1ml of this culture was pelleted at 16 000 x g for 1 minute in a microcentrifuge tube. The supernatant was removed and replaced with 200µl STET buffer containing 1mg/ml lysozyme. Tubes were floated in a boiling water bath for exactly 2 minutes and the reaction was immediately quenched by covering the tubes in ice for 10 minutes. Following this, the tubes were centrifuged at 16 000 x g for 10 minutes. The resulting cell debris pellet was removed with a toothpick and discarded. 10µl 10M NH_4Ac and 400µl ice cold absolute ethanol was added to each tube, mixed with vortexing and incubated on ice for 10 minutes. The precipitated DNA was pelleted by centrifugation at 16 000 x g for 10 minutes. The supernatant was tipped out in one motion and the tube was tapped onto some tissue paper remove any residue. The pellets were then washed in 100µl 70% ethanol and pelleted at 16 000 x g for 5 minutes. The supernatant was discarded and remaining liquid was removed using a pipette. The pellets were allowed to dry next to a Bunsen burner and finally, resuspended in 50µl TE buffer containing 50µg/ml RNase A. The pellets were allowed to swell for an hour at room temperature and mixed with vortexing. Crudely extracted plasmid DNA was digested with restriction enzymes to confirm the presence of inserted DNA.

5.2.21 Small scale preparation of plasmid DNA

Plasmid DNA was prepared for sequencing or transformation using the Qiagen Miniprep kit. A Promega Miniprep kit based on the same principles was used previously with poor

results. During plasmid extraction, cells are lysed to release plasmid DNA, which is precipitated in the presence of high salt. Precipitated DNA is adsorbed to a spin column membrane, washed and eluted. 1ml overnight culture of transformed *E. coli* (in LB broth with 25μg/ml kanamycin) was pelleted by centrifugation at 16 000 x g for 1 minute in a micro-centrifuge tube. Cells were resuspended in 250μl Buffer P1 containing RNase A. The bacteria were resuspended completely by vortexing until no cell clumps were visible. 250μl Buffer P2 was added and the tubes were mixed by inverting 4-6 times. The tubes were not vortexed to avoid shearing of genomic DNA. Mixing was continued until the solution became viscous and slightly clear. The lysis reaction was allowed to proceed no longer than 5 minutes. 350μl Buffer N3 was added to each tube and mixed by inverting the tube 4-6 times. The tubes were centrifuged at 16 000 x g for 10 minutes in order to pellet the cell debris. The supernatant was transferred to a QIAprep spin column and this was centrifuged for 30 seconds. The flow through was discarded and the DNA washed by the addition of 750μl Buffer PE. The column was centrifuged for 30 seconds and the resulting flow through was discarded. The columns were spun again for 1 minute to remove residual wash buffer. The columns were transferred to clean micro-centrifuge tubes and 50μl sterile nanopure water was applied to the centre of each column membrane. The column was left to stand at room temperature for 1 minute and then centrifuged for 1 minute. The eluted DNA was stored at -20°C.

5.2.22 DNA Sequencing

Sequencing of plasmid constructs and PCR products were carried out by MWG AB Biotech (Germany) using specific primers directed to the DNA inserts. DNA to be sequenced was vacuum dried in micro-centrifuge tubes. The received sequences were checked for insertion of the correct DNA using a BLASTn search. All plasmid constructs and PCR products matched the correct gene sequence in the *M. tuberculosis* H37Rv genome sequence and the promoter regions were shown to be present in the plasmid construct inserts.

5.3 Results

5.3.1 vanBODIPY stains the septum of actively growing *B. subtilis*

Vancomycin BODIPY (vanBODIPY) staining of nascent peptidoglycan synthesis of *B. subtilis* was examined in order to establish the staining method using an organism in which the staining pattern of this probe is well characterised. Exponential phase and stationary phase cultures of *B. subtilis* were stained with vanBODIPY. Septum staining was readily visible in log phase cultures and less frequently observed in stationary phase cells (Figure 36).

Figure 36: vanBODIPY localises at the septum of log phase *Bacillus subtilis*

Log (a-b) and stationary phase (c-d) cultures of *B. subtilis* were stained with 1μg/ml vanBODIPY for 15 minutes and viewed by phase (panels to left) and fluorescence microscopy (panels to right). vanBODIPY appeared to localised to the septum of diving cells. Staining was less frequently observed in stationary phase cells. Bar is equal to 2μm.

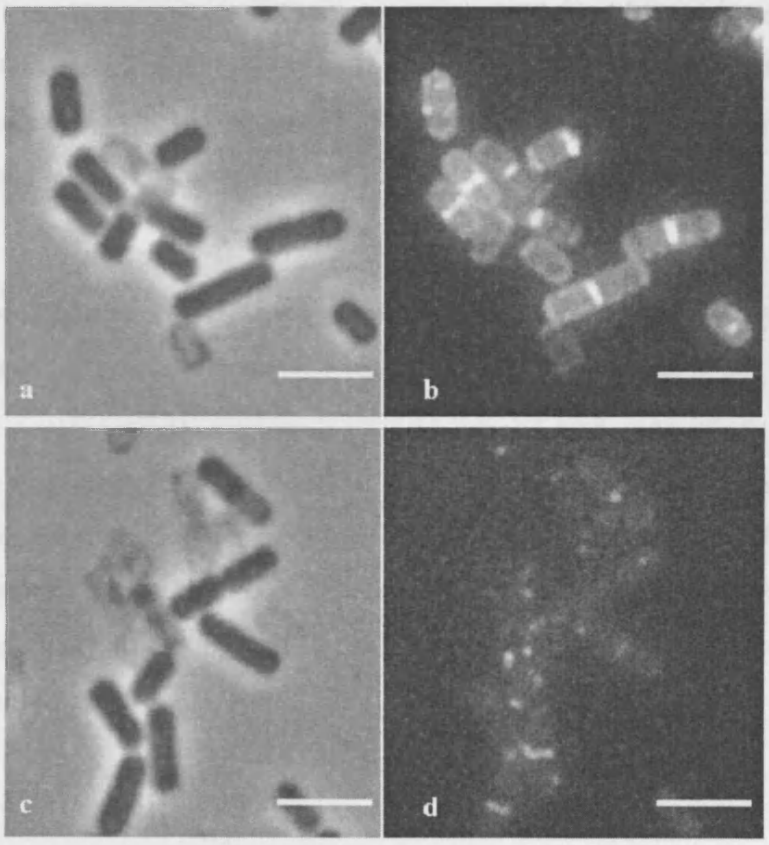

5.3.2 VanBODIPY staining is localised to the cell poles of *M. smegmatis*

Staining of mycobacteria with vanBODIPY was explored as a method for examining the growth status of LB positive mycobacteria. Log and stationary phase cultures of *M. smegmatis* were labelled with 1μg/ml vanBODIPY for 6 hours. Samples were also stained with Nile Red as described previously. The vanBODIPY stain localised to the cell poles and log phase cells appeared to be more frequently stained (37% cells displayed polar staining) than stationary phase cells (8% of cells were stained). However, there appeared to an overlap in the fluorescence emissions of Nile Red and vanBODIPY, which allowed the visualisation of Nile Red stained LBs with the FITC filter used to observe BODIPY staining. Further examination revealed that more polar labelling was observed in dual labelled cells than with vanBODIPY alone. In samples taken from log phase growth 62% of the cells examined displayed polar staining, which is almost twice that observed when cells were stained with vanBODIPY alone. The difference was even more marked in stationary phase cultures, in which 34% of cells were stained, which is over 4 times that observed in cells stained with vanBODIPY. Due to this difficulty in discriminating between Nile Red and BODIPY labelling, this method was considered unsuitable to examine the growth status of LB positive cells.

5.3.3 Carboxyfluorescein diacetate, succinimidyl ester (CFDA/SE) staining of *M. smegmatis* is heterogeneous

M. smegmatis was stained with CFDA/SE and examined by fluorescence microscopy. Staining carried out in triplicate experiments revealed that initial staining of mycobacteria was heterogeneous. Since the stain was intended to be use to examine changes in fluorescence intensity following cell division, it was felt that this inconsistent staining was unacceptable.

Figure 37: VanBODIPY localises at the cell pole of actively replicating *M. smegmatis*

Log (a) and stationary phase (b) cultures of *M. smegmatis* were stained with 1μg/ml vanBODIPY for 6 hours, with or without Nile Red staining. Cells were viewed by phase (panels to left) and fluorescence microscopy (panels to right), using the FITC and G2-A filters to view vanBODIPY and Nile Red staining, respectively. vanBODIPY appeared to be localised to the septum of diving cells. Staining was less frequently observed in stationary phase cells. The emission of the two fluorescence stains overlapped, as evidenced by an apparent increase in staining visualised by the FITC filter when cells were dual labelled. Bar is equal to 2μm.

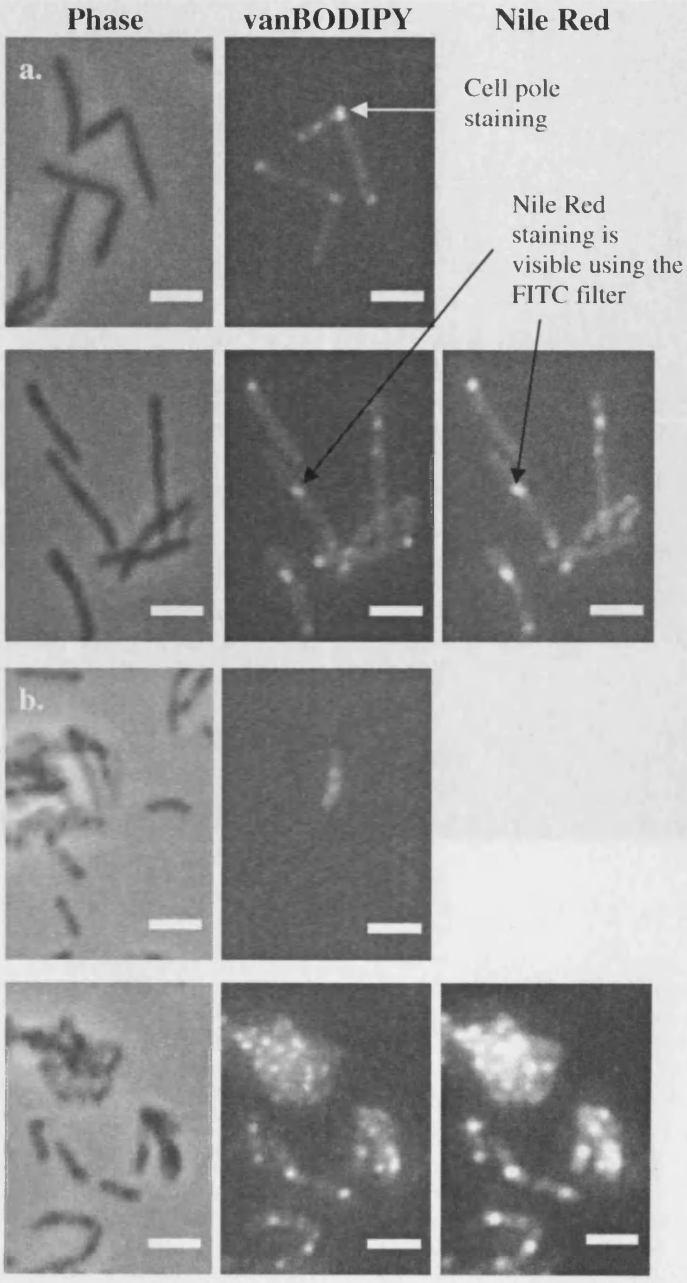

Figure 38: CFDA/SE staining of *M. smegmatis* is heterogenous

Cultures of *M. smegmatis* were stained with 20μM (a-b) or 40μM (c-d) CFDA SE.

Stained cells were observed by phase (left panels) and fluorescence (right panels) microscopy. Cells were observed to be heterogeneously stained. Bar is equal to 2μM.

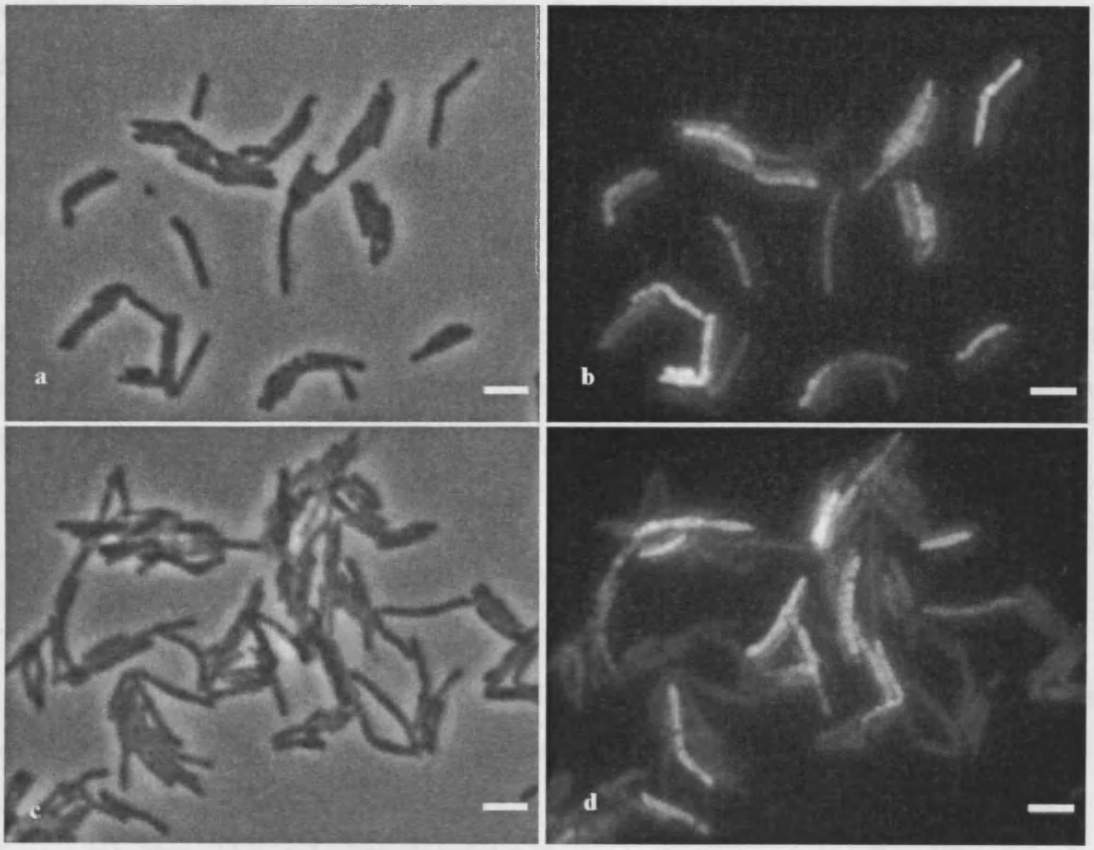

5.3.4 Preparation of GFP cell division reporter constructs

5.3.4.1 Preparation of insert DNA

Reporter vectors were designed to monitor the gene expression of the three *M. tuberculosis* cell division genes: *ftsZ*, *sigB* and *whiB2*. The genes and vector are described in the introduction to this chapter. A region of approximately 15 base pairs (bp) upstream of the -35 promoter element of each gene of interest was amplified from the *M. tuberculosis* H37Rv genome DNA template by PCR using the primers listed in Appendix 1. PCR products were examined by agarose gel electrophoresis in order to ensure amplified regions were of the correct size (Figure 39). Bands were excised and the gel was imaged to confirm that primer dimer bands were excluded (Figure 39). The PCR products were purified and digested with the restriction enzymes Bam HI and Sca I to create the correct sticky ends for insertion into pJFX2. The digested DNA was separated by gel electrophoresis and purified.

5.3.4.2 Preparation of plasmid DNA

E. coli DH5α was transformed with stocks of pJFX2 and pJFX4 plasmid preparations from previous studies in the laboratory. Small scale plasmid preparations were carried out on cultured transformants. Purified plasmid was linearised by digestion with BamHI and cut and uncut plasmids were confirmed to be of the correct size by gel electrophoresis (Figure 40). Plasmid was double digested with the restriction enzymes BamHI and ScaI to form sticky ends to complement those of the insert DNA. The digested DNA was run out on an agarose gel and products were excised and purified.

5.3.4.3 Insertion of promoter sequence into vector

Vector and insert DNA was ligated and *E. coli* alpha select chemically competent cells were transformed with the ligation products. Crude plasmid preparations were carried out on cultivated transformants to confirm the presence of plasmids. Plasmid extracts were

then double digested to demonstrate the insertion of the promoter sequence. A Qiagen spin mini-plasmid preparation was carried out on cultivated clones containing the plasmid and insert of the correct size. Plasmids and gene specific promoters were vacuum dried and sent for sequencing at MWG Biotech AG to verify the presence of promoter sequences. The forward reaction started after the promoter sequence, perhaps due to a lack of stringency of the PCR in sequencing; however the reverse reaction was successful. Sequencing from the reverse reaction was copied into DNA Star, and the complementary sequence was determined. The promoter sequence for each gene of interest was identified in the complemented sequence.

5.3.4.4 Transformation of mycobacteria

Initially, plasmids were transformed into *M. smegmatis* because genetic manipulation of this organism is relatively straightforward and it has a shorter generation time than *M. tuberculosis*. The sequenced plasmids were transformed into *M. smegmatis*, as described. The presence of plasmids was confirmed by transforming the plasmids from *M. smegmatis* into electrocompetent *E. coli* via the "Zap-Zap" method. Plasmids were extracted from transformed *E. coli* and digested to confirm the presence of inserts of the expected size. Transformed strains were inoculated in Middlebrook 7H9 broth, containing 25μg/ml kanamycin for selection, to the same optical density (0.05) and samples were taken every three hours to assess the point at which there was maximum fluorescence. Unfortunately, no fluorescent cells were observed.

M. tuberculosis was transformed with the sequenced plasmids in order to examine the activity of the promoters in their natural host. Colonies were obtained from transformation, however, attempts to culture transformants were unsuccessful.

Figure 39: Amplified promoter insert DNA was visualised by gel electrophoresis

Amplified PCR products were run out on a 2% agarose gel alongside a DNA ladder to allow an approximation of fragment size. Ethidium bromide (0.5µg/ml) was included in the gel for staining DNA. DNA bands were visualised by UV illumination (images are inverted) and gel photography was performed using a gel documentation system and imaging software (Kodak). Bands were excised for purification and an additional image was taken to demonstrate that primer dimmer bands had remained in the gel.

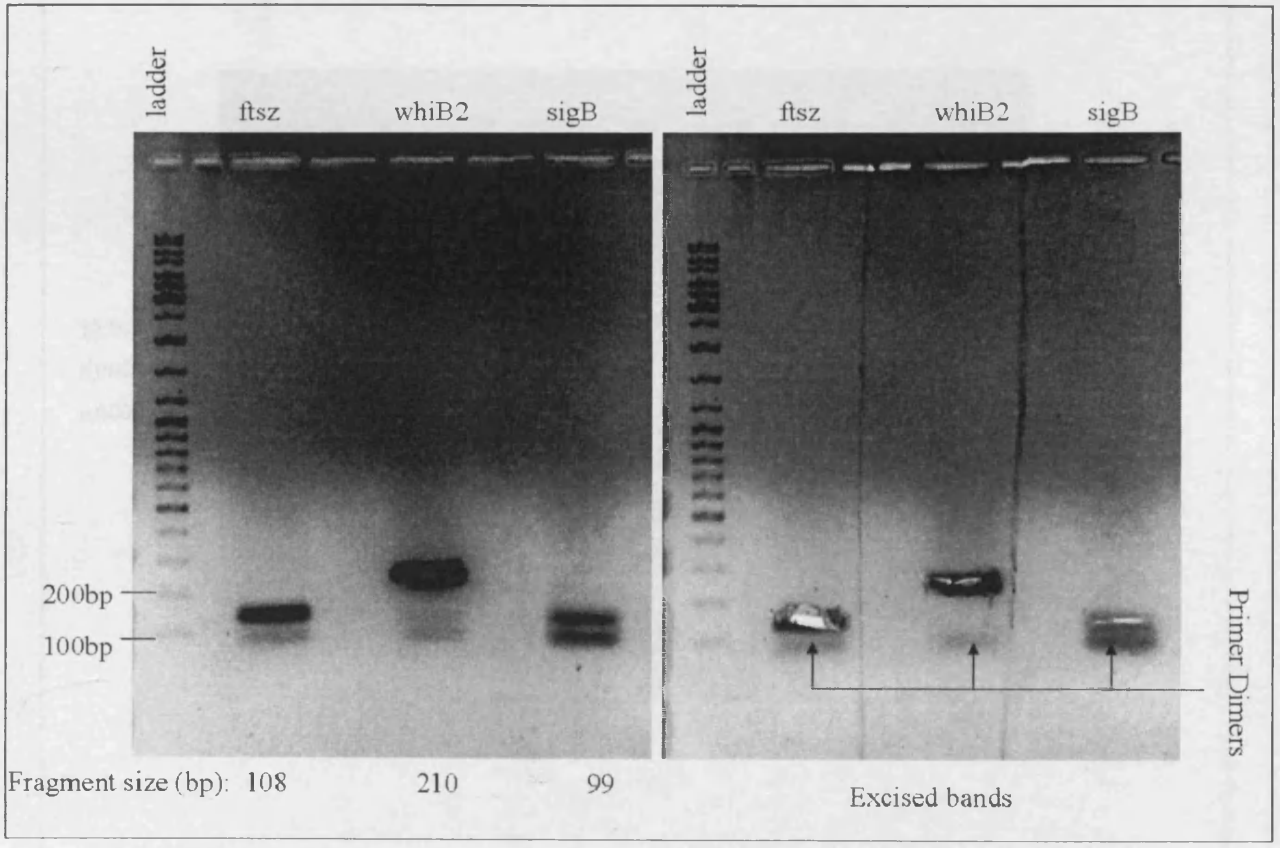

Figure 40: Purified plasmid DNA was confirmed to be of the correct size by gel electrophoresis

Plasmids pJFX2 and pJFX4 were purified from transformed *E. coli* and products were linearised by Bam HI digest. Cut and uncut plasmid DNA was run out on a 1% agarose gel and visualised by UV illumination. Plasmids were shown to be approximately the correct size of 7822bp by comparison with a DNA ladder.

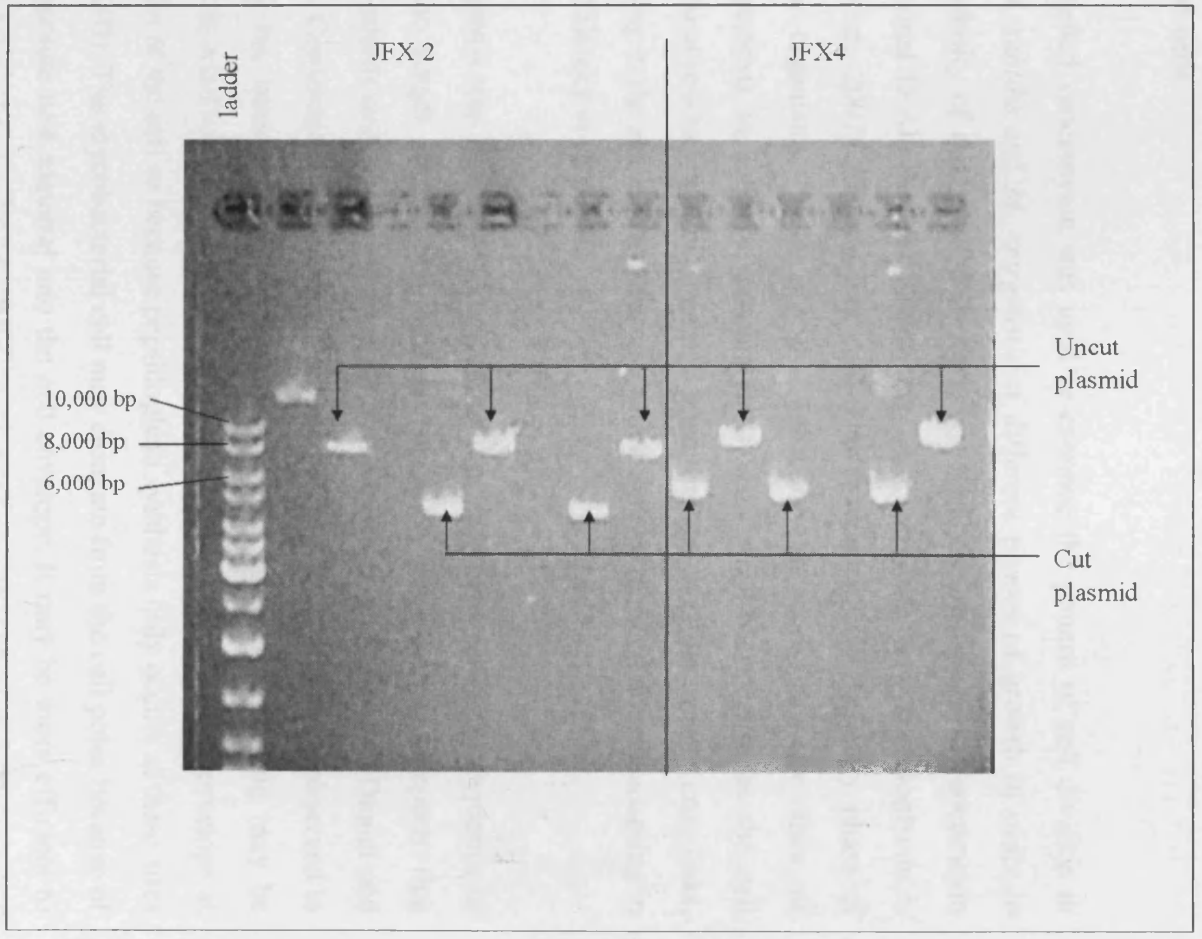

5.4 Discussion

5.4.1 VanBODIPY localises to the cell septum and cell poles of actively growing *M. smegmatis* cells

Fluorescently labelled vancomycin was used to examine the pattern of cell division in populations of *B. subtilis* and *M. smegmatis* at different phases of growth in order to evaluate the suitability of this method to identify actively growing cells. Vancomcyin binds to the terminal D-Ala-D-Ala residues that are exposed as new peptidoglycan is made (Thanky et al., 2007). Labelling of cells was reduced in the stationary phase of growth of both organisms, indicating that vancomycin binds to new sites of peptidoglycan synthesis in actively growing cells. This may be because as the cell matures, the terminal residues will become protected through the formation of crosslinks, limiting the staining to the active growth areas, which may be reduced in cells adapting to stationary phase (Thanky et al., 2007).

Staining of *B. subtilis* was localised to the cell septum and there was some evidence of staining along the length of the cell, this is consistent with previous reports that peptidoglycan synthesis occurs along the length of the cylinder in *B. subtilis* (Daniel and Errington, 2003). Conversely, only polar and occasional septal labelling was observed in *M. smegmatis*. It has been previously suggested that this restricted labelling may be because terminal D-Ala-D-Ala residues are only accessible through the outer envelope at the septa and poles of the cell or because peptidoglcan synthesis only occurs at these sites (Thanky et al., 2007). The mycobacterial cell may elongate from the cell poles because of the need to incorporate new material into the cell envelope. It may be more efficient to limit the biosynthesis and transport of cell envelope lipid components to specific areas of the cell and avoids the introduction of weaknesses along the cell structure that may occur if cell elongation followed the helical pattern (Thanky et al., 2007).

In summary, vanBODIPY staining can be used to discriminate between populations of replicating and non-replicating cells. However, it can not be used to identify the growth status of LB positive cells because its emission spectrum overlaps that of Nile Red.

5.4.2 Carboxyfluorescein diacetate, succinimidyl ester (CFDA/SE) staining of *M. smegmatis* is heterogenous

CFDA/SE staining has been successfully applied in the assessment of environmental bacterial growth rate (Mailloux and Fuller, 2003, Lee et al., 2004). Ideally, each generation should have a unique fluorescence intensity equal to exactly one half the intensity of the preceeding generation, however, it was noted that the intensity of a stained population is actually represented by a range of intensities distributed about a mean (Mailloux and Fuller, 2003). In this particular study, measurement of bacterial growth was carried out using a flow cytometer which allowed the determination of the fluorescence intensity of each cell and a calculation of a mean intensity for the population (Mailloux and Fuller, 2003). However, the range in intensity of staining of *M. smegmatis* was too extreme to be able to determine any changes in fluorescence qualitatively. Therefore, this stain could not be used to assess the growth status of LB positive cells. Future work may include the use of a fluorescence cell sorting method that may allow the separation of populations of cells with different means of intensity. The LB content of these cells could then be examined.

5.4.3 *M. smegmatis* GFP promoter reporter strains did not fluoresce during growth

M. smegmatis transformed with the three GFP promoter reporter strains were assessed for fluorescence throughout growth. No fluorescence was observed in any of the transformed strains. It is unlikely that *ftsZ* was not transcribed because the cells were shown to be doubling by optical density measurements. Therefore, it may be that the *M. tuberculosis*

promoter regions for the genes of interest are not homologous to the *M. smegmatis* promoters.

The inability to culture *M. tuberculosis* transformants may be due to a lethal effect due to overexpression of the promoter regions, leading to overexpression of the genes. Dziadek et al. (2003) demonstrated that overexpression of *ftsZ* in *M. smegmatis* causes FtsZ accumulation, filamentation and lysis. Similarly, overexpression of *whiB2* in *M. smegmatis* caused slow growth in broth and multiple septate bacteria (Gomez and Bishai, 2000).

5.5 Conclusions

The growth status of LB positive cells has yet to be elucidated. The methods used in this study may be developed to address this point in the future.

Chapter 6

Lipid Bodies and Antibiotic Tolerance

6.1 Introduction

Preliminary work in this laboratory has suggested that the presence of LBs in *M. smegmatis* is associated with enhanced survival of rifampicin and isoniazid treatment when compared to cells with minimal LB content (Anna Hartridge, Unpublished Work). This work was repeated in order to confirm this observation. *M. smegmatis* was originally used as a model organism for LB formation in mycobacteria because LBs had not been demonstrated in *M. tuberculosis in vivo*. However, the identification of LB promoting conditions (Chapter 3) has allowed the examination of LB positive *M. tuberculosis* cells *in vitro*.

Demonstration of LB formation in NRP cells strengthened the hypothesis that LBs are associated with antibiotic tolerance because these cells are inherently drug tolerant (Figure 41). The question arose as to whether other LB promoting conditions were capable of inducing antibiotic tolerance in *M. tuberculosis*. Therefore, antibiotic tolerance assays were carried out on Nitric Oxide (NO) treated *M. tuberculosis* in order to establish whether LBs were markers of antibiotic tolerant cells.

NO treatment was selected as a means of promoting LBs in *M. tuberculosis* in this study because of its role as a host defence mechanism against microbial pathogens (Chan et al., 2001). *M. tuberculosis* is likely to encounter NO *in vivo*, as it is released by the activated macrophage (Boshoff and Barry, 2005) and acts as a eukaryotic signalling molecule (Martin et al., 2000). Therefore in addition to hypoxia, NO may also act as an environmental signal of immune activation and allow *M. tuberculosis* to adapt its metabolism to the anticipated changes (Voskuil et al., 2003). The production of NO has been shown to be important in the host control of *M. tuberculosis* in murine models of infection. Disease dissemination and mortality was shown to be significantly higher in a mouse strain with a genetic disruption for inducible NO Synthase (NOS) infected with *M. tuberculosis* when compared to the parent mouse strain (MacMicking et al., 1997). NO also appears to be important in maintaining the chronic disease state. Flynn et al (1998)

demonstrated that administration of the NOS inhibitor aminoguanidine to latently infected mice led to disease reactivation.

The mechanism by which NO acts on mycobacteria is not known but is believed to involve the disruption of bacterial DNA and proteins and may also induce the apoptosis of infected macrophages (Reviewed by Chan et al., 2001). There is some evidence to suggest that NO exposure equivalent to the levels *M. tuberculosis* may encounter *in vivo* may be bacteriostatic rather than bactericidal. Rhoades and Orme (1997) demonstrated that the numbers of intracellular *M. tuberculosis* in activated bone-marrow derived macrophages were not greatly reduced despite production of reactive nitrogen species. Further to this, bacteria recovered from macrophages seemed to replicate at a lower rate, suggesting that these cells had undergone physiological changes (Rhoades and Orme, 1997). If indeed NO exposure does induce a growth arrested state in *M. tuberculosis*, these cells are likely to be phenotypically tolerant of drugs that act on growing cells, in the same manner as NRP cells.

Figure 41: Non Replicating Persistent cultures of *M. tuberculosis* are tolerant of frontline antibiotics

Data adapted from Wayne and Hayes (1996). *M. tuberculosis* subjected to Wayne's hypoxic shift down model become tolerant of isoniazid (0.4μg/ml) and rifampicin (0.1μg/ml) as oxygen is depleted to microaerophilic (NRP1) levels and finally anaerobic levels (NRP2).

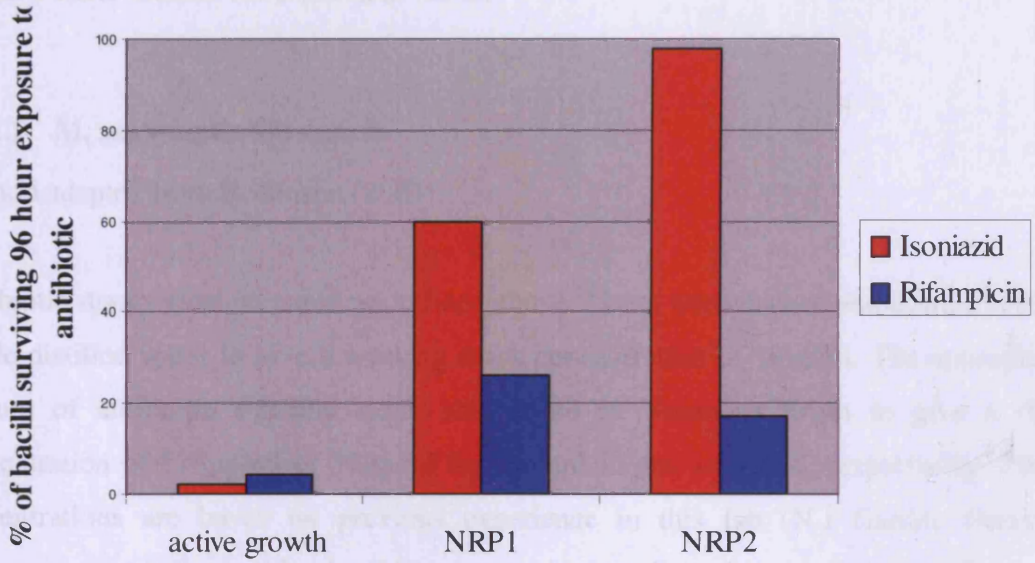

6.2 Materials and Methods

6.2.1 Antibiotic Tolerance Assays

6.2.1.1 Preparation of Antibiotic Stocks

Antibiotic stocks used for antibiotic tolerance assays were prepared at a concentration 10mg/ml. Rifampicin was prepared in DMSO and isoniazid was prepared in sterile distilled water. Stocks were stored at -20°C.

6.2.1.2 M. smegmatis kill curves

Method adapted from Rollinson (2003).

Antibiotic stocks were prepared as outlined above. These were thawed and diluted 1:10 in sterile distilled water to give a working stock concentration of 1mg/ml. The appropriate amount of antibiotic working stock was added to Youmans Broth to give a final concentration of 128µg/ml or 32µg/ml for rifampicin and isoniazid, respectively. These concentrations are based on previous experience in this lab (N.J Garton, Personal Communication). Fresh cultures of *M. smegmatis* were diluted to a calculated OD_{580nm} of 0.2 for rifampicin tolerance assays or 0.1 for isoniazid assays and 1ml of this was used to inoculate 9ml antibiotic containing Youmans broth in triplicate sterile 32ml Universal tubes (Sterilin). Tubes were sealed with laboratory sealing film (Nesco, Osaka, Japan) and incubated with shaking at 37°C. Samples of 100µl were taken at 0, 24, 48 and 78 hours. These were used to carry out colony forming unit (CFU) counts, the method of which is described in Chapter 2.

6.2.1.3 Antibiotic tolerance assays of M. tuberculosis following exposure to Nitric Oxide

Method adapted from Cooney (2000).

Cultures of *M. tuberculosis* grown in Sautons broth was exposed to SPER/NO or SPER.4HCL control as before (Chapter 3) and incubated at 37°C for 4 hours. Colony forming unit (CFU) counts were performed before the addition of NO and after 4 hours of exposure. Samples for LB analysis and antibiotic tolerance assays were taken at 4, 24 and 48 hours. The latter was achieved by adding 7.5ml of culture to 7.5ml Sautons broth containing antibiotics at a final concentration of 1μg/ml and 0.2μg/ml for rifampicin and isoniazid, respectively. This was made using antibiotic stocks (prepared as described above) diluted 1:10 to give a working concentration of 1mg/ml. Incubation of culture in Sautons broth without antibiotics was used as a control. Assays were carried out in 50ml Falcon Centrifuge tubes; which were doubled bagged and incubated with shaking at 37°C. A further CFU count was taken on day 7 to assess the percentage kill.

6.3 Results

6.3.1 Survival of *M. smegmatis* subjected to Rifampicin treatment

M. smegmatis was cultured in medium low in nitrogen or low in carbon, with or without oleic acid supplementation, as described in Chapter 2. An overnight culture of *M. smegmatis* was included in the experiment as a control. All cultures were grown fresh for each antibiotic tolerance assay, which was carried out in triplicate. Figure 42a-c show the survival of groups of *M. smegmatis* over 72 hours, for triplicate experiments.

M. smegmatis grown in a low carbon medium supplemented with oleic acid showed the highest survival of rifampicin treatment, followed by the corresponding cells grown in low carbon broth without oleic acid. *M. smegmatis* cells grown in a low nitrogen broth and cells growing exponentially in Middlebrook broth were extremely susceptible to rifampicin treatment. These cells were usually below the limit of detection (8cfu/ml) after 72 hours antibiotic treatment. The inclusion of Tween in the antibiotic broth seemed to generally increase the number of cells recovered; however, the difference between groups treated with or without Tween was not statistically significant (≤ 0.05), except in the case of LCYB cells in replica c ($p=0.027$) (Figure 42). Antibiotic treated cells seemed to survive better without Tween in replica a (Figure 42); however, there was no statistical significance between the sets of data for each group of cells with and without Tween. The mean survival data after 72 hours treatment from all replica experiments is tabulated in Figure 42. This data appears to agree with the trends observed in individual experiments (discussed above); however, there is substantial variability between data obtained in individual experiments for low carbon and oleic acid treated cells (indicated by the standard deviation). This may be due to some extent to the level of LB content of the populations of cells that were exposed to the antibiotic and not simply the presence or absence of LBs. However, LNYB cultures accumulate LBs but these cells are extremely susceptible to rifampicin. This indicates that the growth condition of *M. smegmatis* cells

to some extent dictates their ability to survive antibiotic exposure (see discussion of results).

6.3.2 Survival of *M. smegmatis* subjected to Isoniazid treatment

Antibiotic tolerance assays were carried out on *M. smegmatis* as described above, with isoniazid in place of rifampicin. Survival of groups of *M. smegmatis* is shown over 48 hours instead of 72 hours (Figure 43a-c) because killing of *M. smegmatis* by isoniazid appeared to be more rapid than that observed for rifampicin. The optical density of the initial inoculum was half of that used in rifampicin tolerance assays because spontaneous mutants that are resistant to isoniazid occur more frequently than rifampicin resistant mutants. This is because a large number of different mutations in mycobacteria have been shown to confer resistance to isoniazid, whereas, the development of resistance to rifampicin is due to mutations in a well-defined, 81 base pair central region of the gene that encodes the β-subunit of RNA polymerase (*rpoB*) (Reviewed by Somoskovi et al., 2001).

Again, the oleic acid supplemented low carbon cells had the highest survival rate during isoniazid treatment, followed by the low carbon cells, except in replica b (Figure 43) but there was no significant difference ($p=0.812$) between these groups. It is difficult to say whether Tween made a difference to survival. In general, Tween seemed to increase survival; however, there was some conflicting evidence shown in replica a, in which survival of most groups was enhanced by the exclusion of Tween. The mean survival of cells exposed to 48 hours isoniazid treatment from all the replica experiments is shown in Figure 43. Again, data obtained from individual experiments was very varied for low carbon and oleic acid supplemented cells but generally represented the data trends observed for individual experiments. The reason for the variation in experimental data will be discussed later.

Figure 42a-c: Survival of *M. smegmatis* subjected to Rifampicin treatment

Cultures of *M. smegmatis* were grown in Low Nitrogen Youmans Broth (**LNYB**) for 5 days or in Low Carbon Youmans Broth for 7 days (**LCYB**) with 1 hour glycerol amendment. A group of glycerol amended LCYB cells were exposed to 630μM Oleic Acid emulsified in BSA (**OA**) for a further hour. An overnight culture of *M. smegmatis* was included as a control. Growth of the control culture was confirmed as exponential by a doubling in OD_{580nm} over a 3 hour period. The OD_{580nm} was adjusted to 0.2 for all cultures and 1ml of culture was used to inoculate 9ml Youmans Broth containing 128μg/ml rifampicin. Triplicate tubes were incubated at 37°C, with shaking. CFU counts were taken immediately following inoculation (time = 0) and after this every 24 hours, for a 72 hour period. Average survival is expressed as the percentage of the initial population (time= 0 hours) that was recovered after antibiotic treatment (time= 24, 48 or 72 hours). Survival shown as 0.0001 was below the limit of detection of 8cfu/ml.

The graphs show three antibiotic tolerance assays, each carried out using fresh inocula, in broth with (top graph) or without (bottom graph) Tween 80 (**T**). Bars show standard error. Statistical difference between LCYB and OA survival rates (≤ 0.05) is indicated by *.

The table below shows the average % survival for all three replica experiments of *M. smegmatis* after 72 hours rifampicin treatment. As discussed, cells were exposed to antibiotics in the presence or absence of Tween (+/- T). The standard deviation (SD) is shown in brackets.

Condition of growth	**Mean % survival at 72 hours (SD)**	**Condition of growth**	**Mean % survival at 72 hours (SD)**
OA + T	7.64 (13)	OA - T	6.66 (10)
LCYB + T	0.06 (0.1)	LCYB - T	0.01 (0.02)
LNYB + T	0 (0)	LNYB -T	0 (0)
EXPO + T	0 (0)	EXPO -T	0.006 (0.01)

(a)

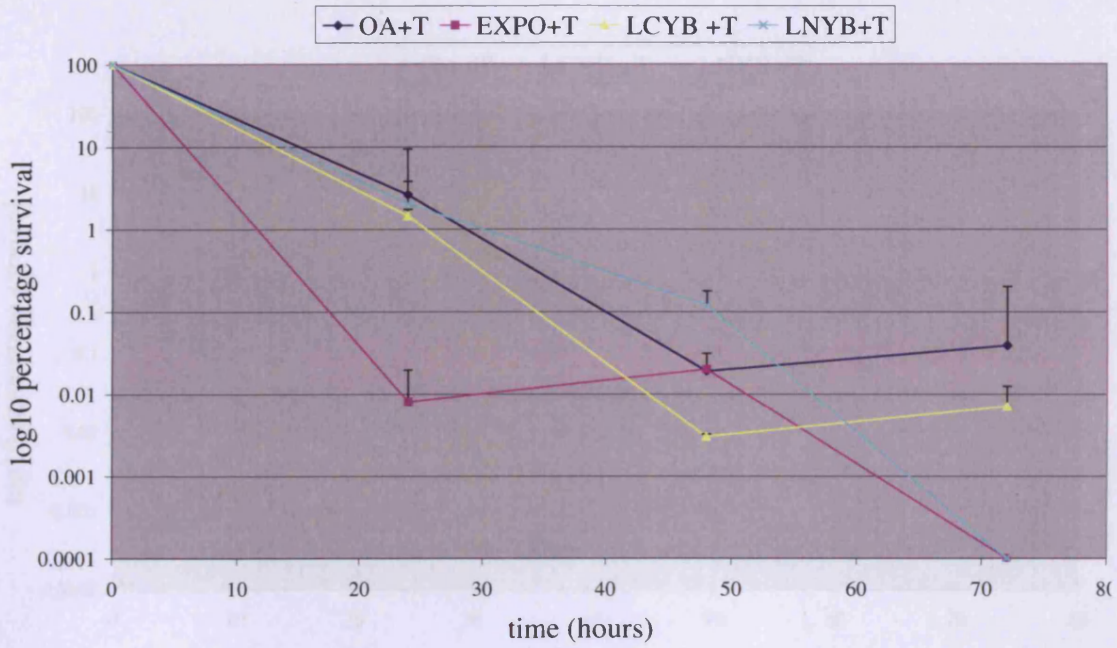
OA+T
EXPO+T
LCYB +T
LNYB+T
log10 percentage survival
100
10
1
0.1
0.01
0.001
0.0001
0
10
20
30
40
50
60
70
time (hours)

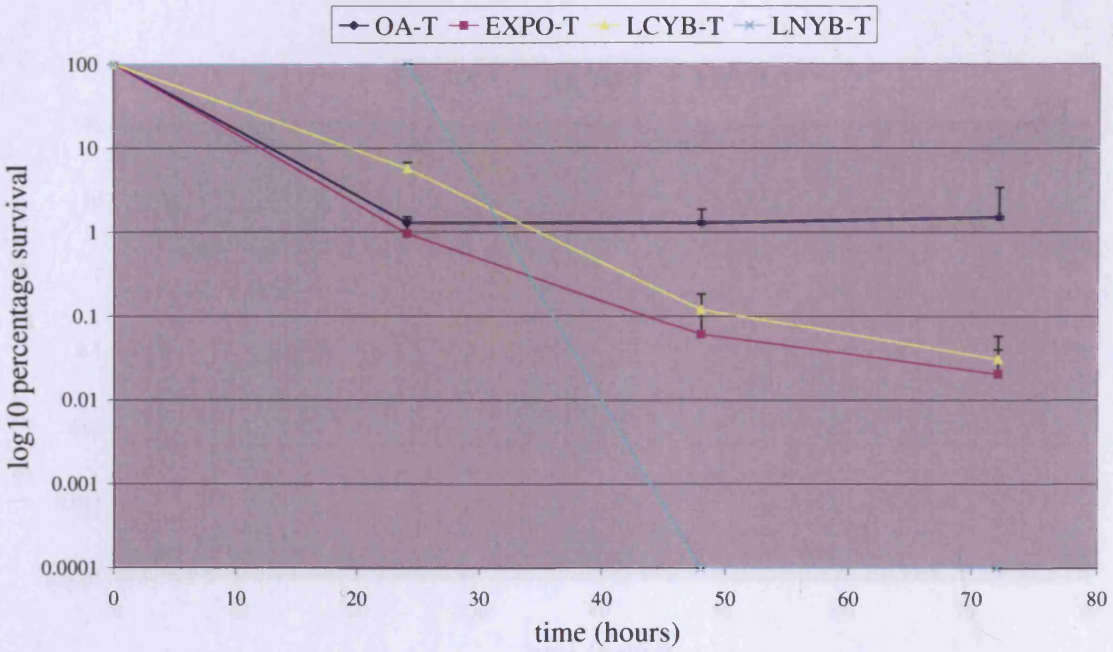
OA-T
EXPO-T
LCYB-T
LNYB-T
log10 percentage survival
100
10
1
0.1
0.01
0.001
0.0001
0
10
20
30
40
50
60
70
80
time (hours)

(b)

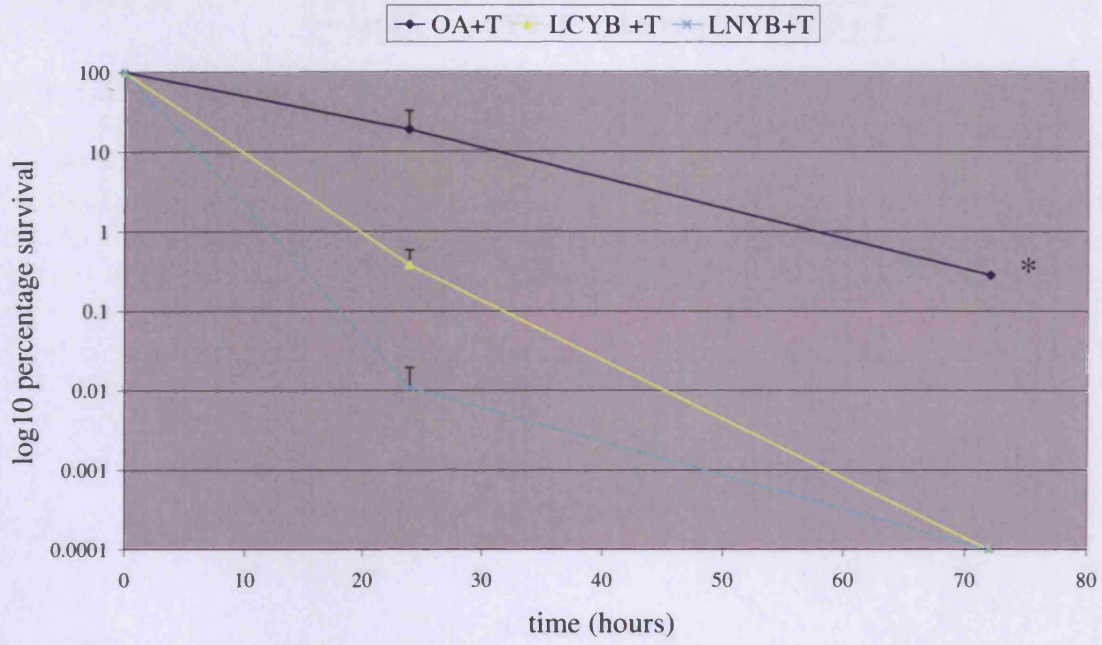
OA+T
LCYB +T
LNYB+T
log10 percentage survival
100
10
1
0.1
0.01
0.001
0.0001
0
10
20
30
40
50
60
70
80
time (hours)
*

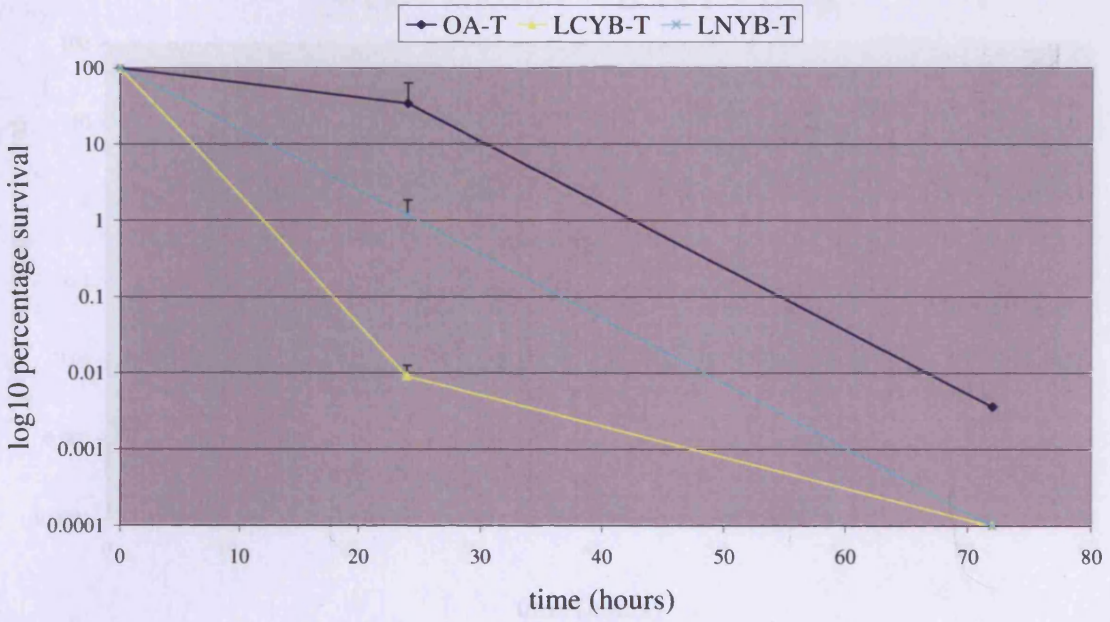
OA-T
LCYB-T
LNYB-T
log10 percentage survival
100
10
1
0.1
0.01
0.001
0.0001
0
10
20
30
40
50
60
70
80
time (hours)

(c)

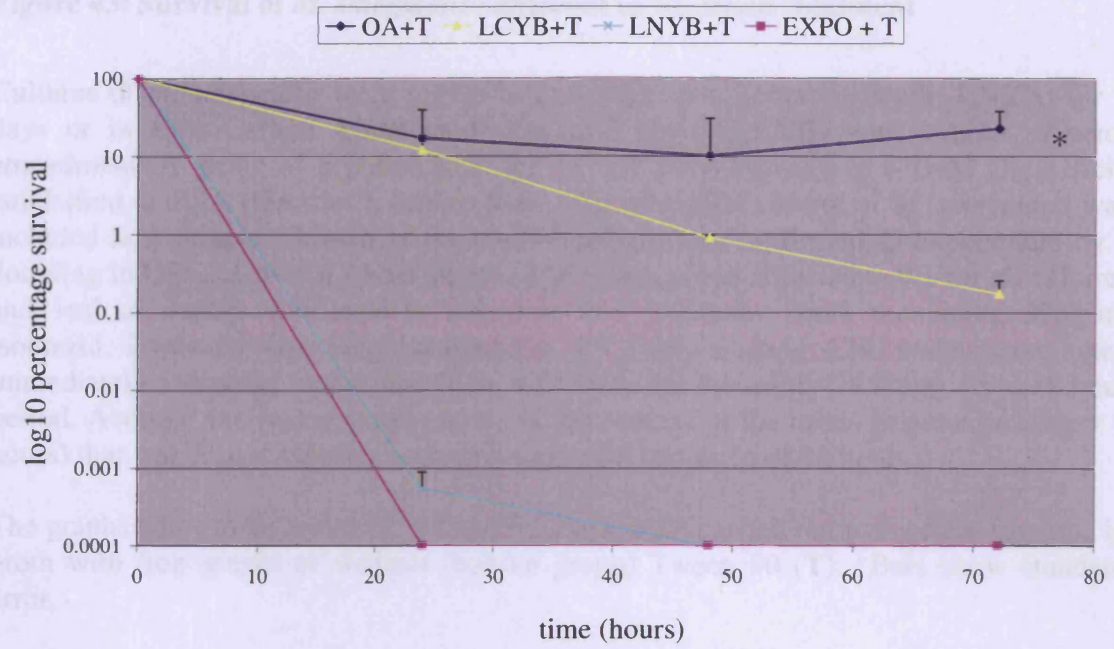
OA+T
LCYB+T
LNYB+T
EXPO + T
log10 percentage survival
100
10
1
0.1
0.01
0.001
0.0001
0
10
20
30
40
50
60
70
80
*
time (hours)

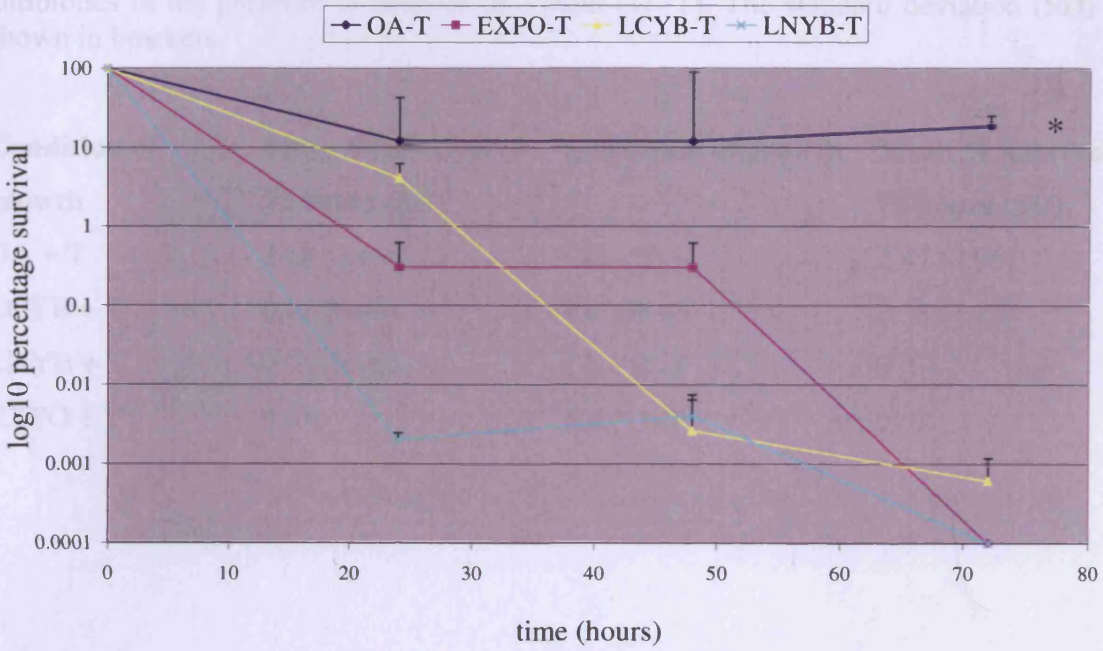
OA-T
EXPO-T
LCYB-T
LNYB-T
log10 percentage survival
100
10
1
0.1
0.01
0.001
0.0001
0
10
20
30
40
50
60
70
80
*
time (hours)

Figure 43: Survival of *M. smegmatis* subjected to Isoniazid treatment

Cultures of *M. smegmatis* were grown in Low Nitrogen Youmans Broth (**LNYB**) for 5 days or in Low Carbon Youmans Broth for 7 days (**LCYB**) with 1 hour glycerol amendment. A group of glycerol amended LCYB were exposed to 630μM Oleic Acid emulsified in BSA (**OA**) for a further hour. An overnight culture of *M. smegmatis* was included as a control. Growth of the control culture was confirmed as exponential by a doubling in OD_{580nm} over a 3 hour period. The OD_{580nm} was adjusted to 0.1 for all cultures and 1ml of culture was used to inoculate 9ml Youmans Broth containing 32μg/ml isoniazid. Triplicate tubes were incubated at 37°C, with shaking. CFU counts were taken immediately following inoculation (time = 0) and after this every 24 hours, for a 48 hour period. Average survival is expressed as the percentage of the initial population (time= 0 hours) that was recovered after antibiotic treatment (time=24 or 48 hours).

The graphs show three antibiotic tolerance assays, each carried out using fresh inocula, in broth with (top graph) or without (bottom graph) Tween 80 (**T**). Bars show standard error.

The table below shows the average % survival for all three replica experiments of *M. smegmatis* after 48 hours isoniazid treatment. As discussed, cells were exposed to antibiotics in the presence or absence of Tween (+/- T). The standard deviation (SD) is shown in brackets.

Condition of growth	**Mean % survival at 72 hours (SD)**	**Condition of growth**	**Mean % survival at 72 hours (SD)**
OA + T	3.18 (2.69)	OA - T	2.47 (3.06)
LCYB + T	0.02 (0.03)	LCYB - T	2.38 (4.12)
LNYB + T	0.04 (0.08)	LNYB -T	0 (0)
EXPO + T	0 (0)	EXPO -T	0 (0)

(a)

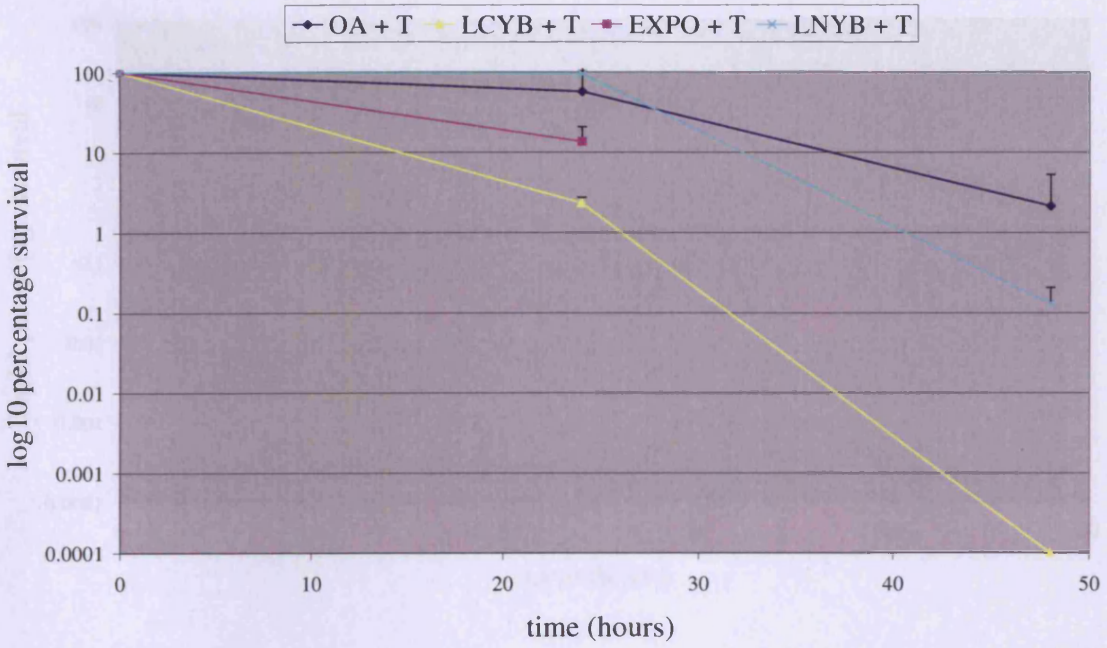
OA + T
LCYB + T
EXPO + T
LNYB + T
log10 percentage survival
100
10
1
0.1
0.01
0.001
0.0001
0
10
20
30
40
50
time (hours)

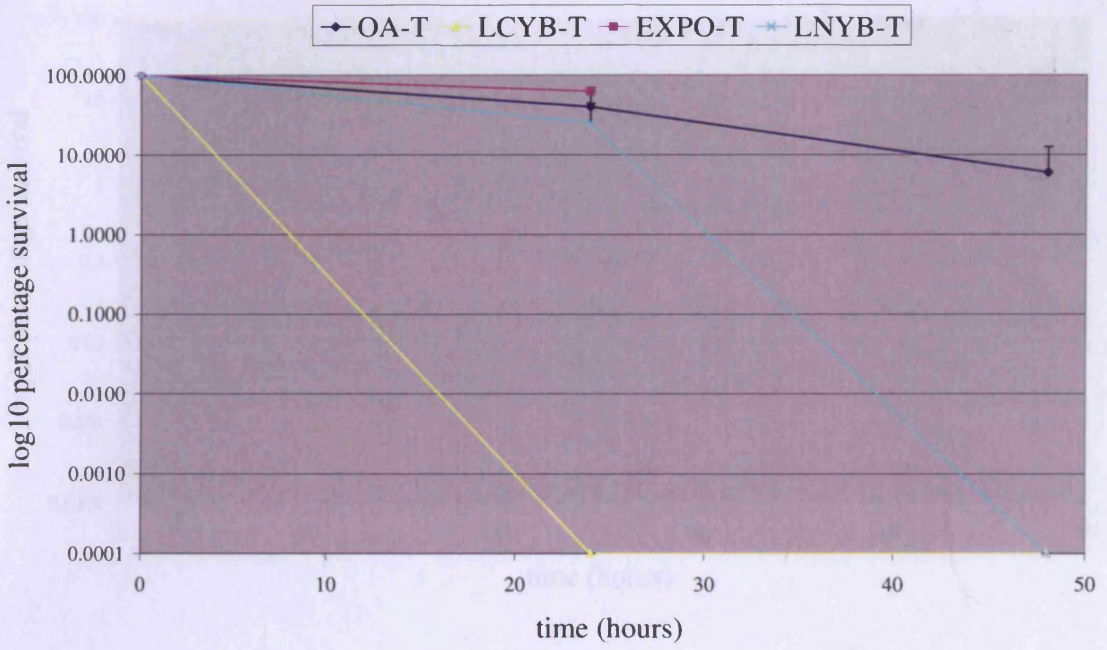
OA-T
LCYB-T
EXPO-T
LNYB-T
log10 percentage survival
100.0000
10.0000
1.0000
0.1000
0.0100
0.0010
0.0001
0
10
20
30
40
50
time (hours)

(b)

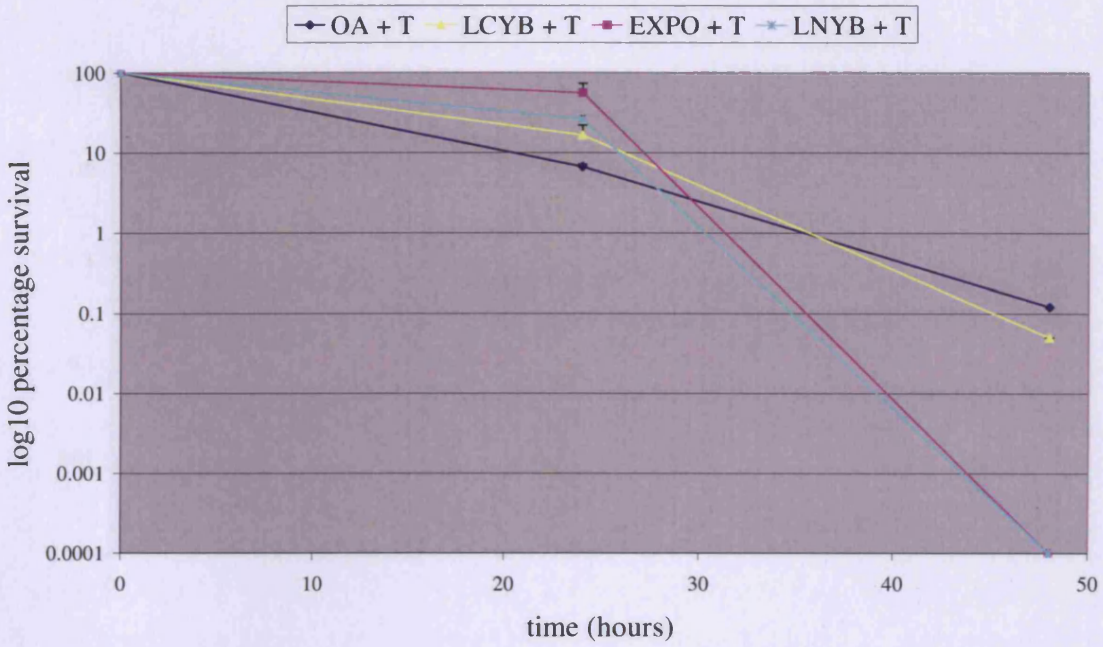
OA + T
LCYB + T
EXPO + T
LNYB + T
log10 percentage survival
100
10
1
0.1
0.01
0.001
0.0001
0
10
20
30
40
50
time (hours)

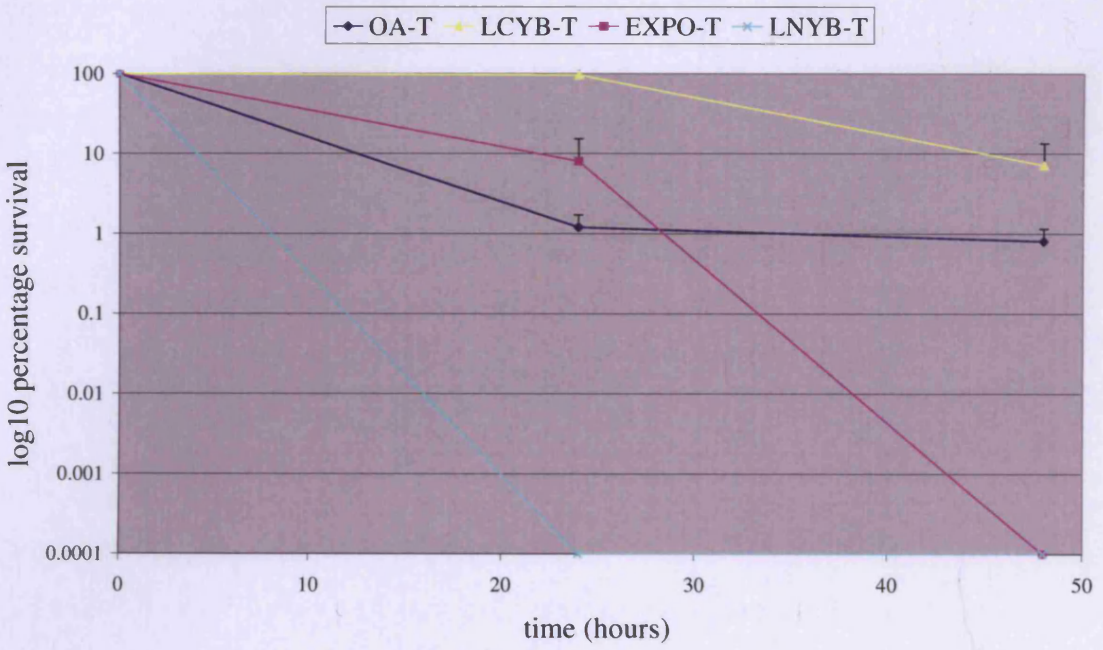
OA-T
LCYB-T
EXPO-T
LNYB-T
log10 percentage survival
100
10
1
0.1
0.01
0.001
0.0001
0
10
20
30
40
50
time (hours)

(c)

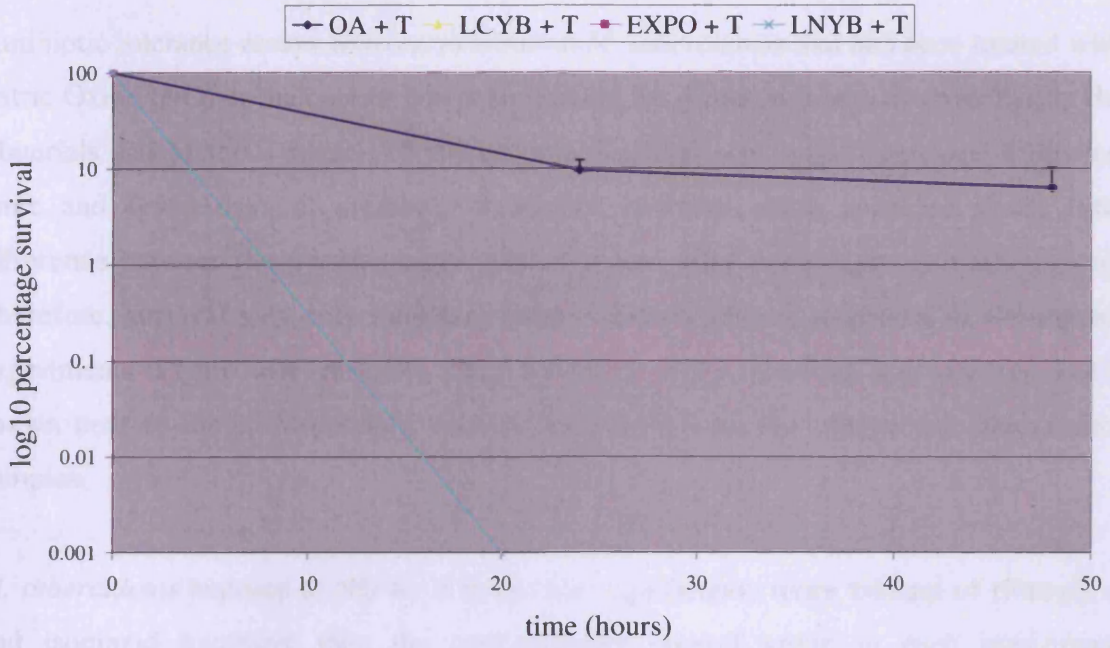
OA + T
LCYB + T
EXPO + T
LNYB + T
log10 percentage survival
100
10
1
0.1
0.01
0.001
0
10
20
30
40
50
time (hours)

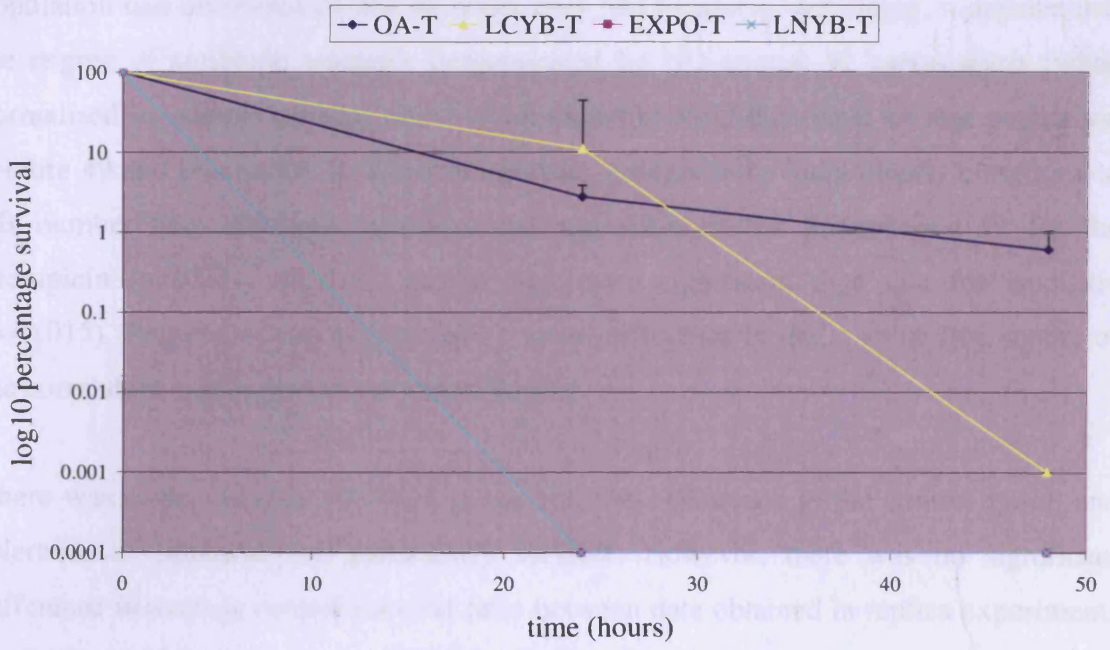
OA-T
LCYB-T
EXPO-T
LNYB-T
log10 percentage survival
100
10
1
0.1
0.01
0.001
0.0001
0
10
20
30
40
50
time (hours)

6.3.3 Antibiotic tolerance in Lipid body positive populations of *M. tuberculosis*

Antibiotic tolerance assays were carried out on *M. tuberculosis* that had been treated with Nitric Oxide (NO) or the control donor compound for 4 and 24 hours, as described in the Materials and Methods section of this chapter. Survival was initially assessed following three and seven days of antibiotic treatment, however, there appeared to be little difference between the treatment and control groups after three days (data not shown). Therefore, survival was only measured after 7 days antibiotic treatment in subsequent experiments (Figure 44-Figure 48). The LB content of the inoculum was assessed and is shown next to the corresponding survival data, LBs were not observed in the control samples.

M. tuberculosis exposed to NO for 4 hours was significantly more tolerant of rifampicin and isoniazid treatment than the corresponding control group in each experiment undertaken (Figure 44-Figure 48). The level of antibiotic tolerance and LB content of the population had decreased 24 and 48 hours after NO treatment. Strikingly, it appears that the degree of antibiotic tolerance demonstrated by NO treated *M. tuberculosis* (when normalised to control survival rates) is correlated to the LB content of that population (Figure 49 and Figure 50). Rifampicin tolerance appears to be more closely correlated to LB number than isoniazid tolerance; the regression of the line of best fit for the rifampicin ($p=0.004$) tolerance dataset was more significant than that for isoniazid ($p=0.015$). Regression analysis revealed a small difference in the r^2 value (the square of the correlation coefficient) of the line of best fit.

There was some variation observed in the antibiotic tolerance in the control group and tolerance to isoniazid was particularly variable. However, there was no significant difference in average control survival rates between data obtained in replica experiments ($p=0.682$ for Rifampicin and $p=0.358$ for Isoniazid) or between average control survival at 4 and 24 hours after treatment ($p=0.902$ for rifampicin and $p=0.966$ for isoniazid). Control isoniazid tolerance was particularly high after 48 hours treatment; however, there

was insufficient data to carry out statistical analysis to show whether this was an anomaly or a genuine result.

6.3.4 Effect of a second Nitric Oxide treatment on the LB content and antibiotic tolerance of *M. tuberculosis*

LB formation was confined to only a subpopulation of NO exposed *M. tuberculosis* cells in previous experiments. Therefore, it was hypothesised that a further dose of NO would increase the LB content and antibiotic tolerance cumulatively. In order to examine this possibility, duplicate cultures of *M. tuberculosis* were exposed to a second dose of NO donor or control compound 4 hours after the initial dose, to coincide with peak LB formation. Antibiotic tolerance was measured 4 hours after the second exposure (Figure 46 and Figure 48).

There was a modest increase in LB number and a corresponding small but statistically insignificant ($p=0.709$) increase in the overall survival after 7 days of isoniazid treatment. Rifampicin tolerance did not increase following the additional NO treatment, indeed survival of singly exposed cells was significantly greater than populations exposed to a second dose of NO ($p=0.040$).

Figure 44-Figure 46: Effect of NO treatment on LB count and survival of *M. tuberculosis* to Rifampicin treatment

Cultures of *M. tuberculosis* were exposed to an overall concentration of 100μM Nitric Oxide donor, Spermine NONOate or control compound Spermine tetrahydrochloride for 4 or 24 hours. Colony forming unit (CFU) counts were taken after 4 and 24 hours treatment. Samples for LB analysis and antibiotic tolerance assays were taken at 4, 24 and 48 hours of NO treatment. The latter was achieved by adding 7.5ml of culture to 7.5ml Sautons broth containing antibiotic. Sautons broth without antibiotics was used as a control. Tubes were incubated for 7 days and CFU counts were performed to assess survival of antibiotic treatment. Experiments examining tolerance to rifampicin (1μg/ml) were carried out in triplicate (using duplicate technical replicas). Isoniazid (0.2μg/ml) tolerance was also examined in two of these experiments and is presented later. Average survival is expressed as the percentage of the initial inoculum that could be recovered after antibiotic treatment. Bars show standard error. Statistical significance is indicated by * for a p-value ≤ 0.05 and ** for a p-value ≤ 0.0001.

Figure 44: Effect of NO treatment on LB content and Rifampicin tolerance of *M. tuberculosis*. Replicate 1.

Graph (i.) shows the average survival of *M. tuberculosis* treated with NO or Control (C) for 4 and 24 hours after 7 days rifampicin (1µg/ml) exposure. The scale is shown in log in order to clearly demonstrate the difference between the NO and C groups. The Graph (ii.) shows the survival ratio (NO survival/ C survival), demonstrating the difference in survival between the 4 and 24 hour NO treated groups after 7 days rifampicin kill. See dataset legend above for experimental details.

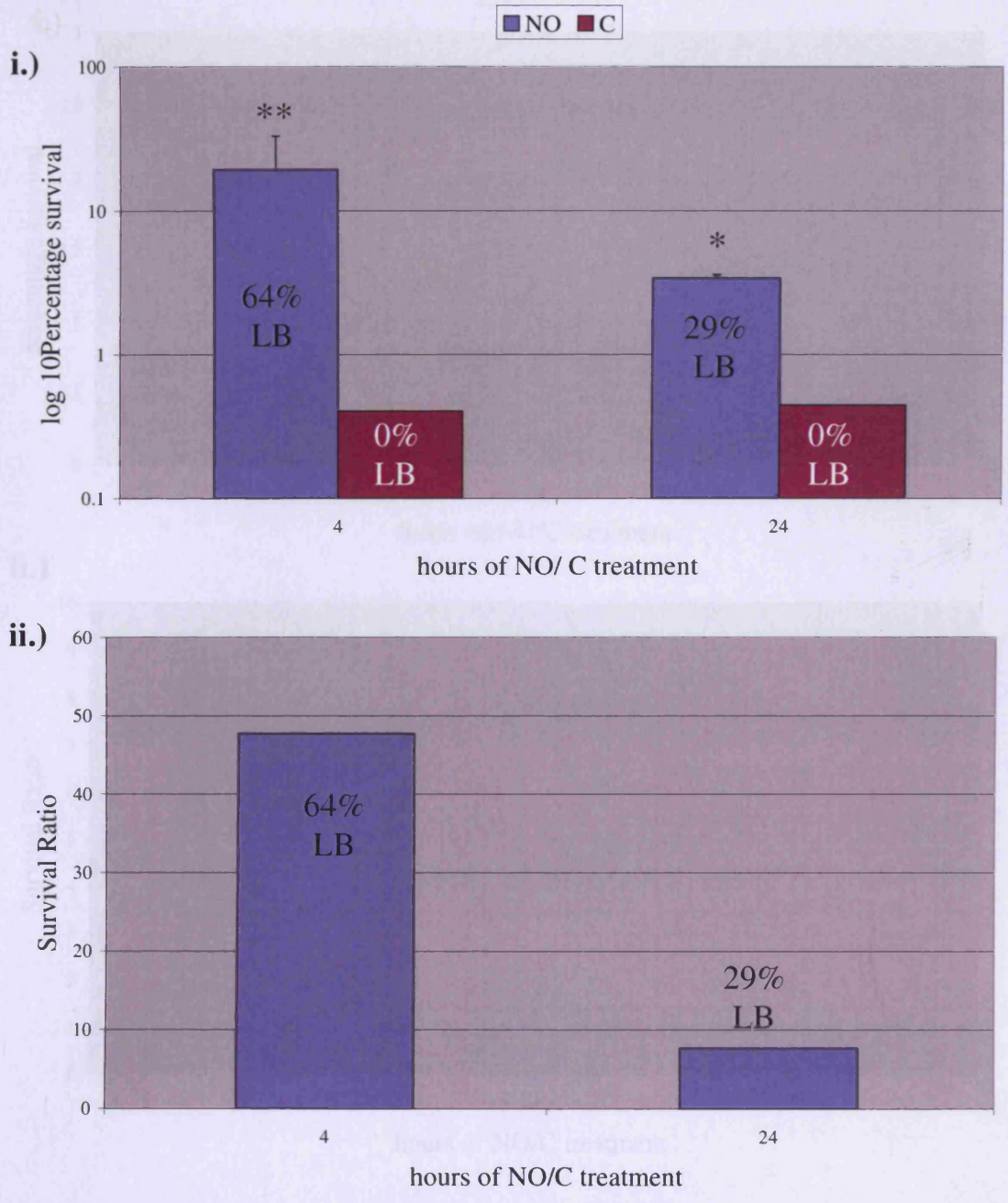

Figure 45: Effect of NO treatment on LB content and Rifampicin tolerance of *M. tuberculosis*. Replicate 2.

Graph (i.) shows the average survival of *M. tuberculosis* treated with NO or Control (C) for 4, 24 and 48 hours after 7 days rifampicin (1µg/ml) exposure. Graph (ii.) shows the survival ratio (NO survival/ C survival), demonstrating the difference in survival between NO treated groups after 7 days rifampicin exposure. For experimental detail see dataset legend above.

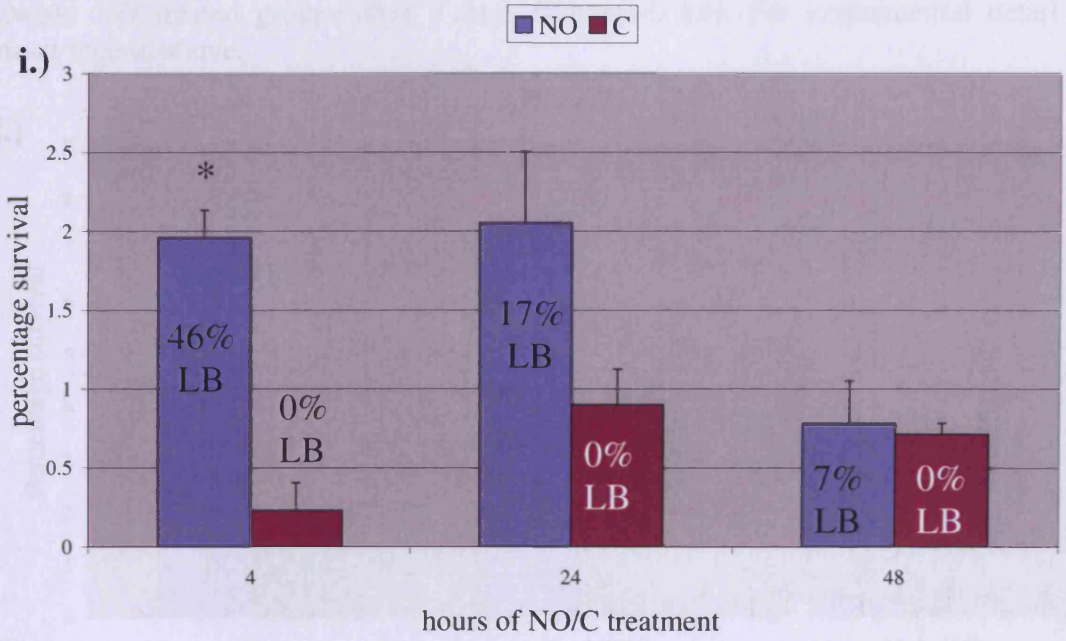

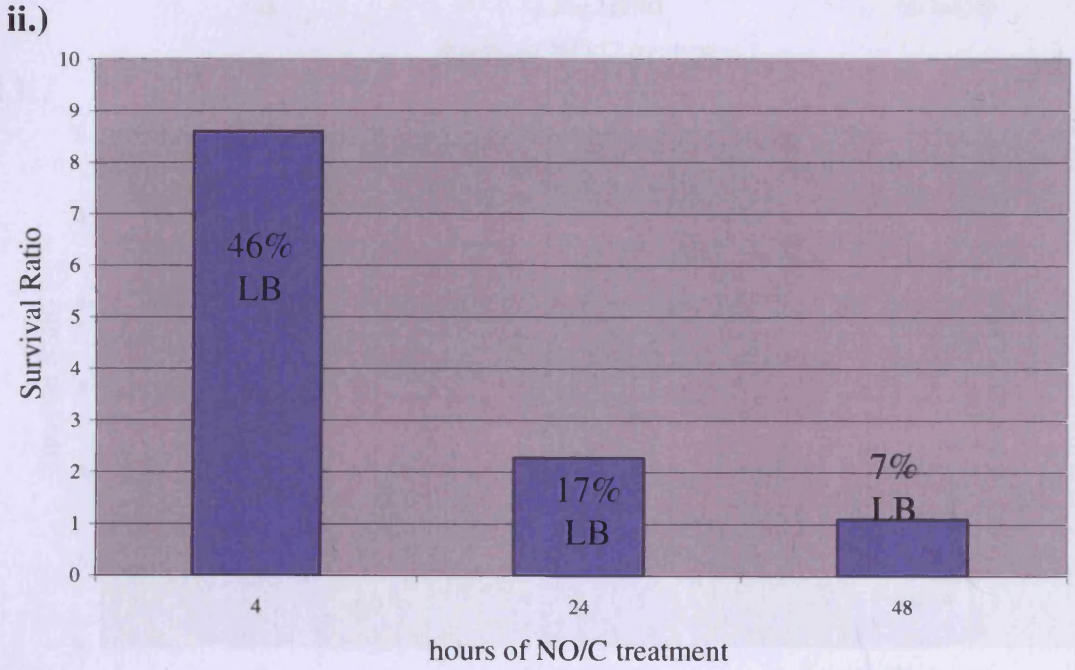

Figure 46: Effect of NO treatment on LB content and Rifampicin tolerance of *M. tuberculosis*. Replicate 3.

Graph (i.) shows the average survival of *M. tuberculosis* treated with NO or Control (C) for 4 and 24 hours after 7 days rifampicin (1μg/ml) kill. The culture was also treated with a second dose of NO or control compound after 4 hours exposure to the initial dose. The 24 hour time point was taken following 24 hours of the second dose. Graph (ii.) shows the survival ratio (NO survival/ C survival), demonstrating the difference in survival between NO treated groups after 7 days rifampicin kill. For experimental detail see dataset legend above.

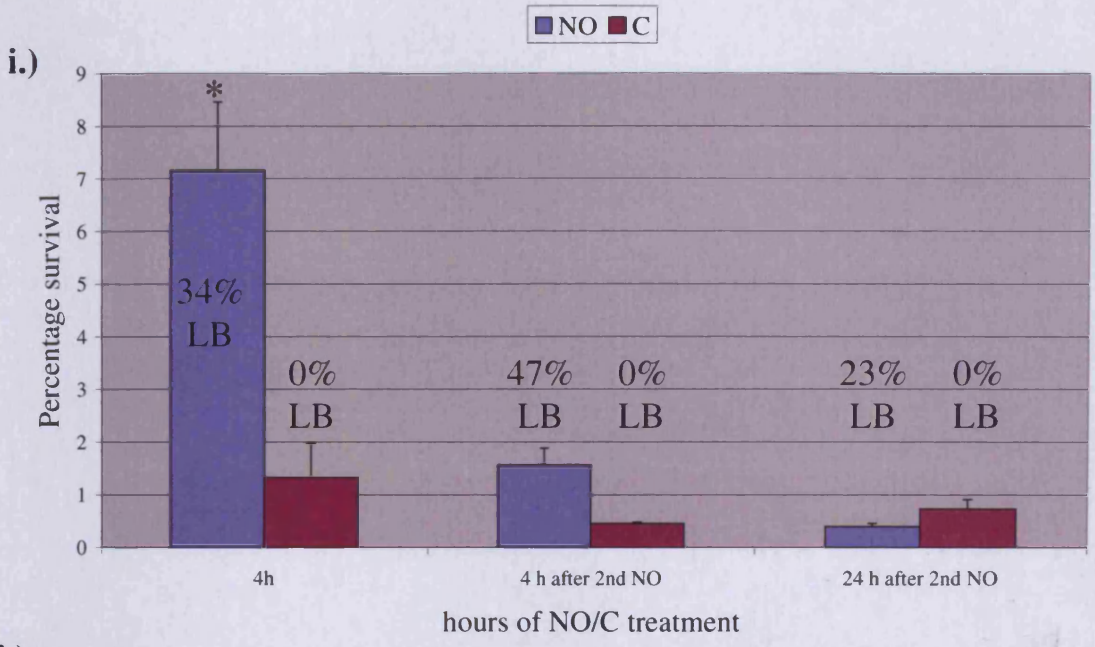

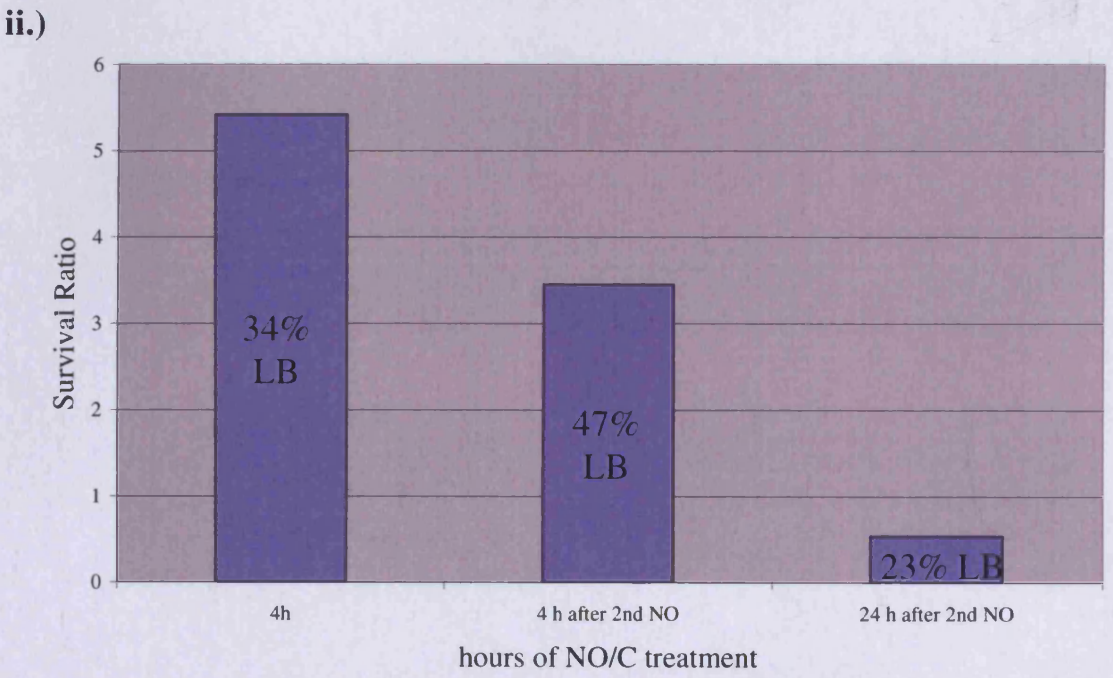

Figure 47-Figure 48: Effect of NO treatment on LB count and survival of *M. tuberculosis* to Isoniazid treatment

Cultures of *M. tuberculosis* were exposed to Spermine NONOate or Spermine tetrahydrochloride for 4 or 24 hours, as before. Colony forming unit (CFU) counts were taken after 4 and 24 hours treatment. Antibiotic tolerance assays were also set up at these times. For experimental detail see figure legend for rifampicin tolerance dataset. Average survival of isoniazid treatment (0.2μM) is expressed as the percentage of initial inoculum that could be recovered after antibiotic treatment. Bars show standard error. Statistical significance is indicated by * for a p-value ≤0.05 and ** for a p-value ≤0.0001.

Figure 47: Effect of NO treatment on LB content and Isoniazid tolerance of *M. tuberculosis*. Replicate 1.

Graph (i.) shows the average survival of *M. tuberculosis* treated with NO or Control (C) for 4, 24 and 48 hours after 7 days isoniazid (0.2µg/ml) exposure. Graph (ii.) shows the survival ratio (NO survival/ C survival), demonstrating the difference in survival between NO treated groups after 7 days isoniazid exposure. For experimental detail see dataset legend above.

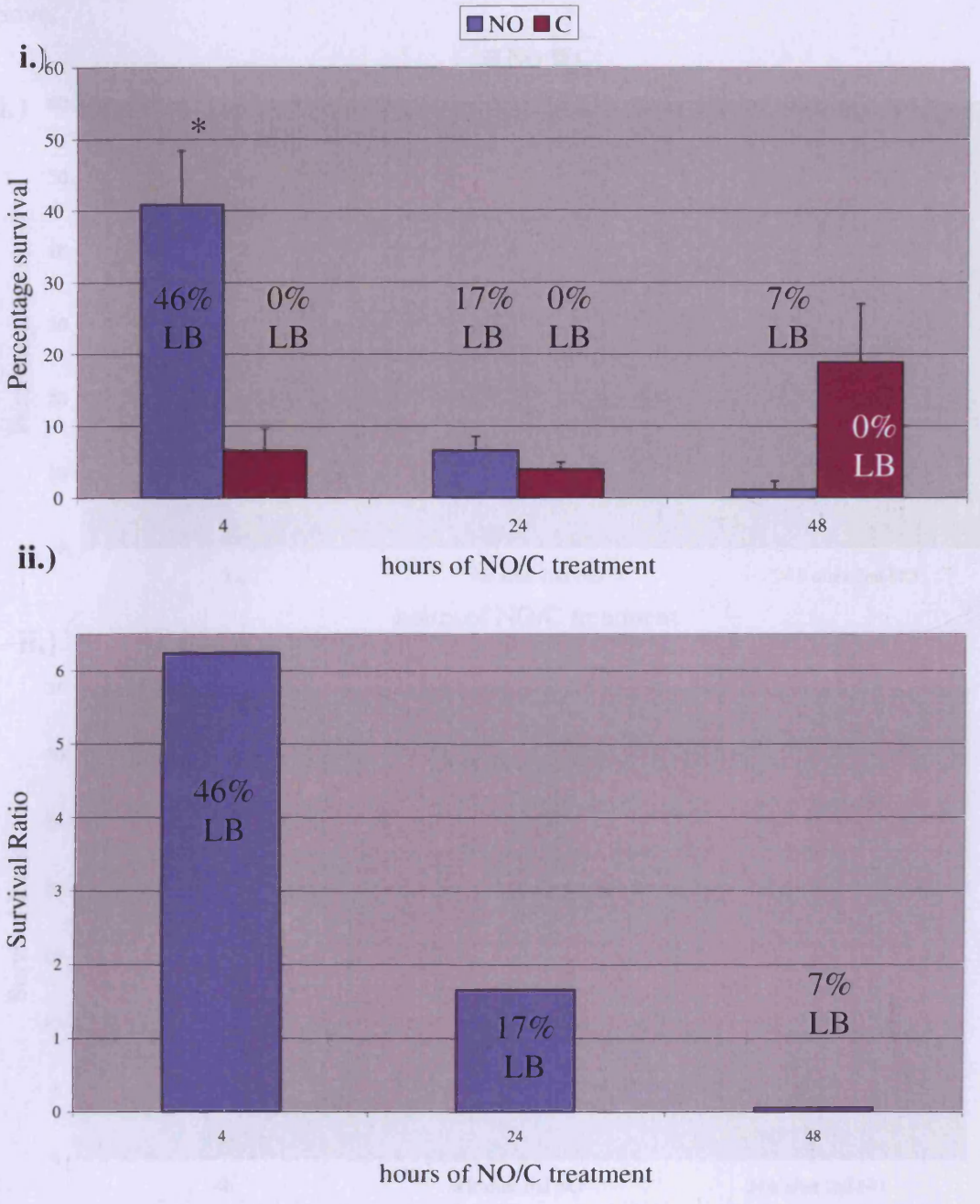

Figure 48: Effect of NO treatment on LB content and Isoniazid tolerance of *M. tuberculosis* – Replicate 2.
Graph (i.) shows the average survival of *M. tuberculosis* treated with NO or Control (C) for 4 and 24 hours after 7 days isoniazid (0.2μg/ml) kill. The culture was also treated to a second dose of NO or control compound after 4 hours exposure to the initial dose. The 24 hour time point was taken following 24 hours of the second dose. Graph (ii.) shows the survival ratio (NO survival/ C survival), demonstrating the difference in survival between NO treated groups after 7 days isoniazid kill. For experimental detail see dataset legend above.

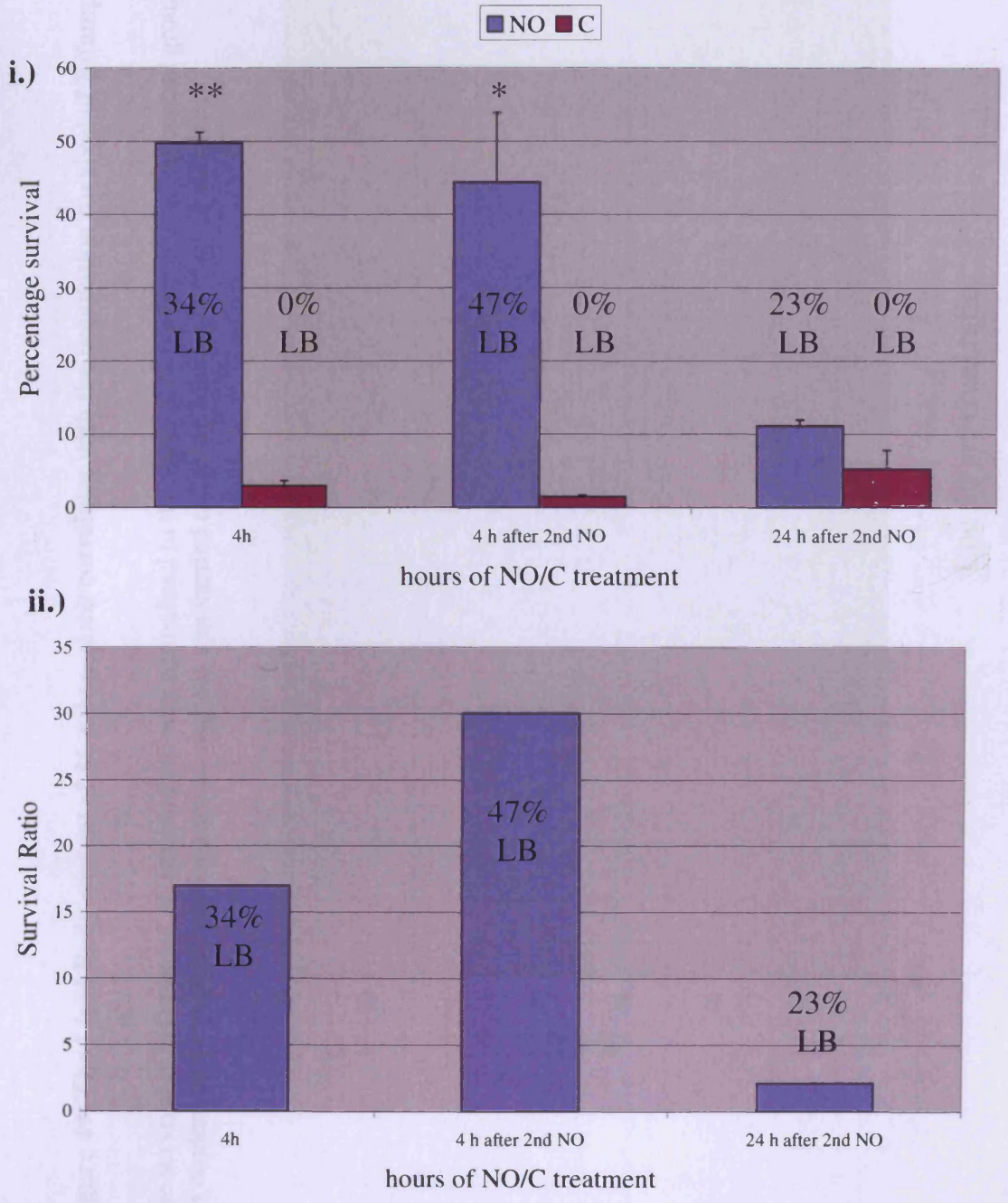

Figure 49: The Lipid Body content of *M. tuberculosis* correlates with the population survival of Rifampicin treatment

The survival of NO treated *M. tuberculosis* was normalised to the survival of the corresponding control group and plotted against the LB content of the population. Regression analysis was carried out using Minitab Statistical software.

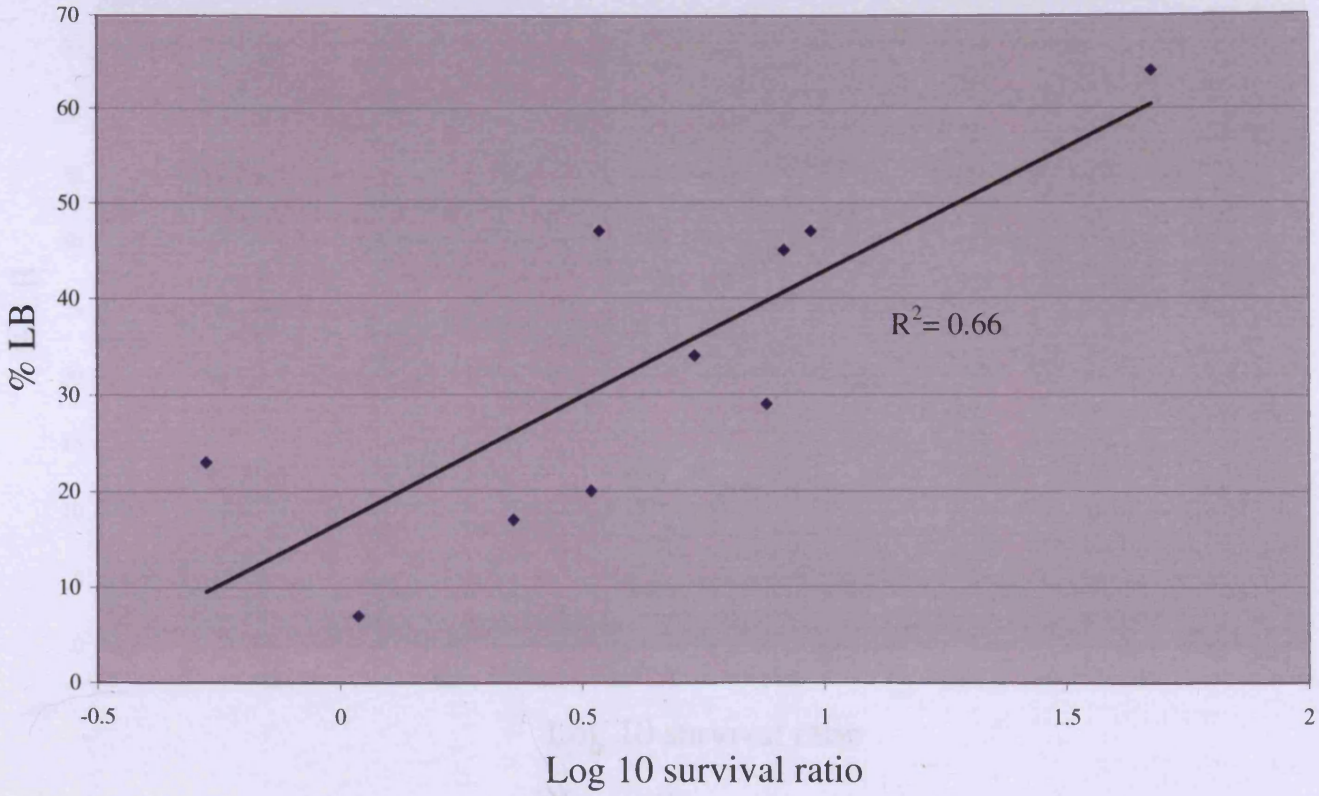

Figure 50: The Lipid Body content of *M. tuberculosis* correlates with the population survival of Isoniazid treatment

The survival of NO treated *M. tuberculosis* was normalised to the survival of the corresponding control group and plotted against the LB content of the population. Regression analysis was carried out using Minitab Statistical software.

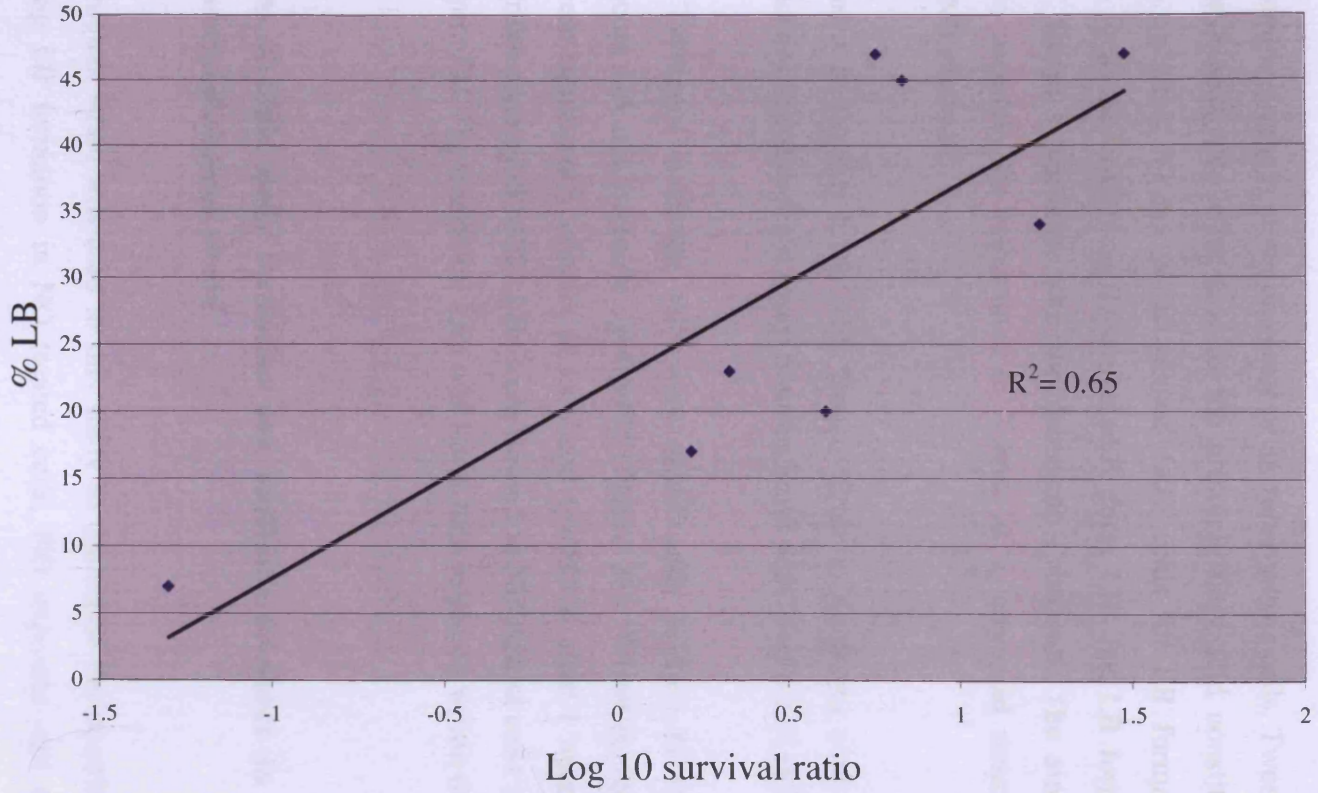

6.3.5 Evaluating the role of Tween 80 in Lipid Body formation and antibiotic tolerance

Tween 80 is included in media to allow dispersal of *M. tuberculosis* cells. Tween 80 is a polyethylene sorbitol ester with oleic acid as the principle fatty acid constituent. *M. tuberculosis* may hydrolyse Tween 80 to release fatty acids for LB formation. *M. smegmatis* grown in media containing Tween readily form LBs but LB formation is diminished when Tween is replaced with the detergent Tyloxapol. The aim of this experiment was to ascertain the importance of Tween as a fatty acid source in LB formation during NO exposure.

Cultures were grown in Sautons broth with Tween. Prior to treatment with NO, the medium was replaced with either pre-warmed Sautons broth with Tween or Tyloxapol.

The NO treated Tyloxapol incubated cells were significantly tolerant of rifampicin ($p=0.037$) at 4 hours but not isoniazid ($p=0.847$) (Figure 51). Whereas, the Tween incubated cells were significantly tolerant of isoniazid ($p=0.030$) after 4 hours of NO treatment but not rifampicin ($p=0.0422$). LBs were formed in NO treated cells incubated in both media (Figure 52). The number of LBs was lower than expected within the Tween incubated group.

6.3.6 Assessment of Lipid Body formation and antibiotic tolerance in a DosR mutant and complemented strain

A DosR deleted mutant strain was used in this study to determine the contribution of DosR in regulating LB formation in NO treated cells. NO exposure and antibiotic tolerance assays were carried out as before (Figure 52).

A small percentage of DosR mutant cells formed LBs after NO exposure (Figure 52). This was accompanied by significant tolerance of isoniazid ($p=0.018$) when compared to

the mutant treated with control (Figure 52). This matched the tolerance displayed by the complemented strain, with no significant difference observed between the two groups ($p=0.140$). However, the mutant did not display tolerance to rifampicin ($p=0.279$).

The complemented strain showed a response comparable to that of the wild type. The NO treated complemented strain showed significant tolerance of both rifampicin and isoniazid ($p=0.000$) at 4 hours after NO treatment. The complemented strain also showed a significantly higher tolerance of rifampicin ($p=0.000$) than the mutant at 4 hours.

Figure 51: The effect of the availability of a fatty acid source on Lipid Body formation and antibiotic tolerance in Nitric Oxide treated *M. tuberculosis*

Duplicate cultures of *M. tuberculosis* were grown in Sautons broth with Tween and prior to the experiment the medium was replaced with either Sautons broth containing Tween or Tyloxapol. Cultures were incubated for 1 hour to allow recovery and NO exposure and antibiotic tolerance was carried out as before. The inoculum for the antibiotic tolerance assay was pelleted and resuspended in Sautons with Tween, with or without antibiotic. Graph (i.) shows the average survival of *M. tuberculosis* treated with NO or Control (C) for 4 hours after 7 days rifampicin (1μg/ml) exposure. Graph (ii.) shows the survival ratio (NO survival/ C survival), demonstrating the difference in survival between NO treated groups after 7 days rifampicin exposure. Graph (iii.) shows the survival of NO or C treated cells after 7 days isoniazid (0.2μg/ml) exposure. Graph (iv.) shows the NO treated groups survival normalised to that of the control group to give the survival ratio for isoniazid.

i.)

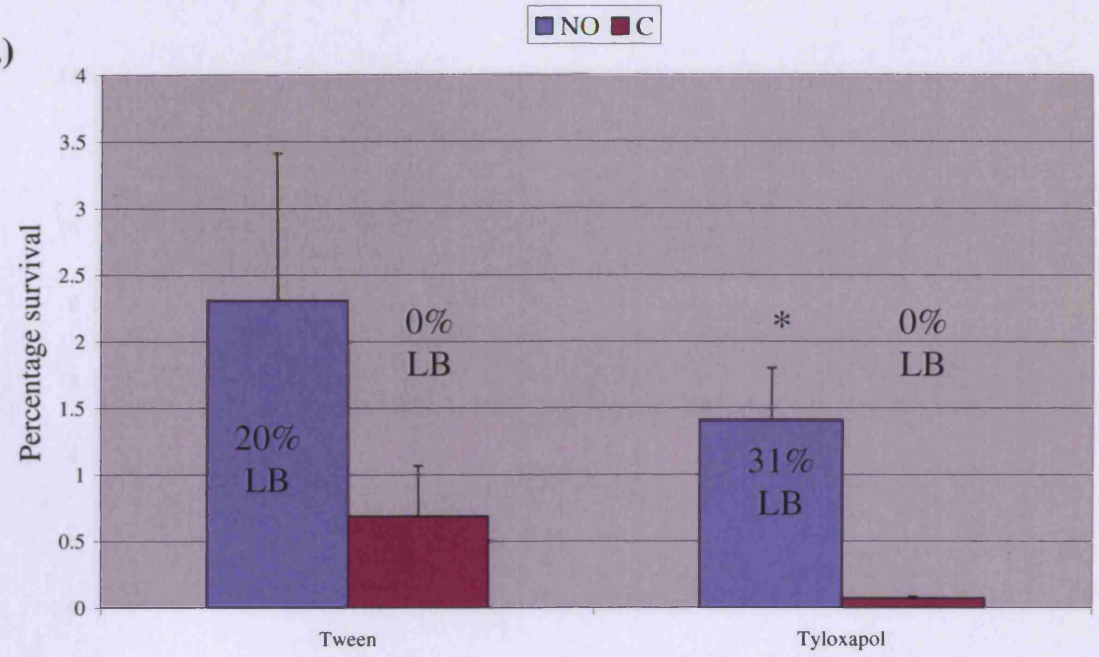
NO
C
Percentage survival
4
3.5
3
2.5
2
1.5
1
0.5
0
20% LB
0% LB
*
31% LB
0% LB
Tween
Tyloxapol

ii.)

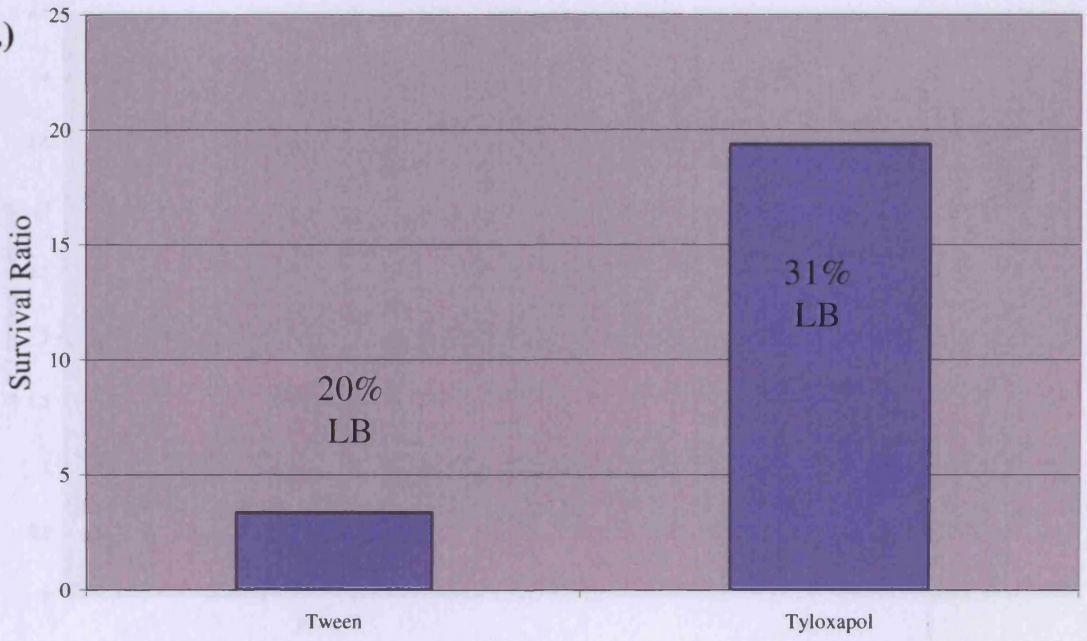
Survival Ratio
25
20
15
10
5
0
20% LB
31% LB
Tween
Tyloxapol

iii.)

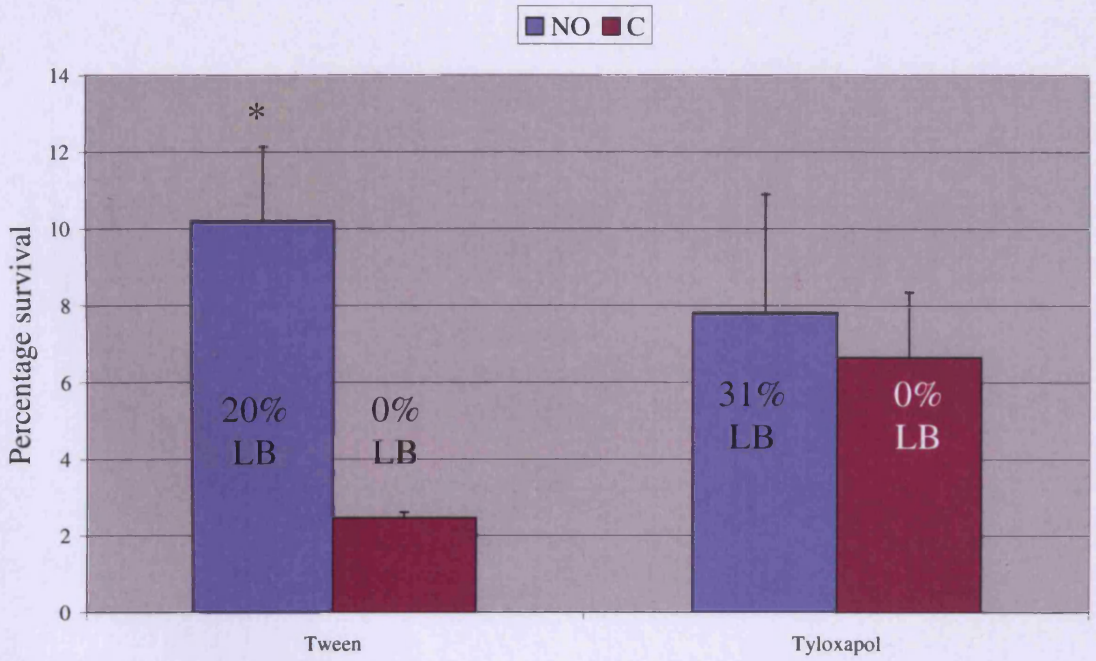
NO
C
Percentage survival
14
12
10
8
6
4
2
0
*
20% LB
0% LB
31% LB
0% LB
Tween
Tyloxapol

iv.)

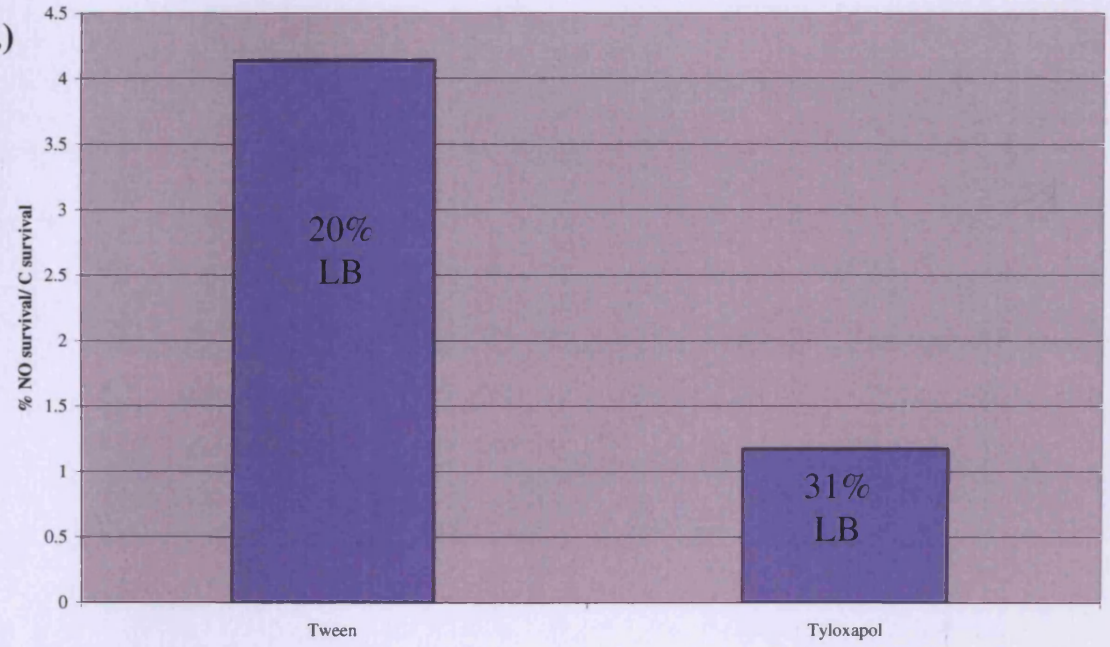
% NO survival/ C survival
4.5
4
3.5
3
2.5
2
1.5
1
0.5
0
20% LB
31% LB
Tween
Tyloxapol

Figure 52: Lipid Body formation and antibiotic tolerance in a DosR deleted mutant and complemented strain

Duplicate cultures of the DosR mutant and complemented strains were exposed to NO and antibiotic tolerance assays were carried out as before. Graph (i.) shows the average survival of *M. tuberculosis* treated with NO or Control (C) for 4 hours after 7 days rifampicin (1μg/ml) exposure. Graph (ii.) shows the survival ratio (NO survival/ C survival), demonstrating the difference in survival between NO treated groups after 7 days rifampicin exposure. Graph (iii.) shows the survival of NO or C treated cells after 7 days isoniazid (0.2μg/ml) exposure. Graph (iv.) shows the NO treated groups survival normalised to that of the control group to give the survival ratio for isoniazid.

i.)

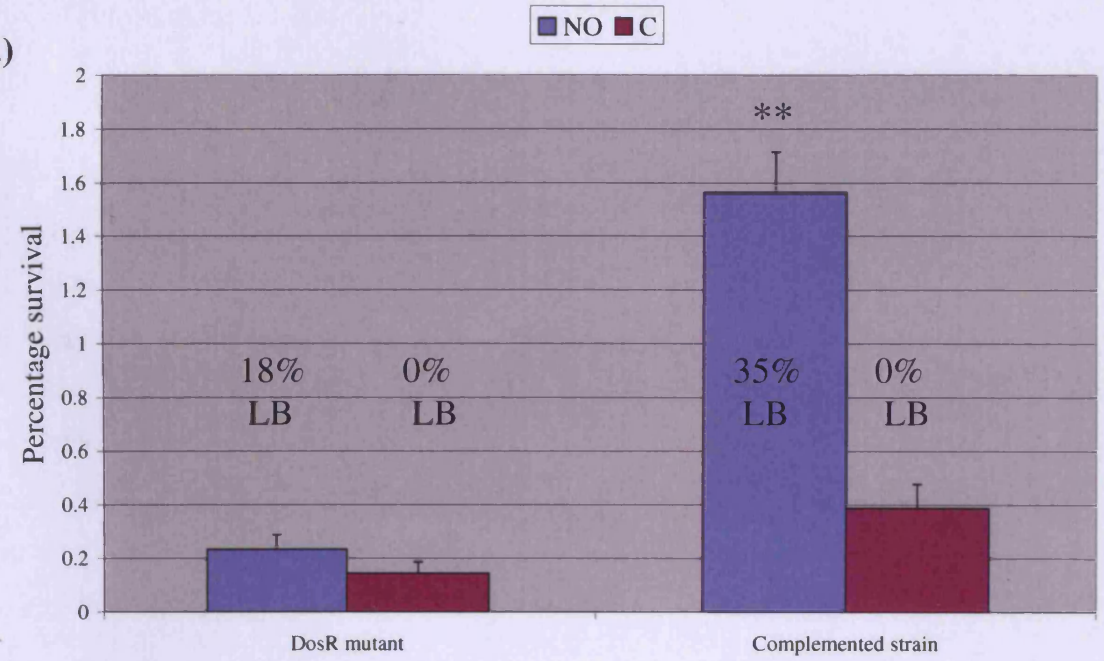
NO
C
Percentage survival
2
1.8
1.6
1.4
1.2
1
0.8
0.6
0.4
0.2
0
**
18% LB
0% LB
35% LB
0% LB
DosR mutant
Complemented strain

ii.)

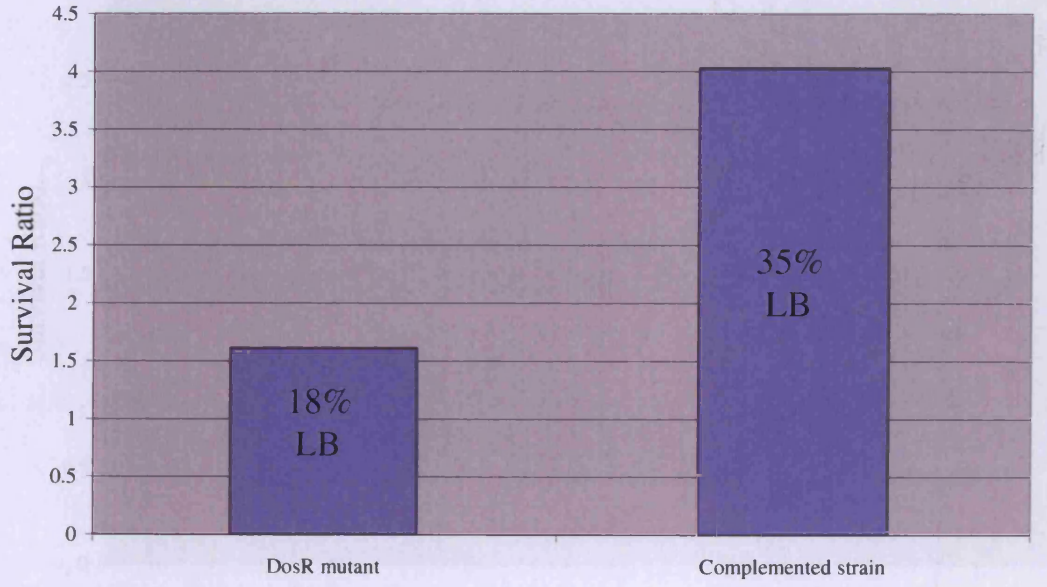
Survival Ratio
4.5
4
3.5
3
2.5
2
1.5
1
0.5
0
18% LB
35% LB
DosR mutant
Complemented strain

iii.)

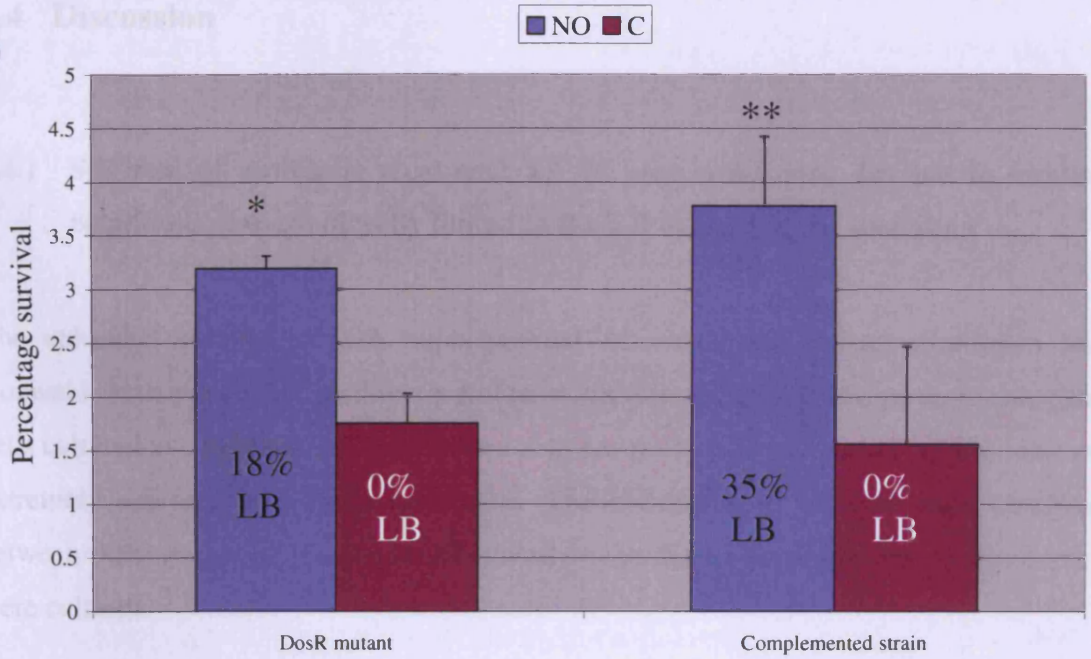
NO
C
Percentage survival
5
4.5
4
3.5
3
2.5
2
1.5
1
0.5
0
*
**
18% LB
0% LB
35% LB
0% LB
DosR mutant
Complemented strain

iv.)

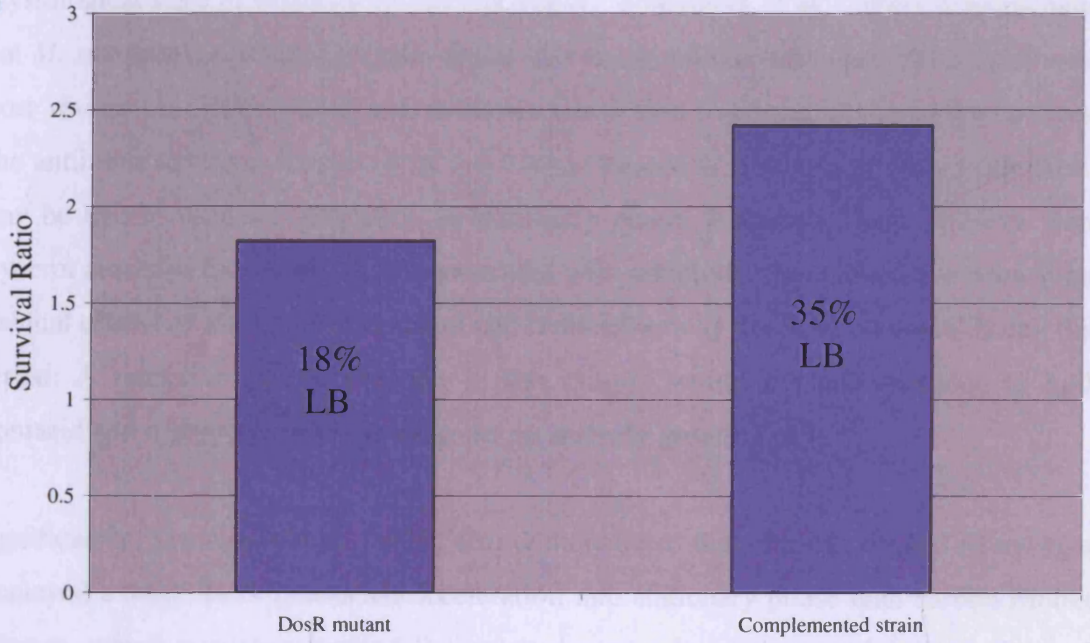
Survival Ratio
3
2.5
2
1.5
1
0.5
0
18% LB
35% LB
DosR mutant
Complemented strain

6.4 Discussion

6.4.1 Survival of antibiotic treatment by *M. smegmatis* may be due to culture conditions and not directly linked to the LB content of the inoculum

The enhanced survival of OA supplemented *M. smegmatis* during rifampicin and isoniazid treatment cannot be directly linked to the LB content of this group because the cells cultured in conditions of low nitrogen also accumulate large numbers of LBs and are extremely susceptible to these antibiotics. The difference in survival rates observed between these groups of *M. smegmatis* is likely to be due to the conditions in which they were cultured.

Cells cultured in low nitrogen or low carbon broth may both adopt an altered physiological state in response to nutrient stress. Smeulders et al. (1999) demonstrated that *M. smegmatis* entered stationary phase due to carbon starvation and these cells were more resistant to acid, osmotic and oxidative stress than exponentially growing cultures. The antibiotic tolerance displayed by low carbon treated *M. smegmatis* within this thesis may be due to such an adaptation to stationary phase. Although, these cultures were glycerol amended for 1 hour prior to treatment with antibiotic, there may have been some residual effects of low carbon treatment and replication may not have resumed during this period. A reduction of cell division in this culture would explain tolerance to both isoniazid and rifampicin, because these act on actively growing cells.

Significantly, Smeulders et al. (1999) also demonstrated that cultures limited in nitrogen displayed a much more protracted deceleration into stationary phase than carbon limited cultures, which was characterised by a slow increase in biomass and cell numbers. A continuation in cell division, albeit at a reduced rate, may explain why the low nitrogen culture of *M. smegmatis* was still susceptible to the activity of rifampicin and isoniazid.

In addition, cultures were exposed to low nitrogen and low carbon by different methods. Low nitrogen broth was simply inoculated with *M. smegmatis* and grown for 5 days, to allow a gradual reduction in nitrogen. Whereas, in order to subject *M. smegmatis* to low carbon conditions, exponentially growing cultures were resuspended in broth containing no glycerol or glucose but with a citrate buffer. Therefore, *M. smegmatis* subjected to low carbon conditions may have had more time to adapt to nutrient stress than those grown under conditions of low nitrogen. In order to evaluate this possibility it would be of interest to examine antibiotic tolerance of *M. smegmatis* subjected to a sudden change in nitrogen availability or cultured under these conditions for longer periods of time.

The induction of the stringent response may be the basis for long term survival during carbon starvation in mycobacteria (Primm et al., 2000). The stringent response is a transcriptional program, brought about by amino acid depletion. This leads to increased levels of two specific hyperphosphorylated guanine nucleotides; the 3' pyrophosphate derivatives of GDP (ppGpp) and GTP (pppGpp), collectively known as (p)ppGpp (Reviewed by Cashel and Rudd, 1987). In *E. coli*, (p)ppGpp binds to the β-subunit of RNA polymerase (Dahl et al., 2003). Interestingly, accumulation of ppGpp in *M. smegmatis* cells grown in low carbon led to a reduction in cell length and cells assumed an almost coccoid morphology (Ojha et al., 2000). Low carbon cells examined in studies presented in this thesis were also noted to have shorter cell lengths than cells growing in rich medium although this has not been correlated with increased ppGpp levels in this study.

The ribosome bound gene product of *relA* has been identified as a (p)ppGpp synthase in *E. coli* and is activated by binding uncharged tRNAs to the ribosome on depletion of amino acids (Reviewed by Primm et al., 2000). Deletion of the *relA* homologue in *M. smegmatis* and *M. tuberculosis* leads to impaired survival during carbon starvation (Mathew et al., 2004, Primm et al., 2000, respectively). The induction of the stringent response may also have important implications for *M. tuberculosis* during infection. Deletion of *relA* in *M. tuberculosis* severely impaired the ability of this strain to sustain chronic infection (Dahl et al., 2003). Expression of *relA* was also associated with the

early stages of *M. tuberculosis* adaptation to *in vitro* carbon starvation; a condition which also induced entry into a non-replicative state and the upregulation of genes involved in virulence (Hampshire et al., 2004). Therefore, it is possible that residual adaptation to low carbon conditions in *M. smegmatis* via the stringent response gives rise to an altered physiological state that renders the bacteria more tolerant to the action of antibiotics. For further discussion of nutrient depletion as a dormancy inducing condition, please see Chapter 1.

The OA supplemented low carbon cells were almost consistently more tolerant of antibiotic treatment than their low carbon counterparts. It is likely that the basis for these cells tolerance is due to a combination of factors; firstly, cells may not have recovered from the physiological changes brought about by low carbon treatment (discussed above) and secondly, exposure of the cells to LCFA. Oleic acid exposure may have a number of effects on the cell.

Exposure to LCFA, which is thought to be toxic to mycobacteria (see Chapter 3 for discussion), may also elicit a transcriptional response that allows further adaptation to stress. In addition, the incorporation of fatty acids into triacylglycerol storage may provide the cell with an additional carbon source for utilisation during antibiotic treatment. It is possible that the high variation in survival of OA supplemented cells during antibiotic treatment is attributable to the LB content of the population. It is also possible that the variation in survival observed for low carbon treated cells is due to the level of residual LBs present in the population. Future experiments should include an assessment of the LB content of the inoculum and the surviving cells in order to determine the role of LBs and their utilisation during antibiotic exposure.

Fatty acids, such as oleic acid or Tween may also become incorporated into the cell envelope (Christensen et al., 1999, discussed in Chapter 1) and thus decrease the permeability of the envelope to drugs. The slight increase in survival observed when cells were incubated with Tween 80 may be attributed to this. Indeed, preliminary results suggest that HAF competes with Tween for insertion into the cell envelope because HAF

labelling decreased as the Tween increased in concentration. Alternatively, Tween may simply allow dispersal of clumps of bacteria to produce a more accurate colony count. Changes in HAF labelling may also provide some indication of the antibiotic tolerance of *M. smegmatis* following growth in a number of conditions.

Overall, *M. smegmatis* is not a suitable model organism in which to assess the significance of LBs and antibiotic tolerance. The difficulty in using this organism for such an experiment is due to the fact that LBs are readily formed during routine culture. LBs are eliminated by culture in low carbon conditions, but as is discussed, this may introduce a further factor that may affect the susceptibility of the bacteria to antibiotic exposure. This could be overcome by increasing the period of time in which the cells are amended with glycerol; which may allow cells to recover completely from low carbon stress. However, recent preliminary work within the laboratory has shown that overexpression of *tgs1* in *M. smegmatis*, via a tetracycline inducible system, leads to enhanced LB formation and increased survival in comparison to the blank plasmid control strain (Saadnah Naidu, Unpublished Results). While these cells were initially carbon starved to eliminate background LB formation, this work has clearly shown that increased LB formation does lead to enhanced survival during antibiotic treatment. However, these experiments will be always be limited to a certain degree by the inability to separate the effects of a changed physiology in the face of nutrient stress and the contribution of LBs in antibiotic tolerance until more suitable growth conditions are found.

6.4.2 Antibiotic tolerance coincides with LB formation in *M. tuberculosis* treated with NO

M. tuberculosis formed LBs after 4 hours NO treatment and this treated population was significantly more tolerant of isoniazid and rifampicin than cultures treated with the control compound. The correlation of LB positivity and antibiotic tolerance (Figure 49 and Figure 50) strongly suggests that the presence of LBs in a population of cells may be

a marker for the overall level of antibiotic tolerance within that population. LB content also appeared to be more correlated with rifampicin tolerance than isoniazid. Although this is not explicit evidence that a LB positive cell is a tolerant cell and this is discussed further below.

The restoration of antibiotic susceptibility and the decline in LBs, presumably occurs as the NO dissipates. This demonstrates that antibiotic tolerance is not constitutive but is due to the physiological response of the bacilli to an environmental factor, in this case NO treatment. The physiological basis for this drug tolerance remains unclear; however, phenotypic drug tolerance is thought to be elicited by an environmental signal that induces the cells to enter an antibiotic refractory growth phase (Michele et al., 1999). Since isoniazid and rifampicin are only effective on actively growing cells, a transitory drop in growth in response to NO may explain the drug tolerance of this population of cells. Voskuil *et al* (2003) demonstrated through optical density readings that exposure of *M. tuberculosis* to a high dose of the NO donor DETA/NO (500μM) caused reversible bacteriostasis. Data from work presented in this thesis showed there was no significant difference in optical density (OD) readings after 4 and 24 hours of NO treatment in comparison to the control group (Appendix 3). Interestingly, exposure to two doses of NO did result in a lower OD measurement in comparison to the control after 24 hours, although this was not a statistically significant difference. This may be because the dose of NO was too low to induce a period of growth arrest long enough to observe a dramatic change in optical density. Voskuil et al. (2003) used 500μM of the NO donor DETA/NO, which releases 2 moles of NO released per mole of donor molecule, to induce growth arrest. This is more than double the concentration of SPER/NO used in experiments in this thesis, as this also releases 2 moles of NO per mole of donor. It is also possible that upon resumption of growth, NO treated cells are able to grow at a faster rate because the components required for the generation of new cell wall lipids and phospholipids are already present in the cell in the form of TAG LBs. Work carried out to determine the growth status of NO treated, LB positive *M. tuberculosis* cells is presented elsewhere (Chapter 5).

The variability of the antibiotic tolerance of the control group was an area of concern. There was no significant difference between the average control survival rates obtained for each replica experiment (see results section) or between the average survival rates at 4 and 24 hours; however, the control survival rate did appear to increase slightly on prolonged incubation. Following 24 and 48 hours incubation, the cultures may be beginning to enter stationary phase, which would have an effect on the antibiotic tolerance of the population. In addition, a preliminary study showed that *M. tuberculosis* incubated with 0.1μg/ml isoniazid formed LBs after 10 days incubation. Therefore, it is also possible that treatment with antibiotic in the presence of Tween for 7 days may promote low level tolerance, indicated by a small increase in LB numbers. Thus the LB content of the antibiotic treated cells may be as significant as that of the initial inoculum and should be examined in future experiments.

6.4.3 LB formation and antibiotic tolerance are induced in *M. tuberculosis* exposed to NO without the presence of Tween

This preliminary experiment showed that cells incubated with the Tween substitute, Tyloxapol, during NO exposure are able to form LBs. This LB formation was correlated with tolerance to rifampicin but not to isoniazid. The Tween incubated cells formed fewer than expected LBs and were only tolerant of isoniazid treatment. This is consistent with the hypothesis that LBs are a more indicative marker of rifampicin tolerance than isoniazid tolerance. Since the Tween incubated cells were as tolerant of isoniazid as the Tyloxapol treated cells, which had a higher LB content, it is possible that tolerance of isoniazid may be explained in part by the presence of Tween in the media. As discussed in this and previous chapters, Tween may insert into the cell envelope and decrease the cells permeability to drugs.

The cells used in this experiment were grown in media containing Tween because previous attempts to grow cultures with a Tyloxapol replacement were unsuccessful. The cells were resuspended in media with Tyloxapol prior to the addition of NO. Therefore, it

is difficult to determine whether LBs were formed from *de novo* synthesised fatty acids or from Tween previously taken up by the cell.

As this was a preliminary study, this experiment needs to be repeated to determine whether this was an anomalous result.

6.4.4 LB formation and antibiotic tolerance in NO treated *M. tuberculosis* are largely under the control of DosR

Preliminary results showed that the DosR deleted mutant strain formed a smaller number of LBs than the complemented strain in response to NO exposure. The NO treated DosR mutant was tolerant of isoniazid but not rifampicin, while the complemented strain was tolerant of both. This is another indication that LBs are a closer marker of rifampicin tolerance.

The diminished level of LB formation and antibiotic tolerance in the DosR mutant following exposure to NO suggests that DosR plays a significant role in mediating this response. As discussed in Chapter 3, the observed low level LB formation and antibiotic tolerance in the DosR mutant may be under the control of a non-DosR regulated pathway; which may induce the expression of *tgs1* or one or more of the *tgs* genes. This requires further investigation by RNA transcriptional analysis.

6.5 Conclusions

M. smegmatis and *M. tuberculosis* with and without LBs were assessed for ability to survive antibiotic treatment. Currently, the inability to reduce the LB content of *M. smegmatis* without its subjection to the initial stress of low carbon treatment limits the use of this organism for such an experiment. *M. tuberculosis* has been shown to form LBs in response to a number of conditions (see Chapter 3). NO exposure was used to promote LB production because of the relatively short exposure period needed and its biological relevance. LB formation was shown to correlate with increased antibiotic tolerance in NO treated populations of *M. tuberculosis* when compared with controls.

Phenotypic drug tolerance is thought to be elicited by an environmental signal that induces the cells to enter an antibiotic refractory growth phase (Michele et al., 1999). As this tolerance is due to a change in cell physiology and is not chromosomally encoded, susceptibility to the antibiotic is regained as the stimulus is withdrawn (Warner and Mizrahi, 2006). This was shown to be the case for NO treated *M. tuberculosis*, which regained its sensitivity to antibiotics, presumably when the NO had dissipated. However, the basis for this phenotypic drug tolerance was not identified. NO treatment was expected to result in a transitory growth arrested population of *M. tuberculosis*, giving rise to phenotypic antibiotic tolerance. There was insufficient evidence to confirm such a hypothesis with these experiments and therefore, the question remains; are LB positive cells growth arrested? This subject was addressed in Chapter 5.

Chapter 7

General Discussion

7.1 General Discussion

The significance of triacylglycerol (TAG) accumulation and Lipid Body (LB) formation in mycobacteria is an issue that has only recently begun to be addressed. Renewed interest followed the report that LBs were present in Acid-Fast Bacilli (AFB) in a sputum specimen taken from a patient with tuberculosis (Garton et al., 2002). Shortly after this discovery, the genetic basis for TAG synthesis was demonstrated through the identification of the triacylglycerol synthase (TGS) gene, *tgs1* (Daniel et al., 2004) and in contemporaneous experiments in the laboratory (Garton et al., 2008). Furthermore, work presented within this thesis (Chapter 3), has demonstrated that expression of this gene is linked with LB formation in mycobacteria. In light of the findings presented in the literature prior to the commencement of this study, the aim of the research presented here was to examine the conditions in which LBs occur in mycobacteria and their physiological significance.

7.1.1 What conditions are required for LB promotion in *M. tuberculosis*?

It has now been demonstrated through findings presented in this study and work within the laboratory (Garton et al., 2008), that LBs are a universal feature of AFB in microscopy positive sputum samples. In addition, the expression of *tgs1* was shown to be upregulated in sputum tubercle bacilli when compared to broth grown culture though microarray and quantitative real time PCR analysis. The absence of LBs in standard broth cultured *M. tuberculosis* suggests that the presence of LBs in AFB represents a change in physiology.

The presence of LBs and similarities in *tgs1* expression in both Non Replicating Persistence (NRP) cells and sputum bacilli suggest that LB AFB are in a NRP-like state. Microarray data indicated that the expression of genes required for aerobic respiration and ribosomal function was down-regulated in sputum bacilli in comparison to *M. tuberculosis* grown aerobically (Garton et al., 2008). When these microarray results were

compared to transcriptomes obtained from nutrient deprived and NRP *M. tuberculosis*, a set of 20 repressed genes were found to be common to all three conditions (Garton et al., 2008). Furthermore, the LB content of AFB was correlated with a delay in the initiation of growth of bacteria isolated from sputum and cultured in BACTEC (Becton Dickinson) media containing a growth indicator (Garton et al., 2008). This is compatible with the hypothesis that LB positive cells are growth arrested or only replicating very slowly, as reactivation of growth by these bacteria would be expected to be at a slower rate in comparison to actively replicating cells.

As discussed in previous chapters, the adaptation to a NRP state in *M. tuberculosis* is mediated by the expression of the DosR regulon, of which *tgs1* is a member (Muttucumaru et al., 2004). However, it is unlikely that LBs are simply a response that is regulated by the expression of DosR because LB formation has been shown to occur in *M. tuberculosis* under conditions in which the DosR regulon is not induced. LB formation also occurred in a DosR disrupted mutant strain of *M. tuberculosis* but at a reduced level (Chapter 3). Interestingly, this DosR mutant has previously been shown to be more virulent in SCID mouse infection than the wild type strain and grew more during acute infection of immunocompetent mice and in activated macrophages (Parish et al., 2003). This suggests that DosR is involved in the establishment of the chronic phase of infection or in regulating growth *in vivo*. However, the role of DosR in adaptation to growth arrest has recently been called into question. DosR was shown to be dispensable on entry to bacteriostasis and for survival under hypoxia (see Chapter 1). This was attributed to a large set of genes that were induced and expressed throughout hypoxia that were thought to be involved in the maintenance of the growth arrested state. The implication of this was that the DosR regulon only functions to prime cells for growth arrest (Rustad et al., 2008). An aspect of this may be the formation of TAG during the growth arrest process. The LBs may then act as energy reserves during chronic infection or dormancy. The low level of LB formation without the input of DosR regulation indicates that *tgs1* expression or expression of other *tgs* genes and LB formation may continue sporadically throughout dormancy to maintain the carbon source or to remove toxic extracellular fatty acid. The contribution of the activity of the other 13 *tgs* genes,

which are not members of the DosR regulon, has not been assessed. It is possible that the products of these genes contribute to LB formation under non-DosR activating conditions. With or without regulation by DosR, LBs appear to be a feature of cells that have been exposed to conditions that are thought to result in a reduction in growth rate. In the event of a cessation of replication Long Chain Fatty Acid (LCFA) that would have been incorporated into the growing cell envelope may then be utilised in TAG synthesis, resulting in the formation of LBs. Therefore, LBs may be markers of growth arrested cells.

7.1.2 Are LBs in mycobacteria associated with enhanced survival following antibiotic treatment?

As we know from studies of NRP cells, a reduction in growth rate results in phenotypic antibiotic tolerance due to a decrease in the cellular functions that are the targets of drugs such as rifampicin and isoniazid (Wayne and Hayes, 1996). In fact, the correlation of antibiotic tolerance and bacterial growth rate is a phenomenon that is widespread among bacteria (Gomez and McKinney, 2004). The antibiotic tolerance of *M. tuberculosis* exposed to NO was examined in order to determine whether this phenomenon was common to LB inducing conditions other than hypoxia. Remarkably, the LB content of a population of *M. tuberculosis* appears to be correlated with the level of antibiotic tolerance by that population of cells (Chapter 6). Interestingly, LB formation and antibiotic tolerance was confined to a subpopulation of cells and this will be discussed in the following section. Phenotypic tolerance when LB positive cells are generated by conditions other than NO exposure has yet to be examined. The underlying basis for antibiotic tolerance was hypothesised to be due to a reduction in growth but attempts to demonstrate the growth status of LB positive cells through the use of differential fluorescent labelling and growth reporter vectors were unsuccessful (Chapter 5). Studies of LB positive populations of *M. smegmatis* also revealed that LBs were associated with survival of antibiotic treatment. However, as there were other factors (residual adaptation to low carbon conditions) that may have been involved in this relationship, it is difficult

to make a general statement about the significance of LBs to *M. smegmatis* survival (this is discussed in more detail in Chapter 6).

Mitchison has previously proposed the existence of physiologically diverse populations of *M. tuberculosis in vivo* to explain the discrepancies between the sterilizing activity of drugs and their bactericidal activities *in vitro* and early treatment *in vivo* (1979). The Mitchison Hypothesis is based on groups of bacteria characterised by their growth state, which varies from active replication to growth inhibition (Figure 53). It is widely recognised that slowly metabolising bacteria are more drug refractory than their actively growing counterparts and, therefore, bacterial growth status impacts on infection treatment (Reviewed by Lewis, 2007). In the treatment of tuberculosis, initial drug chemotherapy results in rapid killing, probably eliminating groups of exponentially growing bacteria. The sterilizing phase of treatment is more protracted and it is thought that this is caused by the residual population of slowly metabolising bacteria (Mitchison, 2004). The existence of such a subpopulation of antibiotic tolerant cells could explain the protracted period required to treat tuberculosis. Interestingly, there is some clinical evidence to suggest that this hypothesis is correct. In tissue obtained from lung lesions taken after prolonged therapy, open and active cavities yielded bacteria that formed colonies in the usual time of 3-8 weeks, these bacteria were antibiotic resistant. However, closed cavities contained bacteria which only formed colonies after 3-10 months incubation, indicating that they had adopted an altered physiological state. The recovered bacteria were drug susceptible but their persistence in the lung suggests that their physiological state *in vivo* rendered them drug refractory (Bloom and McKinney, 1999). The poor drug activity against *in vivo* bacilli is due to the fact that frontline drugs currently used to treat tuberculosis target processes that are involved in cell growth and division (Gomez and McKinney, 2004).

While it has not been shown that LB positive cells are growth arrested, it can be hypothesised that LB positive populations of AFB may be representative of the persistent group of cells observed in chemotherapy. In spite of this, there is no evidence that any of the conditions examined in this study replicate the environment of the bacteria that are

responsible for the prolonged colonisation of the latent tuberculosis state, as little is known about these bacteria. However, a recent study has revealed that *M. tuberculosis* DNA could be detected by conventional and *in situ* PCR in sections of adipose tissue from autopsies of patients who had died of causes other than tuberculosis (Neyrolles et al., 2006). The authors suggest that this tissue may constitute a reservoir where dormant bacilli persist during latent infection, however, the most interesting piece of evidence was the demonstration of LBs in *M. tuberculosis* internalised in adipocytes *in vitro*. Furthermore, accumulation of LBs coincided with maturation of the host cell giving rise to growth arrested bacilli, which were shown to be tolerant of isoniazid (Neyrolles et al., 2006). While no intact bacilli were detected in autopsy tissue specimens, perhaps due to low bacterial load or loss of acid-fastness, this work does provide the first tantalising evidence for the presence of LBs in a population of *M. tuberculosis* that may represent the dormant, long term colonisers that underlie latent disease.

Alternatively, the survival of antibiotic treatment by LB positive mycobacteria may not be connected to the growth rate. It is possible that TAG LBs are mechanistically linked to tolerance. TAG formed in mycobacteria may initially be located in the cell envelope. LB formation may represent cell envelope saturation, whereupon, excess TAG is stored in the LB. The electron transparent material observed at the cell periphery of low carbon treated *M. smegmatis* may be representative of this (Chapter 4). Storage of TAG in the cell envelope may decrease the permeability of the cell to antibiotics. If this is the case Nile Red labelling in mycobacteria exposed to increasing concentrations of oleic acid would be expected to partition with the cell envelope until TAG formation reached a critical level, perhaps during exposure to large amounts of LCFA, whereupon LBs would form in the exposed cells.

Figure 53: The Mitchison Hypothesis

Mitchison proposes that variation in bacterial growth rate accounts for the biphasic killing of *M. tuberculosis in vivo*. Groups of bacteria can be classified by their growth status, which dictates the drug which will have the highest activity against them. The actively growing bacteria are eliminated rapidly through the activity of isoniazid. As replication rate decreases the isoniazid activity is diminished. Rifampicin is thought to be active against bacteria displaying occasional metabolic spurts because, unlike isoniazid, its bactericidal action starts rapidly. Pyrazinamide is active only on organisms in an acid environment and its activity increases as the growth rate of the organisms goes down. The dormant population is unlikely to be killed by any of these antibiotics (Mitchison, 1979). Figure adapted from Mitchison (1979).

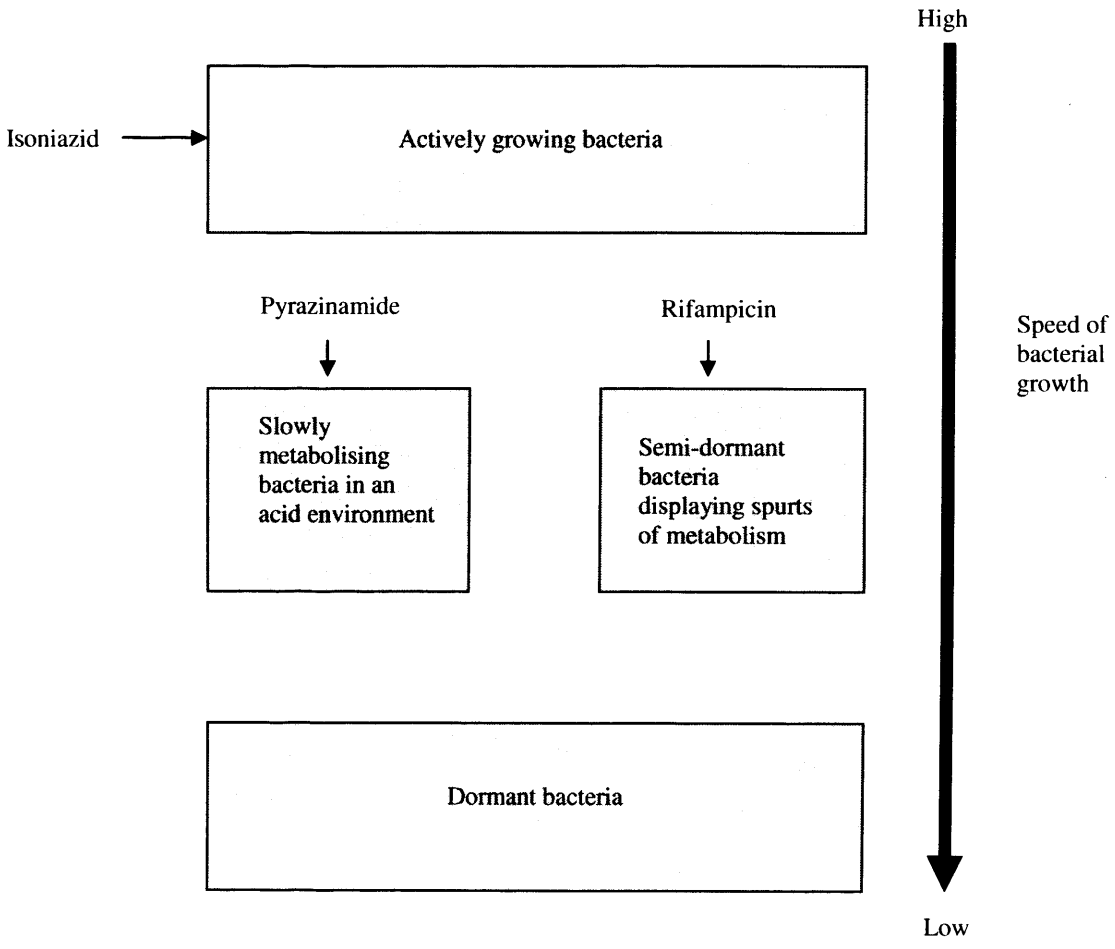

7.1.3 What role may Lipid Bodies Play during Infection?

Examination of sputum gives a unique insight into the population of *M. tuberculosis* responsible for transmission. The similarities between NRP cells and sputum tubercle bacilli, discussed above, may have further implications on the transmissibility of the organism. Growth arrested cells by their very nature are generally more resistant to stresses (Kussell et al., 2005) and the presence of intracellular LBs may provide additional protection against environmental pressures. Just as plant lipid bodies are important for seedling germination and growth (Zweytick et al., 2000); LBs in mycobacteria may act as an immediately available source of LCFA and carbon for reactivation of growth following a period of growth arrest. Therefore, LB positive cells may represent a population of cells with a physiology specifically adapted for transmission.

Three instances in which LB formation appears to increase survival in conditions that may be encountered upon transmission or confer an advantage in virulence have been reported in the literature. Firstly, LB accumulation in Rhodococcus has been shown to enhance survival of the organism on desiccation, perhaps through the oxidation of lipid hydrocarbon, which would release water to be utilised by the cells (Waltermann and Steinbuchel, 2005). The degradation of LBs in *Rhodococcus opacus* during prolonged dehydration corroborates this theory (Waltermann and Steinbuchel, 2005). *M. tuberculosis* may be subjected to a period of desiccation following transmission from the host and therefore, the presence of an internal reservoir of water would confer a selective advantage.

Indeed, chemostat cultures of *M. tuberculosis* grown under conditions of low oxygen, shown in this study to contain a population of LB positive cells, are more infectious to guinea pigs than aerobically grown cultures (Bacon et al., 2004). In addition, it has been suggested that the successful global distribution of strains of *M. tuberculosis* belonging to the Beijing lineage may be related to differential gene expression (Pheiffer et al., 2005).

Although confirmation of LB formation *in vitro* by Beijing strains has proved to be difficult (NJ Garton, Personal Communication), it is known that expression of *tgs1* is up-regulated in cells belonging to this lineage, presumably resulting in the observed accumulation of TAG in these strains (Reed et al., 2007). It is interesting to speculate that LB formation in these strains may contribute to the high transmissibility of this group of pathogens. LB analysis of sputum samples taken from patients infected with Beijing strains of *M. tuberculosis* would perhaps contribute to our understanding of this clinically important lineage.

Lipid bodies may also represent an important carbon storage structure for utilisation during the initial period of replication following infection *in vivo*. The role of TAG LBs during infection remains largely unknown; although there is some evidence to suggest that TAG may act as an energy reserve that is exploited during dormancy and upon reactivation of growth. However, it is thought that fatty acids are in abundance in the host environment; therefore, TAG may be rapidly formed by cells *in vivo* and stored as LBs to buffer the toxic affects of fatty acids that are surplus to the growth requirements of the cell. The gene encoding isocitrate lysase (*icl*), an enzyme involved in the metabolism of fatty acid as a carbon source, is upregulated upon entry to non-replicating persistence (Muttucumaru et al., 2004, Wayne and Lin, 1982) and is essential for bacterial survival during murine infection and in the activated murine macrophage (McKinney et al., 2000). Microarray analysis of sputum bacilli also indicated that *icl* was induced during human infection (Garton et al., 2008). Interestingly, this apparent change in physiology was alluded to by early experiments carried out by Segal and Bloch (1956), who demonstrated that *in vitro* grown *M. tuberculosis* grows preferentially on media in which carbohydrate is the main carbon source, whereas, *in vivo* grown *M. tuberculosis* prefers fatty acids. For further discussion about ICL, the reader is referred to Chapter 1.

Of course, in order for stored lipids to be utilised during periods of nutrient stress or desiccation, the fatty acids must first be released from the acylglycerol molecule. As discussed in Chapter 3, Deb et al. (2006) have identified a lipase with TAG hydrolase activity that appears to be central to TAG utilisation during starvation in *M. tuberculosis*.

7.1.4 What is the basis for variation in Lipid Body numbers between clinical samples?

While it is clear that LB positive cells in sputum represent a group of bacilli with a distinct physiological status not previously demonstrated in batch growth *in vitro*, explanations for the observed variability in size of this population may only be speculative. Differences in population size may be due to host-pathogen interactions, the clinical strain or drug treatment.

Within the lungs of patients with active tuberculosis there exist a number of microenvironments characterised by distinct pathology (Boshoff and Barry, 2005). These include cavitating granulomas, areas of fibrosis and necrotic non-cavitating granulomas (Kaplan et al., 2003). Conditions within these sites of infection may be as diverse as the pathology. There may be varying degrees of hypoxia depending on the proximity of the granuloma to the airway and the thickness of the surrounding tissue, which also has an impact on the immune response (Kaplan et al., 2003). The activation status of macrophages associated with the site of infection is related to the ability of T-cells to infiltrate the tissue (Kaplan et al., 2003) and this in turn adds a further layer of environmental complexity due to the acidic and hypoxic nature of the activated macrophage. Bacterial physiology is likely to adapt in response to environmental signals and therefore, environmental diversity will result in populations of cells displaying various physiological statuses.

The rate of LB accumulation may also be dependent on the clinical strain responsible for the infection, either through differences in gene expression, changes in growth rate or sensitivity to environmental signals. As discussed above, such a difference has been demonstrated in the highly virulent Beijing strains of *M. tuberculosis* which have been shown to accumulate TAG and constitutively express *tgs1* during aerobic log phase growth at a rate 10-fold higher than that observed in the control laboratory strains (Reed

et al., 2007). Interestingly, *M. tuberculosis* strain CH, a highly virulent clinical isolate responsible for a recent outbreak of tuberculosis, did show a higher level of LB accumulation following exposure to hypoxia when compared to the lab strain, H37Rv. This also provides further evidence to suggest that LB formation and variation in the number of LB positive cells may contribute to the transmissibility of a strain.

Chemotherapy may also influence LB positive cell numbers. If LB positive cells do represent a drug tolerant, slowly metabolising population, the population of LB positive cells should become more concentrated as treatment progresses due to the removal of actively replicating cells through the action of isoniazid and rifampicin. This has been shown to be the case for *in vitro* antibiotic treated *E. coli*. Wiuff et al. (2005) demonstrated that antibiotic treatment resulted in the enrichment of subpopulations of phenotypically antibiotic tolerant cells.

The treatment status of the patients who provided sputum samples for this study is unknown and therefore it is not possible to correlate LB numbers with the stage of chemotherapy here but this would be a study of enormous value. Demonstration of such an association could lead to the development of a simple tool, such as dual stained sputum smears, to monitor the bacterial response to chemotherapy. Potentially, treatment could be adjusted according to the LB content of sputum bacilli.

7.1.5 Why are populations of *M. tuberculosis* heterogeneous in terms of their LB content?

If LBs confer a selective advantage to *M. tuberculosis* during antibiotic exposure and survival during transmission and infection, it would seem probable that the majority of cells within that population would contain LBs. However, in cultures of *M. tuberculosis* subjected to all the conditions examined within the course of this study and in populations of sputum bacilli, LBs have been consistently observed in only a subset of cells. As discussed, in studies of NO exposed cells, LB formation coincided with the

development of reversible antibiotic tolerance by a small proportion of the overall population. Therefore, these cells could be described as persisters because of their ability to survive antibiotic exposure, without the apparent generation of resistance mutations (Lewis, 2007) (see Chapter 1 for detailed discussion). Such persistence may be due to a reduction in growth rate (Kussell et al., 2005). It has previously been proposed that within a growing population of bacteria, a small subpopulation of persisters with suppressed growth will be present. And therefore, phenotypic heterogeneity within a population may afford protection against elimination by environmental stresses (Kussell et al., 2005). The small number of slowly growing, stress-resistant cells ensure the survival of the strain, at the expense of non-proliferation and an extended lag time, while the actively growing cell is free to rapidly exploit favourable growth conditions (Lewis, 2007).

A cell is able to swap between persistence and normal growth through a spontaneous switching mechanism (Balaban et al., 2004) and the rate of switching between phenotypes is known to be dependent on the frequency of environmental changes (Kussell et al., 2005). If the switching mechanism is upregulated in *M. tuberculosis* in response to environmental signals, it is possible that this forms the basis for the generation of persister-like/antibiotic tolerant cells observed following NO exposure. In addition, the pre-existence of a small population of slowly growing, persister-like cells within the population may explain the rapid formation of LBs in NO exposed cells. Since the switch to persistence is associated with the frequency of environmental changes, it is possible that the generation of persister cells is artificially lower during *in vitro* culture, in which environmental stress is minimal. Whereas bacilli *in vivo* are much more likely to encounter fluctuations in a variety of adverse conditions and persisters may be generated in higher numbers; cells which are perhaps responsible for the phenomenon of extended drug treatment of tuberculosis. If LBs are a feature of persister-like cells, this may explain why LBs could be observed in every population of sputum bacilli examined. There is little known about the physiology of *M. tuberculosis* during the long term colonisation period of latent disease and whether the presumed dormant state of these cells is distinct to the persistent cell population observed during chemotherapy.

The mechanisms involved in the switch to a persistent-like state have not yet been established but two systems have been suggested for the role. The first is through the stringent response regulator, RelA. As discussed in Chapter 6, RelA is responsible for the synthesis of hyperphosphorylated derivatives of GTP ((p)ppGpp) in response to carbon and amino acid starvation. This (p)ppGpp alarmone binds to the β-subunit of RNA polymerase and thereby inhibits transcription (Reviewed by Gomez and McKinney, 2004). It also increases the recruitment of alternative sigma factors to the RNA polymerase complex in order to prioritise the transcription of stress related genes (Gerdes et al., 2005). As was discussed in Chapter 6, adaptation to low carbon stress, perhaps via the stringent response, seemed to be a factor in the development of phenotypic drug tolerance in *M. smegmatis*. Furthermore, *relA* has been shown to be crucial in *M. tuberculosis* sustaining infection in mice (Dahl et al., 2003). While the physiology of the persister and stringent-like states in bacteria are thought to be similar, other factors involved in mediating the switch to a persister-like state have been identified (Warner and Mizrahi, 2006).

A strain of *E. coli* mutated in the gene *hipA7* has been shown to generate a high number of persister cells during log phase growth (Keren et al., 2004). Expression profiling of cells of this strain recovered from ampicillin treatment revealed that among the induced genes there was a number of toxin components of toxin-antitoxin modules (Keren et al., 2004). Toxin-antitoxin (TA) modules are widespread throughout the prokaryotes and are plasmid and chromosomally encoded modules (Gerdes et al., 2005). The toxin is a protein that inhibits a cellular function, such as translation and is regulated by the antitoxin, which forms an inactive complex with the toxin (Lewis, 2007). In this manner, a persistent–like state may be adopted through the inhibition of transcription that can be reversed through the action of the corresponding antitoxin (Lewis, 2007). Mycobacteria have a high number of TA domains which are largely uncharacterised (Arcus et al., 2006). The MazF toxin of *E. coli* is an mRNA interferase that inhibits protein synthesis and brings about growth arrest. *M. tuberculosis* contains 7 MazF homologues and four of these caused growth arrest when cloned and expressed in *E. coli* (Zhu et al., 2006). Therefore, the switch to a persistent state is likely to be controlled by a combination of

factors such as the stringent response and toxin-antitoxin modules. While studies in mycobacteria have revealed the importance of both systems in mycobacteria, it is clear that further work will need to be carried out to determine whether they are an important part of the adaptation to a persister-like state during chemotherapy in human infection and whether other regulator systems, such as DosR contribute. There is currently no evidence to show that the physiology of *M. tuberculosis* persisters during chemotherapy is the same as that of the bacilli responsible for dormant infection.

7.2 Future work

Through the work reported in this thesis it has been possible to demonstrate that LBs are a widespread occurrence in sputum tubercle bacilli. *In vitro*, LBs are formed by *M. tuberculosis* in response to hypoxia, which is known to bring about a controlled adaptation to growth arrest through regulation by DosR (Park et al., 2003). LBs were also formed in response to NO treatment, and other conditions that are expected to bring about a reduction in growth. Although experiments were preliminary, it was demonstrated that a DosR disrupted mutant was able to form LBs, albeit at a diminished level and that LBs were formed in non-DosR inducing conditions. This suggests that although DosR plays a role in regulating the formation of LBs, it is not the only contributing factor. Expression studies of *dosR* during exposure to LB inducing conditions would resolve what role DosR plays in regulating LB formation. The expression of *tgs1* was shown to be linked with LB formation in *M. smegmatis* and associated with LB formation in *M. tuberculosis* in response to NO exposure. However, in order to show that expression of *tgs1* is inextricably linked with LB formation, a *tgs1* deleted *M. smegmatis* mutant and complemented strain would need to be constructed. LB formation in the mutant should be significantly diminished when compared to the wild type and LB formation should be restored to wild type levels in the complemented strain.

It would be of value to assess the contribution of *tgs1* and LB formation to survival during *in vitro* stresses, such as NO treatment and hypoxia and during infection of mice or macrophages by creating a *tgs1* deleted *M. tuberculosis* mutant strain. If LBs provide an essential source of carbon during a dormancy-like period, it would be expected that long term survival under these conditions would be diminished. Conversely, survival of LB positive populations generated through exposure to LB inducing conditions in comparison to LB negative populations of *M. tuberculosis* could be assessed. If LBs do aid transmission and the establishment of infection, it would be expected that LB positive cells would initiate growth more quickly in macrophages and show enhanced survival.

However, it would be difficult to separate the part that LBs play in survival from other adaptations that may have occurred during exposure to stress.

Reversible growth arrest is thought to form the basis of the antibiotic tolerance displayed by NRP cells adapted to hypoxia (Wayne and Hayes, 1996). The onset of antibiotic tolerance was shown to coincide with LB formation and expression of *tgs1* in *M. tuberculosis* following NO exposure. Although the number of LB positive cells was correlated with the level of antibiotic tolerance displayed by the population as a whole, the nature of the persistent-like population was not resolved. The persister-like cells were not genetic mutants, as sensitivity was restored upon dissipation of the NO. It would seem likely that the basis for the transitory drug tolerance was due to a reduction in growth rate in response to NO exposure, as previously demonstrated by Voskuil et al. (2003) but this still needs to be established. It also remains to be shown whether the tolerant population is characterised by LB positive cells alone. In order to establish absolutely that LBs are markers of antibiotic tolerant cells it would be necessary to demonstrate that antibiotic tolerance in *M. tuberculosis* is inextricably linked with the occurrence of LBs and that one does not exist without the other. The antibiotic tolerance of LB positive *M. tuberculosis* cells generated under a wide range of conditions could be assessed initially; however, it is unlikely that all the LB promoting conditions have been identified. It would be more appropriate to establish the physiology of the LB positive cells. The promoter reporter plasmids constructed in this study could be used or other promoter sequences for cell division reporter genes may show more promise.

It may be possible to separate the LB positive *M. tuberculosis* cells from the LB negative population using fluorescence cell sorting, if the signals from Nile Red or GFP allow differentiation. The antibiotic tolerance of this population alone may then be assessed, along with gene expression for which microarray analysis may be employed. This would produce a whole genome expression pattern that could be compared with gene expression of sputum tubercle bacilli, or *M. tuberculosis* exposed to stress *in vitro*. The presence of LBs may well be advantageous to the cell during the period of growth arrest and upon reactivation of growth but they may not be a requirement for this process.

Of course, LBs in *M. tuberculosis* may form as a result of a number of factors and may not be simply markers of a particular growth rate or cell physiology. Therefore, it must be established whether actively growing *M. tuberculosis* cells can sustain LBs. This is especially important in respect to the chemostat grown cultures of *M. tuberculosis* which were found to form LBs in response to nutrient stress as this finding appears to be somewhat contrary to the hypothesis that LB positive cells are growth arrested. This is dependant on developing a method for examining the growth status of cells. If the use of cell division reporter plasmids proves viable, these may be used to assess the growth rate of cells grown in a chemostat.

The availability of exogenous LCFA may also be crucial in the regulation of LB formation. Preliminary evidence suggests that *M. tuberculosis* forms LBs in the presence of excess Tween (NJ Garton, Personal Communication). It may be that LBs are formed by actively growing cells in which the supply of LCFA exceeds the demands of the cell but must be removed from the environment to avoid toxicity. When this is taken into consideration, it seems more probable that the formation of LBs is actually representative of the balance of available exogenous LCFA and the requirements of the cell. LBs may well be markers of growth arrest, as all biosynthetic processes would be curtailed and LCFA diverted to TAG synthesis. This could be assessed by exposing *M. tuberculosis* to increasing concentrations of LCFA, if the hypothesis is correct, LB formation should be dose dependent. But equally, it would be expected that if growth arrest occurred in the absence of a LCFA source, LBs would not be formed unless *de novo* fatty acid synthesis occurred. *M. tuberculosis* grown in minimal medium could be exposed to LB promoting conditions to assess its ability to form LBs without an exogenous lipid source. Attempts were made to examine this in this study, however due to difficulties in culturing cells the results were inconclusive. The expression of genes involved in fatty acid synthesis would be expected to be higher in cells that are undergoing *de novo* fatty acid synthesis; this could be examined by quantitative real time PCR.

Clearly, given the prevalence of LBs in sputum AFB, definitive demonstration that LBs are markers of antibiotic tolerant cells would have considerable impact on the treatment of disease. Even disregarding a link with drug tolerance, LBs are evidently important for *M. tuberculosis* during infection either as a carbon source, or as a means of detoxifying the environment. There is no evidence as yet to demonstrate that LB positive *M. tuberculosis* bacilli *in vitro* are in the same physiological state as those *in vivo*. While the the underlying mechanism of antibiotic tolerance was not resolved, assessment of the antibiotic tolerance of sputum tubercle bacilli with varying degrees of LB content may provide an insight into the relationship between drug treatment persisters *in vivo* and LBs.

It is possible that the full extent of antibiotic tolerance of LB positive populations of *M. tuberculosis in vitro* was not revealed because cells were in a dormant state and were not culturable on agar. Hu et al. (2000) have shown that long term stationary phase cultures of *M. tuberculosis* are able to grow in liquid culture but do not establish growth on solid media. It was postulated that these represent a dormant subpopulation of cells. These cultures also included a smaller population of cells that were able to grow in both; these may represent a population of survivors from log phase culture. This phenomenon was also observed for *M. tuberculosis* isolated from chronically infected mice but not from those involved in acute infection (Dhillon et al., 2004). Therefore, there may be a greater number of antibiotic tolerant dormant-like cells in the NO exposed cultures of *M. tuberculosis* than originally anticipated. To examine this possibility, the number of cells surviving antibiotic treatment could be measured by plate count and broth counts. The latter is carried out by the most probable number method, in which the presence of growth is assessed in serial broth dilutions. Alternatively the dormant cells could be resuscitated with resuscitation promoting factor (Rpf) (see Introduction). The *Micrococcus luteus* Rpf is a growth promoting factor and has been shown to resuscitate dormant *M. luteus* cells (Mukamolova et al., 1998, Mukamolova et al., 1999).

M. smegmatis largely proved to be an unsuitable host to examine the relationship of LB formation and antibiotic tolerance, due to the current inability to eliminate LBs without introducing further stress. However, there was some evidence to suggest that LB

formation contributed to overall survival following antibiotic treatment. Further work to examine the exact role of the LB in survival could make use of the inducible *tgs1* overexpressing strains that have recently been evaluated in the laboratory. If LBs are important during survival, the proportion of LBs should predict the level of antibiotic tolerance. This could be controlled by altering the concentration of inducer. It would also be of value to transform *M. tuberculosis* with these plasmids and carry out similar experiments.

M. smegmatis did prove to be a model system in which to study LB formation because of the ease at which this organism can be manipulated. LB morphology appears to reflect the composition of the storage lipid in mycobacteria. Lipid extraction of *M. smegmatis* grown in the presence of hexadecanol was unsuccessful and this should be repeated in order to confirm the accumulation of wax ester. The effect of composition of lipid on LB formation and morphology could be examined by incubating *M. smegmatis* with a mixture of hexadecanol and oleic acid in varying proportions. LB formation in mycobacteria seems to be similar to that described in Rhodococcus species (Waltermann and Steinbuchel, 2005). It was not possible to demonstrate conclusively whether LBs are membrane limited or if they are attached to the cell membrane. It may be possible to extract LBs from *M. smegmatis* using a French press and isolate them by centrifugation in glycerol and sucrose density gradients, in the same way that *R. opacus* LBs were isolated. This would allow direct demonstration that mycobacterial LBs are composed of TAG. The associated proteins could also be purified and identified by SDS PAGE analysis (Alverez and Steinbuchel, 2002). This may allow the identification of proteins that are involved in LB formation or lipid utilisation that may have a role during infection.

7.3 Conclusions

The work presented in this thesis has fulfilled the main objective of the study, which was to examine the formation and occurrence of LBs in mycobacteria and has contributed to the understanding of the role of LBs in the physiology of mycobacteria. The specific findings of this report are as follows:

- A survey of clinical specimens collected from tuberculosis patients in Leicester and The Gambia revealed that LBs are a universal feature of AFB in positive sputum specimens.
- A number of conditions were shown to promote LB formation in *M. tuberculosis in vitro*. These included hypoxia, NO exposure, pH shock and heat and cold shock. These conditions were thought to induce transitory growth arrest in *M. tuberculosis*; however, this was not demonstrated.
- LB formation in *M. smegmatis* was shown to contribute to survival of antibiotic exposure; however, the growth condition of the exposed cultures was also thought to play a part. Therefore, the role of LBs in *M. smegmatis* survival was not definitively identified.
- The formation of LBs in *M. tuberculosis* in response to NO treatment was shown to coincide with the development of reversible tolerance to rifampicin and isoniazid. Furthermore, the LB content of NO exposed populations of *M. tuberculosis* was shown to directly correlate with the level of antibiotic tolerance displayed by that population of cells.
- The basis of antibiotic tolerance displayed by LB positive populations of *M. tuberculosis* was hypothesised to be due to a transitory reduction in growth rate. Two fluorescent dyes were evaluated for their ability to differentiate between growing and non-growing cells. The vancomycin BODIPY (vanBODIPY) conjugate labels nascent petidoglycan synthesis and localises to the cell poles of mycobacterial cells. VanBODIPY was shown to label exponentially growing *M. smegmatis* cells more frequently than stationary phase cells; however, overlap between the fluorescence signals of vanBODIPY and Nile Red meant that this method could not be used to

assess the growth status of LB positive cells. The stably inherited dye CFDA/SE distributes equally between daughter cells upon cell division, halving fluorescent intensity. Each generation should be represented by a distinct fluorescent intensity; however, initial labelling of *M. smegmatis* cells was heterogeneous. Therefore, it was impossible to assign reduction of fluorescence intensity to cell division.

- A series of GFP reporter vectors were constructed to report the activity of the promoters of *ftsZ* and *whiB2*, genes involved in cell division and *sigB*, a gene involved in adaptation to stationary phase. *M. smegmatis* and *M. tuberculosis* were transformed with these plasmids; however, no fluorescence was observed in *M. smegmatis* and transformed *M. tuberculosis* failed to grow on subsequent culturing.
- Examination of LBs in *M. smegmatis* and *M. tuberculosis* by TEM revealed that LB morphology reflected the composition of lipid that had previously been shown to be accumulated by the respective cultures. In addition, *M. smegmatis* was shown to form disc-like LBs when cultured in the presence of hexadecanol, which were similar to wax ester LBs previously observed in Acinetobacter. However, lipid extraction of this *M. smegmatis* culture was unsuccessful and therefore, wax ester accumulation was not demonstrated.
- There was some evidence to suggest that LBs in mycobacteria are bound by a unit membrane but this was not demonstrated for all LBs observed by TEM. Attempts to visualise membranes by freeze fracture replication were unsuccessful as the cells did not cleave to reveal intracellular details.
- LBs were shown to be associated with the cell periphery in *M. smegmatis* subjected to low carbon treatment or grown in mimimal medium. Peripheral LBs were not observed in any other growth conditions examined. Peripheral LBs were often associated with an electron transparent thickening at the cell periphery. These structures were morphological similar to those observed in the formation of TAG LBs in *R. opacus*. Therefore, it was hypothesised that LB formation in mycobacteria follows a scheme similar to that suggested for *R. opacus*; however, this requires further evaluation.
- Membranous structures (mesosomes) were observed in LB positive cells and occasionally in association with LBs. These structures were proposed to be involved in LB formation but the role of mesosomes in mycobacteria requires further assessment.

References

AGA, R. G. & HUGHES, M. N. (2008) The preparation and purification of NO gas and the use of NO releasers: the application of NO donors and other agents of nitrosative stress in biological systems. *Methods Enzymol,* 436, 35-48.

ALBERTS, B., BRAY, D., LEWIS, J., RAFF, M., ROBERTS, K. & WATSON, J. D. (1994) *Molecular Biology of The Cell,* New York, Garland Publishing, Inc.

ALVAREZ, H. M., KALSCHEUER, R. & STEINBUCHEL, A. (2000) Accumulation and mobilization of storage lipids by Rhodococcus opacus PD630 and Rhodococcus ruber NCIMB 40126. *Appl Microbiol Biotechnol,* 54, 218-23.

ALVAREZ, H. M., MAYER, F., FABRITIUS, D. & STEINBUCHEL, A. (1996) Formation of intracytoplasmic lipid inclusions by Rhodococcus opacus strain PD630. *Arch Microbiol,* 165, 377-86.

ALVAREZ, H. M. & STEINBUCHEL, A. (2002) Triacylglycerols in prokaryotic microorganisms. *Appl Microbiol Biotechnol,* 60, 367-76.

AMER, A. O. & SWANSON, M. S. (2002) A phagosome of one's own: a microbial guide to life in the macrophage. *Curr Opin Microbiol,* 5, 56-61.

ANDERSON, A. J. & DAWES, E. A. (1990) Occurrence, metabolism, metabolic role, and industrial uses of bacterial polyhydroxyalkanoates. *Microbiol Rev,* 54, 450-72.

ARANAZ, A., COUSINS, D., MATEOS, A. & DOMINGUEZ, L. (2003) Elevation of Mycobacterium tuberculosis subsp. caprae Aranaz et al. 1999 to species rank as Mycobacterium caprae comb. nov., sp. nov. *Int J Syst Evol Microbiol,* 53, 1785-9.

ARCUS, V. L., LOTT, J. S., JOHNSTON, J. M. & BAKER, E. N. (2006) The potential impact of structural genomics on tuberculosis drug discovery. *Drug Discov Today,* 11, 28-34.

AZIZ, M. A., WRIGHT, A., LASZLO, A., DE MUYNCK, A., PORTAELS, F., VAN DEUN, A., WELLS, C., NUNN, P., BLANC, L. & RAVIGLIONE, M. (2006) Epidemiology of antituberculosis drug resistance (the Global Project on Anti-tuberculosis Drug Resistance Surveillance): an updated analysis. *Lancet,* 368, 2142-54.

BACON, J., DOVER, L. G., HATCH, K. A., ZHANG, Y., GOMES, J. M., KENDALL, S., WERNISCH, L., STOKER, N. G., BUTCHER, P. D., BESRA, G. S. & MARSH, P. D. (2007) Lipid composition and transcriptional response of Mycobacterium tuberculosis grown under iron-limitation in continuous culture: identification of a novel wax ester. *Microbiology,* 153, 1435-44.

BACON, J., JAMES, B. W., WERNISCH, L., WILLIAMS, A., MORLEY, K. A., HATCH, G. J., MANGAN, J. A., HINDS, J., STOKER, N. G., BUTCHER, P. D. & MARSH, P. D. (2004) The influence of reduced oxygen availability on pathogenicity and gene expression in Mycobacterium tuberculosis. *Tuberculosis (Edinb),* 84, 205-17.

BALABAN, N. Q., MERRIN, J., CHAIT, R., KOWALIK, L. & LEIBLER, S. (2004) Bacterial persistence as a phenotypic switch. *Science,* 305, 1622-5.

BARER, M. R. (1991) New possibilities for bacterial cytochemistry: light microscopical demonstration of beta-galactosidase in unfixed immobilized bacteria. *Histochem J,* 23, 529-33.

BARKSDALE, L. & KIM, K. S. (1977) Mycobacterium. *Bacteriol Rev,* 41, 217-372.

BETTS, J. C., LUKEY, P. T., ROBB, L. C., MCADAM, R. A. & DUNCAN, K. (2002) Evaluation of a nutrient starvation model of Mycobacterium tuberculosis persistence by gene and protein expression profiling. *Mol Microbiol,* 43, 717-31.

BHATT, A., MOLLE, V., BESRA, G. S., JACOBS, W. R., JR. & KREMER, L. (2007) The Mycobacterium tuberculosis FAS-II condensing enzymes: their role in mycolic acid biosynthesis, acid-fastness, pathogenesis and in future drug development. *Mol Microbiol,* 64, 1442-54.

BIGGER, J. W. (1944) Treatment of staphylococcal infections with penicillin. *Lancet,* 244, 497-500.

BIKETOV, S., MUKAMOLOVA, G. V., POTAPOV, V., GILENKOV, E., VOSTROKNUTOVA, G., KELL, D. B., YOUNG, M. & KAPRELYANTS, A. S. (2000) Culturability of Mycobacterium tuberculosis cells isolated from murine macrophages: a bacterial growth factor promotes recovery. *FEMS Immunol Med Microbiol,* 29, 233-40.

BLOCH, H. & SEGAL, W. (1956) Biochemical differentiation of Mycobacterium tuberculosis grown in vivo and in vitro. *J Bacteriol,* 72, 132-41.

BOSHOFF, H. I. & BARRY, C. E., 3RD (2005) Tuberculosis - metabolism and respiration in the absence of growth. *Nat Rev Microbiol,* 3, 70-80.

BRANDLI, O. (1998) The clinical presentation of tuberculosis. *Respiration,* 65, 97-105.

BRENNAN, P. J. (1988) Mycobacterium and other actinomycetes. IN RATLEDGE, C. & WILKINSON, S. G. (Eds.) *Microbial Lipids.* London, Academic Press Limited.

BRENNAN, P. J. (2003) Structure, function, and biogenesis of the cell wall of Mycobacterium tuberculosis. *Tuberculosis (Edinb),* 83, 91-7.

BRENNAN, P. J. & NIKAIDO, H. (1995) The envelope of mycobacteria. *Annu Rev Biochem,* 64, 29-63.

BRIEGER, E. M. & GLAUERT, A. M. (1956) Electron microscopy of the leprosy bacillus: a study of submicroscopical structure. *Tubercle,* 37, 195-206.

BROSCH, R., GORDON, S. V., MARMIESSE, M., BRODIN, P., BUCHRIESER, C., EIGLMEIER, K., GARNIER, T., GUTIERREZ, C., HEWINSON, G., KREMER, K., PARSONS, L. M., PYM, A. S., SAMPER, S., VAN SOOLINGEN, D. & COLE, S. T. (2002) A new evolutionary scenario for the Mycobacterium tuberculosis complex. *Proc Natl Acad Sci U S A,* 99, 3684-9.

BURDON, K. L. (1946) Fatty Material in Bacteria and Fungi Revealed by Staining Dried, Fixed Slide Preparations. *J Bacteriol,* 52, 665-78.

CASHEL, M. & RUDD, K. E. (1987) The Stringent Response. IN NEIDHARDT, F. C., INGRAHAM, J. L., LOW, K. B., MAGASANIK, B., SCHAECHTER, M. & UMBARGER, H. E. (Eds.) *Escherichia Coli and Salmonella Typhimurium Cellular and Molecular Biology.* Washington, D.C., American Society for Microbiology.

CHAN, E. D., CHAN, J. & SCHLUGER, N. W. (2001) What is the role of nitric oxide in murine and human host defense against tuberculosis?Current knowledge. *Am J Respir Cell Mol Biol,* 25, 606-12.

CHATTERJEE, D. (1997) The mycobacterial cell wall: structure, biosynthesis and sites of drug action. *Curr Opin Chem Biol,* 1, 579-88.

CHEN, P., RUIZ, R. E., LI, Q., SILVER, R. F. & BISHAI, W. R. (2000) Construction and characterization of a Mycobacterium tuberculosis mutant lacking the alternate sigma factor gene, sigF. *Infect Immun,* 68, 5575-80.

CHRISTENSEN, H., GARTON, N. J., HOROBIN, R. W., MINNIKIN, D. E. & BARER, M. R. (1999) Lipid domains of mycobacteria studied with fluorescent molecular probes. *Mol Microbiol,* 31, 1561-72.

COLE, S. T. (2002) Comparative and functional genomics of the Mycobacterium tuberculosis complex. *Microbiology,* 148, 2919-28.

COLE, S. T., BROSCH, R., PARKHILL, J., GARNIER, T., CHURCHER, C., HARRIS, D., GORDON, S. V., EIGLMEIER, K., GAS, S., BARRY, C. E., 3RD, TEKAIA, F., BADCOCK, K., BASHAM, D., BROWN, D., CHILLINGWORTH, T., CONNOR, R., DAVIES, R., DEVLIN, K., FELTWELL, T., GENTLES, S., HAMLIN, N., HOLROYD, S., HORNSBY, T., JAGELS, K., KROGH, A., MCLEAN, J., MOULE, S., MURPHY, L., OLIVER, K., OSBORNE, J., QUAIL, M. A., RAJANDREAM, M. A., ROGERS, J., RUTTER, S., SEEGER, K., SKELTON, J., SQUARES, R., SQUARES, S., SULSTON, J. E., TAYLOR, K., WHITEHEAD, S. & BARRELL, B. G. (1998) Deciphering the biology of Mycobacterium tuberculosis from the complete genome sequence. *Nature,* 393, 537-44.

COONEY, R. P. (2000) Cellular responses of *Mycobacterium tuberculosis* to antimycobacterial agents. *School of Cell and Molecular Biosciences.* Newcastle upon Tyne, University of Newcastle.

CORBETT, E. L., WATT, C. J., WALKER, N., MAHER, D., WILLIAMS, B. G., RAVIGLIONE, M. C. & DYE, C. (2003) The growing burden of tuberculosis: global trends and interactions with the HIV epidemic. *Arch Intern Med,* 163, 1009-21.

COSMA, C. L., SHERMAN, D. R. & RAMAKRISHNAN, L. (2003) The secret lives of the pathogenic mycobacteria. *Annu Rev Microbiol,* 57, 641-76.

COUSINS, D. V., BASTIDA, R., CATALDI, A., QUSE, V., REDROBE, S., DOW, S., DUIGNAN, P., MURRAY, A., DUPONT, C., AHMED, N., COLLINS, D. M., BUTLER, W. R., DAWSON, D., RODRIGUEZ, D., LOUREIRO, J., ROMANO, M. I., ALITO, A., ZUMARRAGA, M. & BERNARDELLI, A. (2003) Tuberculosis in seals caused by a novel member of the Mycobacterium tuberculosis complex: Mycobacterium pinnipedii sp. nov. *Int J Syst Evol Microbiol,* 53, 1305-14.

CUNNINGHAM, A. F. & SPREADBURY, C. L. (1998) Mycobacterial stationary phase induced by low oxygen tension: cell wall thickening and localization of the 16-kilodalton alpha-crystallin homolog. *J Bacteriol,* 180, 801-8.

DAFFE, M. & DRAPER, P. (1998) The envelope layers of mycobacteria with reference to their pathogenicity. *Adv Microb Physiol,* 39, 131-203.

DAHL, J. L., KRAUS, C. N., BOSHOFF, H. I., DOAN, B., FOLEY, K., AVARBOCK, D., KAPLAN, G., MIZRAHI, V., RUBIN, H. & BARRY, C. E., 3RD (2003) The role of RelMtb-mediated adaptation to stationary phase in long-term persistence of Mycobacterium tuberculosis in mice. *Proc Natl Acad Sci U S A,* 100, 10026-31.

DANIEL, J., DEB, C., DUBEY, V. S., SIRAKOVA, T. D., ABOMOELAK, B., MORBIDONI, H. R. & KOLATTUKUDY, P. E. (2004) Induction of a novel class of diacylglycerol acyltransferases and triacylglycerol accumulation in Mycobacterium tuberculosis as it goes into a dormancy-like state in culture. *J Bacteriol,* 186, 5017-30.

DANIEL, R. A. & ERRINGTON, J. (2003) Control of cell morphogenesis in bacteria: two distinct ways to make a rod-shaped cell. *Cell,* 113, 767-76.

DE JONG, B. C., HILL, P. C., AIKEN, A., JEFFRIES, D. J., ONIPEDE, A., SMALL, P. M., ADEGBOLA, R. A. & CORRAH, T. P. (2007) Clinical presentation and outcome of tuberculosis patients infected by M. africanum versus M. tuberculosis. *Int J Tuberc Lung Dis,* 11, 450-6.

DEB, C., DANIEL, J., SIRAKOVA, T. D., ABOMOELAK, B., DUBEY, V. S. & KOLATTUKUDY, P. E. (2006) A novel lipase belonging to the hormone-sensitive lipase family induced under starvation to utilize stored triacylglycerol in Mycobacterium tuberculosis. *J Biol Chem,* 281, 3866-75.

DHILLON, J., LOWRIE, D. B. & MITCHISON, D. A. (2004) Mycobacterium tuberculosis from chronic murine infections that grows in liquid but not on solid medium. *BMC Infect Dis,* 4, 51.

DOUKHAN, L., PREDICH, M., NAIR, G., DUSSURGET, O., MANDIC-MULEC, I., COLE, S. T., SMITH, D. R. & SMITH, I. (1995) Genomic organization of the mycobacterial sigma gene cluster. *Gene,* 165, 67-70.

DOWNING, K. J., BETTS, J. C., YOUNG, D. I., MCADAM, R. A., KELLY, F., YOUNG, M. & MIZRAHI, V. (2004) Global expression profiling of strains harbouring null mutations reveals that the five rpf-like genes of Mycobacterium tuberculosis show functional redundancy. *Tuberculosis (Edinb),* 84, 167-79.

DU TOIT, L. C., PILLAY, V. & DANCKWERTS, M. P. (2006) Tuberculosis chemotherapy: current drug delivery approaches. *Respir Res,* 7, 118.

DUNLOP, W. F. & ROBARDS, A. W. (1973) Ultrastructural study of poly- -hydroxybutyrate granules from Bacillus cereus. *J Bacteriol,* 114, 1271-80.

DYE, C. (2006) Global epidemiology of tuberculosis. *Lancet,* 367, 938-40.

DYE, C., FLOYD, K. & UPLEKER, M. (2008) Global tuberculosis control: surveillance, planning, financing: WHO report 2008. Geneva, World Health Organization.

DYE, C., SCHEELE, S., DOLIN, P., PATHANIA, V. & RAVIGLIONE, M. C. (1999) Consensus statement. Global burden of tuberculosis: estimated incidence, prevalence, and mortality by country. WHO Global Surveillance and Monitoring Project. *Jama,* 282, 677-86.

DZIADEK, J., RUTHERFORD, S. A., MADIRAJU, M. V., ATKINSON, M. A. & RAJAGOPALAN, M. (2003) Conditional expression of Mycobacterium smegmatis ftsZ, an essential cell division gene. *Microbiology,* 149, 1593-603.

EBERSOLD, H. R., CORDIER, J. L. & LUTHY, P. (1981) Bacterial mesosomes: method dependent artifacts. *Arch Microbiol,* 130, 19-22.

ELBEIN, A. D., PAN, Y. T., PASTUSZAK, I. & CARROLL, D. (2003) New insights on trehalose: a multifunctional molecule. *Glycobiology,* 13, 17R-27R.

ESPINAL, M. A. (2003) The global situation of MDR-TB. *Tuberculosis (Edinb),* 83, 44-51.

FANG, F. C., LIBBY, S. J., CASTOR, M. E. & FUNG, A. M. (2005) Isocitrate lyase (AceA) is required for Salmonella persistence but not for acute lethal infection in mice. *Infect Immun,* 73, 2547-9.

FELDMAN, W. H. & BAGGENSTOSS, A. H. (1939) The occurrence of virulent tubercle bacilli in presumably non-tuberculous lung tissue. *American Journal of Pathology,* 15, 501-15.

FENHALLS, G., STEVENS-MULLER, L., WARREN, R., CARROLL, N., BEZUIDENHOUT, J., VAN HELDEN, P. & BARDIN, P. (2002) Localisation of mycobacterial DNA and mRNA in human tuberculous granulomas. *J Microbiol Methods,* 51, 197-208.

FEUCHT, A. & ERRINGTON, J. (2005) ftsZ mutations affecting cell division frequency, placement and morphology in Bacillus subtilis. *Microbiology,* 151, 2053-64.

FISHER, M. A., PLIKAYTIS, B. B. & SHINNICK, T. M. (2002) Microarray analysis of the Mycobacterium tuberculosis transcriptional response to the acidic conditions found in phagosomes. *J Bacteriol,* 184, 4025-32.

FLEISCHMANN, R. D., ALLAND, D., EISEN, J. A., CARPENTER, L., WHITE, O., PETERSON, J., DEBOY, R., DODSON, R., GWINN, M., HAFT, D., HICKEY, E., KOLONAY, J. F., NELSON, W. C., UMAYAM, L. A., ERMOLAEVA, M., SALZBERG, S. L., DELCHER, A., UTTERBACK, T., WEIDMAN, J., KHOURI, H., GILL, J., MIKULA, A., BISHAI, W., JACOBS JR, W. R., JR., VENTER, J. C. & FRASER, C. M. (2002) Whole-genome comparison of Mycobacterium tuberculosis clinical and laboratory strains. *J Bacteriol,* 184, 5479-90.

FLYNN, J. L., SCANGA, C. A., TANAKA, K. E. & CHAN, J. (1998) Effects of aminoguanidine on latent murine tuberculosis. *J Immunol,* 160, 1796-803.

FRIEDEN, T. R., STERLING, T. R., MUNSIFF, S. S., WATT, C. J. & DYE, C. (2003) Tuberculosis. *Lancet,* 362, 887-99.

FRIEDRICH, C. L., MOYLES, D., BEVERIDGE, T. J. & HANCOCK, R. E. (2000) Antibacterial action of structurally diverse cationic peptides on gram-positive bacteria. *Antimicrob Agents Chemother,* 44, 2086-92.

GALE, G. R. & MCLAIN, H. H. (1963) Effect of Ethambutol on Cytology of Mycobacterium Smegmatis. *J Bacteriol,* 86, 749-56.

GANDHI, N. R., MOLL, A., STURM, A. W., PAWINSKI, R., GOVENDER, T., LALLOO, U., ZELLER, K., ANDREWS, J. & FRIEDLAND, G. (2006) Extensively drug-resistant tuberculosis as a cause of death in patients co-infected with tuberculosis and HIV in a rural area of South Africa. *Lancet,* 368, 1575-80.

GARTON, N. J., CHRISTENSEN, H., MINNIKIN, D. E., ADEGBOLA, R. A. & BARER, M. R. (2002) Intracellular lipophilic inclusions of mycobacteria in vitro and in sputum. *Microbiology,* 148, 2951-8.

GARTON, N. J., WADDELL, S. J., SHERRATT, A. L., LEE, S. M., SMITH, R. J., SENNER, C., HINDS, J., RAJAKUMAR, K., ADEGBOLA, R. A., BESRA, G. S., BUTCHER, P. D. & BARER, M. R. (2008) Cytological and transcript analyses reveal fat and lazy persister-like bacilli in tuberculous sputum. *PLoS Med,* 5, e75.

GEIMAN, D. E., KAUSHAL, D., KO, C., TYAGI, S., MANABE, Y. C., SCHROEDER, B. G., FLEISCHMANN, R. D., MORRISON, N. E., CONVERSE, P. J., CHEN, P. & BISHAI, W. R. (2004) Attenuation of late-stage disease in mice infected by the Mycobacterium tuberculosis mutant lacking the SigF alternate sigma factor and identification of SigF-dependent genes by microarray analysis. *Infect Immun,* 72, 1733-45.

GERDES, K., CHRISTENSEN, S. K. & LOBNER-OLESEN, A. (2005) Prokaryotic toxin-antitoxin stress response loci. *Nat Rev Microbiol,* 3, 371-82.

GLAUERT, A. M. (1975) *Fixation, Dehydration and Embedding of Biological Specimens,* Amsterdam, North-Holland Publishing Company, American Elsevier Publishing Company.

GOMEZ, J. E. & BISHAI, W. R. (2000) whmD is an essential mycobacterial gene required for proper septation and cell division. *Proc Natl Acad Sci U S A,* 97, 8554-9.

GOMEZ, J. E., CHEN, J. M. & BISHAI, W. R. (1997) Sigma factors of Mycobacterium tuberculosis. *Tuber Lung Dis,* 78, 175-83.

GOMEZ, J. E. & MCKINNEY, J. D. (2004) M. tuberculosis persistence, latency, and drug tolerance. *Tuberculosis (Edinb),* 84, 29-44.

GOODFELLOW, M. & MINNIKIN, D. E. (1980) Definition of the genus *Mycobacterium vis a vis* other allied taxa. IN KUBICA, G. P., WAYNE, L. G. & GOOD, R. C. (Eds.) *1954-1979: Twenty-Five Years of Mycobacterial Taxonomy.* Atlanta, United States Department of Health, Education and Welfare, Center for Disease Control.

GREENAWALT, J. W. & WHITESIDE, T. L. (1975) Mesosomes: membranous bacterial organelles. *Bacteriol Rev,* 39, 405-63.

GURR, M. I. & JAMES, A. T. (1975) *Lipid Biochemistry: An Introduction,* London, Chapman and Hall.

HAMPSHIRE, T., SONEJI, S., BACON, J., JAMES, B. W., HINDS, J., LAING, K., STABLER, R. A., MARSH, P. D. & BUTCHER, P. D. (2004) Stationary phase gene expression of Mycobacterium tuberculosis following a progressive nutrient depletion: a model for persistent organisms? *Tuberculosis (Edinb),* 84, 228-38.

HERNANDEZ-PANDO, R., JEYANATHAN, M., MENGISTU, G., AGUILAR, D., OROZCO, H., HARBOE, M., ROOK, G. A. & BJUNE, G. (2000) Persistence of DNA from Mycobacterium tuberculosis in superficially normal lung tissue during latent infection. *Lancet,* 356, 2133-8.

HETT, E. C., CHAO, M. C., DENG, L. L. & RUBIN, E. J. (2008) A mycobacterial enzyme essential for cell division synergizes with resuscitation-promoting factor. *PLoS Pathog,* 4, e1000001.

HETT, E. C., CHAO, M. C., STEYN, A. J., FORTUNE, S. M., DENG, L. L. & RUBIN, E. J. (2007) A partner for the resuscitation-promoting factors of Mycobacterium tuberculosis. *Mol Microbiol,* 66, 658-68.

HIGGINS, M. L. & DANEO-MOORE, L. (1972) Morphokinetic reaction of cells of Streptococcus faecalis (ATCC 9790) to specific inhibition of macromolecular synthesis: dependence of mesosome growth on deoxyribonucleic acid synthesis. *J Bacteriol,* 109, 1221-31.

HIGGINS, M. L., TSIEN, H. C. & DANEO-MOORE, L. (1976) Organization of mesosomes in fixed and unfixed cells. *J Bacteriol,* 127, 1519-23.

HONER ZU BENTRUP, K. & RUSSELL, D. G. (2001) Mycobacterial persistence: adaptation to a changing environment. *Trends Microbiol,* 9, 597-605.

HOPEWELL, P. C. (1994) Overview of Clinical Tuberculosis. IN BLOOM, B. R. (Ed.) *Tuberculosis: Pathogenesis, Protection, and Control.* Washington, D.C., ASM Press.

HOWARD, S. T. & BYRD, T. F. (2000) The rapidly growing mycobacteria: saprophytes and parasites. *Microbes Infect,* 2, 1845-53.

HU, Y. & COATES, A. R. (1999) Transcription of two sigma 70 homologue genes, sigA and sigB, in stationary-phase Mycobacterium tuberculosis. *J Bacteriol,* 181, 469-76.

HU, Y., MANGAN, J. A., DHILLON, J., SOLE, K. M., MITCHISON, D. A., BUTCHER, P. D. & COATES, A. R. (2000) Detection of mRNA transcripts and active transcription in persistent Mycobacterium tuberculosis induced by exposure to rifampin or pyrazinamide. *J Bacteriol,* 182, 6358-65.

HU, Y., MOVAHEDZADEH, F., STOKER, N. G. & COATES, A. R. (2006) Deletion of the Mycobacterium tuberculosis alpha-crystallin-like hspX gene causes increased bacterial growth in vivo. *Infect Immun,* 74, 861-8.

HU, Y. M., BUTCHER, P. D., SOLE, K., MITCHISON, D. A. & COATES, A. R. (1998) Protein synthesis is shutdown in dormant Mycobacterium tuberculosis and is reversed by oxygen or heat shock. *FEMS Microbiol Lett,* 158, 139-45.

ISHIGE, T., TANI, A., TAKABE, K., KAWASAKI, K., SAKAI, Y. & KATO, N. (2002) Wax ester production from n-alkanes by Acinetobacter sp. strain M-1: ultrastructure of cellular inclusions and role of acyl coenzyme A reductase. *Appl Environ Microbiol,* 68, 1192-5.

JACKSON, S. K., STARK, J. M., TAYLOR, S. & HARWOOD, J. L. (1989) Changes in phospholipid fatty acid composition and triacylglycerol content in mouse tissues after infection with bacille Calmette-Guerin. *Br J Exp Pathol,* 70, 435-41.

JARLIER, V. & NIKAIDO, H. (1994) Mycobacterial cell wall: structure and role in natural resistance to antibiotics. *FEMS Microbiol Lett,* 123, 11-8.

KALSCHEUER, R. & STEINBUCHEL, A. (2003) A novel bifunctional wax ester synthase/acyl-CoA:diacylglycerol acyltransferase mediates wax ester and triacylglycerol biosynthesis in Acinetobacter calcoaceticus ADP1. *J Biol Chem,* 278, 8075-82.

KALSCHEUER, R., WALTERMANN, M., ALVAREZ, M. & STEINBUCHEL, A. (2001) Preparative isolation of lipid inclusions from Rhodococcus opacus and Rhodococcus ruber and identification of granule-associated proteins. *Arch Microbiol,* 177, 20-8.

KANA, B. D., GORDHAN, B. G., DOWNING, K. J., SUNG, N., VOSTROKTUNOVA, G., MACHOWSKI, E. E., TSENOVA, L., YOUNG, M., KAPRELYANTS, A., KAPLAN, G. & MIZRAHI, V. (2008) The resuscitation-promoting factors of Mycobacterium tuberculosis are required for virulence and resuscitation from dormancy but are collectively dispensable for growth in vitro. *Mol Microbiol,* 67, 672-84.

KAPLAN, G., POST, F. A., MOREIRA, A. L., WAINWRIGHT, H., KREISWIRTH, B. N., TANVERDI, M., MATHEMA, B., RAMASWAMY, S. V., WALTHER, G., STEYN, L. M., BARRY, C. E., 3RD & BEKKER, L. G. (2003) Mycobacterium tuberculosis growth at the cavity surface: a microenvironment with failed immunity. *Infect Immun,* 71, 7099-108.

KAPRELYANTS, A. S. & KELL, D. B. (1993) Dormancy in Stationary-Phase Cultures of Micrococcus luteus: Flow Cytometric Analysis of Starvation and Resuscitation. *Appl Environ Microbiol,* 59, 3187-3196.

KARAKOUSIS, P. C., YOSHIMATSU, T., LAMICHHANE, G., WOOLWINE, S. C., NUERMBERGER, E. L., GROSSET, J. & BISHAI, W. R. (2004) Dormancy phenotype displayed by extracellular Mycobacterium tuberculosis within artificial granulomas in mice. *J Exp Med,* 200, 647-57.

KEEP, N. H., WARD, J. M., COHEN-GONSAUD, M. & HENDERSON, B. (2006) Wake up! Peptidoglycan lysis and bacterial non-growth states. *Trends Microbiol,* 14, 271-6.

KENDALL, S. L., MOVAHEDZADEH, F., RISON, S. C., WERNISCH, L., PARISH, T., DUNCAN, K., BETTS, J. C. & STOKER, N. G. (2004) The Mycobacterium tuberculosis dosRS two-component system is induced by multiple stresses. *Tuberculosis (Edinb),* 84, 247-55.

KEREN, I., KALDALU, N., SPOERING, A., WANG, Y. & LEWIS, K. (2004) Persister cells and tolerance to antimicrobials. *FEMS Microbiol Lett,* 230, 13-8.

KHOMENKO, A. G. (1987) The variability of Mycobacterium tuberculosis in patients with cavitary pulmonary tuberculosis in the course of chemotherapy. *Tubercle,* 68, 243-53.

KIM, K. S., SALTON, M. R. & BARKSDALE, L. (1976) Ultrastructure of superficial mycosidic integuments of Mycobacterium sp. *J Bacteriol,* 125, 739-43.

KNAYSI, G., HILLIER, J. & FABRICANT, C. (1950) The cytology of an avian strain of Mycobacterium tuberculosis studied with the electron and light microscopes. *J Bacteriol,* 60, 423-47.

KONDO, E. & KANAI, K. (1972) The lethal effect of long-chain fatty acids on mycobacteria. *Jpn J Med Sci Biol,* 25, 1-13.

KUSSELL, E., KISHONY, R., BALABAN, N. Q. & LEIBLER, S. (2005) Bacterial persistence: a model of survival in changing environments. *Genetics,* 169, 1807-14.

LEE, S. M. (2007) Studies on Mycobacterial Lipid Bodies on Patients with Tuberculosis in The Gambia. *Department of Infection, Immunity and Inflammation.* Leicester, University of Leicester.

LEE, Y. K., HO, P. S., LOW, C. S., ARVILOMMI, H. & SALMINEN, S. (2004) Permanent colonization by Lactobacillus casei is hindered by the low rate of cell division in mouse gut. *Appl Environ Microbiol,* 70, 670-4.

LEWIS, K. (2007) Persister cells, dormancy and infectious disease. *Nat Rev Microbiol,* 5, 48-56.

LEWIS, P. R. & KNIGHT, D. P. (1980) *Staining Methods for Sectioned Material,* Amsterdam, North-Holland Publishing Company.

LOEBEL, R. O., SHORR, E. & RICHARDSON, H. B. (1933) The Influence of Adverse Conditions upon the Respiratory Metabolism and Growth of Human Tubercle Bacilli. *J Bacteriol,* 26, 167-200.

LOUNATMAA, K. & BRANDER, E. (1989) Crystalline cell surface layer of Mycobacterium bovis BCG. *J Bacteriol,* 171, 5756-8.

LOWE, J. & AMOS, L. A. (1999) Tubulin-like protofilaments in Ca2+-induced FtsZ sheets. *Embo J,* 18, 2364-71.

MAARTENS, G. & WILKINSON, R. J. (2007) Tuberculosis. *Lancet,* 370, 2030-43.

MACMICKING, J. D., NORTH, R. J., LACOURSE, R., MUDGETT, J. S., SHAH, S. K. & NATHAN, C. F. (1997) Identification of nitric oxide synthase as a protective locus against tuberculosis. *Proc Natl Acad Sci U S A,* 94, 5243-8.

MAILLOUX, B. J. & FULLER, M. E. (2003) Determination of in situ bacterial growth rates in aquifers and aquifer sediments. *Appl Environ Microbiol,* 69, 3798-808.

MALHOTRA, V., SHARMA, D., RAMANATHAN, V. D., SHAKILA, H., SAINI, D. K., CHAKRAVORTY, S., DAS, T. K., LI, Q., SILVER, R. F., NARAYANAN, P. R. & TYAGI, J. S. (2004) Disruption of response regulator gene, devR, leads to attenuation in virulence of Mycobacterium tuberculosis. *FEMS Microbiol Lett,* 231, 237-45.

MANGANELLI, R., DUBNAU, E., TYAGI, S., KRAMER, F. R. & SMITH, I. (1999) Differential expression of 10 sigma factor genes in Mycobacterium tuberculosis. *Mol Microbiol,* 31, 715-24.

MANGANELLI, R., VOSKUIL, M. I., SCHOOLNIK, G. K., DUBNAU, E., GOMEZ, M. & SMITH, I. (2002) Role of the extracytoplasmic-function sigma factor sigma(H) in Mycobacterium tuberculosis global gene expression. *Mol Microbiol,* 45, 365-74.

MARTIN, E., DAVIS, K., BIAN, K., LEE, Y. C. & MURAD, F. (2000) Cellular signaling with nitric oxide and cyclic guanosine monophosphate. *Semin Perinatol,* 24, 2-6.

MATHEW, R., OHJA, A. K., KARANDE, A. A. & CHATTERJI, D. (2004) Deletion of the *rel* gene in *Mycobacterium smegmatis* reduces its stationary phase survival without altering the cell-surface associated properties. *Current Science,* 86, 149-53.

MCCARTHY, C. (1971) Utilization of palmitic acid by Mycobacterium avium. *Infect Immun,* 4, 199-204.

MCKINNEY, J. D. (2000) In vivo veritas: the search for TB drug targets goes live. *Nat Med,* 6, 1330-3.

MCKINNEY, J. D. & GOMEZ, J. E. (2003) Life on the inside for Mycobacterium tuberculosis. *Nat Med,* 9, 1356-7.

MCKINNEY, J. D., HONER ZU BENTRUP, K., MUNOZ-ELIAS, E. J., MICZAK, A., CHEN, B., CHAN, W. T., SWENSON, D., SACCHETTINI, J. C., JACOBS, W. R., JR. & RUSSELL, D. G. (2000) Persistence of Mycobacterium tuberculosis in macrophages and mice requires the glyoxylate shunt enzyme isocitrate lyase. *Nature,* 406, 735-8.

MICHELE, T. M., KO, C. & BISHAI, W. R. (1999) Exposure to antibiotics induces expression of the Mycobacterium tuberculosis sigF gene: implications for chemotherapy against mycobacterial persistors. *Antimicrob Agents Chemother,* 43, 218-25.

MINNIKIN, D. E. (1982) Lipids: complex lipids, their chemistry, biosynthesis and roles. IN RATLEDGE, C. & STANFORD, J. L. (Eds.) *The Biology of the Mycobacteria.* London, Academic Press Limited.

MINNIKIN, D. E., KREMER, L., DOVER, L. G. & BESRA, G. S. (2002) The methyl-branched fortifications of Mycobacterium tuberculosis. *Chem Biol,* 9, 545-53.

MITCHISON, D. A. (1979) Basic mechanisms of chemotherapy. *Chest,* 76, 771-81.

MITCHISON, D. A. (2004) The search for new sterilizing anti-tuberculosis drugs. *Front Biosci,* 9, 1059-72.

MITCHISON, D. A. (2005) The diagnosis and therapy of tuberculosis during the past 100 years. *Am J Respir Crit Care Med,* 171, 699-706.

MORITA, Y. S., VELASQUEZ, R., TAIG, E., WALLER, R. F., PATTERSON, J. H., TULL, D., WILLIAMS, S. J., BILLMAN-JACOBE, H. & MCCONVILLE, M. J. (2005) Compartmentalization of lipid biosynthesis in mycobacteria. *J Biol Chem,* 280, 21645-52.

MUELLER, P. & PIETERS, J. (2006) Modulation of macrophage antimicrobial mechanisms by pathogenic mycobacteria. *Immunobiology,* 211, 549-56.

MUKAMOLOVA, G. V., KAPRELYANTS, A. S., YOUNG, D. I., YOUNG, M. & KELL, D. B. (1998) A bacterial cytokine. *Proc Natl Acad Sci U S A,* 95, 8916-21.

MUKAMOLOVA, G. V., KORMER, S. S., KELL, D. B. & KAPRELYANTS, A. S. (1999) Stimulation of the multiplication of Micrococcus luteus by an autocrine growth factor. *Arch Microbiol,* 172, 9-14.

MUKAMOLOVA, G. V., TURAPOV, O. A., YOUNG, D. I., KAPRELYANTS, A. S., KELL, D. B. & YOUNG, M. (2002) A family of autocrine growth factors in Mycobacterium tuberculosis. *Mol Microbiol,* 46, 623-35.

MUNOZ-ELIAS, E. J. & MCKINNEY, J. D. (2005) Mycobacterium tuberculosis isocitrate lyases 1 and 2 are jointly required for in vivo growth and virulence. *Nat Med,* 11, 638-44.

MUNOZ-ELIAS, E. J. & MCKINNEY, J. D. (2006) Carbon metabolism of intracellular bacteria. *Cell Microbiol,* 8, 10-22.

MUTTUCUMARU, D. G., ROBERTS, G., HINDS, J., STABLER, R. A. & PARISH, T. (2004) Gene expression profile of Mycobacterium tuberculosis in a non-replicating state. *Tuberculosis (Edinb),* 84, 239-46.

NEYROLLES, O., HERNANDEZ-PANDO, R., PIETRI-ROUXEL, F., FORNES, P., TAILLEUX, L., BARRIOS PAYAN, J. A., PIVERT, E., BORDAT, Y., AGUILAR, D., PREVOST, M. C., PETIT, C. & GICQUEL, B. (2006) Is adipose tissue a place for Mycobacterium tuberculosis persistence? *PLoS ONE,* 1, e43.

NGUYEN, H. T., TRACH, D. D., MAN, N. V., NGOAN, T. H., DUNIA, I., LUDOSKY-DIAWARA, M. A. & BENEDETTI, E. L. (1979) Comparative ultrastructure of Mycobacterium leprae and Mycobacterium lepraemurium cell envelopes. *J Bacteriol,* 138, 552-8.

NOZAKI, Y., HASEGAWA, Y., ICHIYAMA, S., NAKASHIMA, I. & SHIMOKATA, K. (1997) Mechanism of nitric oxide-dependent killing of Mycobacterium bovis BCG in human alveolar macrophages. *Infect Immun,* 65, 3644-7.

OHNO, H., ZHU, G., MOHAN, V. P., CHU, D., KOHNO, S., JACOBS, W. R., JR. & CHAN, J. (2003) The effects of reactive nitrogen intermediates on gene expression in Mycobacterium tuberculosis. *Cell Microbiol,* 5, 637-48.

OJHA, A. K., MUKHERJEE, T. K. & CHATTERJI, D. (2000) High intracellular level of guanosine tetraphosphate in Mycobacterium smegmatis changes the morphology of the bacterium. *Infect Immun,* 68, 4084-91.

OLUKOSHI, E. R. & PACKTER, N. M. (1994) Importance of stored triacylglycerols in Streptomyces: possible carbon source for antibiotics. *Microbiology,* 140 (Pt 4), 931-43.

OPIE, E. L. & ARONSON, J. D. (1927) Tubercle bacilli in latent tuberculous lesions and in lung tissue without tuberculous lesions. *Archives in Pathology,* 4, 1-21.

ORMEROD, L. P. (2005) Multidrug-resistant tuberculosis (MDR-TB): epidemiology, prevention and treatment. *Br Med Bull,* 73-74, 17-24.

PACKTER, N. M. & OLUKOSHI, E. R. (1995) Ultrastructural studies of neutral lipid localisation in Streptomyces. *Arch Microbiol,* 164, 420-7.

PARISH, T., SMITH, D. A., KENDALL, S., CASALI, N., BANCROFT, G. J. & STOCKER, N. G. (2003) Deletion of Two-Component Regulatory Systems Increases the Virulence of *Mycobacterium tuberculosis. Infection and Immunity,* 71, 1134-40.

PARK, H. D., GUINN, K. M., HARRELL, M. I., LIAO, R., VOSKUIL, M. I., TOMPA, M., SCHOOLNIK, G. K. & SHERMAN, D. R. (2003) Rv3133c/dosR is a transcription factor that mediates the hypoxic response of Mycobacterium tuberculosis. *Mol Microbiol,* 48, 833-43.

PARRISH, N. M., DICK, J. D. & BISHAI, W. R. (1998) Mechanisms of latency in Mycobacterium tuberculosis. *Trends Microbiol,* 6, 107-12.

PAUL, T. R. & BEVERIDGE, T. J. (1992) Reevaluation of envelope profiles and cytoplasmic ultrastructure of mycobacteria processed by conventional embedding and freeze-substitution protocols. *J Bacteriol,* 174, 6508-17.

PHEIFFER, C., BETTS, J. C., FLYNN, H. R., LUKEY, P. T. & VAN HELDEN, P. (2005) Protein expression by a Beijing strain differs from that of another clinical isolate and Mycobacterium tuberculosis H37Rv. *Microbiology,* 151, 1139-50.

PRIMM, T. P., ANDERSEN, S. J., MIZRAHI, V., AVARBOCK, D., RUBIN, H. & BARRY, C. E., 3RD (2000) The stringent response of Mycobacterium tuberculosis is required for long-term survival. *J Bacteriol,* 182, 4889-98.

QUAST, T. M. & BROWNING, R. F. (2006) Pathogenesis and clinical manifestations of pulmonary tuberculosis. *Dis Mon,* 52, 413-9.

RACHMAN, H., LEE, J. S., ANGERMANN, J., KOWALL, J. & KAUFMANN, S. H. (2006) Reliable amplification method for bacterial RNA. *J Biotechnol,* 126, 61-8.

RAGHUNAND, T. R. & BISHAI, W. R. (2006a) Mapping essential domains of Mycobacterium smegmatis WhmD: insights into WhiB structure and function. *J Bacteriol,* 188, 6966-76.

RAGHUNAND, T. R. & BISHAI, W. R. (2006b) Mycobacterium smegmatis whmD and its homologue Mycobacterium tuberculosis whiB2 are functionally equivalent. *Microbiology,* 152, 2735-47.

RAJAKUMAR, K., SHAFI, J., SMITH, R. J., STABLER, R. A., ANDREW, P. W., MODHA, D., BRYANT, G., MONK, P., HINDS, J., BUTCHER, P. D. & BARER, M. R. (2004) Use of genome level-informed PCR as a new investigational approach for analysis of outbreak-associated Mycobacterium tuberculosis isolates. *J Clin Microbiol,* 42, 1890-6.

RATLEDGE, C. & WILKINSON, S. G. (1988) Fatty acids, related and derived lipids. IN RATLEDGE, C. (Ed.) *Microbial Lipids.* Washington, D.C, Academic Press Limited.

REED, M. B., GAGNEUX, S., DERIEMER, K., SMALL, P. M. & BARRY, C. E., 3RD (2007) The W-Beijing lineage of Mycobacterium tuberculosis overproduces triglycerides and has the DosR dormancy regulon constitutively upregulated. *J Bacteriol,* 189, 2583-9.

REID, N. (1975) *Ultramicrotomy,* Amsterdam, North-Holland Publishing Company.

RHOADES, E. R. & ORME, I. M. (1997) Susceptibility of a panel of virulent strains of Mycobacterium tuberculosis to reactive nitrogen intermediates. *Infect Immun,* 65, 1189-95.

RICH, E. A., TORRES, M., SADA, E., FINEGAN, C. K., HAMILTON, B. D. & TOOSSI, Z. (1997) Mycobacterium tuberculosis (MTB)-stimulated production of nitric oxide by human alveolar macrophages and relationship of nitric oxide production to growth inhibition of MTB. *Tuber Lung Dis,* 78, 247-55.

ROLLINSON, S. (2003) Physiological activities and expression of *Mycobacterium tuberculosis rpf* homologues. *School of Cell and Molecular Biosciences.* Newcastlen upon Tyne, University of Newcastle.

ROY, S. & AJITKUMAR, P. (2005) Transcriptional analysis of the principal cell division gene, ftsZ, of Mycobacterium tuberculosis. *J Bacteriol,* 187, 2540-50.

RUSSELL, D. G. (2001) Mycobacterium tuberculosis: here today, and here tomorrow. *Nat Rev Mol Cell Biol,* 2, 569-77.

RUSSELL, D. G. (2007) Who puts the tubercle in tuberculosis? *Nat Rev Microbiol,* 5, 39-47.

RUSSELL, D. G., MWANDUMBA, H. C. & RHOADES, E. E. (2002) Mycobacterium and the coat of many lipids. *J Cell Biol,* 158, 421-6.

RUSTAD, T. R., HARRELL, M. I., LIAO, R. & SHERMAN, D. R. (2008) The enduring hypoxic response of Mycobacterium tuberculosis. *PLoS ONE,* 3, e1502.

SALKIN, D. & WAYNE, L. G. (1956) The bacteriology of resected tuberculous pulmonary lesions. I. The effect of interval between reversal of infectiousness and subsequent surgery. *Am Rev Tuberc,* 74, 376-87.

SANTHANA RAJ, L., HING, H. L., BAHARUDIN, O., TEH HAMIDAH, Z., AIDA SUHANA, R., NOR ASIHA, C. P., VIMALA, B., PARAMSARVARAN, S., SUMARNI, G. & HANJEET, K. (2007) Mesosomes are a definite event in antibiotic-treated Staphylococcus aureus ATCC 25923. *Trop Biomed,* 24, 105-9.

SCHAEFER, W. B. & LEWIS, C. W., JR. (1965) Effect of oleic acid on growth and cell structure of mycobacteria. *J Bacteriol,* 90, 1438-47.

SCHLEGEL, H. G., KALTWASSER, H. & GOTTSCHALK, G. (1961) [A submersion method for culture of hydrogen-oxidizing bacteria: growth physiological studies.]. *Arch Mikrobiol,* 38, 209-22.

SCHNAPPINGER, D., EHRT, S., VOSKUIL, M. I., LIU, Y., MANGAN, J. A., MONAHAN, I. M., DOLGANOV, G., EFRON, B., BUTCHER, P. D., NATHAN, C. & SCHOOLNIK, G. K. (2003) Transcriptional Adaptation of Mycobacterium tuberculosis within Macrophages: Insights into the Phagosomal Environment. *J Exp Med,* 198, 693-704.

SCHWEIZER, E. & HOFMANN, J. (2004) Microbial type I fatty acid synthases (FAS): major players in a network of cellular FAS systems. *Microbiol Mol Biol Rev,* 68, 501-17.

SCOTT, C. C. & FINNERTY, W. R. (1976) Characterization of intracytoplasmic hydrocarbon inclusions from the hydrocarbon-oxidizing Acinetobacter species HO1-N. *J Bacteriol,* 127, 481-9.

SHARMA, V., SHARMA, S., HOENER ZU BENTRUP, K., MCKINNEY, J. D., RUSSELL, D. G., JACOBS, W. R., JR. & SACCHETTINI, J. C. (2000) Structure of isocitrate lyase, a persistence factor of Mycobacterium tuberculosis. *Nat Struct Biol,* 7, 663-8.

SHERMAN, D. R., VOSKUIL, M., SCHNAPPINGER, D., LIAO, R., HARRELL, M. I. & SCHOOLNIK, G. K. (2001) Regulation of the Mycobacterium tuberculosis hypoxic response gene encoding alpha -crystallin. *Proc Natl Acad Sci U S A,* 98, 7534-9.

SHI, L., SOHASKEY, C. D., KANA, B. D., DAWES, S., NORTH, R. J., MIZRAHI, V. & GENNARO, M. L. (2005) Changes in energy metabolism of Mycobacterium tuberculosis in mouse lung and under in vitro conditions affecting aerobic respiration. *Proc Natl Acad Sci U S A,* 102, 15629-34.

SHIVELY, J. M. (1974) Inclusion bodies of prokaryotes. *Annu Rev Microbiol,* 28, 167-87.

SHOTTON, D. M. & SEVERS, N. J. (1995) An Introduction to Freeze Fracture and Deep Etching. IN SEVERS, N. J. & SHOTTON, D. M. (Eds.) *Rapid Freezing, Freeze Fracture and Deep Etching.* 1st ed. New York, Wiley-liss.

SIRAKOVA, T. D., DUBEY, V. S., DEB, C., DANIEL, J., KOROTKOVA, T. A., ABOMOELAK, B. & KOLATTUKUDY, P. E. (2006) Identification of a diacylglycerol acyltransferase gene involved in accumulation of triacylglycerol in Mycobacterium tuberculosis under stress. *Microbiology,* 152, 2717-25.

SLAYDEN, R. A., KNUDSON, D. L. & BELISLE, J. T. (2006) Identification of cell cycle regulators in Mycobacterium tuberculosis by inhibition of septum formation and global transcriptional analysis. *Microbiology,* 152, 1789-97.

SMEULDERS, M. J., KEER, J., SPEIGHT, R. A. & WILLIAMS, H. D. (1999) Adaptation of Mycobacterium smegmatis to stationary phase. *J Bacteriol,* 181, 270-83.

SMITH, S., WITKOWSKI, A. & JOSHI, A. K. (2003) Structural and functional organization of the animal fatty acid synthase. *Prog Lipid Res,* 42, 289-317.

SOHASKEY, C. D. & WAYNE, L. G. (2003) Role of narK2X and narGHJI in hypoxic upregulation of nitrate reduction by Mycobacterium tuberculosis. *J Bacteriol,* 185, 7247-56.

SOMOSKOVI, A., PARSONS, L. M. & SALFINGER, M. (2001) The molecular basis of resistance to isoniazid, rifampin, and pyrazinamide in Mycobacterium tuberculosis. *Respir Res,* 2, 164-8.

SPURR, A. R. (1969) A low-viscosity epoxy resin embedding medium for electron microscopy. *J Ultrastruct Res,* 26, 31-43.

SREEVATSAN, S., PAN, X., STOCKBAUER, K. E., CONNELL, N. D., KREISWIRTH, B. N., WHITTAM, T. S. & MUSSER, J. M. (1997) Restricted structural gene polymorphism in the Mycobacterium tuberculosis complex indicates evolutionarily recent global dissemination. *Proc Natl Acad Sci U S A,* 94, 9869-74.

STEINBUCHEL, A. & FUCHTENBUSCH, B. (1998) Bacterial and other biological systems for polyester production. *Trends Biotechnol,* 16, 419-27.

STOVEKEN, T., KALSCHEUER, R., MALKUS, U., REICHELT, R. & STEINBUCHEL, A. (2005) The wax ester synthase/acyl coenzyme A:diacylglycerol acyltransferase from Acinetobacter sp. strain ADP1: characterization of a novel type of acyltransferase. *J Bacteriol,* 187, 1369-76.

SUMMERS, H. M. & GOOD, R. C. (1985) Mycobacterium. IN LENNETTE, E. H., BALAUS, A., HAUSLER, W. J. & SHADONNY, H. J. (Eds.) *Manual of Clinical Microbiology.* 4th ed. Washington, D.C., American Society for Microbiology.

SUNDARAMURTHY, V. & PIETERS, J. (2007) Interactions of pathogenic mycobacteria with host macrophages. *Microbes Infect,* 9, 1671-9.

TAKAYAMA, K., WANG, C. & BESRA, G. S. (2005) Pathway to synthesis and processing of mycolic acids in Mycobacterium tuberculosis. *Clin Microbiol Rev,* 18, 81-101.

THANKY, N. R., YOUNG, D. B. & ROBERTSON, B. D. (2007) Unusual features of the cell cycle in mycobacteria: polar-restricted growth and the snapping-model of cell division. *Tuberculosis (Edinb),* 87, 231-6.

TIMM, J., POST, F. A., BEKKER, L. G., WALTHER, G. B., WAINWRIGHT, H. C., MANGANELLI, R., CHAN, W. T., TSENOVA, L., GOLD, B., SMITH, I., KAPLAN, G. & MCKINNEY, J. D. (2003) Differential expression of iron-, carbon-, and oxygen-responsive mycobacterial genes in the lungs of chronically infected mice and tuberculosis patients. *Proc Natl Acad Sci U S A,* 100, 14321-6.

TIMMINS, G. S. & DERETIC, V. (2006) Mechanisms of action of isoniazid. *Mol Microbiol,* 62, 1220-7.

TRICCAS, J. A., BERTHET, F. X., PELICIC, V. & GICQUEL, B. (1999) Use of fluorescence induction and sucrose counterselection to identify Mycobacterium tuberculosis genes expressed within host cells. *Microbiology,* 145 (Pt 10), 2923-30.

TSIEN, R. Y. (1998) The green fluorescent protein. *Annu Rev Biochem,* 67, 509-44.

TUFARIELLO, J. M., CHAN, J. & FLYNN, J. L. (2003) Latent tuberculosis: mechanisms of host and bacillus that contribute to persistent infection. *Lancet Infect Dis,* 3, 578-90.

TUMMON, R. (1975) Growth inhibition of mycobacterium tuberculosis by oleate in acidified medium. *Med Lab Technol,* 32, 229-32.

ULRICHS, T., KOSMIADI, G. A., JORG, S., PRADL, L., TITUKHINA, M., MISHENKO, V., GUSHINA, N. & KAUFMANN, S. H. (2005) Differential Organization of the Local Immune Response in Patients with Active Cavitary Tuberculosis or with Nonprogressive Tuberculoma. *Journal of Infectious Diseases,* 192.

VERLINDEN, R. A., HILL, D. J., KENWARD, M. A., WILLIAMS, C. D. & RADECKA, I. (2007) Bacterial synthesis of biodegradable polyhydroxyalkanoates. *J Appl Microbiol,* 102, 1437-49.

VOSKUIL, M. I. (2004) Mycobacterium tuberculosis gene expression during environmental conditions associated with latency. *Tuberculosis (Edinb),* 84, 138-43.

VOSKUIL, M. I., SCHNAPPINGER, D., VISCONTI, K. C., HARRELL, M. I., DOLGANOV, G. M., SHERMAN, D. R. & SCHOOLNIK, G. K. (2003) Inhibition of respiration by nitric oxide induces a Mycobacterium tuberculosis dormancy program. *J Exp Med,* 198, 705-13.

VOSKUIL, M. I., VISCONTI, K. C. & SCHOOLNIK, G. K. (2004) Mycobacterium tuberculosis gene expression during adaptation to stationary phase and low-oxygen dormancy. *Tuberculosis (Edinb),* 84, 218-27.

VOTYAKOVA, T. V., KAPRELYANTS, A. S. & KELL, D. B. (1994) Influence of Viable Cells on the Resuscitation of Dormant Cells in Micrococcus luteus Cultures Held in an Extended Stationary Phase: the Population Effect. *Appl Environ Microbiol,* 60, 3284-3291.

WALKER, D. R., NWOGUH, C. E. & BARER, M. R. (1994) A microchamber system for the rapid cytochemical demonstration of beta-galactosidase and other properties in pathogenic microbes. *Lett Appl Microbiol,* 18, 102-4.

WALL, D. M., DUFFY, P. S., DUPONT, C., PRESCOTT, J. F. & MEIJER, W. G. (2005) Isocitrate lyase activity is required for virulence of the intracellular pathogen Rhodococcus equi. *Infect Immun,* 73, 6736-41.

WALTERMANN, M., HINZ, A., ROBENEK, H., TROYER, D., REICHELT, R., MALKUS, U., GALLA, H. J., KALSCHEUER, R., STOVEKEN, T., VON LANDENBERG, P. & STEINBUCHEL, A. (2005) Mechanism of lipid-body formation in prokaryotes: how bacteria fatten up. *Mol Microbiol,* 55, 750-63.

WALTERMANN, M. & STEINBUCHEL, A. (2005) Neutral lipid bodies in prokaryotes: recent insights into structure, formation, and relationship to eukaryotic lipid depots. *J Bacteriol,* 187, 3607-19.

WALTERMANN, M., STOVEKEN, T. & STEINBUCHEL, A. (2007) Key enzymes for biosynthesis of neutral lipid storage compounds in prokaryotes: properties, function and occurrence of wax ester synthases/acyl-CoA: diacylglycerol acyltransferases. *Biochimie,* 89, 230-42.

WARNER, D. F. & MIZRAHI, V. (2006) Tuberculosis chemotherapy: the influence of bacillary stress and damage response pathways on drug efficacy. *Clin Microbiol Rev,* 19, 558-70.

WAYNE, L. G. & HAYES, L. G. (1996) An in vitro model for sequential study of shiftdown of Mycobacterium tuberculosis through two stages of nonreplicating persistence. *Infect Immun,* 64, 2062-9.

WAYNE, L. G. & KUBICA, G. P. (1986) Mycobacteria. IN SNEATH, P. H. A., MAIR, N. S., SHARPE, M. E. & HOLT, J. G. (Eds.) *Bergey's Manual of Systematic Bateriology.* Baltimore, Williams & Wilkins.

WAYNE, L. G. & LIN, K. Y. (1982) Glyoxylate metabolism and adaptation of Mycobacterium tuberculosis to survival under anaerobic conditions. *Infect Immun,* 37, 1042-9.

WAYNE, L. G. & SOHASKEY, C. D. (2001) Nonreplicating persistence of mycobacterium tuberculosis. *Annu Rev Microbiol,* 55, 139-63.

WEBER, I., FRITZ, C., RUTTKOWSKI, S., KREFT, A. & BANGE, F. C. (2000) Anaerobic nitrate reductase (narGHJI) activity of Mycobacterium bovis BCG in vitro and its contribution to virulence in immunodeficient mice. *Mol Microbiol,* 35, 1017-25.

WEIR, M. P., LANGRIDGE, W. H., 3RD & WALKER, R. W. (1972) Relationships between oleic acid uptake and lipid metabolism in Mycobacterium smegmatis. *Am Rev Respir Dis,* 106, 450-7.

WEYER, K., RUSTOMJEE, J., MIZRAHI, V. & VAN HELDEN, P. (1999) Part II: Microscopy acid-fast staining procedures. *Tuberculosis.* SA HealthInfo.

WHEELER, P. R. & BLANCHARD, J. S. (2005) General Metabolism and Biochemical Pathways of Tubercle Bacilli. IN COLE, S. T. (Ed.) *Tuberculosis and the Tubercle Bacillus.* Washington, D.C., ASM Press.

WHITEHOUSE, R. L., WONG, P. C. & JACKSON, F. L. (1971) Ultrastructure of Mycobacterium lepraemurium. *Int J Lepr Other Mycobact Dis,* 39, 151-63.

WILKINSON, M. H. F. & SCHUT, F. (1998) *Digital Image Analysis of Microbes: Imaging, Morphology, Fluormetry, and Motility: Techniques and Applications,* London, John Wiley & Sons.

WIUFF, C., ZAPPALA, R. M., REGOES, R. R., GARNER, K. N., BAQUERO, F. & LEVIN, B. R. (2005) Phenotypic tolerance: antibiotic enrichment of noninherited resistance in bacterial populations. *Antimicrob Agents Chemother,* 49, 1483-94.

YOUNG, D. B. & DUNCAN, K. (1995) Prospects for new interventions in the treatment and prevention of mycobacterial disease. *Annu Rev Microbiol,* 49, 641-73.

YUAN, Y., CRANE, D. D. & BARRY, C. E., 3RD (1996) Stationary phase-associated protein expression in Mycobacterium tuberculosis: function of the mycobacterial alpha-crystallin homolog. *J Bacteriol,* 178, 4484-92.

YUAN, Y., CRANE, D. D., SIMPSON, R. M., ZHU, Y. Q., HICKEY, M. J., SHERMAN, D. R. & BARRY, C. E., 3RD (1998) The 16-kDa alpha-crystallin (Acr) protein of Mycobacterium tuberculosis is required for growth in macrophages. *Proc Natl Acad Sci U S A,* 95, 9578-83.

ZHANG, Y. & AMZEL, L. M. (2002) Tuberculosis drug targets. *Curr Drug Targets,* 3, 131-54.

ZHU, L., ZHANG, Y., TEH, J. S., ZHANG, J., CONNELL, N., RUBIN, H. & INOUYE, M. (2006) Characterization of mRNA interferases from Mycobacterium tuberculosis. *J Biol Chem,* 281, 18638-43.

ZWEYTICK, D., ATHENSTAEDT, K. & DAUM, G. (2000) Intracellular lipid particles of eukaryotic cells. *Biochim Biophys Acta,* 1469, 101-20.

Appendices

Appendix 1: Primers

Genome-Directed Primers

Primer Name	Sequence
mtGDP1	5' CGG CCA GC 3'
mtGDP2	5' CGG CGG CG 3'
mtGDP3	5' CGC CGC CG 3'
mtGDP4	5' CGT CGG CG 3'
mtGDP5	5' CGC CGG CG 3'
mtGDP6	5' CGG CCG CG 3'
mtGDP7	5' CGC CGT CG 3'
mtGDP8	5' CGG CGT CG 3'
mtGDP9	5' CGG CGA CC 3'
mtGDP10	5' CGG CGA TG 3'
mtGDP11	5' CGT CGT CG 3'
mtGDP12	5' GGC CGC CG 3'
mtGDP13	5' CGC CAC CG 3'
mtGDP14	5' GCA GCA GC 3'
mtGDP15	5' CGG TGC CG 3'
mtGDP16	5' CAC CGC G 3'
mtGDP17	5' GTC GCC G 3'
mtGDP18	5' GTC GAC G 3'
mtGDP19	5' CGC CAG C 3'
mtGDP20	5' GAT CGG C 3'
mtGDP21	5' CGC CGC G 3'
mtGDP22	5' CGG TGG C 3'
mtGDP23	5' CAC CGT C 3'
mtGDP24	5' GCG GCC A 3'
mtGDP25	5' CAC CGG C 3'

mtGDP26	5' GCG GCC G 3'
mtGDP27	5' CCG CGC C 3'
mtGDP28	5' GCC CAG C 3'
mtGDP29	5' TCG GCC A 3'
mtGDP30	5' CCC GGC G 3'
mtGDP31	5' CAC CAG C 3'
mtGDP32	5' CAC CGC C 3'
mtGDP33	5' CGG GCC G 3'
mtGDP34	5' CGC TGA C 3'
mtGDP35	5' GGT GTT G 3'
mtGDP36	5' ACG CAG C 3'
mtGDP37	5' ACC GGA C 3'

Primer sequences obtained from Rachman et al. (2006)

Taqman Probe and Primer Sequences

Primer Name	Sequence	Reference
3130c TaqMan	5' FAM – AAC CTG CCG GTG GAT CAA GAG AAC – TAMRA 3'	(Sequence kindly provided by Rebecca Smith)
3130c F	5' CCG ATA ACC GTG TTT CGT TA 3'	(Sequence kindly provided by Rebecca Smith)
3130c R	5' TTT CCG AAT TGT CTC TGT CC 3'	(Sequence kindly provided by Rebecca Smith)
sigA TaqMan	5' JOE – CCT GCG CCT GGT GGT TTC GC – TAMRA 3'	(Hampshire et al., 2004)
sigA	5' AAA CCA TCT GCT GGA AGC CA 3'	(Hampshire et al., 2004)
sigA	5' CGG CCG GTG TAG CGC 3'	(Hampshire et al., 2004)

PCR Primers for Amplication of Promoter Regions of Cell Division Genes
Primers designed in this study

Primer Name	Sequence
FtsZ F	5'AAA AGT ACT CTA AGC CTA TGG TTG 3'
FtsZ R	5'AAA GGA TCC GAC GGC CAG GTA GTT3'
WhiB2 F	5'AAA AGT ACT GAC CGA GAT TCG ATC3'
WhiB2 R	5'AAA GGA TCC CGC CTC GGG AAC CAA3'
sigB F	5'AAA AGT ACT GCG TCA GAT CAC TGC3'
sigB R	5'AAA GGA TCC GGG TGC ATC GGC CAT3'

Appendix 2: CFU Counts for *M. tuberculosis* recovered from Primary Blood Monocytes

Figure 54: Growth of *M. tuberculosis* in Primary Blood Monocytes assessed by Colony Forming Unit Counts (CFU/ml)

Differentiated Primary Blood Monocytes (with or without activation by interferon-γ) were infected with *M. tuberculosis* strains H37Rv and CH as described in Chapter 3. Infected macrophages were cultured under normoxia, hypoxia or were switched to hypoxia during the course of the experiment, as indicated. Bacterial growth was assessed by colony forming Colony Unit Counts (CFU) were performed on wells of infected macrophage lysates, which are show in the graph below. The CFU count is shown per well of infected macrophage, as an assessment of macrophage numbers was not possible. Bernard Burke carried bacterial growth assays and kindly supplied the data presented below.

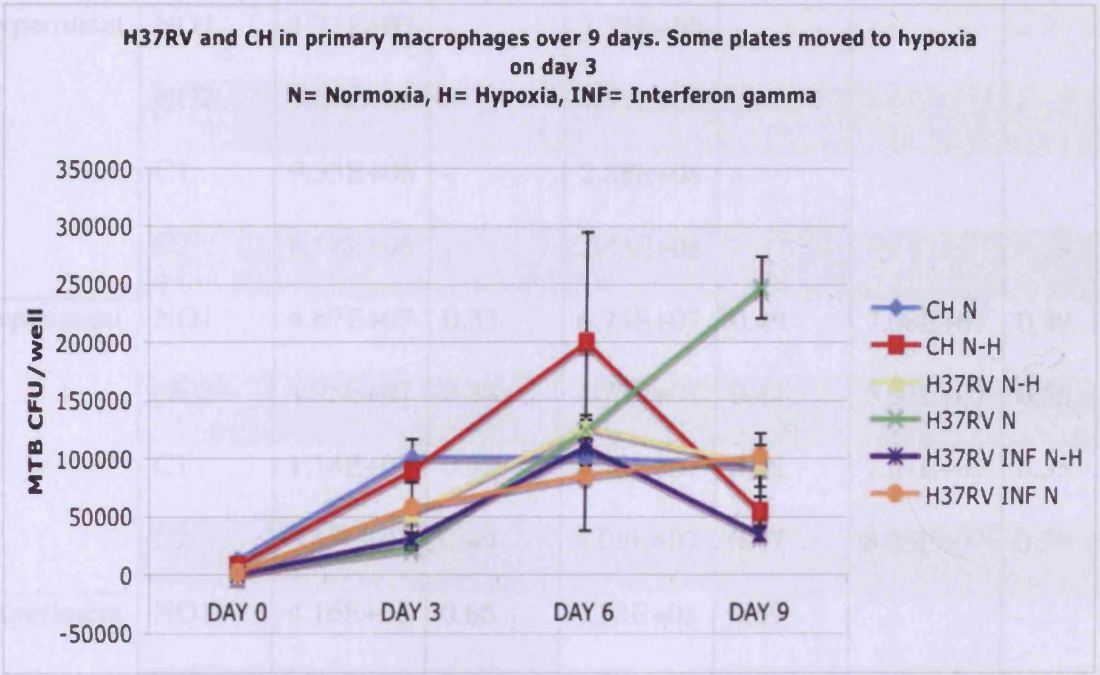

Appendix 3: CFU Counts for NO treated *M. tuberculosis* Cultures

Table 12: Colony Forming Unit Counts per ml (CFU/ml) for NO treated *M. tuberculosis*.

CFU counts were taken for duplicate cultures of *M. tuberculosis* after 4 and 24 hours of treatment with the NO releasing agent SPER/NO or the control compound (C) and represent the initial inoculum used in antibiotic tolerance assays. Optical density at 580nm (OD_{580nm}) measurements, where available, are shown alongside.

		Time after NO added					
		4 hours		24 hours		48 hours	
		CFU/ml	OD_{580nm}	CFU/ml	OD_{580nm}	CFU/ml	OD_{580nm}
Experiment 1	NO1	1.21E+07	-	2.73E+08	-	-	-
	NO2	7.67E+06	-	1.89E+08	-	-	-
	C1	9.33E+06	-	2.88E+08	-	-	-
	C2	6.58E+06	-	2.83E+08	-	-	-
Experiment 2	NO1	4.67E+07	0.33	6.75E+07	0.49	7.08E+07	0.49
	NO2	4.95E+07	0.38	4.75E+07	0.44	5.33E+07	0.55
	C1	1.14E+08	0.38	4.42E+07	0.48	7.67E+07	0.55
	C2	3.49E+07	0.40	4.08E+07	0.47	8.25E+07	0.59
Experiment 3	NO1	4.16E+08	0.66	4.38E+08	0.69	-	-
	NO2	1.01E+08	0.65	4.73E+08	0.64	-	-
	C1	3.36E+08	0.69	5.95E+08	0.79	-	-
	C2	3.14E+08	0.62	4.07E+08	0.763	-	-

Appendix 4: Cytological and Transcript Analyses Reveal Fat and Lazy Persister-Like Bacilli in Tuberculous Sputum

Cytological and Transcript Analyses Reveal Fat and Lazy Persister-Like Bacilli in Tuberculous Sputum

Natalie J. Garton[1☯], Simon J. Waddell[2☯], Anna L. Sherratt[1], Su-Min Lee[1], Rebecca J. Smith[1], Claire Senner[2], Jason Hinds[2], Kumar Rajakumar[1,3], Richard A. Adegbola[4], Gurdyal S. Besra[5], Philip D. Butcher[2*], Michael R. Barer[1,3*]

1 Department of Infection, Immunity and Inflammation, University of Leicester Medical School, Leicester, United Kingdom, **2** Medical Microbiology, Division of Cellular and Molecular Medicine, St George's University of London, London, United Kingdom, **3** Department of Clinical Microbiology, University Hospitals of Leicester National Health Service Trust, Leicester, United Kingdom, **4** Medical Research Council Laboratories, Fajara, Banjul, The Gambia, **5** School of Biosciences, University of Birmingham, Edgbaston, Birmingham, United Kingdom

Funding: This work was supported by grants from the Medical Research Council (UK) to MRB and GSB, the Henry Smith Charity and the British Lung Foundation to MRB and the Wellcome Trust to NJG. The whole genome *M. tuberculosis* microarray was constructed and analysed at St George's University of London as part of the multi-collaborative microbial pathogen microarray facility (BμG@S), for which funding from The Wellcome Trust's Functional Genomics Resources Initiative is acknowledged (grant number 062511). These funding agencies played no part in study design, data collection and analysis, decision to publish, or preparation of the manuscript.

Competing Interests: The authors have declared that no competing interests exist.

Academic Editor: Olivier Neyrolles, Institut de Pharmacologie et de Biologie Structurale-CNRS, France

Citation: Garton NJ, Waddell SJ, Sherratt AL, Lee S-M, Smith RJ, et al. (2008) Cytological and transcript analyses reveal fat and lazy persister-like bacilli in tuberculous sputum. PLoS Med 5(4) e75. doi:10.1371/journal.pmed.0050075

Received: August 24, 2007
Accepted: February 14, 2008
Published: April 1, 2008

Abbreviations: AFB, acid-fast bacilli; NRP, nonreplicating persistent

* To whom correspondence should be addressed. E-mail: butcherp@sgul.ac.uk (PDB); mrb19@le.ac.uk (MRB)

☯ These authors contributed equally to this work.

ABSTRACT

Background

Tuberculous sputum provides a sample of bacilli that must be eliminated by chemotherapy and that may go on to transmit infection. A preliminary observation that *Mycobacterium tuberculosis* cells contain triacylglycerol lipid bodies in sputum, but not when growing in vitro, led us to investigate the extent of this phenomenon and its physiological basis.

Methods and Findings

Microscopy-positive sputum samples from the UK and The Gambia were investigated for their content of lipid body–positive mycobacteria by combined Nile red and auramine staining. All samples contained a lipid body–positive population varying from 3% to 86% of the acid-fast bacilli present. The recent finding that triacylglycerol synthase is expressed by mycobacteria when they enter in vitro nonreplicating persistence led us to investigate whether this state was also associated with lipid body formation. We found that, when placed in laboratory conditions inducing nonreplicating persistence, two *M. tuberculosis* strains had lipid body levels comparable to those found in sputum. We investigated these physiological findings further by comparing the *M. tuberculosis* transcriptome of growing and nonreplicating persistence cultures with that obtained directly from sputum samples. Although sputum has traditionally been thought to contain actively growing tubercle bacilli, our transcript analyses refute the hypothesis that these cells predominate. Rather, they reinforce the results of the lipid body analyses by revealing transcriptional signatures that can be clearly attributed to slowly replicating or nonreplicating mycobacteria. Finally, the lipid body count was highly correlated ($R^2 = 0.64$, $p < 0.03$) with time to positivity in diagnostic liquid cultures, thereby establishing a direct link between this cytological feature and the size of a potential nonreplicating population.

Conclusion

As nonreplicating tubercle bacilli are tolerant to the cidal action of antibiotics and resistant to multiple stresses, identification of this persister-like population of tubercle bacilli in sputum presents exciting and tractable new opportunities to investigate both responses to chemotherapy and the transmission of tuberculosis.

The Editors' Summary of this article follows the references.

Introduction

Mycobacterium tuberculosis infects one in three worldwide and kills more people each year than any other bacterial pathogen. Routine treatment of tuberculosis requires combination antibiotic therapy for a minimum of six months, and places a substantial burden on health care systems, particularly in resource-poor countries. Over eight million new cases every year testify to this obligate pathogen's ongoing success in transmission [1], yet we know little about what the organism needs to achieve this essential step.

Expectorated tubercle bacilli have been thought to originate from rapid and extensive bacterial growth at the margins of liquefied lesions in the lung [2,3]. Sputum provides a tractable sample of the bacterial population that must be targeted by antibiotic therapy and a snapshot of the organism on its way to a new host. It follows that the bacilli in microscopy smear-positive tuberculosis sputum express properties required for transmission—properties that might explain the existence of drug-tolerant persister subpopulations and account for the prolonged antibiotic therapy necessary for relapse-free treatment [4]. Since transmission is required for evolutionary survival, we may assume that *M. tuberculosis* experiences powerful selection pressures to maintain and express these as-yet unidentified properties. Thus, any bacillary phenotype recognised preferentially in sputum could provide clues to these properties.

We have previously shown that nonpathogenic mycobacteria readily accumulate intracellular triacylglycerol lipid bodies in vitro [5]; these bodies could not be demonstrated under similar conditions with *M. tuberculosis*, yet anecdotally have been seen in acid-fast bacilli (AFB) in tuberculous sputum [5]. The recent discovery of a novel class of diacylglycerol acyl transferase enzymes in *Acinetobacter* [6] and the subsequent characterisation of 15 members of this class as triacylglycerol synthase-encoding genes (*tgs1–tgs15*) in *M. tuberculosis* [7] provide a biochemical basis for the presence of lipid bodies in this organism. Intriguingly, Tgs1, the most active of these enzymes, is a member of the DosR regulon [8], a set of genes responsive to hypoxia and linked to long-term survival of *M. tuberculosis* in animal hosts [9–13]. It has recently been shown that triacylglycerol is accumulated by *M. tuberculosis* following hypoxic and other stresses [7,14] and may contribute to long-term mycobacterial survival. These observations raise the possibility that lipid body–positive cells in sputum may be in a nonreplicating persistent (NRP) state, which, given that NRP bacilli display antibiotic tolerance [11,13,15], would have implications for chemotherapy.

Defining the phenotypes of bacterial pathogens in their natural environments remains a key challenge. Accurate knowledge of the properties expressed at different stages of infection enables precise targeting of therapeutic and preventive measures. While much has been learnt about bacterial pathogens from in vitro and in vivo (animal model) transcriptome studies [16,17] as well as from human lung tissue [18], there have, to the best of our knowledge, been no published studies of transcript profiles in sputum samples—a clinically tractable sample. Such methods as rapidly stabilised RNA, differential cell lysis, and RNA amplification have enabled us to report here the transcriptome of *M. tuberculosis* in the sputum of patients prior to treatment.

Methods

Patients

Patients attending the public clinic at the MRC Laboratories, Fajara, The Gambia and identified as sputum smear-positive by routine microscopy were invited to provide early-morning samples for transcriptome analysis. Patients who agreed to participate gave informed oral consent (study nos. L2002.52 and L2006.60, ethical committee, MRC Laboratories, Fajara, The Gambia). Sputum from nine patients yielded sufficient mycobacterial RNA for analysis by microarray or PCR; these were designated sputum samples 1–9.

Mycobacterial Strains and Growth Conditions

M. tuberculosis complex for direct microarray transcriptome analysis was isolated from an aliquot of sputum 1 using standard methods [19]. *M. tuberculosis* complex was grown on 7H10 agar with oleic acid-albumin-dextrose-catalase [20] supplement or in 7H9 broth with albumin-dextrose-catalase supplement [20], 0.2% glycerol and 0.05% Tween-80. For hypoxic (nonreplicating persistence) cultures *M. tuberculosis* strains H37Rv and CH [21] were grown in Dubos Tween-albumin broth.

Routine Culturing of Smear-Positive Sputum Samples

Diagnostic sputum specimens were stained with auramine-phenol [19], and positive smears confirmed and scored by Ziehl-Neelsen staining after initial examination by fluorescence microscopy. Smears were scored as either 1+ (1–10 AFB in 100 fields of view), 2+ (1–10 AFB in ten fields of view), or 3+ (1–10 AFB in one field of view). Decontamination of specimens was performed by the NaOH-NALC method [19]. Each decontaminated specimen was inoculated into one vial of BACTEC 9000 MB medium for isolation of *M. tuberculosis*. The time to positivity of the BACTEC culture was recorded in days. All mycobacterial cultures were identified and confirmed as *M. tuberculosis* complex using standard procedures.

Auramine-Nile Red Labelling of Sputum Samples

Whole sputum (~1–4 ml) was digested for 15 min with an equal volume of 0.5% w/v *N*-acetyl L-cysteine in 50 mM sodium citrate [19]. Phosphate buffer (67 mM [pH 6.8]) was added to a final volume of 20 ml, and bacteria were concentrated (1,398*g*, 20 min). The pellet was resuspended in 0.5 ml of phosphate-buffered saline and a smear prepared with ~10 μl of the suspension. Heat-fixed smears were labelled with auramine-Nile red as previously described [5]. Preparations were observed by epifluorescence microscopy using a Nikon Diphot 300 inverted microscope with a 100 W mercury light source. Images were recorded using a 12/10bit, high speed Peltier-cooled CCD camera (FDI, Photonic Science) using Image-Pro Plus (Media Cybernetics) software. The 11001V2 Blue (excitation 470 ± 40 nm; emission > 515 nm; Chroma Technology) and the G-2A (excitation 510–560 nm; emission: 590 ± 10 nm, Nikon) filter sets were used for epifluorescence microscopy.

Nile Red Labelling of Nonreplicating Persistence *M. tuberculosis* Cultures

M. tuberculosis H37Rv and strain CH [21] were grown as agitated, aerated cultures (370 rpm) to mid-log phase in Dubos liquid medium, supplemented with Dubos medium albumin. *M. tuberculosis* NRP1/2 (nonreplicating persistence

stage 1 and 2) cultures were incubated with continuous stirring at 37 °C for 168, 288, and 504 h, respectively, according to Wayne and Hayes [15]. At these time points one tube of each culture was destructively sampled for microscopic analysis. 10 µl of each sample was spread on a slide, heat fixed, and labelled with Nile red as previously described [5].

RNA Extraction from Tuberculous Sputa

With the exception of sputum sample 1, which was frozen in liquid nitrogen within 10 min of expectoration, approximately four volumes of GTC solution (5 M guanidinium thiocyanate, 0.5% w/v sodium N-lauryl sarcosine, 25 mM trisodium citrate, 0.1 M 2-mercaptoethanol, 0.5% w/v Tween 80 [pH 7.0]) [22] were added to sputum within 5 min of collection. Mycobacteria were harvested by centrifugation (1398*g*, 30 min), resuspended in 400 µl of sterile deionized water, and added to 1 ml of Trizol LS (Invitrogen). RNA was extracted using a method modified from that of DesJardin et al. [23] with chloroform replacing chloroform:isoamyl alcohol washes and the Cleanascite step omitted. The mixture was transferred to a glass matrix tube for cell lysis (Lysing matrix B; Q-Biogene) and processed in a spin/rotation instrument for cell lysis (Ribolyser; Hybaid), with a speed setting of 6.5 and a time setting of 45 s. After processing, 200 µl of chloroform was added to the mixture and it was vortex-mixed for 2 min. The aqueous and organic layers were separated by microcentrifugation for 15 min at room temperature at 16,000*g*. The aqueous phase containing the RNA was washed once with an equal volume of chloroform. The aqueous phase was removed to a fresh tube and 1 µl of glycoblue (Ambion), 0.1 volume of 5 M ammonium acetate, and an equal volume of isopropanol were added. The RNA was precipitated overnight at −20 °C. The resulting RNA pellet was washed once with 70% v/v and once with 95% v/v ethanol, dried and resuspended in 100 µl of RNase-free H_2O (Sigma). The cognate *M. tuberculosis* complex isolate from sputum sample 1 was cultured for 6 d in 100ml 7H9 broth at 37 °C, 200 rpm at which time the absorbance was 0.22 at 580 nm. Mycobacterial RNA was stabilised with GTC solution and extracted as previously described. Total RNA from sputum samples (5, 7, 8, and 9) for amplification was quantified using the NanoDrop ND-1000 Spectrophotometer (NanoDrop Technologies) and Agilent 2100 Bioanalyser (Agilent Technologies).

Microarray Analysis of RNA from Sputum 1

RNA from sputum 1 and the in vitro-grown cognate isolate was cleaned using the RNeasy kit (Qiagen). A *M. tuberculosis* whole genome microarray, generated by the Bacterial Microarray Group at St. George's (University of London) and consisting of 3,924 gene-specific PCR products (designed with minimal cross-homology) to the *M. tuberculosis* H37Rv [24], was utilised (ArrayExpress accession number A-BUGS-1; http://bugs.sgul.ac.uk/A-BUGS-1). Hybridisations were conducted as previously described [25] with 15 µg of Cy5-labelled cDNA derived from *M. tuberculosis* RNA against 1 µg Cy3-labelled *M. tuberculosis* H37Rv genomic DNA. The hybridised slides were scanned sequentially at 532 nm and 635 nm corresponding to Cy3 and Cy5 excitation maxima using the Affymetrix 428 Array Scanner (MWG). Comparative spot intensities from the images were calculated using Imagene 5.5 (BioDiscovery), and imported into GeneSpring GX 7.2 (Agilent Technologies) for further analysis. After local background subtraction the measured intensity in the cDNA channel for each gene was divided by its intensity in the genomic DNA control channel. The array data were normalised to the 50th percentile of all genes detected to be present on the array and filtered to remove unreliable low intensity data (below a value of 500 in either channel).Genes were identified as differentially expressed in sputum with a cut-off of >3-fold relative to in vitro growth.

Growth Conditions and RNA Extraction for Microarray Analysis

M. tuberculosis H37Rv was grown as agitated, aerated cultures (370 rpm) to mid-log phase at 37 °C in Dubos liquid medium, supplemented with Dubos medium albumin. *M. tuberculosis* NRP1/2 cultures were set up and cultured in a stirred model for 72 h and 240 h, respectively, according to Wayne and Hayes [15]. Mycobacterial RNA was extracted from in vitro models (collected straight into GTC solution) using the GTC/Trizol method as developed by Mangan et al. [26]; RNA was DNase-treated and purified using RNeasy columns (Qiagen). Total RNA was quantified using the NanoDrop ND-1000 Spectrophotometer (NanoDrop Technologies) and Agilent 2100 Bioanalyser (Agilent Technologies).

RNA Amplification

An aliquot of 5 ng of total *M. tuberculosis* RNA was amplified using an Eberwine T7-oligo-dT based system after an initial polyadenylation step (MessageAmp II Bacteria, Ambion). Using this method, bacterial RNA was polyadenylated before priming the first-strand cDNA synthesis reaction with T7-linked oligo-dT. Amplified RNA was generated after second-strand cDNA synthesis and cDNA purification by in vitro run-off transcription (IVT) using T7 polymerase. Single rounds of amplification were performed, with an in vitro transcription reaction of 16 h at 37 °C. This amplification method has been previously demonstrated to be reproducible and capable of identifying representative changes in gene expression [27,28]. The yield and size distribution of amplified products was assessed spectrophotometrically at OD260 and using the Agilent 2100 Bioanalyser (Agilent Technologies).

Microarray Analyses of Samples 5, 7, 8, and 9

An *M. tuberculosis* whole-genome microarray, generated by the Bacterial Microarray Group at St. George's (ArrayExpress accession number A-BUGS-23; http://bugs.sgul.ac.uk/A-BUGS-23), and consisting of 4,410 gene-specific PCR products (designed with minimal cross-homology) to the *M. tuberculosis* H37Rv [24], CDC1551 [29], and *M. bovis* AF2122/97 [30] genomes was utilised. Hybridisations were conducted as previously described [25] except for the use of *M. tuberculosis* genomic DNA as a common reference [31]. Using genomic DNA reduced technical variation between replicate hybridisations and allowed RNA profiles to be used in multiple comparisons. 5 µg of Cy5-labelled cDNA derived from amplified *M. tuberculosis* RNA was hybridised with 2 µg of Cy3-labelled *M. tuberculosis* H37Rv genomic DNA. A lower ratio of test cDNA to comparator gDNA was used than with sample 1, as we were able to confirm the purity of our preparations with the Bioanalyser at the same time and perform technical replicates. The *M. tuberculosis* H37Rv

reference DNA was kindly provided by Colorado State University (http://www.cvmbs.colostate.edu/microbiology/tb/top.htm). Two biological replicates of each in vitro growth condition and four sputum samples (5, 7, 8, and 9) were hybridised in triplicate. The microarrays were scanned and spot intensities calculated as described above. The array data were normalised to the 50th percentile of all genes detected to be present on the array. The dataset was filtered to include only cDNA elements flagged to be present on 80% of the arrays. Significantly differentially expressed genes were identified using ANOVA ($p < 0.05$ with Benjamini and Hochberg multiple testing correction) and a fold change of > 2.5. The significantly differentially expressed genes were hierarchically clustered using Cluster and the results displayed using Treeview software [32]. The hypergeometric distribution was used to determine if functional categories of genes were significantly enriched in the sputum profile [33]. Fully annotated microarray data are deposited in BμG@Sbase and ArrayExpress.

Quantitative Real-Time RT-PCR

Mycobacterial RNA (0.5 μg) from sputum sample 1 and its cognate isolate and eight further sputum samples (samples 2–9) were reverse transcribed in a total volume of 30 μl using random primers and Superscript II (Invitrogen Technologies) according to manufacturer's instructions. To estimate DNA contamination of samples, all were subjected to a no reverse transcriptase control, which was then subtracted from the RNA result. A no-reverse transcriptase threshold of 10% of the test value was taken, with the exception of four reactions in which values which were <20% were used for correction. PCR reactions for *tgs1* were set up using Absolute QPCR SYBR green mix (ABgene), 0.4 μM primers [7] and 2 μl of cDNA. PCR was performed using the Rotor-Gene RG-3000 system (Corbett Research) heating to 56 °C for 2 min, then 95 °C for 15 min, before 40 cycles of 95 °C for 30s, 60 °C for 30s, and 72 °C for 30s, acquiring fluorescence at 85 °C. No-reverse transcriptase controls for both the sputum and isolate RNA were included, and these showed no PCR product. PCR for *icl1* was set up with the primers of Dubnau et al. [34] using the same cycling conditions and acquiring fluorescence at 86 °C. An *hspX* PCR was performed using primers of Wilkinson et al. [35] with 40 cycles of 95 °C for 30s, 59 °C for 30s, 72 °C for 30s, acquisition of fluorescence at 85 °C. For normalisation, PCR of *sigA* was performed using the primers of Manganelli et al. [36], and cycling conditions used for *tgs1* with fluorescence acquisition at 86 °C. PCRs for *nuoB*, *qcrC*, and *ctaD* were performed using primers of Shi et al. [37] with conditions as previously described with annealing steps performed at 61 °C, 56 °C, and 56 °C, and acquisition of fluorescence at 84 °C, 82 °C, and 83 °C, respectively. The quantity of target DNA in each cDNA sample was determined by the threshold cycle (C_T) with reference to a standard curve generated by the amplification of known amounts of *M. tuberculosis* H37Rv genomic DNA.

Statistics

The proportion of lipid body–positive AFB and time to positivity of routine cultures were analysed by linear regression to provide R^2 correlation coefficients. As the lipid body content of these samples was not normally distributed, Pearson correlations were also performed.

Results

Lipid Body–Positive Acid-Fast Bacilli Are a Universal Feature of Smear-Positive Tuberculous Sputum

If lipid body–positive cells are a transmission-adapted phenotype for *M. tuberculosis*, then such cells should be present in most smear-positive sputum samples. We confirm this hypothesis in 82 smear-positive samples from patients from The Gambia and the UK (69 and 13, respectively). In samples with >100 assessable bacilli, the frequency of lipid body–positive cells varied from 3% to 86% (mean 45%, standard deviation 20%), and these contained between two and eight lipid bodies per cell (Figure 1). Thus, lipid body–positive tubercle bacilli are readily demonstrable in smear-positive samples from tuberculosis patients in two well-separated geographic locations and are present in a subpopulation of mycobacterial cells.

Lipid Bodies Are Readily Observed in *M. tuberculosis* Cells in Nonreplicating Persistence

The discovery and characterisation of *tgs1* [6,7] raised the possibility that lipid bodies might be formed in response to the hypoxic growth shift-down conditions that have been described by Wayne and Hayes [15], conditions known to cause up-regulation of the DosR regulon [9,10]. When *M. tuberculosis* H37Rv, a laboratory strain, and CH, a recent clinical isolate responsible for a large outbreak [21], were exposed in vitro to these conditions, abundant Nile red-staining lipid bodies were observed in both strains; respectively, 29% and 42% in NRP1 (168 h), 50% and 65% in NRP2 (288 h), and 41% and 56% in late NRP2 (504 h). An average of two lipid bodies per cell (range one to five) was observed in all samples except for the H37Rv NRP1 sample in which only one (range one to three) was seen in positive cells. Thus, NRP *M. tuberculosis* cultures contain lipid bodies at levels comparable to those seen in sputum.

Expression Profiling of *M. tuberculosis* Recovered from Sputum

If lipid bodies are a biomarker for cells in an NRP state, then the *M. tuberculosis* transcripts present in sputum should be compatible with those observed in NRP in vitro studies [9,10]. We therefore compared the transcriptome of *M. tuberculosis* recovered from human sputum to that obtained from in vitro aerobic cultures and NRP-inducing conditions [15]. Twenty sputa were collected from known microscopy-positive Gambian patients before they started antibiotic treatment, and the samples were rapidly stabilized against RNA degradation. Five samples (designated 1, 5, 7, 8, and 9) were analysed by microarray hybridisation, four with and one without prior polyadenylation/oligo-dT based amplification. Although the results from sputum 1, the single direct (nonamplified) array, are not discussed further, they confirm the essential details of the amplified analyses (Tables S1 and S2). This high-volume sample (~30 ml) had an exceptionally high bacterial load, and we estimate that $>10^{10}$ bacilli were present. The data from the four amplified samples were analysed with array hybridisations of amplified RNA extracted from *M. tuberculosis* H37Rv under different conditions: log-phase aerobic growth, the two stages of NRP (NRP1 t = 72 h; NRP2 t = 240 h) [15], and a mixed preparation containing RNA from aerobic and NRP2 cells mixed in the proportion 70:30 (w/w total RNA). This latter preparation was included

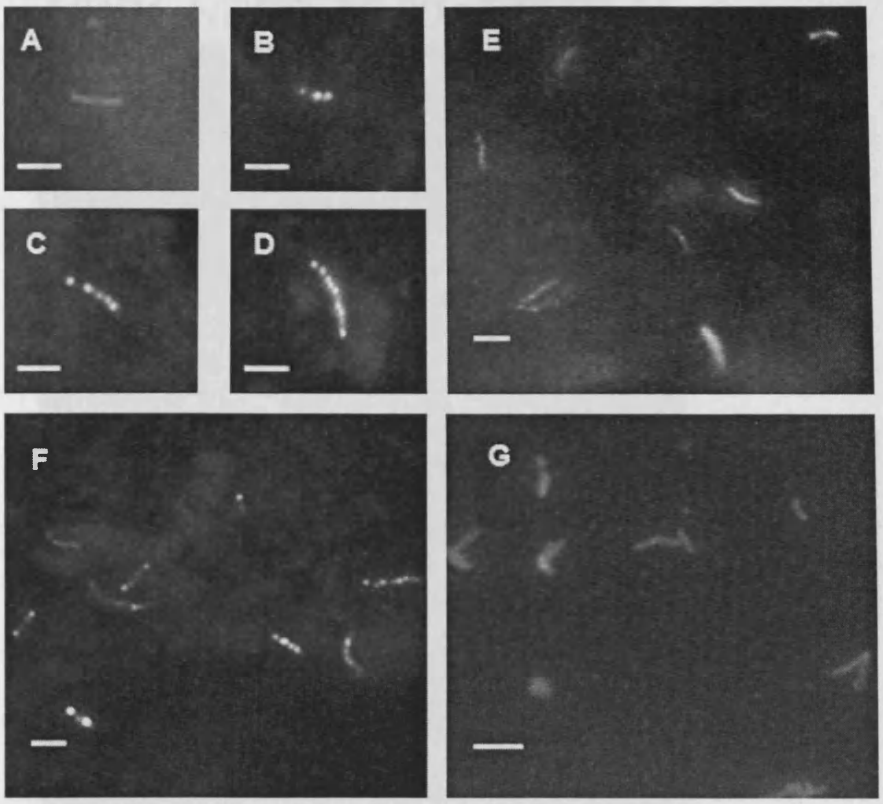

Figure 1. Lipid Bodies in Tuberculous Sputum Samples

Auramine/Nile red-fixed sputum smears [5] and aerobic *M. tuberculosis* growth. Variation in lipid bodies per cell: (A) none, (B) three, (C) five, and (D) eight. Samples are shown with (E) low and (F) high proportions of lipid body–positive cells. (G) Aerobically grown mid-log *M. tuberculosis* H37Rv contained negligible lipid bodies. Scale bar 2μm.

doi:10.1371/journal.pmed.0050075.g001

because this mixture was representative of the lipid body–positive population in sputum. This preparation therefore enabled us to test the hypothesis that sputum comprises a mixture of the rapidly and aerobically growing bacilli expected at the margins of liquefying caseous lesions [2] with the NRP-like cells indicated by our lipid body studies.

Microarray data analysis revealed that, after filtering to remove genes with low signals in either channel, 182 genes were significantly induced in sputum compared to aerobic growth, and 334 genes were significantly repressed (Tables S3 and S4). Figure 2 displays the results of gene cluster analysis of array data from the biological and technical replicates for these genes across the sputa, NRP and mixed aerobic:NRP2 sample sets. Boxes 1 and 2 highlight gene clusters similarly regulated in NRP2 and sputum relative to aerobic growth. We note the large cluster of strongly down-regulated signals in sputum, a feature lost in box 1 in the 70:30 mix, presumably due to the aerobic signals obscuring the NRP2 signals. A similar pattern of differential expression is apparent for the amplified RNA from the four sputum samples, even though they came from separate, untreated patients.

The data show that none of our comparator conditions, including the 70:30 aerobically replicating:NRP2 mixture, closely parallel the sputum transcriptome. While significant overlaps between the genes differentially expressed in sputum were revealed by hypergeometric probability values (Tables S5 and S6), no single or obvious combination of defined conditions herein, nor previously reported in vitro or in vivo, correspond to the signature we have obtained from sputum. Amongst the different functional categories of genes, relative to aerobic growth there were significant decreases in expression of genes required for aerobic respiration and ribosomal function and an increase in transcripts associated with cholesterol utilisation (Figure 3) [38]. We note also that genes previously observed to be repressed during bacillary stasis in a chronic murine infection model [37], *nuoB, ctaD, qcrC, atpA*, and *atpD*, followed this pattern in our data while *narK2* was up-regulated, as was the case in the murine studies. DosR was the most prominently activated regulon in sputum (box 2 in Figure 2; Tables S2 and S5), although the level of activation was lower than in the comparator conditions.

The induction of the isocitrate lyase gene, *icl1*, is consistent with the expected shift to utilisation of lipids as a source of carbon and energy [39]. This in vivo–associated metabolic pattern has emerged from other in vivo studies [11,12,39–42]; we particularly note the signals indicating cholesterol utilisation related to the putative KstR regulon [38,43], a feature that corresponds well with prominent sputum cholesterol content detected by thin layer chromatography (NJG, unpublished data) and the presence of this lipid in pulmonary exudates. The combination of DosR activation, lipid utilisation, and a slow growth signature is similar to experimental conditions previously studied in animal and macrophage infections [11,12], as depicted in Figures 3 and 4.

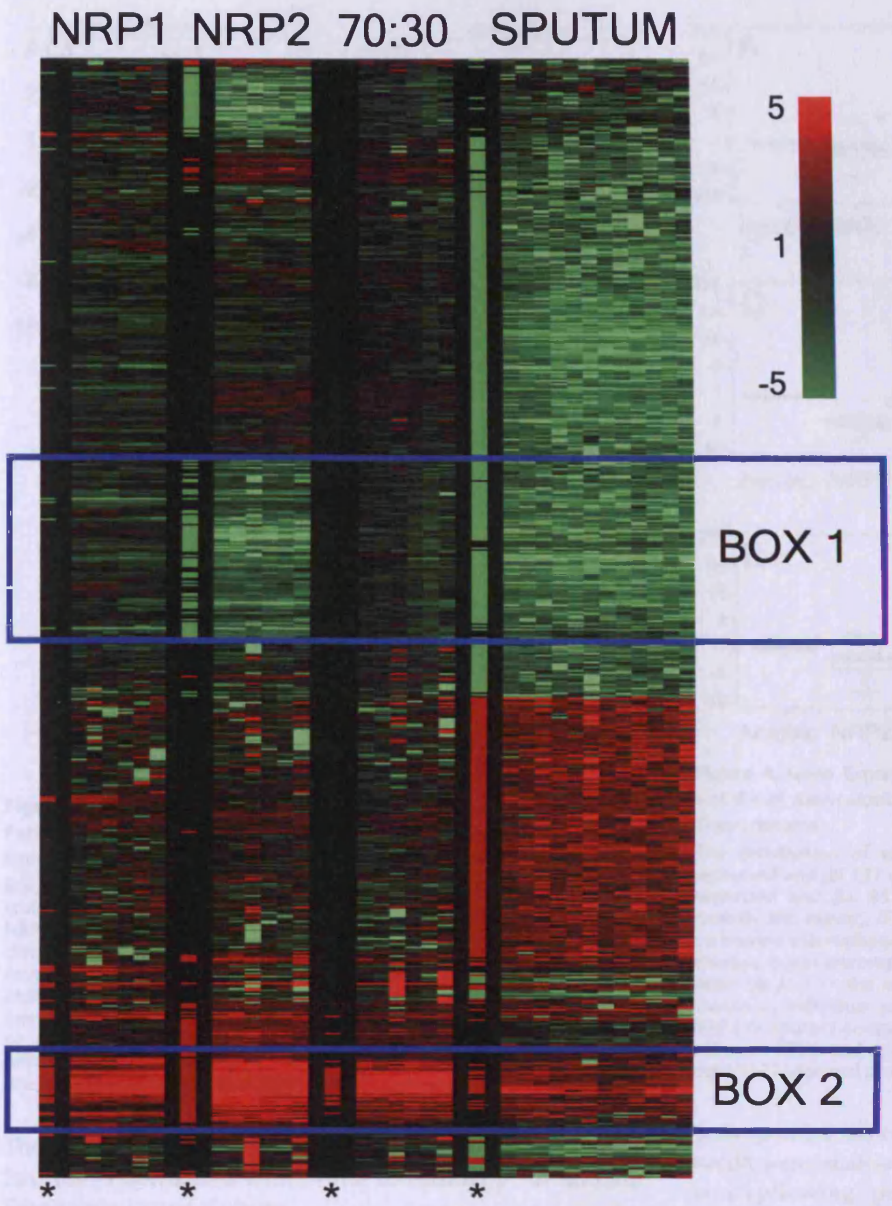

Figure 2. Display of Genes Differentially Regulated in Sputum and NRP versus Aerobic Culture

Clustering of 648 genes significantly differentially expressed in either sputum, NRP1, NRP2, or a 70:30 mix of aerobic:NRP2 compared to aerobic growth. Biological and technical replicates of conditions are displayed as columns, genes as rows. Red represents the induction of gene expression relative to aerobic growth, green repression. Asterisked columns mark the conditions in which genes were identified as significantly differentially expressed compared to aerobic growth. Boxes 1 and 2 highlight clusters of genes similarly regulated in NRP2 and sputum.

doi:10.1371/journal.pmed.0050075.g002

However, induction of Fe^{2+} scavenging was absent from our dataset, presumably due to an excess of available Fe^{2+} in necrotic liquefying tissue (Tables S3–S6).

We have confirmed key features of the sputum transcriptome and its relation to the metabolic states of bacilli in sputum with selected qRT-PCR analyses applied to up- and down-regulated transcripts (Figure 5). Up-regulation of *tgs1* was detected in unamplified (Table S1) and amplified (Table S3) array analyses and qRT-PCR confirmed this in these and four further samples (designated 2–4 and 6). While the up-regulation of *icl1* confirms the shift towards lipid utilisation, the strong *hspX* (α-crystallin homologue), *narK2* (nitrate/nitrite transporter), and *tgs1* transcript signals confirm DosR up-regulation [8]. Down-regulation of *nuoB* (type-I NADH dehydrogenase), *qcrC* (cytochrome bc_1 complex), and *ctaD* (aa_3-type cytochrome *c* oxidase) confirms a reduction in efficiency of the aerobic respiratory chain [37].

The strong expression of *tgs1* in sputum and the presence of lipid body–positive *M. tuberculosis* cells therein suggest a likely direct link between *tgs1* expression, lipid body formation, and increased bacillary triacylglycerol content. We have demonstrated such a link in *M. smegmatis* by overexpressing *tgs1* in this organism (see Figure S1): both increased triacylglycerol and lipid body content were observed following *tgs1* induction.

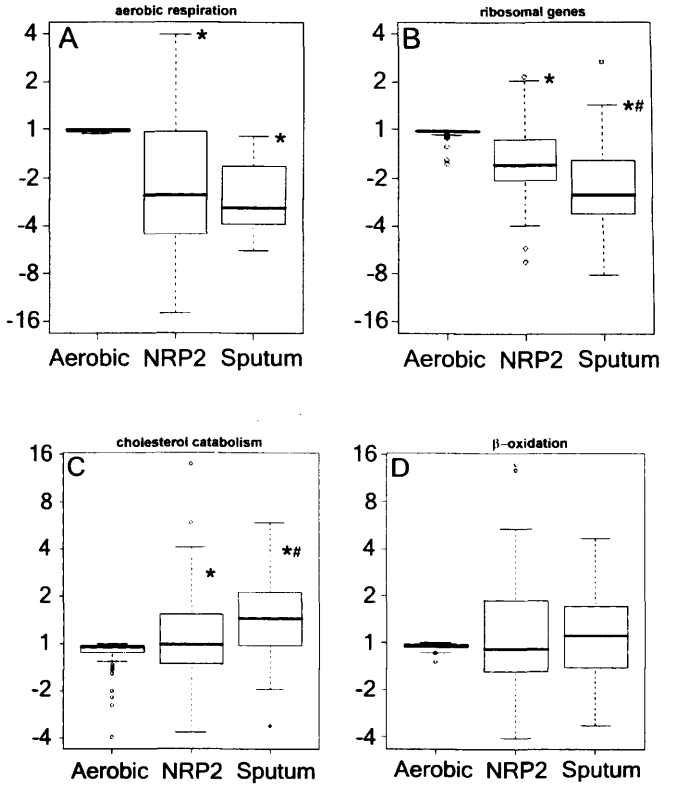

Figure 3. Genes Required for Aerobic Respiration and Ribosomal Function Show Decreased Expression in Sputum Compared with Aerobic Growth while Genes Involved in Lipid Metabolism Were Induced

Box and whisker plots showing the distribution of expression ratios (log2 scale) of (A) 21 aerobic respiration genes and (B) 45 ribosomal genes in NRP2 and sputum relative to aerobic growth using functional classifications defined by Cole et al., 1998 [24]; also (C) 64 genes that may be involved in cholesterol catabolism [38] and (D) 45 genes in the *fadB, echA, fadE,* and *fadA* families, which may be involved in the β-oxidation of fatty acids. *Significant difference ($p < 0.01$) between NRP2 or sputum compared to aerobic; #Significant difference ($p < 0.01$) between NRP2 and sputum.

doi:10.1371/journal.pmed.0050075.g003

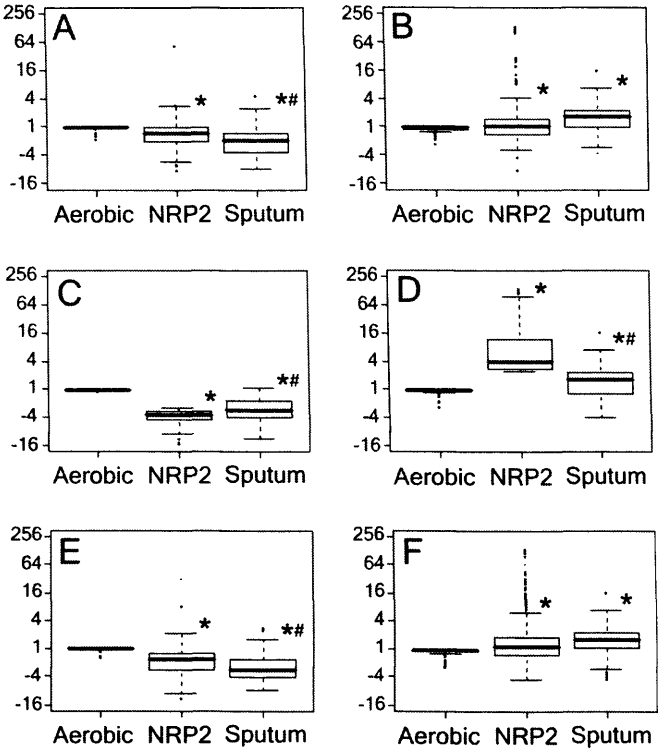

Figure 4. Gene Expression Signatures Representative of Slow Growth and the *M. tuberculosis* In Vivo Phenotype Were Identified in the Sputum Transcriptome

The distribution of expression ratios (log2 scale) of (A) 129 genes repressed and (B) 127 genes induced by slow growth [53]; (C) 106 genes repressed and (D) 85 genes induced by NRP2 compared to aerobic growth (this report); (E) 111 genes repressed and (F) 339 genes induced on murine macrophage infection [12]. In all plots the y-axis denotes fold change, boxes encompass the 25th and 75th percentiles, whiskers have been set at 1.5× the range between these values, and only outliers are shown as individual points. *Significant difference ($p < 0.01$) between NRP2 or sputum compared to aerobic; #Significant difference ($p < 0.01$) between NRP2 and sputum.

doi:10.1371/journal.pmed.0050075.g004

The Frequency of Lipid Body–Positive Acid-Fast Bacilli in Sputum Is Correlated with "Time to Positivity" in Routine Diagnostic Liquid Culture

Although both the lipid body and the transcriptome results are consistent with the presence of a NRP-like population in sputum, more direct evidence that the lipid body–positive cells have the properties one might expect of cells in this state would be desirable. Standard bacteriology tells us that nonreplicating bacterial cells take longer to initiate growth than their replicating counterparts (longer lag phase) [44,45]. If the lipid body–positive cell count provides an estimate of a NRP population in sputum, then this should be reflected in the "time to positivity" in liquid culture. Figure 6 demonstrates that "time to positivity" is significantly associated with lipid body percentage in 15 diagnostic samples with $p < 0.03$ and $R^2 = 0.64$.

Discussion

We applied a combination of ex vivo and in vitro analyses to study the phenotypes of *M. tuberculosis* cells in smear-positive sputum samples. We found a subpopulation of lipid body–positive acid-fast cells in all samples for which >100 bacilli were analysable. Our further in vitro studies revealed nonreplicating persistence, as defined by Wayne and colleagues [46], to be a condition in which *M. tuberculosis* cells are induced to form lipid bodies at frequencies comparable to those observed among tubercle bacilli in sputum. Consistent with this finding, transcriptome analysis of *M. tuberculosis* in sputum revealed signals compatible with slow or non-growth and absence of aerobic respiration. Moreover, the time to positivity in diagnostic liquid culture was shown to be directly related to sputum lipid body content, adding further weight to the view that lipid body–positive cells are not replicating. While other explanations remain possible, we conclude that the lipid body–positive cells in sputum have a persister-like phenotype, with important implications for the treatment and transmission of tuberculosis. Further studies should elucidate the impact of chemotherapy on the frequency of lipid body–positive populations of *M. tuberculosis* in patient sputum, and the relationship between this candidate biomarker and both infectivity and the clinical response to treatment.

The analysis of tuberculous sputum has played a central

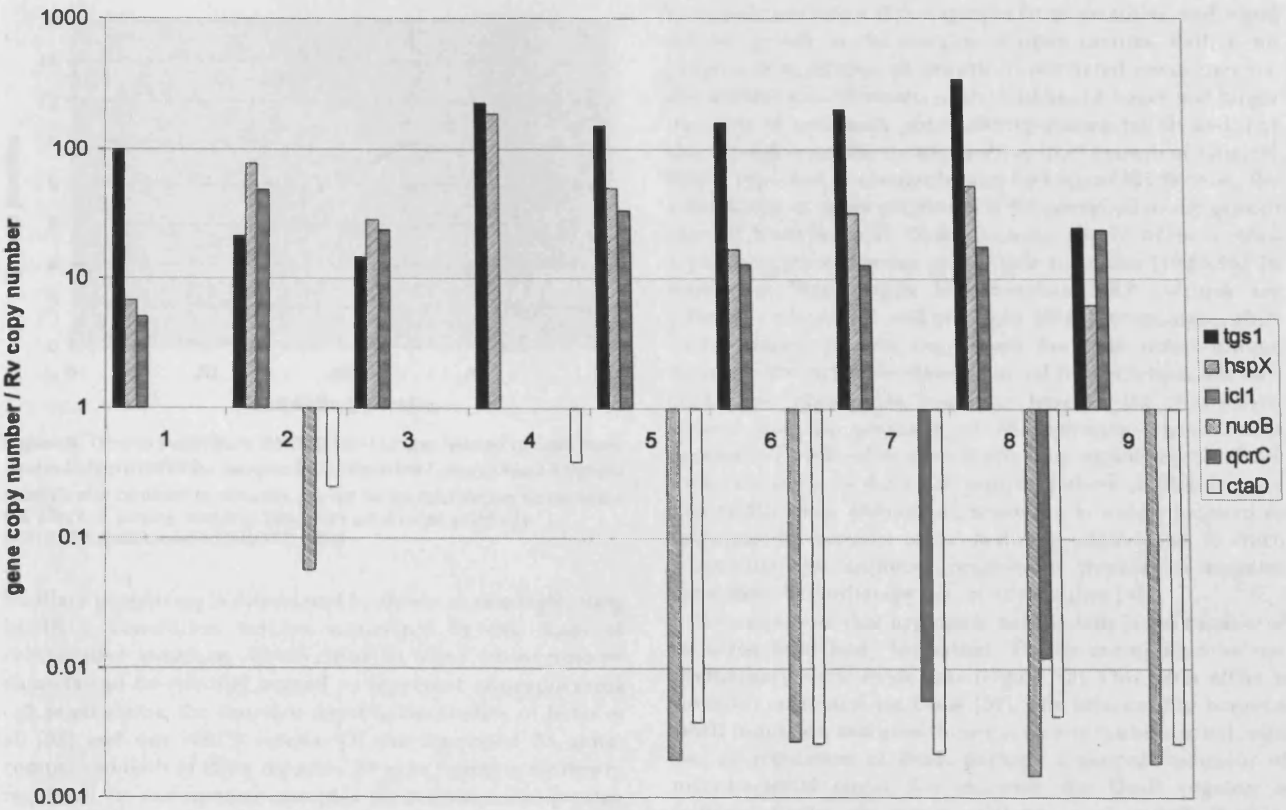

Figure 5. Specific Transcript Ratios for *tgs1*, *hspX*, *icl1*, *nuoB*, *qcrC*, and *ctaD* in AFB-Positive Sputum Samples Determined by qRT-PCR and Normalized to Values for Aerobically Grown Mid-Log *M. tuberculosis* H37Rv

Individual target gene transcript copy numbers were normalized against transcript copy numbers of *sigA* in the samples concerned. Numbers on the abscissa refer to the designated sputum sample numbers.

doi:10.1371/journal.pmed.0050075.g005

role in the diagnosis and management of tuberculosis. While the presence of acid-fast bacilli in sputum is the feature most prominently linked to the potential of a patient to disseminate infection, there are other influential factors. Setting aside those associated with human behaviour and the immediate atmospheric conditions, a transmitted tubercle bacillus must survive transit and master new environmental pressures if it is to establish infection in a new individual. From what we know about bacterial adaptation, it is highly probable that specific traits are expressed to achieve this ability. Furthermore, it is recognised that in the treatment of tuberculosis and other bacterial infections, bacterial burden correlates not only with increased potential for onward transmission, but also with the duration of chemotherapy required for a cure [47]. Bacterial populations often show heterogeneous properties. The presence of a slow or non-growing subpopulation of bacteria phenotypically resistant to antibiotics has been proposed to account for the extended time required for treatment of tuberculosis [4,48]. Although never directly identified, the presence of such a population is inferred from the biphasic reduction of viable bacterial counts recovered from serial sputum samples collected during therapy [4]. Such antibiotic-tolerant "persister" populations have been recognised in many bacterial infections [49]; a greater bacterial burden being associated with a higher frequency of phenotypic resistance. The results we present here are a first step towards defining the transmission phenotype of *M. tuberculosis* and also reveal directly, to our knowledge for the first time, a substantial population of persister-like bacilli in sputum prior to commencement of therapy.

Lipid bodies must now be recognised as a universal feature of smear-positive tuberculosis, and the significance of this finding and of the variation in the proportion of positive cells between samples must be established. While lipid bodies are a well-established feature of eukaryotic cell biology [50], their recognition in prokaryotes is relatively recent [51]. The link between *tgs1*, the DosR regulon, the hypoxia-induced NRP state, and lipid bodies that is strengthened and made clinically relevant by our findings, relates these structures to a coherent set of laboratory studies. Lipid body–positive cells must now be factored into the debate about mycobacterial dormancy and persistence. Fourteen functional Tgs enzymes that are not DosR regulated have been identified [7]. However, none of the mRNAs encoding these enzymes was found to be up-regulated in our transcriptional studies, while Tgs1, the most active enzyme, and the DosR regulon itself were.

While the microarray results can be analysed in several different contexts, we focus here on the data that have a bearing on the growth state and lipid body content of our samples. The transcriptome clearly shows that the sputum

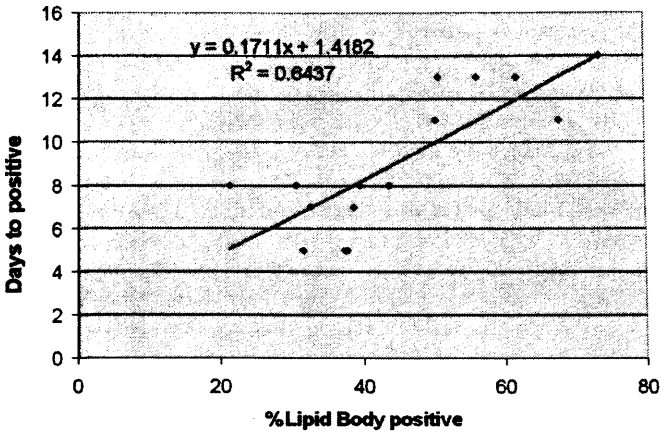

Figure 6. Time to Positivity in BACTEC 960 Cultures Related to Lipid Body Counts Determined in the Samples from Which the Cultures Were Prepared
Analysis was confined to samples graded 3+ by microscopy to minimize the effect of varying bacterial inoculum on time to positivity.
doi:10.1371/journal.pmed.0050075.g006

bacillary population is dominated by slowly or nonreplicating bacilli, a contention further supported by two lines of comparative evidence. Firstly, two in vitro transcriptome datasets can be robustly argued to represent nonreplicating cell populations: the nutrient deprivation studies of Betts et al. [52] and our NRP2 results. Of the repressed 33 genes common to both of these datasets, 20 were found to be down-regulated in our sputum samples (hypergeometric p-value 2.56×10^{-11}), a feature that is further supported by strong correlations with the recently published reduced growth rate dataset (Figure 5) [53]. Secondly, Shi and colleagues studied specific gene expression in chronic mouse infections [37] under conditions in which there is clear evidence for lack of replication [54]. In common with this study, our results show repression of *nuoB, ctaD, qcrC, atpA,* and *atpD* and up-regulation of *narK2*. This supports the view that our sputum samples contained many nonreplicating bacilli in respiratory state III defined by these authors [37], that is, a shift from oxygen electron transfer to anaerobic electron transfer.

If the frequency of lipid body–positive mycobacteria in sputum provides an estimate of the NRP cells present, then other NRP-related features should be correlated. Remarkably, we found this to be the case with time to positivity in routine diagnostic cultures performed on samples that we had analysed for their lipid body content (Figure 6). These results provide direct evidence that the frequency of lipid body–positive cells provide an estimate of the nonreplicating mycobacterial population in sputum in these samples.

Drawing all these results together, we now reject the commonly held belief that smear-positive sputum is dominated by aerobically replicating *Mycobacterium tuberculosis*. The transcriptome data in particular show that such cells could only be a minor component in the samples analysed in this way. In contrast, we conclude that our samples contained nonreplicating mycobacteria at levels proportional to the lipid body-positive cells therein.

While the significance of this finding to clinical tuberculosis will only be established by long-term studies, several important implications can be recognised at this stage. First, it is clear that the large numbers of tubercle bacilli observed in sputum are not a direct sample from extensive and rapid aerobic growth at the margins of open cavities. Rather, we propose that, as with all growth in restricted environments, this aerobic growth results in the buildup of larger and larger numbers of stationary phase nonreplicating bacilli and that this accords with the mature "colony-like" growth of tubercle bacilli reported in caseous lesions by Canetti [2]. Second, the cidal action of many antibiotics is proportional to the growth rate of bacteria, with those growing slowly or in a non-replicating state showing phenotypic tolerance [49,55,56]. In particular, Wayne type *M. tuberculosis* NRP cultures are tolerant to isoniazid and rifampin [15]. Interestingly, while such cultures provide the closest available transcriptome match to the signals we have obtained from sputum, our own studies on phenotypic resistance have so far consistently shown that the presence of *M. tuberculosis* lipid bodies accumulated following growth-arresting stimuli, is correlated with tolerance to the cidal action of these antibiotics (see Figure S2). Such phenotypic resistance is widely believed to underpin the persister phenomenon in tuberculosis, in which a residual and antibiotic-recalcitrant population requires extended chemotherapy for its elimination [4].

We emphasise that hypoxia is not the only stress capable of inducing lipid body formation. This is exemplified by our preliminary nitric oxide data (Figure S2). This latter effect is probably mediated via DosR [57]. The relationship between DosR induction and growth rate is clearly multifactorial, with the up-regulation of DosR perhaps a general indicator of mycobacterial stress, for example the DosR regulon is induced during the exponential phase of growth in mice [31]. It is the slow/nongrowth transcriptional profile and our time-to-positivity results that indicate the presence of a nonreplicating population in sputum rather than *dosR* expression, which is found in both growing and nongrowing populations. However, it should be noted that bacterial populations are evidently nonuniform. Thus lipid body–positive cells may also represent a slower or nonreplicating population within a growing culture.

We cannot say whether the expectorated persister-like population we report here reflects the persister population revealed during chemotherapy. Initial establishment of persisters in growing populations is probably random and at a low level; however, during infection these populations will be influenced by specific conditions, including the development of colonial/biofilm-like growth [2] and inflammatory responses that may increase the numbers of persister-like cells observed [49,57]. We note that all the sputum samples we examined were collected prior to the commencement of chemotherapy; the status of bacilli within patients treated with antibiotics is not clear. Nonetheless, this question is amenable to further study through the analysis of the responses of patients to therapy and serial analyses of the lipid body content of their sputum samples.

Finally, returning to the proposal that the bacilli in sputum display traits that underpin the transmission of tuberculosis, the relative resistance of nonreplicating bacteria, including *M. tuberculosis*, to a variety of stresses is well established [59–61]. Global stress resistance will promote survival that is essential for transmission. More specifically, we note that formation of lipid bodies in *Rhodococcus*, another actinomoycete, has been linked to improved survival during desiccation [62]. Even more intriguing is the observation that

hypoxically grown *M. tuberculosis* cultures, in which we have demonstrated ~34% lipid body–positive cells (unpublished data), are 10-fold more infectious for guinea pigs by the aerosol route than their aerobically grown counterparts [63]. Moreover, recent investigation of Beijing strains of *M. tuberculosis* revealed that they accumulate more triacylglycerol and express *tgs1* at levels 10-fold higher than laboratory strains, during aerobic log-phase growth [64]. The enhanced transmissibility, evidenced by the rapid global spread of these strains, may reflect a greater propensity for lipid body formation in vivo.

We propose that lipid body positive (fat) acid fast bacilli are a biomarker for nonreplicating (lazy) *M. tuberculosis* cells in sputum; their further study offers exciting and tractable avenues for research into the treatment and prevention of tuberculosis.

Supporting Information

Figure S1. Overexpression of *tgs1* in *M. smegmatis* Leads to Enhanced Accumulation of Triacylglycerol and Lipid Bodies

We cloned *tgs1* under the control of the acetamide-inducible promoter pSD26 [65] and expressed it in *Mycobacterium smegmatis*, which readily forms tiacylglycerol (TAG) lipid bodies in vitro. Test and control cells were exposed to radiolabelled oleic acid for 10 min and incorporation into TAG determined [66].

(A) Triacylglycerol synthase (TGS) activity of induced MspSD26-*tgs1* and MspSD26 vector control, $p < 0.001$.

(B) Pseudo-coloured fluorescence images of induced MspSD26 vector control (i) and MspSD26-*tgs1* (ii) incubated with 630 μM oleic acid for 10 min and labelled with Nile red [5]. Pseudo-colour (blue/min to red/max) was applied to grey levels 101–255 to demonstrate enhanced lipid body formation in the *tgs1*-overexpressing cells. Scale bar = 2 μm.

Found at doi:10.1371/journal.pmed.0050075.sg001 (6.7 MB TIF).

Figure S2. Nitric Oxide Exposure Stimulates Lipid Body Formation and Tolerance to the Cidal Action of Rifampin

Exponential phase *M. tuberculosis* H37Rv cultures in Sauton's medium (~10^5 cfu/ml) were treated with 100 μM spermine.NO (NO donor) for 4 or 24 h. These test cultures respectively contained 65% and 22% lipid body–positive cells, while the control cultures, exposed to 100 μM spermine.HCl for the same times, contained < 1% . Subsequent exposure of test and control cultures to rifampin (1 μg/ml) for 7 d revealed diminished killing in the NO exposed cultures. Error bars = − 1 standard deviation ($n = 3$).

Found at doi:10.1371/journal.pmed.0050075.sg002 (194 KB TIF).

Table S1. Genes Determined to Be Greater than 3-fold Up-regulated in Sputum 1 Compared with In Vitro Growth of the Cognate Isolate by Direct Microarray

Found at doi:10.1371/journal.pmed.0050075.st001 (52 KB DOC).

Table S2. Hypergeometric Probability Analysis of Genes Determined to be > 3-Fold Up-regulated in Sputum 1 Compared to In Vitro Cognate Isolate Growth by Direct Microarray

Found at doi:10.1371/journal.pmed.0050075.st002 (85 KB DOC).

Table S3. Genes Determined to be Greater than 2.5-Fold Up-regulated in Sputum Compared with In Vitro Growth by Amplified Microarray

Found at doi:10.1371/journal.pmed.0050075.st003 (403 KB DOC).

Table S4. Genes Determined to be Greater than 2.5-fold Down-regulated in Sputum Compared with In Vitro Growth by Amplified Microarray

Found at doi:10.1371/journal.pmed.0050075.st004 (664 KB DOC).

Table S5. Hypergeometric Probability Analysis of Genes Determined to be >2.5-Fold Up-regulated in Sputum Compared to In Vitro H37Rv Growth by Amplified Microarray

Found at doi:10.1371/journal.pmed.0050075.st005 (104 KB DOC).

Table S6. Hypergeometric Probability Analysis of Genes Determined to be >2.5-Fold Down-regulated in Sputum Compared to In Vitro H37Rv Growth by Amplified Microarray

Found at doi:10.1371/journal.pmed.0050075.st006 (86 KB DOC).

Accession Numbers

The fully annotated microarray data from this study are deposited in BμG@Sbase (accession number: E-BUGS-52; http://bugs.sgul.ac.uk/E-BUGS-52) and ArrayExpress (accession number: E-BUGS-52; http://www.ebi.ac.uk/arrayexpress/experiments/E-BUGS-52).

Acknowledgments

We thank Sarah Fandrich and Helen Smith for technical assistance; Jenny Bryan for helpful comments on the manuscript; and Keith McAdam, Tumani Corah, Bouke de Jong, Omar Ceesay, Babou Faye, and Jacob Otu for their assistance in The Gambia. *M. tuberculosis* H37Rv reference DNA was kindly provided by Colorado State University (Contract No. HHSN266200400091C; NIH, NIAID N01-AI-40091; "Tuberculosis Vaccine Testing and Research Materials Contract"; http://www.cvmbs.colostate.edu/microbiology/tb/top.htm). Joanna Bacon, Health Protection Agency, Porton Down, UK, kindly supplied a sample of her hypoxically grown bacilli for lipid body analysis.

Author contributions. NJG, SJW, RAA, PDB, and MRB designed the study, analysed results and contributed to the writing of the paper. KR and GSB contributed to the analysis of results and writing of the paper. NJG, SJW, ALS, SML, RJS, CS, and JH were involved in performing the experiments and analysing the data.

References

1. WHO (2007) Global tuberculosis control: surveillance, planning, financing. Geneva: WHO. WHO/HTM/TB/2007.376. Available: http://www.who.int/tb/publications/global_report/en/. Accessed 20 February 2008.
2. Canetti G (1955) The tubercle bacillus in the pulmonary lesion of man. Histobacteriology and its bearing on therapy of pulmonary tuberculosis. The tubercle bacillus in the pulmonary tuberculous lesion. New York: Springer Publishing Company. pp. 29–85.
3. Young DB, Duncan K (1995) Prospects for new interventions in the treatment and prevention of mycobacterial disease. Annu Rev Microbiol 49: 641–673.
4. Mitchison DA (2004) The search for new sterilizing anti-tuberculosis drugs. Front Biosci 9: 1059–1072.
5. Garton NJ, Christensen H, Minnikin DE, Adegbola RA, Barer MR (2002) Intracellular lipophilic inclusions of mycobacteria in vitro and in sputum. Microbiology 148: 2951–2958.
6. Kalscheuer R, Steinbüchel A (2003) A novel bifunctional wax ester synthase/acyl-CoA:diacylglycerol acyltransferase mediates wax ester and triacylglycerol biosynthesis in *Acinetobacter calcoaceticus* ADP1. J Biol Chem 278: 8075–8082.
7. Daniel J, Deb C, Dubey VS, Sirakova TD, Abomoelak B, et al. (2004) Induction of a novel class of diacylglycerol acyltransferases and triacylglycerol accumulation in *Mycobacterium tuberculosis* as it goes into a dormancy-like state in culture. J Bacteriol 186: 5017–5030.
8. Park HD, Guinn KM, Harrell MI, Liao R, Voskuil MI, et al. (2003) *Rv3133c/dosR* is a transcription factor that mediates the hypoxic response of *Mycobacterium tuberculosis*. Mol Microbiol 48: 833–843.
9. Voskuil MI, Visconti KC, Schoolnik GK (2004) *Mycobacterium tuberculosis* gene expression during adaptation to stationary phase and low-oxygen dormancy. Tuberculosis (Edinb) 84: 218–227.
10. Muttucumaru DG, Roberts G, Hinds J, Stabler RA, Parish T (2004) Gene expression profile of *Mycobacterium tuberculosis* in a nonreplicating state. Tuberculosis (Edinb) 84: 239–246.
11. Karakousis PC, Yoshimatsu T, Lamichhane G, Woolwine SC, Nuermberger EL, et al. (2004) Dormancy phenotype displayed by extracellular *Mycobacterium tuberculosis* within artificial granulomas in mice. J Exp Med 200: 647–657.
12. Schnappinger D, Ehrt S, Voskuil MI, Liu Y, Mangan JA, et al. (2003) Transcriptional adaptation of *Mycobacterium tuberculosis* within macrophages: Insights into the phagosomal environment. J Exp Med 198: 693–704.
13. Neyrolles O, Hernandez-Pando R, Pietri-Rouxel F, Fornes P, Tailleux L, et al. (2006) Is adipose tissue a place for *Mycobacterium tuberculosis* persistence? PLoS ONE 1: e43. doi:10.1371/journal.pone.0000043
14. Sirakova TD, Dubey VS, Deb C, Daniel J, Korotkova TA, et al. (2006) Identification of a diacylglycerol acyltransferase gene involved in accumulation of triacylglycerol in *Mycobacterium tuberculosis* under stress. Microbiology 152: 2717–2725.
15. Wayne LG, Hayes LG (1996) An in vitro model for sequential study of shiftdown of *Mycobacterium tuberculosis* through two stages of nonreplicating persistence. Infect Immun 64: 2062–2069.

16. Conway T, Schoolnik GK (2003) Microarray expression profiling: capturing a genome-wide portrait of the transcriptome. Mol Microbiol 47: 879–889.
17. Waddell SJ, Butcher PD (2007) Microarray analysis of whole genome expression of intracellular *Mycobacterium tuberculosis*. Curr Mol Med 7: 287–296.
18. Rachman H, Strong M, Ulrichs T, Grode L, Schuchhardt J, et al. (2006) Unique transcriptome signature of *Mycobacterium tuberculosis* in pulmonary tuberculosis. Infect Immun 74: 1233–1242.
19. Sommers HM, Good RC (1985) Mycobacterium. In: Lennette EH, Balows A, Hausler Jr WJ, Shadomy HJ, editors. Manual of clinical microbiology. Washington (D.C.): ASM. pp. 216–248.
20. Larsen MH (2000) Some common methods in mycobacterial genetics. In: Hatfull GF, Jacobs J W. R., editors. Molecular genetics of mycobacteria. Washington (D.C.): ASM. pp. 216–248.
21. Rajakumar K, Shafi J, Smith RJ, Stabler RA, Andrew PW, et al. (2004) Use of genome level-informed PCR as a new investigational approach for analysis of outbreak-associated *Mycobacterium tuberculosis* isolates. J Clin Microbiol 42: 1890–1896.
22. Monahan IM, Mangan JA, Butcher PD (2001) Extraction of RNA from intracellular *Mycobacterium tuberculosis*: Methods, considerations and applications. In: Stoker TPaNG, editor. Mycobacterium tuberculosis Protocols. Totowa (New Jersey): Humana Press. pp. 31–42.
23. Desjardin LE, Perkins MD, Wolski K, Haun S, Teixeira L, et al. (1999) Measurement of sputum *Mycobacterium tuberculosis* messenger RNA as a surrogate for response to chemotherapy. Am J Respir Crit Care Med 160: 203–210.
24. Cole ST, Brosch R, Parkhill J, Garnier T, Churcher C, et al. (1998) Deciphering the biology of *Mycobacterium tuberculosis* from the complete genome sequence. Nature 393: 537–544.
25. Stewart GR, Wernisch L, Stabler R, Mangan JA, Hinds J, et al. (2002) Dissection of the heat-shock response in *Mycobacterium tuberculosis* using mutants and microarrays. Microbiology 148: 3129–3138.
26. Mangan JA, Monahan IM, Butcher PD (2002) Gene expression during host-pathogen interactions: approaches to bacterial mRNA extraction and labelling for microarray analysis. In: Wren Dorrell, editors. Methods in microbiology. London: Academic Press. pp. 137–151.
27. Waddell SJ, Laing K, Senner C, Butcher PD (2008) Microarray analysis of defined *Mycobacterium tuberculosis* populations using RNA amplification strategies BMC Genomics 2008, 9: 94 (25 February 2008)
28. Rohde KH, Abramovitch RB, Russell DG (2007) *Mycobacterium tuberculosis* invasion of macrophages: linking bacterial gene expression to environmental cues. Cell Host Microbe 2: 352–364.
29. Fleischmann RD, Alland D, Eisen JA, Carpenter L, White O, et al. (2002) Whole-genome comparison of *Mycobacterium tuberculosis* clinical and laboratory strains. J Bacteriol 184: 5479–5490.
30. Garnier T, Eiglmeier K, Camus JC, Medina N, Mansoor H, et al. (2003) The complete genome sequence of *Mycobacterium bovis*. Proc Natl Acad Sci U S A 100: 7877–7882.
31. Talaat AM, Lyons R, Howard ST, Johnston SA (2004) The temporal expression profile of *Mycobacterium tuberculosis* infection in mice. Proc Natl Acad Sci U S A 101: 4602–4607.
32. Eisen MB, Spellman PT, Brown PO, Botstein D (1998) Cluster analysis and display of genome-wide expression patterns. Proc Natl Acad Sci U S A 95: 14863–14868.
33. Waddell SJ, Stabler RA, Laing K, Kremer L, Reynolds RC, et al. (2004) The use of microarray analysis to determine the gene expression profiles of *Mycobacterium tuberculosis* in response to anti-bacterial compounds. Tuberculosis (Edinb) 84: 263–274.
34. Dubnau E, Fontan P, Manganelli R, Soares-Appel S, Smith I (2002) *Mycobacterium tuberculosis* genes induced during infection of human macrophages. Infect Immun 70: 2787–2795.
35. Wilkinson RJ, DesJardin LE, Islam N, Gibson BM, Kanost RA, et al. (2001) An increase in expression of a *Mycobacterium tuberculosis* mycolyl transferase gene (*fbpB*) occurs early after infection of human monocytes. Mol Microbiol 39: 813–821.
36. Manganelli R, Dubnau E, Tyagi S, Kramer FR, Smith I (1999) Differential expression of 10 sigma factor genes in *Mycobacterium tuberculosis*. Mol Microbiol 31: 715–724.
37. Shi L, Sohaskey CD, Kana BD, Dawes S, North RJ, et al. (2005) Changes in energy metabolism of *Mycobacterium tuberculosis* in mouse lung and under in vitro conditions affecting aerobic respiration. Proc Natl Acad Sci U S A 102: 15629–15634.
38. Van der Geize R, Yam K, Heuser T, Wilbrink MH, Hara H, et al. (2007) A gene cluster encoding cholesterol catabolism in a soil actinomycete provides insight into *Mycobacterium tuberculosis* survival in macrophages. Proc Natl Acad Sci U S A 104: 1947–1952.
39. McKinney JD, Honer zu Bentrup K, Munoz-Elias EJ, Miczak A, Chen B, et al. (2000) Persistence of *Mycobacterium tuberculosis* in macrophages and mice requires the glyoxylate shunt enzyme isocitrate lyase. Nature 406: 735–738.
40. Timm J, Post FA, Bekker LG, Walther GB, Wainwright HC, et al. (2003) Differential expression of iron-, carbon-, and oxygen-responsive mycobacterial genes in the lungs of chronically infected mice and tuberculosis patients. Proc Natl Acad Sci U S A 100: 14321–14326.
41. Talaat AM, Ward SK, Wu CW, Rondon E, Tavano C, et al. (2007) Mycobacterial bacilli are metabolically active during chronic tuberculosis in murine lungs: Insights from genome-wide transcriptional profiling. J Bacteriol 189: 4265–4274.
42. Fenhalls G, Stevens L, Moses L, Bezuidenhout J, Betts JC, et al. (2002) In situ detection of *Mycobacterium tuberculosis* transcripts in human lung granulomas reveals differential gene expression in necrotic lesions. Infect Immun 70: 6330–6338.
43. Kendall SL, Withers M, Soffair CN, Moreland NJ, Gurcha S, et al. (2007) A highly conserved transcriptional repressor controls a large regulon involved in lipid degradation in *Mycobacterium smegmatis* and *Mycobacterium tuberculosis*. Mol Microbiol 65: 684–699.
44. Weichart DH, Kell DB (2001) Characterization of an autostimulatory substance produced by *Escherichia coli*. Microbiology 147: 1875–1885.
45. Mukamolova GV, Turapov OA, Young DI, Kaprelyants AS, Kell DB, et al. (2002) A family of autocrine growth factors in *Mycobacterium tuberculosis*. Mol Microbiol 46: 623–635.
46. Wayne LG, Sohaskey CD (2001) Nonreplicating persistence of *Mycobacterium tuberculosis*. Annu Rev Microbiol 55: 139–163.
47. Connolly LE, Edelstein PH, Ramakrishnan L (2007) Why is long-term therapy required to cure tuberculosis? PLoS Med 4: e120. doi:10.1371/journal.pmed.0040120
48. Mitchison DA (1979) Basic mechanisms of chemotherapy. Chest 76: 771–781.
49. Dhar N, McKinney JD (2007) Microbial phenotypic heterogeneity and antibiotic tolerance. Curr Opin Microbiol 10: 30–38.
50. Murphy DJ (2001) The biogenesis and functions of lipid bodies in animals, plants and microorganisms. Prog Lipid Res 40: 325–438.
51. Waltermann M, Steinbüchel A (2005) Neutral lipid bodies in prokaryotes: recent insights into structure, formation, and relationship to eukaryotic lipid depots. J Bacteriol 187: 3607–3619.
52. Betts JC, Lukey PT, Robb LC, McAdam RA, Duncan K (2002) Evaluation of a nutrient starvation model of *Mycobacterium tuberculosis* persistence by gene and protein expression profiling. Mol Microbiol 43: 717–731.
53. Beste DJ, Laing E, Bonde B, Avignone-Rossa C, Bushell ME, et al. (2007) Transcriptomic analysis identifies growth rate modulation as a component of the adaptation of mycobacteria to survival inside the macrophage. J Bacteriol 189: 3969–3976.
54. Munoz-Elias EJ, Timm J, Botha T, Chan WT, Gomez JE, et al. (2005) Replication dynamics of *Mycobacterium tuberculosis* in chronically infected mice. Infect Immun 73: 546–551.
55. Gomez JE, McKinney JD (2004) M. tuberculosis persistence, latency, and drug tolerance. Tuberculosis (Edinb) 84: 29–44.
56. Paramasivan CN, Sulochana S, Kubendiran G, Venkatesan P, Mitchison DA (2005) Bactericidal action of gatifloxacin, rifampin, and isoniazid on logarithmic- and stationary-phase cultures of *Mycobacterium tuberculosis*. Antimicrob Agents Chemother 49: 627–631.
57. Kumar A, Toledo JC, Patel RP, Lancaster JR Jr., Steyn AJ (2007) *Mycobacterium tuberculosis* DosS is a redox sensor and DosT is a hypoxia sensor. Proc Natl Acad Sci U S A 104: 11568–11573.
58. Levin BR, Rozen DE (2006) Non-inherited antibiotic resistance. Nat Rev Microbiol 4: 556–562.
59. Siegele DA, Kolter R (1992) Life after log. J Bacteriol 174: 345–348.
60. Kolter R, Siegele DA, Tormo A (1993) The stationary phase of the bacterial life cycle. Annu Rev Microbiol 47: 855–874.
61. Smeulders MJ, Keer J, Speight RA, Williams HD (1999) Adaptation of *Mycobacterium smegmatis* to stationary phase. J Bacteriol 181: 270–283.
62. Alvarez HM, Silva RA, Cesari AC, Zamit AL, Peressutti SR, et al. (2004) Physiological and morphological responses of the soil bacterium *Rhodococcus opacus* strain PD630 to water stress. FEMS Microbiol Ecol 50: 75–86.
63. Bacon J, James BW, Wernisch L, Williams A, Morley KA, et al. (2004) The influence of reduced oxygen availability on pathogenicity and gene expression in *Mycobacterium tuberculosis*. Tuberculosis (Edinb) 84: 205–217.
64. Reed MB, Gagneux S, Deriemer K, Small PM, Barry CE 3rd (2007) The W-Beijing lineage of *Mycobacterium tuberculosis* overproduces triglycerides and has the DosR dormancy regulon constitutively upregulated. J Bacteriol 189: 2583–2589.
65. Daugelat S, Kowall J, Mattow J, Bumann D, Winter R, et al. (2003) The RD1 proteins of *Mycobacterium tuberculosis*: expression in *Mycobacterium smegmatis* and biochemical characterization. Microbes Infect 5: 1082–95.
66. Nakagawa H, Kashiwabara Y, Matsuki G (1976) Metabolism of triacylglycerol in *Mycobacterium smegmatis*. J Biochem (Tokyo) 80: 923–928.

Editors' Summary

Background. Every year, nearly nine million people develop tuberculosis—a contagious infection usually of the lungs—and about two million people die from the disease. Tuberculosis is caused by *Mycobacterium tuberculosis*, bacteria that are spread in airborne droplets when people with the disease cough or sneeze. The symptoms of tuberculosis include a persistent cough, weight loss, and night sweats. Diagnostic tests include chest X-rays, the tuberculin skin test, and sputum analysis. For the last of these tests, a sample of sputum (mucus and other matter brought up from the lungs by coughing) is collected and then taken to a laboratory where bacteriologists look for *M. tuberculosis* using special stains—tuberculosis-positive sputum contains "acid-fast bacilli"—and also try to grow bacteria from the sample. Tuberculosis can be cured by taking several powerful antibiotics for several months. It is very important that this treatment is completed to ensure that all the *M. tuberculosis* bacteria in the body are killed and to prevent the emergence of drug-resistant bacteria.

Why Was This Study Done? Strenuous efforts are being made to reduce the global burden of tuberculosis but with limited success so far for many reasons. One barrier to success is the efficiency with which *M. tuberculosis* spreads from one person to another. Very little is known about this part of the bacteria's life cycle. If scientists could understand more about the transmission of *M. tuberculosis* between people, they might identify new therapeutic and preventative targets. In the study, therefore, the researchers examine the acid-fast bacilli in tuberculosis-positive sputum samples to get a snapshot of *M. tuberculosis* at the point of its transmission to a new person and ask how the characteristics of these bacilli compare with those of *M. tuberculosis* growing in the laboratory.

What Did the Researchers Do and Find? The researchers collected sputum samples from patients with tuberculosis in the UK and The Gambia before they received any treatment, and looked for the presence of acid-fast bacilli containing "lipid bodies." These small structures contain a fat called triacylglycerol. *M. tuberculosis* accumulates triacylglycerol when it is exposed to several stresses present during infection (for example, reduced oxygen or hypoxia) and the researchers suggest that the presence of this fat may help the bacteria survive during transmission and establish a new infection. They found that all the samples contained some lipid body–positive acid-fast bacilli. Next, the researchers showed that *M. tuberculosis* grown in the laboratory under hypoxic conditions, which induce the bacteria to enter an antibiotic-tolerant condition called a "nonreplicating persistent" (NRP) state, also accumulated lipid bodies. This result suggests that the lipid body–positive acid-fast bacilli in sputum might be in an NRP state. To test this idea, the researchers compared the pattern of mRNAs (the templates from which proteins are produced; the pattern of mRNAs is called the transcriptome and gives an idea of which proteins a cell is making under given conditions) made by growing cultures of *M. tuberculosis*, by *M. tuberculosis* maintained in the NRP state, and by the acid-fast bacilli in several sputum samples. The transcriptome of the sputum sample revealed production of many proteins made in the NRP state. Finally, the researchers showed that the time needed to grow *M. tuberculosis* from sputum samples increased as the proportion of lipid body–positive acid-fast bacilli in the sputum increased, just as one would suspect if the presence of lipid bodies signifies nongrowing cells.

What Do These Findings Mean? It has been generally assumed that the acid-fast bacilli in sputum collected from patients with tuberculosis are rapidly replicating *M. tuberculosis* released from infected areas of the lungs. By identifying a population of bacteria that contain lipid bodies and that are in an NRP-like state in all the samples of sputum examined from two geographical sites, this study strongly challenges this assumption. The characteristics of this population of bacteria, the researchers suggest, might help them survive the adverse conditions that *M. tuberculosis* encounters during transmission between people and might partly explain why complete clearance of *M. tuberculosis* requires extended treatment with antibiotics. To establish the clinical significance of these findings, future studies will need to examine whether antibiotic treatment affects the frequency of lipid body–positive *M. tuberculosis* bacteria in patients' sputum and whether there is any relationship between this measurement and infectiousness, or clinical response to treatment.

Additional Information. Please access these Web sites via the online version of this summary at http://dx.doi.org/10.1371/journal.pmed.0050075.

- The MedlinePlus encyclopedia contains pages on tuberculosis and on sputum culture (in English and Spanish)
- The US National Institute of Allergy and Infectious Diseases provides information on all aspects of tuberculosis
- The US Centers for Disease Control and Prevention Division of Tuberculosis Elimination provides several fact sheets and other information resources about tuberculosis
- The World Health Organization provides information on efforts to reduce the global burden of tuberculosis